Uncovering the role of the epithelial-mesenchymal transition in ovarian cancer immunogenicity

Edward Yakubovich

Thesis submitted to the University of Ottawa
in partial Fulfillment of the requirements for the
Doctorate in Philosophy (PhD) program in Cellular and Molecular Medicine

Department of Cellular and Molecular Medicine Faculty of Medicine
University of Ottawa

Table of Contents

Abstract

Cancer cells often metastasize by undergoing an epithelial-mesenchymal transition (EMT). While undergoing EMT, epithelial cells lose defining characteristics, such as stable cell-cell junctions, and gain the ability to migrate and invade through extracellular matrices. In addition to these changes in characteristics, mesenchymal cells gain the ability to better regulate the immune system around them. Immune regulation by mesenchymal cells in cancer has been a topic of extensive study and has recently started receiving focus in ovarian cancer. Combined with the emergence of advanced single-cell sequencing techniques, there is now great potential in unraveling the interactions underlying immune regulation by mesenchymal cells and the contribution of the EMT to the phenomenon of immunosuppression in cancer. Here, I present my studies applying a combined approach of single-cell transcriptomics (scRNA-seq) and lab-based techniques to characterize the relationship between the EMT and immune regulation in ovarian cancer. First, by characterizing human ovarian tumors and murine ovarian cancer models I identified that mesenchymal cells secrete chemokines and interleukins into their environment such as CCL2, CCL5, and IL1A. The primary immunosuppressive factor secreted by mesenchymal cells against NK cells was determined to be TGF-β1. I also discovered a possible link between infiltration of immune cells into the tumor microenvironment (TME) and EMT where greater numbers of mesenchymal cells in the TME correlated with a greater number and variety of immune cells in both human ovarian tumors and murine ovarian cancer models. Second, by cell-cell communication analysis of scRNA-seq data, I discovered that LGALS3 expressed by mesenchymal cells may exhaust $CD8^+$ T-cells through the LAG3

receptor in human ovarian cancers. Finally, I uncovered links between EMT and the antigen presentation machinery of ovarian cancer cells where higher expression levels of major histocompatibility complex I (MHC I) positively correlated with the presence of mesenchymal cells in the TME. This work further expands the knowledge base of EMT and immunosuppression in ovarian cancer and can be used to inform researchers and clinicians on new targets and mechanisms for future research and therapy, such as targeting the LGALS3-LAG3 axis in ovarian cancer to relieve exhaustion of T-cells.

List of Figures

List of Tables

List of Abbreviations

α-SMA - α-smooth muscle actin
APM - antigen presenting machinery
bHLH - basic helix-loop-helix
BMP - Bone morphogenetic protein
BRCA - Breast cancer gene 1
BSA - bovine serum albumin
CAF - Cancer-associated fibroblasts
CRTAM - cytotoxic and regulatory T cell-associated
cDNA - Complementary DNA
CTZ - Coelenterazine
CSC - cancer stem cells
CCL - cytokine signaling molecules C-C motif ligand
DMEM - Dulbecco's Modified Eagle Medium
Dox – Doxycycline
DEG – Differentially expressed genes
ECM - Extracellular matrix
E-cad - E-cadherin
EDTA - Ethylenediaminetetraacetic acid
EGF - Epidermal growth factor
EGFR - Epidermal growth factor receptor
EMT - Epithelial-mesenchymal transition
EMT-TFs - Epithelial-mesenchymal transition growth factors
EOC - Epithelial ovarian cancer
FACS - Fluorescence-activated cell sorting
FAK - Focal adhesion kinase
FBS - Fetal bovine serum
FCS - fetal calf serum
FDA - US Food and Drug administration
FGF - Fibroblast growth factor
FN - Fibronectin
Gal-3 - Galectin-3/*LGALS3*
GAM - Generalized additive model
GOBP - Gene Ontology biological pathways
GSEA - Gene set enrichment analysis
GSK-3 - glycogen synthase kinase 3
FGSEA - Fast gene set enrichment analysis
FGL1 - Fibrinogen-like protein 1
HDAC - Histone deacetylase
HGSOC - High-grade serous ovarian cancer
HGF - Hepatocyte growth factor
HIF - hypoxia-inducing factor
HLA - Human leukocyte antigen
IL - Interleukin
ILK - Integrin-linked kinase (ILK)

ITSS - insulin-transferrin-sodium-selenite solution
JAK2 - Janus kinase 2
KLRG1 - killer lectin-like receptor G1
LAG3 - Lymphocyte Activation Gene-3
LCN2 - Lipocalin 2
LGALS3BP - LGALS3 Binding Protein
LIANA - LIgand-receptor ANalysis frAmework
LMO - Lipid-modified DNA oligonucleotide
LOX - Lysyl oxidase
MAPK - Mitogen-activated protein kinase
MAST - model-based analysis of single-cell transcriptomics
MEM - Minimal essential media
MET - Mesenchymal-epithelial transition
MHC - Major histocompatibility complex
MMP - matrix metalloproteinase
MDSC - myeloid derived suppressor cells
N-cad - N-cadherin
NK - Natural killer
NKG2D - NK cell group 2 member D
NMF - Non-negative matrix factorization
NFκB - Nuclear factor kappa beta
OVCA - Ovarian cancer
PBS - Phosphate-buffered saline
PC - Principal component
PCA - Principal component analysis
PDGFR - Platelet derived growth factor receptor
PRC2 - Polycomb repressive complex 2
PD-1 - Programmed cell death protein 1
PD-L1 - Programmed death receptor-ligand 1
pEMT - Partial epithelial-mesenchymal transition
PI3K - Phosphoinositide 3-kinase ()
PINCH - Cys–His protein 1/*LIMS1*
PARP - poly ADP-ribose polymerase
qPCR - Quantitative polymerase chain reaction
RNA-seq - RNA sequencing
RPMI - Roswell Park Memorial Institute medium
shRNA - Short hairpin RNA
scRNA-seq - Single-cell RNA sequencing
OSCC – Oral squamous cell carcinoma cell
SCID - Severe combined immunodeficient
SMAD - Small mothers against decapentaplegic
Shh - Sonic hedgehog
STAT3 - signal transducer and activator of transcription 3
TAM - Tumor associated macrophage
TAZ - Transcriptional coactivator with PDZ-binding motif
TCGA - The Cancer Genome Atlas

TCR - T-Cell Receptor complex
TG2 - Transglutaminase 2
TGF - Transforming growth factor
TGF-β - Transforming growth factor beta
TGF-βR - Transforming growth factor beta receptor
TIL - Tumor infiltrating lymphocytes
TME - Tumor microenvironment
TNF - Tumor necrosis factor
TNFR - TNF receptor
Treg - Regulatory T cell
UMAP - Uniform Manifold Approximation and Projection
UMI - Unique molecular index
VIM - Vimentin
WT - Wild-type
YAP - Yes-associated protein
YY1 - Yin Yang 1
ZEB1 - Zinc finger E-box–binding homeobox 1
ZO-1 - Zona occludens 1

Contributions

This dissertation contains results reported in the following publications:

1. Galaxia M. Rodriguez* and Kristianne J.C. Galpin*, David P. Cook, **Edward Yakubovich**, Vincent Maranda, Elizabeth Macdonald, Juliette Wilson-Sanchez, Anjali L. Thomas, Joanna E. Burdette, Barbara C. Vanderhyden. The Tumor Immune Profile of Murine Ovarian Cancer Models: An Essential Tool for Ovarian Cancer Immunotherapy Research. *Cancer Res. Commun.* **2**, 417–433 (2022).

2. Yakubovich, E., Cook, D. P., Rodriguez, G. M. & Vanderhyden, B. C. Mesenchymal ovarian cancer cells promote CD8+ T cell exhaustion through the LGALS3-LAG3 axis. *Npj Syst. Biol. Appl.* **9**, 1–17 (2023).

3. Rodriguez, G. M., Yakubovich, E. & Vanderhyden, B. C. Unveiling the Immunogenicity of Ovarian Tumors as the Crucial Catalyst for Therapeutic Success. *Cancers* **15**, 5694 (2023).

Dr. David Cook performed sample preparation of OVCA420 cells treated with various EMT inducers *in vitro*. Katayoun Sheikheleslamy and Caroline Vergette from StemCore (Ottawa Hospital Research Institute) processed scRNA-seq samples, performed library preparation, and sequencing. Beyond this, I performed all experimental and computational components.

Complete publication list

Abou-Hamad, J., Hodgins, J. J., **Yakubovich, E.**, Vanderhyden, B. C., Ardolino, M., & Sabourin, L. A. (2024). Sox10-Deficient Drug-Resistant Melanoma Cells Are Refractory to Oncolytic RNA Viruses. *Cells*, *13*(1), Article 1. https://doi.org/10.3390/cells13010073

Farokhi Boroujeni, S., Rodriguez, G., Galpin, K., **Yakubovich, E.**, Murshed, H., Ibrahim, D., Asif, S., & Vanderhyden, B. C. (2023). BRCA1 and BRCA2 deficient tumour models generate distinct ovarian tumour microenvironments and differential responses to therapy. *Journal of Ovarian Research*, *16*(1), 231. https://doi.org/10.1186/s13048-023-01313-z

Fong, B. C., Chakroun, I., Iqbal, M. A., Paul, S., Bastasic, J., O'Neil, D., **Yakubovich, E.**, Bejjani, A. T., Ahmadi, N., Carter, A., Clark, A., Leone, G., Park, D. S., Ghanem, N., Vandenbosch, R., & Slack, R. S. (2022). The Rb/E2F axis is a key regulator of the molecular signatures instructing the quiescent and activated adult neural stem cell state. *Cell Reports*, *41*(5). https://doi.org/10.1016/j.celrep.2022.111578

Hodgins, J. J., Abou-Hamad, J., Hagerman, A., **Yakubovich, E.**, Souza, C. T. de, Marotel, M., Buchler, A., Fadel, S., Park, M. M., Fong-McMaster, C., Crupi, M. F., Bell, J. C., Harper, M.-E., Rotstein, B. H., Auer, R. C., Vanderhyden, B. C., Sabourin, L. A.,

Bourgeois-Daigneault, M.-C., Cook, D. P., & Ardolino, M. (2022). *More than a ligand: PD-L1 promotes oncolytic virus infection via a metabolic shift that inhibits the type I interferon pathway* (p. 2022.08.31.506095). bioRxiv. https://doi.org/10.1101/2022.08.31.506095

Landry, D. A., **Yakubovich, E**., Cook, D. P., Fasih, S., Upham, J., & Vanderhyden, B. C. (2022). Metformin prevents age-associated ovarian fibrosis by modulating the immune landscape in female mice. *Science Advances*, *8*(35), eabq1475. https://doi.org/10.1126/sciadv.abq1475

Maranda, V., & **Yakubovich, E**. (2020). The biomedical lab after COVID-19: Cascading effects of the lockdown on lab-based research programs and graduate students in Canada. *FACETS*, *5*(1), 831–835. https://doi.org/10.1139/facets-2020-0036

Rodriguez, G. M., Galpin, K. J. C., Cook, D. P., **Yakubovich, E**., Maranda, V., Macdonald, E. A., Wilson-Sanchez, J., Thomas, A. L., Burdette, J. E., & Vanderhyden, B. C. (2022). The Tumor Immune Profile of Murine Ovarian Cancer Models: An Essential Tool for Ovarian Cancer Immunotherapy Research. *Cancer Research Communications*, *2*(6), 417–433. https://doi.org/10.1158/2767-9764.CRC-22-0017

Rodriguez, G. M., **Yakubovich, E**., & Vanderhyden, B. C. (2023). Unveiling the Immunogenicity of Ovarian Tumors as the Crucial Catalyst for Therapeutic Success. *Cancers*, *15*(23), Article 23. https://doi.org/10.3390/cancers15235694

Rodriguez, G. M., **Yakubovich, E.**, Murshed, H., Galpin, K. J. C., Vanderhyden, B.C. (2024). NLRC5 expression results in modulation of immune cell activity through Class I MHC. Manuscript accepted for publication in *Frontiers in Immunology*.

Yakubovich, E., Cook, D. P., Rodriguez, G. M. & Vanderhyden, B. C. Mesenchymal ovarian cancer cells promote CD8+ T cell exhaustion through the LGALS3-LAG3 axis. *Npj Syst. Biol. Appl.* **9**, 1–17 (2023). https://doi.org/10.1038/s41540-023-00322-4

Acknowledgements

4 years and change, what a time it has been. From starting in September of 2019, to contending with the consequences of COVID lockdowns starting in March of 2020 just when I was beginning to solidify my role and place in the lab, to pivoting my research objectives in tandem with the circumstances of the time, to frantically learning bioinformatics and data science during the lockdowns, to intense and real efforts at job applications and interviews, to assisting with multiple collaborative projects and my own manuscripts at the same time in the latter half of my tenure, to making friendships and lifelong companionships. As a result of all these experiences and events, I think I have experienced the most growth and development as a person and academic in the last 4 years than at any other time. Looking back, I will miss the process and the journey more than I will celebrate the outcome.

None of this would have been possible of course without Dr. Barbara Vanderhyden. When I came to your office for the first time sometime in the winter of 2019, I really did not know what to expect. I was just finishing my tenure as a master's student and all I knew is that I wanted to work on cancer biology and apply computational techniques to biological research. Honestly, I lacked the skills and the domain knowledge, and I expected you to reject me, but you still took a chance taking me on and for that I will forever be grateful. Giving me that chance opened a whole new world of possibilities, and it is my tenure in your lab that allowed me to unlock the next steps of my career. Without your guidance and your trust in me, in giving me the freedom to pursue the skills and research I wanted to tackle, I would not have succeeded. Barb, I thank you for everything from the bottom of my heart.

Likewise, I owe a lot of my success to Dr. David Cook. Without your patience and your guidance in developing my computational skills, I would still be stuck today trying to wrangle data frames using 'for' loops. I will never forget the summer of 2019 when you got me started with understanding how computational analysis can be used to answer real-world biological questions … a fundamental skill I am still using to this day. And for that, I will always call you 'sensei'. Also, I extend a special thank you to Dr. Kristianne Galpin for being a colleague, mentor, and friend during and after my tenure in the lab. I will miss our chats. Another thank you is extended to Dr. Galaxia Rodriguez for her invaluable mentorship and collaborative endeavours with myself. And to everybody else who was there during my journey – you are all equally valued.

Finally, without my family's endless love and support, I would have never been able to complete or indeed pursue graduate school. To my parents Gennady and Elena, and to my sister Naomi, you are the cornerstone and the treasure of my successes, and you are forever and always in my heart and in my mind. And last, but never least, a heartfelt thank you of adoration to Margarita for being such an incredible and kind person and supporting me at the finish line, when I needed that the most. I love and cherish you.

Chapter 1: Introduction

1.1 The epithelial-mesenchymal transition: history and discovery

At the 18th Hahnemann symposium in 1968, Dr. Elizabeth D. Hay presented the first evidence of epithelial-mesenchymal cellular interactions when she presented findings showing how, in the development of the neural tube during embryogenesis, epithelial cells transformed into mesenchymal cells (Lachat et al., 2021). Then, in 1982, Gary Greenburg and Elizabeth D. Hay published the first seminal research work demonstrating the "epithelial to mesenchymal transformation" by placing adult and embryonic epithelial cells in collagen gel culture systems and observing them lose their polarity and cell-cell junctions while acquiring invasive properties common in mesenchymal cells (Greenburg & Hay, 1982). Epithelial cells are connected by cell-to-cell junctions and possess apical-basal polarity whereas mesenchymal cells have reduced cell-to-cell connectivity, and increased motility with a spindle-like morphology that allows for increased invasiveness while lacking any polarity (Dongre & Weinberg, 2019; J. Yang et al., 2020). Though Dr. Hay's work extends as far back as the 1960s, the term "epithelial-mesenchymal transition" was first proposed by Elizabeth herself in 1995 (Hay & Zuk, 1995) and finally officially adopted in 2003 at the meeting of the EMT International Association (J. Yang et al., 2020).

Other important discoveries in the field of epithelial-mesenchymal transition (EMT) research included the discovery that treatment with hepatocyte growth factor (HGF) in epithelial cells lose their cell-cell junctions, allowing them to detach from each other and migrate (Stoker & Perryman, 1985). In 1990, EMT was tentatively linked to cancer when researchers found that fibroblast growth factor (FGF), transforming growth factor (TGF),

hepatocyte growth factor (HGF), and epidermal growth factor (EGF) can induce EMT *in vitro* in cancer cell lines such as rat bladder carcinoma cells (Gavrilović et al., 1990; Pagan et al., 1997; Stoker et al., 1987; Stoker & Perryman, 1985; Vallés et al., 1990). Then, in 1998, researchers demonstrated that TGFβ-induced EMT increased the invasiveness of epithelial cancer cells (Oft et al., 1998), linking EMT to tumor metastasis and elucidating its role in cancer disease.

Alongside the discovery of the role of EMT in cancer and metastasis, researchers discovered EMT transcription factors (EMT-TFs): a myriad of proteins that, once activated by an upstream pathway, begin a series of complex transcriptional changes that causes cells to undergo detachment from each other and the basement membrane, reorganize their cytoskeleton, change morphology, and promote migration and invasion into other tissues (Z. Huang et al., 2022). The first EMT-TFs to be discovered were proteins encoded by the zinc finger genes SNAIL or *SNAI1* in 1992 (Smith et al., 1992) and SLUG or *SNAI2* in 1994 (*Control of Cell Behavior During Vertebrate Development by Slug, a Zinc Finger Gene* | *Science*, n.d.), followed by Twist and ZEB in 2001 (Bloch-Zupan et al., 2001; Comijn et al., 2001). Furthermore, the role of EMT-TFs as it relates to the EMT in cancer and metastasis was further elucidated in the 2000s with the discovery that upregulation of EMT-TFs Snail (Blanco et al., 2002) and Twist in breast cancer (J. Yang et al., 2004) promotes metastasis.

1.2 Characteristics of cellular changes in EMT

As mentioned in the previous section, epithelial cells are connected via tight cell-cell junctions to each other and to their membrane thus limiting their ability to traverse their

immediate environment. Loss of these junctions leads to loss of apical-basal polarity enabling metastatic spread in cancer (Mendonsa et al., 2018). Loss of these epithelial features is marked by loss of the protein E-cadherin (E-cad), which is encoded by the *CDH1* gene, mutations in which have been linked to various cancers (Guilford et al., 1998; Huels et al., 2015). Loss of E-cad occurs in tandem with loss of tight junction proteins such as zona occludens 1 (ZO-1), claudins, occludins (Z. Huang et al., 2022) and various cytokeratins such as KRT19, with an increase in proteins that enable loss of apical-basal polarity and the acquisition of mesenchymal phenotypes such as N-cadherin (N-cad) encoded by the *CDH2* gene, Vimentin (VIM), Fibronectin (FN) and α-smooth muscle actin (α-SMA) (Kalluri & Weinberg, 2009). During this process, E-cad normally found at the plasma membrane is cleaved and rapidly degraded, resulting in loss of contact with β-catenin, an intracellular cell-cell adhesion and transcriptional protein, resulting in rapid deterioration of epithelial cell adhesion (Niehrs, 2012; Yilmaz & Christofori, 2009). Thus, one of the first hallmarks of EMT is the loss of E-cad.

N-cad, which contributes to actin cytoskeleton remodeling inside the cell, becomes the predominant cadherin in mesenchymal cells following a “cadherin switch” from its counterpart E-cad in epithelial cells (Yilmaz & Christofori, 2009). N-cad replaces E-cad in binding to β-catenin molecules, enabling a different kind of adhesion that is more amenable to motility (Bard et al., 2008). For that reason, N-cad is primarily found in lamellopodia of cells (Comunale et al., 2007), a hallmark of mesenchymal cells in cancer (Greaves & Calle, 2022), allowing it to promote greater motility of the cell through different types of adhesion-based interactions with other cells (Yilmaz & Christofori, 2009). Other mechanisms through which N-cad enables actin reorganization

within the cell to promote loss of polarity and increase motility involves interacting with platelet derived growth factor receptor (PDGFR) (Heldin et al., 1998; Kong et al., 2008), activation of Rac and inhibition of RhoA (Nimnual et al., 2003; Wildenberg et al., 2006), and sustained MAPK pathway activation leading to increased secretion of matrix metalloproteinases (MMPs) (Hazan et al., 2000; Williams et al., 2001). Therefore, the cadherin switch from E-cad to N-cad changes a cell's identity from epithelial to mesenchymal cells while also promoting other changes to the cytoskeletal structure of a cell that allows it to shed cell-cell junction and apical-basal polarity.

Another characteristic of cellular and structural changes during EMT is the loss of contact with the basement membrane that happens due to changes in how the cell interacts with the extracellular matrix (ECM). As described earlier, actin-rich lamellipodia allow cells undergoing EMT to extend their cytoskeleton and act as sensory feelers that provide directional motility (McNiven, 2013). These actin-rich lamellipodia express proteases, such as MT1-MMP and MMP-2, that degrade the ECM-rich environment around them allowing the mesenchymal cells to traverse, migrate to, and invade other tissues (McNiven, 2013; Wolf & Friedl, 2009). Many interactions between epithelial cells and the ECM are handled by integrin complexes through signalling mediators such as integrin-linked kinase (ILK), Cys–His protein 1 (PINCH, LIMS1), and parvin (Hansen et al., 2008; Yilmaz & Christofori, 2009). Changes to the composition of these factors, particularly a shift in the presence of different integrins in the cells, happens during EMT to allow the mesenchymal cells to modify the ECM around them (Lamouille et al., 2014). Thus, EMT promotes a host of cellular structural changes that influence the ability of mesenchymal cells to become motile and invade neighbouring tissues.

1.3 Molecular mechanisms of EMT

With EMT's involvement in cancer metastasis (Brabletz et al., 2018), embryogenesis (Owusu-Akyaw et al., 2019), wound healing (Cheng et al., 2016), and fibrosis (Kalluri & Neilson, 2003), it is important to mention the general molecular mechanisms underlying the transition. Many of the cellular changes in the previous section are driven by EMT-TFs that promote in mesenchymal cells the ability to detach from each other and their basement membranes and proceed to traverse tissues and migrate elsewhere. EMT-TFs such as zinc finger binding transcription factors Snail and Slug, basic helix-loop-helix (bHLH) factors such as zinc finger E-box–binding homeobox 1 (ZEB1) (Peinado et al., 2004), ZEB2, and Twist (J. Yang et al., 2004), and T cell factor (TCF) transcription factor family member lymphoid enhancer binding factor-1 (LEF-1) (Nawshad & Hay, 2003) can all induce EMT by repressing the transcription of cell-cell adhesion genes such as E-cad by binding to their promoter regions.

Both Snail and Slug repress transcription of E-cad by binding to the promoter of the *CDH1* gene (Batlle et al., 2000; Cano et al., 2000; Park et al., 2018; J. Yang & Weinberg, 2008), which is a sufficient trigger for EMT initiation through the cadherin switch (Oda et al., 1998). The role of Snail in cancer and metastasis has been well established (Barrallo-Gimeno & Nieto, 2005), with either knock-in models demonstrating that upregulation of Snail alone can induce EMT in cancer such as breast cancer (Ye et al., 2015) or its accumulation in the nucleus is associated with mesenchymal phenotypes (Yook et al., 2006). When binding to the E-box DNA sequence of other target genes (Cano et al., 2000), Snail recruits polycomb repressive complex 2 (PRC2) leading to DNA methylation and repressive histone modification on the promoter region

of these target genes, such as E-cad, claudins, occludin, and ZO-1 (Cano et al., 2000; Dong et al., 2012; Vincent et al., 2009). Snail can also effect repression of E-cad and other targets leading to EMT by recruiting epigenetic regulators such as histone deacetylases (HDACs) (Burstin et al., 2009). Snail can be regulated by itself in some cases (Peiró et al., 2006) and by other transcription factors such as nuclear factor kappa beta (NFκB) (Barberà et al., 2004), Yin Yang 1 (YY1) (Palmer et al., 2009), YAP (Noce et al., 2019), Sonic hedgehog (Shh) (X. Li et al., 2006), and Smads (Leng et al., 2020), which are part of the canonical TGFβ1 pathway. Interestingly, Snail is not only an important EMT-TF, but it also binds to the promoters of immunosuppressive genes (Dongre et al., 2021), suggesting its role extends beyond EMT induction into different modalities of immunoregulation by mesenchymal cells.

As for other members of the Snail family of transcription factors, they too have a role in EMT induction (Nieto et al., 1994). Like Snail, Slug can also form complexes with other major regulators such as YAP/TAZ and control development, wound healing, and metastasis (Savagner et al., 2005; Tang & Weiss, 2017). Slug's key role in cancer EMT was revealed when overexpression of Slug in non-metastatic cells turned them into cells that were capable of migration, invasion, and establishment of satellite colonies (Guo et al., 2012). Like Snail's recently discovered promotion of immunosuppressive phenotypes in cancer cells, Slug has certain auxiliary functions in cancer EMT, for example in promoting tumor angiogenesis (Hultgren et al., 2020). Additionally, both Snail and Slug contribute to chemoresistance in ovarian, breast, and pancreatic cancers by disrupting p53-mediated apoptosis mechanisms (Guo et al., 2012; S. Lim et al., 2013), once again suggesting they have roles that extend beyond induction of EMT

through repression of E-cad into regulation of cell death (Dongre & Weinberg, 2019). Another interesting mechanism of action of Snail and Slug in cancer involves co-expression of both to increase TGFβ pathway activity, creating a positive feedback loop in breast cancer (Dhasarathy et al., 2011). Taken together, both Snail and Slug possess key roles in EMT induction, especially in cancer contexts.

Another important set of EMT-TFs are bHLH transcription factors belonging to the Twist family, members of which are Twist1 and Twist2 who share redundancies in both structure and function (Franco et al., 2011; Qin et al., 2012). Twist1 has been linked to cancer progression and metastasis in breast cancer (Y. Xu, Lee, et al., 2017), bladder cancer (Fondrevelle et al., 2009), cervical cancer (Shibata et al., 2008), and ovarian cancer (Hosono et al., 2007; Kajiyama et al., 2007). For example in breast cancer, Twist1 can bind the promoter for *SNAI2* (Slug) to initiate the EMT and promote metastatic spread (Casas et al., 2011; J. Yang et al., 2004). Furthermore, in murine breast cancer models, Twist1 expression is detected at early stages of metastasis (Hüsemann et al., 2008). Like Snail and Slug, Twist1 represses expression of E-cad in epithelial cells and upregulates N-cad, VIM, and FN in mesenchymal cells in the context of cancer (J. Yang et al., 2004). Interestingly, recent findings show that Twist1 can contribute to metastasis through repression of Fox1a separately from its contributions to EMT induction because Fox1a arrests metastasis of mesenchymal cells in breast cancer and Twist1 has been shown to bind to its promoter region and silence it (Y. Xu, Qin, et al., 2017).

The final members of the EMT-TFs are ZEB1 and ZEB2, which are also inducers of EMT that repress E-cad (Galván et al., 2015), ZO-1 (M. Liu et al., 2018), and claudins

(M. Liu et al., 2018) and play a role in metastasis in colon cancer (SINGH et al., 2011), pancreatic cancer (M. Liu et al., 2018), liver cancer (Nath et al., 2021), breast cancer (Nath et al., 2021), and ovarian cancer (Sakata et al., 2017; Sestito et al., 2022). Interestingly, expression of either ZEB1 or ZEB2 exclusively affects cancer cells in opposite ways. For example, in melanoma, high expression of ZEB1 but low expression of ZEB2 is associated with tumor progression (Caramel et al., 2013), suggesting context dependency of these EMT-TFs. In addition, ZEB1 and ZEB2 modulate expression of MMPs (Miyoshi et al., 2004), suggesting they are involved in the ECM remodeling component of EMT. Taken together, both the Twist and Zeb proteins are another class of EMT-TFs that work to induce and regulate the EMT.

In conclusion, all EMT-TFs repress E-cad which is sufficient to induce EMT in most cells under most contexts. It is no surprise then that low expression of E-cad has been associated with worsening cancer progression and metastasis (Hirohashi, 1998).

1.4 Signaling mechanisms of EMT

The most characterized and well-known signaling pathway to effect EMT is the TGF-β pathway. TGFβ receptors (TGF-βR) can bind TGF-β ligands 1, 2 and 3 as well as the BMP family of proteins (2-7) (Gonzalez & Medici, 2014). The receptor is composed of a heterodimer consisting of type I and type II TGF-β receptors (TGF-βRI, TGF-βRII), with seven type I allotypes and five type II allotypes (Gonzalez & Medici, 2014), different combinations of which allow different isoforms of TGF-β family ligands to bind (Derynck & Feng, 1997; Gilboa et al., 2000). Any binding of a TGF-β superfamily ligand results in transphosphorylation of TGF-βRI by TGF-βRII leading to recruitment of

SMAD2/3 (mothers against decapentaplegic homologs 2 and 3) (Gonzalez & Medici, 2014). Subsequently, SMAD2/3 (R-SMADS) form a complex with SMAD4 and following phosphorylation of the MH2 domain on the C-terminus, the entire complex translocates to the nucleus to affect transcription (Gonzalez & Medici, 2014). One such gene targeted by R-SMAD complexes is *SNAI1* (Snail) that, once expressed, can further form a supercomplex with R-SMAD complexes to repress E-cad, claudin, and occludin expression (Peinado et al., 2003; Vincent et al., 2009). In the nucleus, R-SMADs can also form supercomplexes with Zeb family EMT-TFs to upregulate other EMT-TFs in a positive feedback loop that results in EMT (Peinado et al., 2003; Thuault et al., 2008). Degradation of p53, a common hallmark of many cancers such as ovarian cancer, can be accelerated by R-SMAD complexes which leads to even more Snail expression, further supercharging EMT (Chang et al., 2011; Siemens et al., 2011). TGF-β signaling can also drive EMT through activation of *LEF1* expression which inhibits glycogen synthase kinase 3β (GSK-3β) through the phosphoinositide 3-kinase (PI3K)–Akt pathway which in turn drives EMT induction (Hannigan et al., 2005; Medici et al., 2006).

In a healthy developmental context, TGF-β activation and EMT are required for formation of endocardial cushions and palatal fusion (Mercado-Pimentel & Runyan, 2007; Nawshad et al., 2004). Fibrosis and wound healing are also driven by TGF-β activation of the EMT in many tissues such as epidermis, kidney, liver, and pulmonary airways (Gressner et al., 2002; Willis & Borok, 2007). In cancer contexts, the TGF-β pathway's activation of the EMT is hijacked to enable metastasis (Dongre & Weinberg, 2019). As mentioned in the previous section, a positive feedback loop exists between TGF-β pathway activation, EMT, and upregulation of EMT-TF expression where, for

example, Snail can induce expression of TGF-β1 in renal cancer which signals back to the cell through TGF-βR in an autocrine fashion (Dhasarathy et al., 2011; Grande et al., 2015). In breast cancer, expression of both Snail and Slug leads to expression of TGF-β pathway genes that synergizes with the two to drive EMT (Dhasarathy et al., 2011). Another mechanism by which TGF-β pathway activation interacts with EMT-TFs is through post-translational modifications where, for example in one study, sumoylation at the Lys234 residue of SNAIL occurred after TGF-β pathway was activated (Gudey et al., 2017; Ye & Weinberg, 2017). In another study, inhibition of histone-lysine methyltransferase SETDB1 increased Snail and induced EMT (Du et al., 2018). Taken together, the TGF-β pathway is one of the most well characterized signaling pathways of EMT, and once active, the most potent at driving gene changes to promote EMT.

The tumor necrosis factor (TNF)/NFκB pathway is another important signaling cascade in the induction and modulation of EMT. Canonically, the binding of a ligand such as TNFα to TNF receptor 1 and 2 (TNFR1, TNFR2) leads to activation of the NFκB pathway (Parameswaran & Patial, 2010). Once TNFRs 1 and 2 are stimulated, the NFκB inhibitor, IκBα is phosphorylated by IKKβ leading to release of NFκB and allowing it to translocate to the nucleus to induce gene expression of EMT-TFs such as Snail (Karin & Greten, 2005; Luo et al., 2005). Twist1 and its promoter were recently shown to be targeted by active NFκB following TNFα stimulation in breast cancer (C.-W. Li et al., 2012), while in colorectal cancer TNFα stimulation resulted in enhanced translation of Snail protein but not increased expression at the mRNA level (H. Wang et al., 2013), suggesting that TNFα produces different downstream effects in activation of the EMT pathway than another inducer like TGF-β1 (L. Yu et al., 2014).

Another important signaling pathway inducing EMT is the mitogen growth factor epidermal growth factor (EGF) and its receptor epidermal growth factor receptor (EGFR). Binding of EGF to EGFR induces EMT through activation of the MEK-ERK cascade the result of which is the canonical repression of E-cad (Tashiro et al., 2016; Tian et al., 2007). EGF driven EMT is also possible through the Janus kinase 2 (JAK2) signal transducer and activator of transcription 3 (STAT3) pathway wherein STAT3 binds to Twist's promoter in MCF7 breast cancer cells *in vitro* (Colomiere et al., 2009; Lo et al., 2007). Similar observations have been noted in ovarian OVCA 433 and SKOV3 cells, with increased expression of N-cad and VIM following EGFR activation (Colomiere et al., 2009). Additionally, EGF can synergize with activated TGF-β pathway proteins, helping to colocalize Snail and SMAD2/3 in the nucleus of breast cancer cells, and induce EMT (J. Kim et al., 2016; Uttamsingh et al., 2008). As well, high-affinity binding of EGF to EGFR in MCF7 breast cancer cells results in EMT and mesenchymal phenotypes capable of motility while low-affinity binding of AREG to the same receptor does not induce EMT, suggesting EGF is highly specific to EMT induction in breast cancer (Fukuda et al., 2016).

To summarize, the TGF-β1, TNFα, and EGF signaling pathways are crucial in inducing EMT either in developmental, healthy, or disease conditions, with a certain degree of synergy between the three used to induce EMT and metastasis in cancer. A graphical summary of all these activators and their signaling pathways in EMT can be found in **Figure 1**.

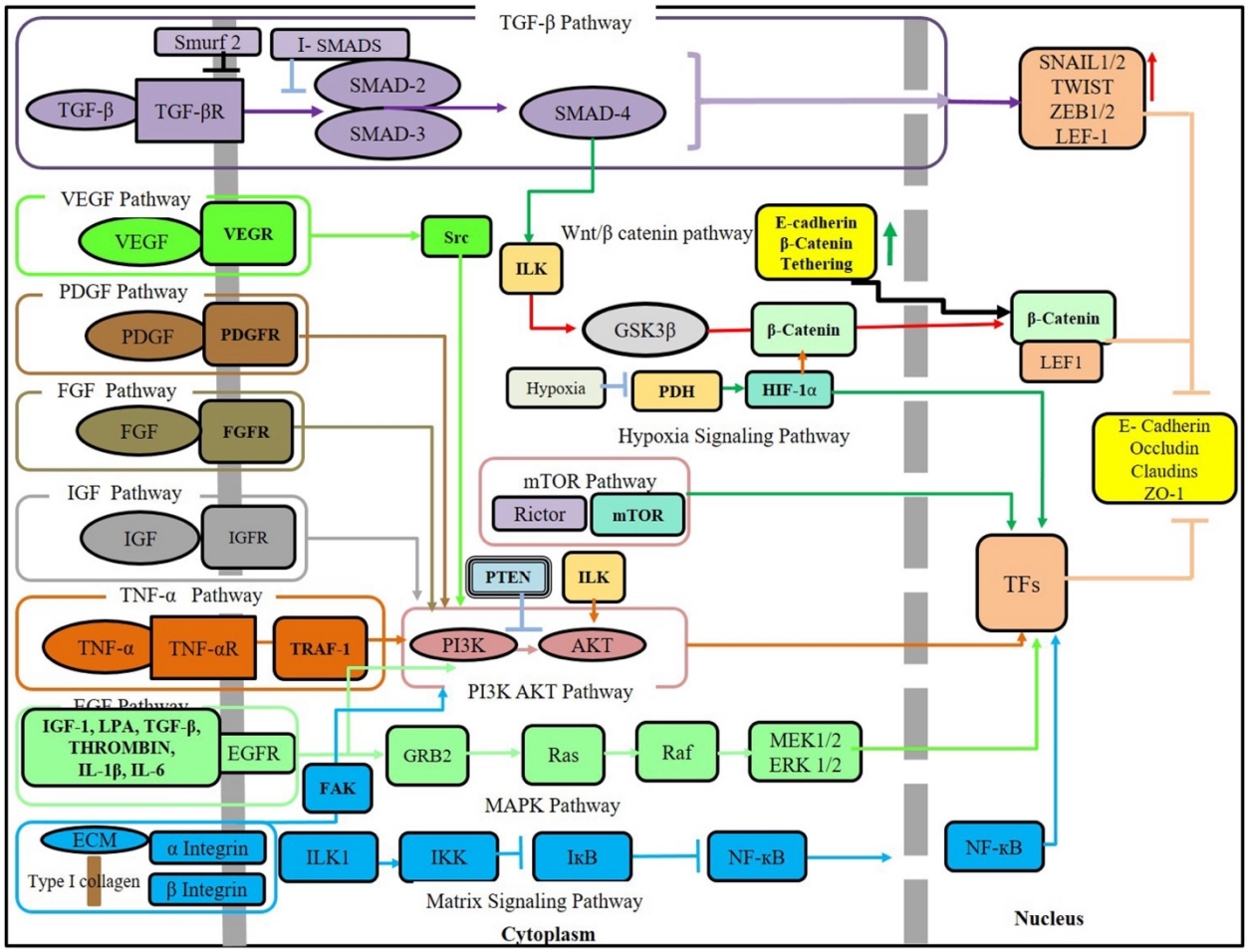

Figure 1. Summary graphic of activators and signaling pathways of EMT (Taken with permission from (Shetty et al., 2020).

1.5 Ovarian cancer: the disease at large

Ovarian cancer (OVCA) is the fifth leading cause of cancer-related deaths in Canadian women and the second most fatal gynecological cancer (Canadian Cancer Statistics, 2023). OVCA 5-year survival rates have largely stagnated at around 45%. It is not uncommon for OVCA diagnosis to occur at Stage III and Stage IV (the later stages) due to the appearance of only subtle symptoms during early disease development and a lack of clinical screening procedures for early detection.

Current therapeutic strategies following diagnosis include the combination of surgical debulking and platinum/taxane-based chemotherapy, with some advances made in recent years in improving the therapies available, namely poly ADP-ribose polymerase (PARP) inhibitors (Piver, 2006). There are several types of OVCA, with the most common diagnosis being epithelial ovarian cancer, which accounts for more than 95% of diagnoses (Torre et al., 2018). Less common types include germ cell and sex-cord stromal cancers and the rare small cell carcinoma and ovarian sarcoma, which collectively account for the other 5% (Torre et al., 2018). Further classification of epithelial OVCA falls into five major subtypes based on histology and grade: high-grade serous (HGSOC), low-grade serous, clear cell, endometrioid, and mucinous ovarian cancer (Lheureux et al., 2019). Distinct features of each of these subtypes contribute to distinct clinical presentation and treatment strategies, paving the way for stratified treatment strategies tailored to each subtype and dependent on specific histological biomarkers unique to each subtype (Lheureux et al., 2019).

Over 70% of epithelial OVCAs are diagnosed as HGSOC, presenting with large mononuclear cells exhibiting pleomorphic nuclei with upregulated mitotic activity and

papillary and solid growth (Prat, 2012). While the majority of HGSCs are sporadic, a strong hereditary component is present in women with *BRCA1*/*BRCA2* tumor suppressor mutations, representing approximately 15% to 20% of HGSOCs (Alsop et al., 2012). HGSOC characterization reveals acquired or inherited mutations in the *TP53* tumor suppressor pathway almost universally (>97% of HGSOC) (Tuna et al., 2020). Chromosomal copy number alterations are a hallmark of HGSOCs that are influenced and promoted by the presence of *TP53* mutations. For example, a common HGSOC copy number alteration resulting in the amplification of the 19q12 locus results in overexpression of *CCNE1*, the gene responsible for the cell-cycle protein E1-driven increase in cellular division (Etemadmoghadam et al., 2010; Kroeger & Drapkin, 2017). Other common pathways affected in HGSOCs tend to be those involved in DNA repair, tumor suppression, and cellular proliferation such as *FXM1*, *Rb*, *PI3K*, and *Notch1* pathways (Cancer Genome Atlas Research Network, 2011).

Efforts by The Cancer Genome Atlas (TCGA) project to further classify HGSOCs into distinct prognostic groups via gene expression analysis resulted in the following stratifications: differentiated, mesenchymal, immunoreactive, and proliferative (Konecny et al., 2014). The stratifications are each associated with different aspects of HGSOC presentation and progression. For example, the immunoreactive subtype in which there is a strong presence of immune cells in the TME, has been correlated with better survival outcomes compared to the mesenchymal subtype which has the worst outcomes (Lheureux et al., 2019). Advancements in genome sequencing and better HGSOC stratification schemas have developed predictive mechanisms for susceptibility of some HGSOC to chemotherapy and even chance of relapse (Macintyre et al., 2018).

Further innovations in genome sequencing techniques and better analysis strategies may improve targeted treatment selection and predictability of disease progression.

1.6 EMT in Cancer: a general overview

In cancer biology, the EMT has been associated with metastatic spread and immunosuppression. In the case of metastasis, cancer cells responsible for invasiveness and migration appear to be in at least a partial EMT (pEMT) state, if not a fully mesenchymal state (Latifi et al., 2012; Saxena et al., 2020; Simeonov et al., 2021). Mesenchymal and pEMT states also appear to be primarily responsible for the immunosuppressive burden in the ovarian tumor microenvironment (TME) (Latifi et al., 2012; Loret et al., 2019; Taki et al., 2021), as will be discussed in greater detail later.

1.6.1 EMT and Stemness:

Cells undergoing EMT show a gradual acquisition of stemness and stem-like properties. Factors such as *Slug*, *Snail*, and *Sox9* have been demonstrated to tightly regulate entrance and exit from the stem-like condition of both healthy and cancer cells (Dongre & Weinberg, 2019). A causal link has been demonstrated between expression of these transcription factors, EMT progression, and the presence of cancer-initiating cancer stem cells (CSCs) (Mani et al., 2008; Morel et al., 2008). It is unknown whether the EMT driving the stemness program of healthy cells is different from that of neoplastic cells, though some differences have been noted in breast cancer (Ye et al., 2015). The significance of EMT driving formation of CSCs while also controlling the ability of non-neoplastic cells to turn into stem-like mesenchymal cells presents potential for the EMT

to convert non-CSCs into CSCs. In mice, non-CSCs have been shown to spontaneously undergo EMT and acquire cell-surface markers associated with CSCs, thus demonstrating the robust ability of the EMT to induce plasticity in cells under the appropriate context and in appropriate tissues (Chaffer et al., 2011).

1.6.2 EMT and chemoresistance:

EMT in cancer cells has been previously linked to chemoresistance in ovarian cancer. Robust research has implicated EMT-related mechanisms in chemoresistance: TGF-β/SMAD signalling drives resistance to paclitaxel; BMP9 activates EMT through TGF-β1 and promotes platinum resistance; and expression of lysyl oxidase (LOX) induced EMT through SLUG and TWIST1 and contributed to chemoresistance by activating PI3K/AKT (Loret et al., 2019; Shayesteh et al., 1999). In another example, cisplatin-resistant oral squamous cell carcinoma cells (OSCC) were generated by continuously exposing them to cisplatin, and the resultant resistant cells had decreased expression of E-cad, suggesting that those cells that had undergone some kind of EMT were more resistant that those that did not (Ghosh et al., 2016). Another gene possibly linking EMT to chemoresistance is transglutaminase 2 (TG2) (Agnihotri et al., 2013), where silencing of TG2 in the breast cancer cell line MDA-MB-231 using short hairpin RNA (shRNA) resulted in increased sensitivity to docetaxel and reversal of EMT. Another interesting link between EMT and chemoresistance was found in colorectal cancer cells that, when treated with neoadjuvant radio-chemotherapy, began to upregulate RNA expression of EMT-related genes such as *Snail*, *Slug*, and *Vim* (Tato-Costa et al., 2016), suggesting that chemotherapy can promote EMT and genes such as TG2 that act through NF-kB, Akt, focal adhesion kinase (FAK), and hypoxia-inducing factor (HIF) pathways (Agnihotri

et al., 2013) to further promote mechanisms of chemoresistance such as senescence (Chakrabarty et al., 2021; Guillon et al., 2019).

1.6.3 EMT and immunosuppression:

Recent attempts have been made to elucidate the role of EMT in cancer cells' ability to facilitate an immunosuppressive TME. A distinct reduction in $CD8^+$ TILs has been reported in ovarian cancer patients with the worst prognosis and a high expression of EMT-related gene signatures (Murakami et al., 2016). NFκβ activation by EMT-TF SNAIL has been linked to CXCL1 and CXCL2 binding to CXCR2 as a mechanism for recruitment of myeloid derived suppressor cells (MDSCs) into the TME, which are immune cells possessing the ability to suppress T-cell activity (Taki et al., 2018; Y. Wu et al., 2022). TGF-β1, on the other hand, a potent inducer of EMT, has been linked to expression of programmed death receptor-ligand 1 (PD-L1) by way of PI3K/AKT pathway activation (Alsuliman et al., 2015). PD-L1 is a checkpoint inhibitor ligand that suppresses the effector function of $CD8^+$ T-cells by binding to the receptor PD-1 in many different carcinomas, and its expression is increased during EMT (Aghajani et al., 2020; L. Chen et al., 2017; Muralidharan et al., 2022). While several pathways have been implicated in EMT-driven immunosuppression by ovarian cancer cells, recently mechanisms underlying exhaustion of $CD8^+$ tumor infiltrating lymphocytes (TILs) have become a focus (Kandalaft et al., 2022). Anti-PD1 therapy has been shown to improve the function of exhausted $CD8^+$ TILs in ovarian cancer (Leem et al., 2020). Despite the interest in how ovarian cancer cells affect $CD8^+$ T-cell exhaustion in HGSOC, the role of the EMT has yet to be explored in this context. We propose that ovarian cancer cells

undergoing EMT, particularly mesenchymal cells, may play a key role in the exhaustion of $CD8^+$ T-cells.

1.6.4 EMT and Metastasis:

During cancer progression, activation of the EMT has been demonstrated to be a major player in metastatic progression. Cancer metastasis presents the most fatal stage of disease progression for patients, with over 90% of cancer-related deaths caused by metastasis rather than the primary tumor (Mehlen & Puisieux, 2006). In epithelial carcinomas, epithelial cells receive context cues from their environment and other nearby cells to undergo an EMT or a partial EMT (pEMT), allowing them to mobilize invasion of local tissues, such as stroma, vasculature, and epithelial tissues. These cells, with EMT-induced mesenchymal characteristics such as loss of E-cad expression and cell-to-cell junctions, intravasate into local blood vessels, travel through the circulatory system, extravasate and implant in the parenchyma of distant tissues to form satellite deposits of malignant cells. It is common for cells undergoing EMT to lose expression of their epithelial cell-surface markers, such as *EpCAM* and *E-cadherin*, though this is not always the case (Lambert et al., 2017). Furthermore, in some contexts, successful formation of metastatic colonies requires cells to be in a pEMT state, rather than in a fully mesenchymal state (Ocaña et al., 2012). Cells that undergo EMT can be capable of reversion, commonly seen at the tail-end of the metastatic process where now-embedded mesenchymal cells may undergo a mesenchymal-to-epithelial transition (MET), reverting to their more-epithelial state along the EMT axis. Recent studies have shown that cancer cells show tremendous plasticity, and it is rare to find cancer cells in either a completely epithelial or mesenchymal state; rather, most

cancer cells' gene expression profile and behavior puts them somewhere along the EMT-axis, in a pEMT state (Grigore et al., 2016; Saitoh, 2018; Saxena et al., 2020).

It is important to mention that in OVCA, metastasis primarily occurs in the immediate environment to the ovaries, spreading throughout the peritoneal cavity rather than travelling through the circulatory system to distant organs. This form of metastasis is facilitated by the accumulation of abdominal fluid known as ascites. Clusters of cells found in ascites fluid possess more mesenchymal characteristics suggesting that EMT is relevant to ovarian cancer metastases. This was shown in experiments where cells derived from patient ascites had gone EMT when aggregating into spheroids *in vitro* (Rafehi et al., 2016). In the same experiment, inhibition of the EMT and attenuated metastatic behavior was seen when the spheroids were treated with a TGF-β1 receptor inhibitor and showed reduced motility, migration, and re-attachment of the cells across a Transwell membrane, suggesting that ascites-derived cells possess strong EMT programming and that the TGF-β1 pathway is key to metastatic spread.

A significant barrier to our understanding of the EMT is the overall complexity of the EMT phenotypic spectrum. EMT programs can participate in the modulation of cellular phenotypes at any point along the multistage progression of cancer – from the initial epithelial cells at the very outset to the malignant cells present at the terminal end of the disease (Y. Zhang & Weinberg, 2018). EMT signature genes can be found in cancer cells from a very early stage of the disease (Berx et al., 1995, 1998). The EMT can influence the cancer cells' resistance to immune cell killing and chemotherapy at the early stages of the disease while promoting their ability to proliferate and disseminate at later stages (Y. Huang et al., 2022; Ribatti et al., 2020; M. Yu et al., 2013). As such, a

wide breadth of phenotypic heterogeneity in cancer cells can be generated through activation of the EMT program at any point along the entire course of the disease. For example, while a host of master regulators (e.g., *SLUG*, *SNAIL*, *ZEB1*) appear to underlie the EMT program in many tissues, their presence alone is not enough to suppress the epithelial characteristics of cancer cells (Stemmler et al., 2019; Y. Wang et al., 2013; Y. Zhang & Weinberg, 2018). In another example, TGF-β1 has been shown to be a potent activator of the EMT program in both healthy and cancer cells, though its EMT inductive capabilities are heavily reliant on the presence of an appropriate intracellular context (K. A. Brown et al., 2004). The combination of these regulators along with the arrangement of cancer cells in the TME, their exposure to different environmental cues, variable hypoxic conditions, and genetic differences of the host can all dictate EMT progression.

Important questions regarding the EMT, such as which genes define the EMT axis, the impact of the EMT axis on metastasis and resistance to treatment, and its contribution to heterogeneity of cancer cells in the TME are yet to be fully elucidated. Recent attempts to formulate lists of genes, or modules, that can be used to calculate an average EMT score for cells have been ongoing in the field of bulk and single-cell genomics (Liberzon et al., 2015) with recent publication of an EMT module based on a census from a large pan-cancer dataset demonstrating the context dependency of these lists (Cook & Vanderhyden, 2022).

1.7 EMT and the immune system

EMT induction in cancer cells by environmental and contextual cues in the TME

results in the transition of cells to acquire mesenchymal characteristics that can modify their immediate environment, particularly targeting cells of the immune system that can affect tumor progression. In certain cancer phenotypes, such as a 'hot' tumor where there are abundant immune cells in the TME, the tumor can exist in a state of constant immune cell activity, with cytotoxic anti-tumor cells [eg. CD8 T-cells, Natural Killer (NK) cells, M1 macrophages] counterbalanced by the presence of suppressive immune cells [eg. regulatory T cells (Treg), M2 macrophages, myeloid-derived suppressor cells (MDSCs)]. Cancer cells undergoing EMT may play a significant role in both the recruitment of immunosuppressive cells and direct suppression of their anti-tumor activity. In melanoma, malignant cells expressing the transcription factor *SNAIL* secrete TGF-β resulting in promotion of Treg differentiation, reduction in antigen presentation by dendritic cells, and promotion of EMT in neighbouring tumor cells (Kudo-Saito et al., 2009). Breast cancer cells which have undergone EMT are less susceptible to immune attack compared to their epithelial neoplastic counterparts through downregulation of MHC I machinery (Dongre et al., 2017; Terry et al., 2017). Another mechanism through which mesenchymal cells possess reduced susceptibility to immunosurveillance is through the recruitment of Treg cells in breast cancer, which are involved in direct suppression of cytotoxic T cells' effector function (Dongre et al., 2017). In another demonstration of how cells undergoing EMT rebuff the immune system, when the human breast cancer cell line MCF-7 was co-cultured with an antigen specific T-cell clone, T-cell function was severely impaired when the cell line expressed *SNAIL* compared with otherwise effective cytotoxicity in absence of *SNAIL* (Akalay et al., 2013).

These various studies show the effects that the EMT program in the cancer cells can have on immune cell activity, though the mechanisms and factors that facilitate mesenchymal cell resistance to immune cell killing are still unknown. In addition to the mesenchymal cell-secreted immunosuppressive factor TGF-β, cytokine signaling molecules C-C motif ligand 2 (CCL2) and Lipocalin 2 (LCN2) have been implicated as factors that can upregulate programmed cell death 1 ligand (*PD-L1*) in neighbouring cells, leading to reduction in the cytolytic activity of T-cells (Kudo-Saito et al., 2013). Cytokines and chemokines such as *TNF* and *CCL5* are also upregulated during an EMT program and are secreted by cancer cells and adjacent fibroblasts (Hsu et al., 2014). Other mechanisms by which the EMT may contribute to impaired immune cell activity include induction of autophagy in cancer cells to escape CD8 T-cell cytotoxicity, attenuation of *MHC-1* and other HLA molecules displayed on the cell surface, and expression of *PD-L1* by carcinoma cells (Dongre & Weinberg, 2019). While research into immune escape by cancer cells is still ongoing, the contribution of EMT to immunosuppression and the crosstalk between cancer cells and immune cells is of great interest and is undergoing investigation. Preliminary analysis of chemokine, cytokine, and interleukin genes' expression in ovarian cancer cell line OVCA420 after induction of EMT with TGF-β1 treatment shows there are many changes in their expression during the course of EMT, with mesenchymal cells upregulating expression of aforementioned factors like *CCL2* (**Figure 2**). Also, certain immunoregulatory factors have recently been implicated in having extensive function in cancer as a function of the EMT, such as Interleukin-32 (IL32). For example, IL32 has either pro-tumorigenic or anti-tumorigenic roles in cancer depending on which isoform is predominantly present,

and has been shown to induce EMT in human lung adenocarcinoma A549 cells, suggesting it is a powerful immunoregulatory molecule capable of a wide range of possible functions in cancer (L. Gong et al., 2020a; Shim et al., 2022).

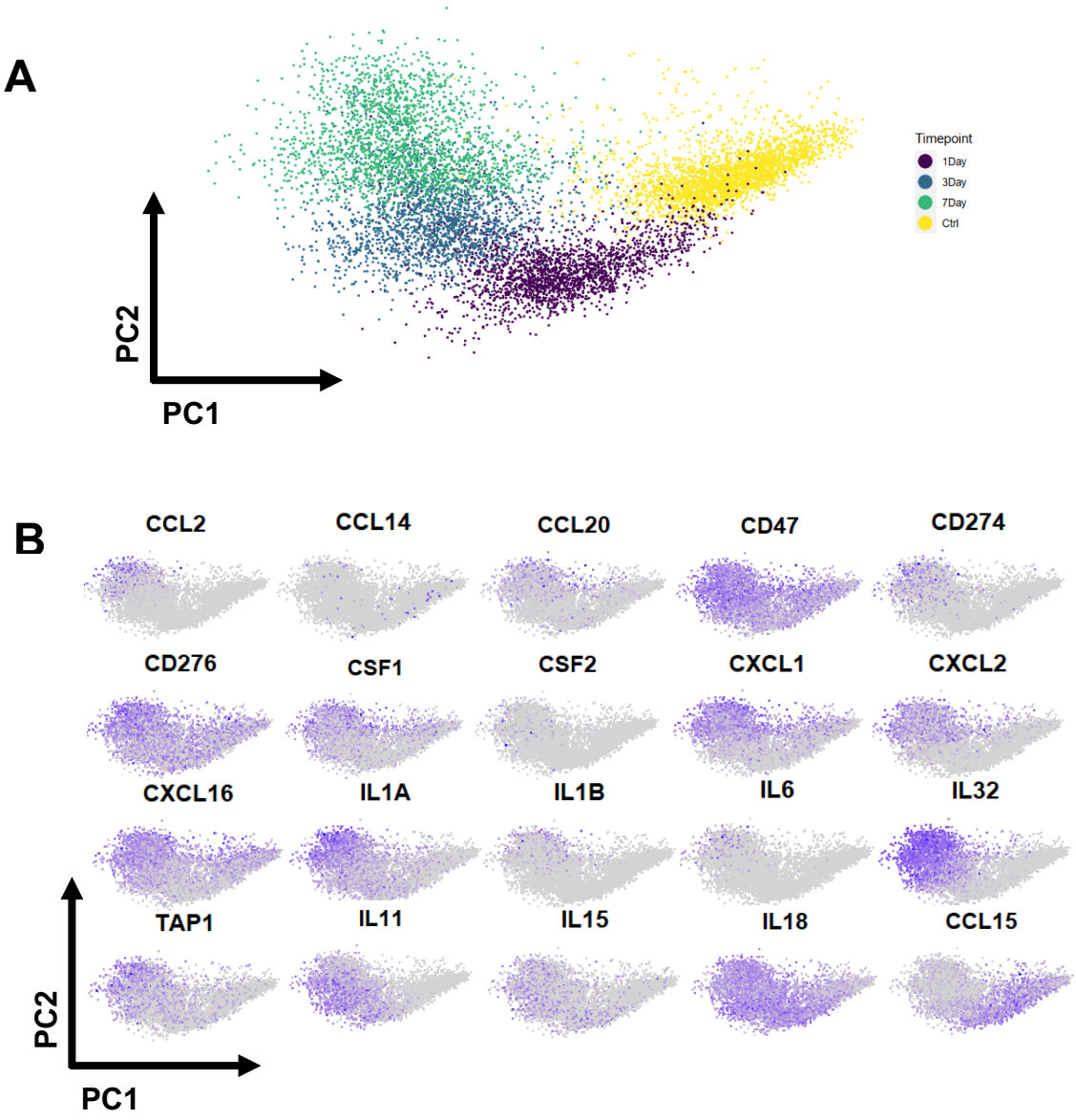

Figure 2. EMT is associated with changes in expression levels of various immunomodulatory factors. (A) PCA clustering of single-cell RNA-sequencing data from OVCA420 cells treated with TGF-β1 (10 ng/mL) at 4 different time points: Ctrl (no treatment), and treated for 1, 3, and 7 days. (B) PCA enrichment plots of cytokines, chemokines, interleukins, and other immune modulatory factors.

Immune infiltration and inflammation play an important role in tumor development in a variety of cancers (Hobson et al., 2013; Stuelten et al., 2008). Inflammation facilitated by immune infiltration has been associated with carcinogenesis, particularly through enhanced metastasis through secreted factors such as TGF-β1 and TNF-α from myeloid cells, particularly MDSCs (Bates & Mercurio, 2003; L. Yang, 2010). In ovarian cancer an 'infiltrated' tumor environment is a TME that is enriched with immune cell infiltration and is associated with better survival prognosis and survival when compared to 'excluded' tumors where immune cells rest on the periphery of the neoplastic mass or 'desert' tumors where immune cells are largely absent from the TME (Kandalaft et al., 2022; Woude et al., 2017). Infiltration by $CD8^+$ cytotoxic T lymphocytes (CTLs) into the TME has been associated with better prognosis and overall survival in many cancers (Bachmayr-Heyda et al., 2013; Ovarian Tumor Tissue Analysis (OTTA) Consortium, 2017).

In ovarian cancer, particularly HGSOC, immune infiltration by $CD8^+CD103^+$ cytotoxic T lymphocytes (CTLs) has been associated with better overall and progression-free survival. However, recent findings show a large portion of infiltrating CTLs in HGSOC are $TIM3^+$ (Fucikova et al., 2019, 2021) and $LAG3^+$ (Fucikova et al., 2021; R.-Y. Huang et al., 2015), suggesting they are prone to exhaustion and attenuated cytolytic action. In many cases, both *TIM3* and *LAG3* act as co-inhibitory molecules together with PDL-1 to dampen antitumor immunity by infiltrating $CD8^+$ T-cells (Chihara et al., 2018; R.-Y. Huang et al., 2015).

1.8 Exhaustion of $CD8^+$ T cells by mesenchymal cells

$CD8^+$ T-cell exhaustion is often induced by a prolonged stimulation by an antigen that leads to loss of effector function, such as scenarios often involving chronic exposure to a pathogen or cancer (Kurachi, 2019). For example, murine studies of HIV-1 infection have demonstrated that both duration of exposure to an antigen and levels of antigen can be synergistic in imposing T-cell exhaustion (Blackburn et al., 2009). Reduction in the cytotoxic potential of $CD8^+$ T-cells from exhaustion culminates in defects in IL-2 production, a decrease in TNF, IFN-γ, and granzyme B secretion, and a reduction in proliferative capacity (Kurachi, 2019). Expression of receptors inhibitory to T-cell effector function, such as LAG3, PD-1, TIM-3, TIGIT, CTLA-4, CD160 and others emerges on the cell surface of these exhausted cells (Kurachi, 2019). Expression of these receptors, or checkpoint inhibitors, is primarily driven by downstream TCR signaling molecules such as NFAT and Sprouty (SRRY2) where, for example, increased PD-1 expression was observed through NFATc2 signaling in EL4 and primary $CD8^+$ T-cells (Oestreich et al., 2008). Some other transcription factors implicated in T-cell exhaustion are Tbet, Eomes, Blimp1, IRF4, BATF, FOXP1, and TCF1 with some of these factors having differential roles in different T-cell populations (Kurachi, 2019). For example, Eomes is implicated in T-cell exhaustion in peripheral tissues but is indispensable for $CD8^+$ T-cell turnover and quiescence in central memory contexts (Banerjee et al., 2010; Paley et al., 2012). An important finding that may bear relevance in the context of $CD8^+$ T-cell exhaustion to EMT is when a dominant negative inhibitor of TGF-β signalling is used, the effector function of exhausted cells was improved in a chronic infection model (Tinoco et al., 2009). Most importantly, phosphorylation of TGF-β1-related downstream signalling target Smad2 in $CD8^+$ T-cells has been associated

with greater exhaustion in chronic infection models, similar to cancer contexts that engage the immune system on a prolonged scale (Tinoco et al., 2009). Overall, prolonged antigen exposure and intensity of exposure to $CD8^+$ T-cells has a role in inducing exhaustion especially in disease contexts such as cancer (P. P. Lee et al., 1999).

Lymphocyte Activation Gene-3 (*LAG3*) encodes a cell surface protein CD223 that associates with the T-Cell Receptor complex (TCR), or CD3, on both $CD4^+$ and $CD8^+$ T-cells and acts as an immune checkpoint. Like the CD4-receptor, LAG3 binds to MHC Class II and Gal-3 but with even stronger affinity. Chronic LAG3 activation on $CD8^+$ tumor antigen-specific T-cells through persistent tumor antigen stimulation has been implicated in exhaustion of TILs and a reduction in their cytolytic capacity (Andrews et al., 2017; Ruffo et al., 2019). High expression levels of *LAG3* have been found in the TME of patients with recurrent HGSOC, along with other immune checkpoints such as *TIGIT* and *CTLA4* (Westergaard et al., 2020). In an ID8 murine model of ovarian cancer, LAG3 was found to associate with PD1 and reduce $CD8^+$ T-cell cytolytic activity leading to attenuated antitumor activity (R.-Y. Huang et al., 2015). In *BRCA*-mutated HGSOC patients, LAG3 was found to be positively correlated with PD1; however, combination immunotherapies to block the activity of both checkpoints were found to have a negligible effect, suggesting that more research can be done in this area to better understand the underlying correlates of *LAG3* expression (Whitehair et al., 2020). Finally, LAG3 plays an important role in $CD8^+$ T-cell exhaustion where single deletion or blockade of LAG3 together with single deletion or blockade of PD-1 was shown to synergistically enhance immune response to tumors or infection, and LAG3 deletion

alone was shown to enhance effector function (Grebinoski et al., 2022; Woo et al., 2012).

Galectin-3 (Gal-3/LGALS3), encoded by the *LGALS3* gene is a glycoprotein that can bind the TCR and suppress T-cell activation through TCR signaling pathways as well as enact TCR downregulation (H.-Y. Chen et al., 2009; Grigorian & Demetriou, 2010). *LGALS3* can be both expressed on the cell surface (Farhad et al., 2018) and secreted (Krześlak & Lipińska, 2004, p. 3). *LGALS3* has been previously linked to poor prognosis in OVCA (Luk et al., 2020) with the assertion that it may be activating the Wnt/β-Catenin pathway to effect cancer stemness mechanisms (Y. Liu et al., 2018). Additionally, overexpression of Galectin-1 (*LGALS1*), a protein similar to *LGALS3*, can promote EMT in fibroblasts through TGF-β signalling pathways (T. Wu et al., 2018, p. 3). LGALS3 has also been linked to the EMT previously where EMT in retinal pigment epithelial (RPE) cells enhanced the binding affinity of Gal-3 to its targets (Priglinger et al., 2016), and thus Gal-3 downregulation by recombinant antibodies has been suggested for future therapy. In both endometrial carcinoma (Friedman et al., 2020) and vulvar squamous carcinoma (Cocks & Mills, 2022) immune checkpoint therapy targeting LGALS3 as well as LAG3 has been suggested, as their co-expression correlated with worse prognosis. Overall, new and emerging evidence for the roles of LGALS3 and LAG3 in carcinoma demonstrates the potential for targeted therapy. However, the link between LGALS3, LAG3, and the EMT has yet to be fully elucidated despite all three elements being linked together under different contexts.

1.9 Project Rationale, Hypotheses and Objectives

The transcriptomic composition of various cellular populations within the ovarian cancer TME has yet to be fully characterized. Ovarian cancer TMEs are complex systems rife with different cell types, cells in varying states, networks of communication, and presence of regulatory molecules that dictate progression and outcomes in concert. The EMT has been previously implicated (Dongre & Weinberg, 2019) in dissemination of metastatic disease in OVCA and has multitudes of auxiliary roles such as cancer therapy resistance and acquisition of stemness. Modulation of the EMT and its downstream effects, and reduction of mesenchymal phenotypes could be a viable strategy for antitumoral therapy in OVCA. It is evident from the literature that the EMT plays a major role in other female cancers such as breast cancer. In a preliminary finding (**Figure 2**), many immune-related signaling factors were upregulated in correlation with the EMT in an *in vitro* model of OVCA.

To better understand the consequences of the EMT in OVCA, we first characterized EMT behavior in the OVCA TME using orthotopic syngeneic murine tumor models and *in vitro* models of EMT by single-cell RNA-sequencing (scRNA-seq). **We hypothesized that there is a strong presence of cancer cells with a mesenchymal phenotype,** and that the murine cancer cell lines ID8 and STOSE experience similar transcriptional changes when undergoing EMT *in vitro*.

We then determined how mesenchymal cancer cells interact with the immune cells in the TME. This was done by assessing the effects of EMT and EMT-related secretions by human HGSOC cell lines on NK cells *in vitro* and characterizing the interactome of cancer cells undergoing EMT and immune cells *in silico* by scRNA-Seq.

In this case, **we hypothesized that mesenchymal cancer cells are more immunosuppressive than epithelial cells in HGSOC.**

EMT has been previously linked to modulation of antigen presentation by cancer cells (Mullins et al., 2022). **We hypothesized that EMT modulates expression of classical and non-classical class I HLA antigen machinery in human HGSOC**. To test this, we characterized links between the expression of various HLA I allotypes and cancer cells undergoing EMT in HGSOC and other types of cancers. Additionally, we assessed links between EMT and HLA I allotypes *in silico* by scRNA-seq of cancer cell lines from various cancers undergoing EMT.

Objectives:

1. To characterize the TME in mouse models of OVCA and the phenotypic behavior of cancer cells in the context of the EMT.
2. To determine the possible effects of the EMT on immunosuppression of cytotoxic immune cells in the TME of HGSOC.
3. To determine the transcriptional expression of class I HLA allotypes in the context of the EMT.

Chapter 2: Materials and Methods

2.1 Cell culture and cell lines

Unmodified (parental, WT) ID8 mouse ovarian cancer cells were provided by Kathy Roby (Roby et al., 2000) and maintained in Dulbecco's Modified Eagle Medium (DMEM, Corning) + 4% fetal bovine serum (FBS, Hyclone) and 0.01 mg/mL insulin-transferrin-sodium-selenite solution (ITSS; Roche) as previously described (J. Walton et al., 2016; J. B. Walton et al., 2017). STOSE ovarian cancer cells were generated in our lab and maintained in α-MEM (minimal essential media) + 4% FBS and ITSS and 2μg/ml epithelial growth factor (EGF, R&D) as previously reported (McCloskey et al., 2014). NK92 cells were maintained in complete leukocyte media (RPMI (HyClone) + 4% FBS (Seradigm) + 1% penicillin/streptomycin (Gibco), 10mM HEPES (Sigma), 55 μM 2-mercaptoethanol (Gibco)) and were provided by Dr. Rebecca Auer (Ottawa Hospital Research Institute, OHRI). K562 and K562-NL cells were maintained in complete media (RPMI + 4% FBS) and were also provided by Dr. Rebecca Auer. The human ovarian cancer cell line OVCA420 was kindly provided by Dr. Gordon Mills. Cells were cultured in Dulbecco's Modified Eagle Medium (DMEM) with 4.5g/L glucose, L-glutamine, and sodium pyruvate (Corning, 10-013-CV), supplemented with 10% FBS and cultured at 37°C with 5% CO_2. Mycoplasma testing was performed prior to animal experiments. Cells were incubated at 37°C with 5% carbon dioxide.

2.2 Induction of EMT in human ovarian cancer cells

OVCA420 cells (10,000/well) were plated into 6-well plates and treated with 10ng/mL TGF-β1 (R&D Systems, #240-B-010), with treatment timed in such a way that all time-

points were synchronized at the time of collection. Cells were passaged as needed to avoid confluence, and fresh TGF-β1 was added every two days with refreshed media. Cells were not passaged in the 2 days prior to final collection to avoid artifacts during sequencing.

2.2.1 OVCA420 EMT time course sample processing, sequencing, and alignment

Single-cell suspensions were processed using the 10x Genomics Single Cell 3' RNA-seq kit v3. Final libraries were sequenced on an Illumina HiSeq 4000 after gene expression libraries were prepared according to the manufacturer's protocol. Raw sequencing reads were processed using CellRanger v2.0.1 using the GRCh38 build of the human genome and default parameters. Raw sequencing files and processed UMI count matrices have been deposited in the NCBI Gene Expression Omnibus under the accession GSE247098.

2.2.2 OVCA420 EMT time course data quality control and post-processing

Quality control was first performed independently on each 10x Genomic library, and all main processing steps were performed with Seurat V3 (Stuart et al., 2019) for the OVCA420 cells' dataset. Expression matrices for the OVCA420 cells were imported into R as Seurat objects. Only cells with more than 200 genes detected were retained and cells with a high percentage of mitochondrial gene expression were also removed. In the OVCA420 treatment time course, an independent Seurat object was made combining all time points, followed by a standard workflow by first removing genes detected in fewer than 1% of the cells for each time point. The top 2000 most variable

genes were selected using the ‘vst’ selection method in Seurat, scaled RNA expression values and regressed out mitochondrial reads, total UMI count, and cell cycle scoring. Cell cycle regression was handled by ‘SCTransform’ (Choudhary & Satija, 2022; Hafemeister & Satija, 2019), which was also used to normalize the RNA matrices for each sample using regularized negative binomial regression. After this, PCA was run on the variable genes and all UMAP embeddings were calculated from the first 30 principal components.

2.3 Multiplexed mouse cell line EMT time course experiment

ID8 and STOSE cells (10,000/well) were plated into 6-well plates. Cells were treated with 10ng/mL TGF-β1 (R&D Systems, #240-B-010), with treatment timed in such a way that all time-points were synchronized at the time of collection with 5 time points (untreated, 8 hours, 1 day, 3 days, and 7 days). Cells were passaged as needed to avoid confluence, and fresh TGF-β1 was added every two days with refreshed media. Cells were not passaged in the 2 days prior to final collection to avoid artifacts during sequencing. Reagents for multiplexing were kindly provided by Dr. Zev Gartner, and multiplexing was performed according to the MULTI-seq protocol (McGinnis et al., 2019). First, culture media was removed and cells from each well were washed with 1x PBS (Corning, #21-031-CV). Next, a lipid-modified DNA oligonucleotide (LMO) and a unique sample barcode oligonucleotide were added at 200nM to 0.05% trypsin with 0.53mM EDTA. Each sample received a different barcode, with each time point in each cell line receiving a unique barcode on the day of collection. Cells were incubated with this trypsin mixture for 5 minutes at 37^{o}C and gently mixed periodically for 5 minutes.

Then, a common lipid-modified co-anchor was added to each well at 200nM and cells were incubated for an additional 5 minutes at 37^{o}C with periodic gentle mixing. All cells were then lifted from the plate, trypsin was neutralized with cultured media, and the cells were triturated by pipetting to ensure a single cell suspension. Samples were then transferred to V-bottom 96-well plates and pelleted at 400xg for 5 minutes. Barcode-containing media was removed, and the cells were then washed with PBS + 1% bovine serum albumin (BSA). After two PBS washes, cells were resuspended in PBS + 1% BSA, pooled together, re-pelleted, and resuspended in PBS + 1% BSA. Viability and cell counts were then determined before preparation of the scRNA-seq libraries.

2.3.1 Mouse cell line time course sample processing, sequencing, and alignment

Single-cell suspensions were processed using the 10x Genomics Single Cell 3' RNA-seq kit v3. Gene expression libraries were prepared according to the manufacturer's protocol. MULTI-seq barcode libraries were retrieved from the samples and libraries were prepared independently according to the MULTI-seq library preparation protocol (McGinnis et al., 2019). Final libraries were sequenced on a NextSeq500 (Illumina). Expression libraries were sequenced so that time course libraries reached an approximate depth of 20,000-25,000 reads per cell.

2.3.2 Processing of raw sequencing reads

Raw sequencing reads from the gene expression libraries were processed using CellRanger and v3.0.2 for the kinase inhibitor data (G. X. Y. Zheng et al., 2017). The mm9 build of the murine genome was used for alignment. Default parameters were

used for all samples. MULTI-seq barcode libraries were simply trimmed to 28bp using Trimmomatic (Bolger et al., 2014) (v0.39) prior to demultiplexing.

2.3.3 Demultiplexing expression data with MULTI-seq barcode libraries

Demultiplexing was performed using the 'deMULTIplex' R package (v1.0.2). The key concepts for demultiplexing are described in McGinnis *et al.* (2019). Briefly, the tool takes the barcode sequencing reads and counts the number of times each of the 96 barcodes appears for each cell. Then, for each barcode, it assesses the distribution of counts in cells and determines an optimal quantile threshold to deem a cell positive for a given barcode. Cells positive for more than one barcode are classified as doublets and are removed. Only cells positive for a single barcode are retained for downstream analysis. As each barcode corresponds to a specific sample in the experiment, the sample annotations were then added to all cells in the dataset.

2.3.4 Mouse cell line time course data quality control and processing

For the mouse time course experiments, the quality control pipeline was identical to human time course experiment data quality control and processing except all main processing steps were performed with Seurat v4 (Hao et al., 2021).

2.4 Visualization and graphics

All visualizations of scRNA-Seq data were drawn using either graphing functions within Seurat, the 'ggplot2' package, or the 'SCPubr' package.

2.5 Pseudotemporal ordering of cells

R package ‘psupertime’ (Macnair et al., 2022) v0.2.6 (https://github.com/wmacnair/psupertime) was used to calculate pseudotime scores on the top 3000 most variable genes for the OVCA420, ID8, and STOSE Seurat objects. Psupertime requires scRNA-seq data with ordinal labels to build a linear combination of genes that vary consistently over the time course and are used to assign a pseudotemporal value to individual cells. Individual cells with pseudotemporal values were correlated with other genes or modules (eg. EMT signature scores).

2.6 EMT scoring strategy

EMT scores on the OVCA420 dataset were calculated using the ‘AddModuleScore()’ Seurat function together with a previously published cancer-specific EMT signature from our lab (Cook & Vanderhyden, 2022), to assign an EMT score to each cancer cell. This EMT signature reflects the most consistent expression pattern associated with epithelial-mesenchymal plasticity in cancer(Cook & Vanderhyden, 2022). We then calculated the mean of each individual samples’ EMT scores and labeled every cell that fell under a threshold of ‘mean–1 standard deviation’ an epithelial cell and every cell above a threshold of ‘mean+1 standard deviation’ a mesenchymal cell, with all cells in-between labeled as partial-EMT (pEMT). A similar strategy was employed for the ID8 and STOSE time course experiments but genes within the cancer-specific EMT signature were converted into their murine orthologs.

2.7 Differential gene expression analysis

The Wilcoxon rank sum test implemented in the 'FindMarkers()' or 'FindAllMarkers()' functions of Seurat were used to calculate all differentially expressed genes between the input populations. For volcano plots and analysis of most differentially expressed genes a cutoff of p-adjusted < 0.05 and for log2 fold-change (log2fc) the mean of the log2fc ± 2*standard deviation of log2fc was used.

2.8 Gene set enrichment analysis

Gene set enrichment analysis (GSEA) was performed using the 'fgsea' R package (Korotkevich et al., 2021). Input genes were ranked by their log2 fold-change values. Reference gene sets were collected from the Molecular Signatures Database (MSigDB) v6.2.

2.9 Cell-cell communication analysis

For cell-cell communication analysis, we used LIANA (Dimitrov et al., 2022), a tool that integrates multiple methods for cell-cell communication inference in single-cell data. LIANA provides a consensus-based rank aggregate for receptor-ligand pairs from the results of multiple cell-cell communication algorithms through 'robust rank aggregation' (RRA). The default settings of LIANA for the analysis use various algorithms in ensemble: SCA, NATMI, Connectome, CellPhoneDB, and CytoTalk, used to evaluate receptor-ligand pairs. We ran LIANA using the function 'liana_wrap()' on our integrated object. The cancer cell population was divided into unique identities based on EMT score, resulting in 3 identities: epithelial cancer cells (EPI), partial EMT cancer cells (FLUX), mesenchymal cancer cells (MES). We then aggregated all the methods into a

single matrix using ‘liana_aggregate()’ to construct maps of cell-cell communications with ‘Circlize’(Z. Gu et al., 2014) based on the top ‘aggregate_rank’ of receptor-ligand pairs.

2.10 Quantitative RT-PCR (qPCR)

RNA was extracted using the RNeasy Mini Kit (Qiagen) and cDNA was synthesized using the OneStep RT-PCR Kit (Qiagen). The ABI 7500 FAST RT-qPCR machine (Applied Biosystems) was used for qPCR using the ssoFast gene expression (Bio-rad) assays for 45 cycles with the ‘SYBR Green’ setting. *Ppia*, *Gapdh*, and *Actin-β* were used as endogenous controls for the assays. Primers for target genes are listed in Table 1. Cycle threshold (Ct) values were taken from the output of the Applied Biosystems 7500 FAST v2.3 software. To calculate relative expression values, the geometric mean of the endogenous genes was first calculated using the GEOMEAN function in Excel on the Ct values of those genes. Then, delta Ct (dCt) values were calculated by subtracting the Ct values of the target genes from the geometric mean of endogenous controls and delta dCt (ddCt) were calculated by subtracting the dCt of treatment groups from their respective control groups. Finally, 2-fold change values were calculated by taking 2 to the power of negative ddCt values.

Table 1: Sequences of gene targets used for qPCR analysis

Target	Forward sequence	Reverse sequence
Ppia	AGGGTGGTGACTTTACACGC	GATGCCAGGACCTGTATGCT
Gapdh	CTCAGGAGAGTGTTTCCTCGT	ATGAAGGGGTCGTTGATGGC

Actin-β	CCTTCCTTCTTGGGTATGGA	ACGGATGTCAACGTCACACT
Cdh1	GGTTTTCTACAGCATCACCG	GCTTCCCCATTTGATGACAC
Cdh2	CCTCCATGTGCCGGATAG	CACCAGAAGCCTCCACAGAC
Vimentin	CGGAAAGTGGAATCCTTGCAGG	AGCAGTGAGGTCAGGCTTGGAA
Snai1	GTCTGCACGACCTGTGGAA	CAGGAGAATGGCTTCTCACC
Snai2	TGCAAGATCTGTGGCAAGG	CAGTGAGGGCAAGAGAAAGG
Sox4	GACAGCGACAAGATTCCGTTC	GTTGCCCGACTTCACCTTC
Il-18	GACTCTTGCGTCAACTTCAAGG	CAGGCTGTCTTTTGTCAACGA
Il-18R	TCACCGATCACAAATTCATGTGG	TGGTGGCTGTTTCATTCCTGT
Col1a1	GCTCCTCTTAGGGGCCACT	CCACGTCTCACCATTGGGG
Col1a2	CTTCGTGCCTAGCAACATGC	TGAGCAGCAAAGTTCCCAGT
Cnn1	TGCGCTTGTCTGTGTCATCT	TCTGGGCCAGCTTGTTCTTT
Actg2	CGTACCACAGGCATCGTTCT	CAAGACGCATGATGGCATGG
Krt19	AAAACACTGAACCCTGATTCTTG	TCTGAAGTCATCTGCAGCCA

2.11 Flow cytometry-based cytotoxicity assays

K562 were harvested and spun down at 500xg for 5 minutes and resuspended in PBS at 2e6 cells/mL, with a few cells reserved in a separate 15 mL Falcon tube as unstained control. CP450 (65-0842-85, ThermoFisher) dye was added to the volume of K562 cells at a 1:500 ratio and the cells were incubated with the dye for 15 minutes in a CO_2 incubator at 37^{o}C with the tube flicked every 5 minutes to maintain equal mixing. Labeling was halted by adding growth media to the top of the tube and the cells were spun down and washed with PBS three times, when the cells were then resuspended at

1e6 cells/mL. 0.5e6 stained CP450-K562 cells are placed in a new 15 mL Falcon tube with growth media added to a final volume of 10 mL. In tandem, NK92 cells were harvested and spun at 500xg for 5 minutes before being resuspended in leukocyte media at 1e6 cell/mL. 100 µL of NK92 cells are then played in triplicate in a 96-well V-bottom plate (Sarstedt) and serially diluted 4 times in 100 µL of leukocyte media with the addition of 100 µL of CP450-K562 cells to match ratios of 10:1, 5:1, 2.5:1 and 1.25:1 of effector (NK92) to target (CP450-K562) cells. The co-cultured cells were then incubated for 4 hours in a CO_2 incubator at 37°C. At the end of the assay the cells were collected into FACS tubes (Corning), 50 µL of a 5x solution of Ethidium Homodimer (E1169, ThemoFisher) was added to each well, and the cells were analyzed by flow cytometry with setting a gate around $CP450^+$ cells.

2.12 Luciferase-release cytotoxicity assays

NK92 effector cells were co-cultured with nano-Luciferase expressing K562 target cells (K562-NL) in 20:1, 10:1, 5:1, 2.5:1, 1.25:1, 0.625:1, 0.3125:1 effector-to-target ratios in 5% RPMI in V bottom plates for 5 hours at 37°C, with 1e5 target cells seeded in triplicate per ratio. After incubation, 50µL supernatant from each well was transferred to non-translucent white round-bottom plates (Corning), with 25µL of CTZ substrate added manually to each well. Coelenterazine (CTZ) stock is made by reconstituting 500 µg of CTZ substrate (Gold Biotechnology, CZ2.5) in 610µL of 100% ethanol and 6.2µL of 12N HCl. For quantifying luciferase as a working dilution, CTZ is mixed with 1X salt buffer (45 mM EDTA, 30 mM sodium pyrophosphate, 1.425 M NaCl) at a 1:200 dilution.

Luminescence was measured using the BioTek Cytation 5 cell imaging multimode reader. Percentage of specific lysis was calculated using the following equation:

$$\%\ Specific\ lysis = \frac{(experimental\ release - spontaneous\ release)}{(maximal\ release - sponteneous\ release)}\ x\ 100$$

Where experimental release refers to raw luminescence values from NK92:K562-NL experimental wells, spontaneous release are luminescence values from K562-NL cells in the absence of any effector cell or induced cell death, and maximal release are luminescence values from K562-NL cells induced to die using 30 µg/mL digitonin (Sigma-Aldrich).

2.13 LEGENDplex™ Bead-Based Immunoassay

Supernatant was acquired from OVCA420 cells after they had been treated with 10ng/mL TGF-β1 (R&D Systems, #240-B-010) every 2 days for 7 days alongside untreated controls. Samples were diluted 1:2 in assay buffer and assayed according to the manufacturer's protocol for the LEGENDplex™ Human Cytokine Panel 2 (13-plex), Human Proinflammatory Chemokine Panel (13-plex), Human Inflammation Panel 1 (13-plex) (BioLegend). Samples were run in duplicate the same day of staining, on a BD LSR Fortessa™ flow cytometer and analyzed using LEGENDplex Quognit software (Biolegend).

2.14 Lentivirus production for *Snai1* and *Snai2* overexpression

Lentivirus production was done according to Lipofectamine3000 manufacturer protocol (Invitrogen) using the reverse transfection protocol. Briefly, 293T maintained in DMEM high glucose + 10% fetal calf serum (FCS) were split and grown in OptiMem + 5% FCS + 0.2 mM sodium pyruvate prior to transfection of plasmid. Using three plasmids, the cells were transfected: 1.3 µg of vector, 1 µg of packaging (pCMV-dR8.74), and 0.7 µg of the envelope plasmid (pCAG-ECO). The vector plasmids were: pEF1-tet (rtTA transactivator), pLVX-imSNAIL-PGK-Hyg (murine *Snai1* overexpression), pLVX-imSLUG-PGK-Hyg (murine *Snai2* overexpression), pLVX-iGFP-PGK-Hyg (inducible GFP), pLVX-PGK-Hyg (empty vector). After addition of vectors, media was changed 6 hours post-transfection. In the first morning post-transfection, media was carefully collected into 50 mL falcon tubes and labeled as the first batch of virus-containing supernatant, with the second and final batch harvested that afternoon. Supernatant was filtered through a 0.45µM syringe filter and was mixed well with virus precipitation solution (Benchmark BioSciences) due to its high viscosity in 15mL conical tubes and left at 4^{o}C overnight on a rocker. After this, the 15 mL conical tubes were spun at 1500xg for 30 minutes until a pellet was visible at the bottom of tubes. Supernatant was aspirated and the tubes were re-spun at 1500xg for 10 minutes and after aspirating remaining supernatant 500µL of virus resuspension buffer (Benchmark BioSciences) was added to create concentrated viral media.

2.15 Infection of target cells

ID8 parental cells were transduced with lentivirus (with 10µg/mL polybrene) carrying pEF1-tet to create a stable ID8-tet cell line with a tetracycline transactivator. Briefly, 1mL

of target cells were resuspended in media with 10μg/mL to each well of a 6-well plate. 100μL of virus was added to each well with the plate placed in an incubator at 37^{o}C, with an additional 1mL of media added after 6 hours. The cells were incubated with the concentrated virus for 3 days before selection was commenced with 1mg/mL Geneticin/G418 (Gibco) per 10,000 ID8-tet cells, given that the pEF1-tet construct contains a G418 resistance cassette. Once ID8-tet cells were selected for, they were further infected either with pLVX-imSNAIL-PGK-Hyg, pLVX-imSLUG-PGK-Hyg, pLVX-iGFP-PGK-Hyg, or pLVX-PGK-Hyg. Cells infected with these constructs were selected for with 10 μg/mL hygromycin (H3274, Sigma).

2.16 IL-18 ELISA

ID8 and STOSE cell lines were plated at 10,000 cells/well in triplicate in a 6-well plate (Corning) and treated with 10ng/mL TGF-β1 every 2 days for a period of 7 days and split as necessary once reaching 75% confluency. Frozen stocks of ID8 and STOSE tumor ascites preserved from a previous study (Rodriguez et al., 2022) were thawed from -80^{o}C at room temperature. IL-18 ELISA was done according to manufacturer's protocol (ab216165, AbCam).

2.17 Snail western blot analysis

Protein was extracted from ID8-WT, ID8-Tet-Empty, ID8-Tet-iGFP, ID8-Tet-imSnail cells (generated as described in section 2.14) using M-PER Mammalian Protein Extraction Reagent (GE Healthcare). Protein extracts were run on a precast Nupage 4-12% Bis-Tris gradient gel (Life Technologies) and transferred to a polyvinylidene fluoride

membrane. Following 1 hour blocking in 5% non-fat milk, membranes were incubated with mouse monoclonal Snail (1:1000, Novus) overnight at 4^{o}C. Following 3x washing with TBS-T, the membrane was incubated with rabbit anti-mouse IgG-HRP (1:5000, Abcam) for 1 hour and developed using SelectTM Western Blotting Detection Reagent (GE Healthcare). The same protocol was used for β-ACTIN using mouse monoclonal anti β-ACTIN (1:10000, Sigma Aldrich).

2.18 Microscopy

Widefield imaging was done at 10X magnification for experiment comparing size and morphology of ID8-Tet-iSnail and ID8-Tet-iiSlug cells to ID8-WT and ID8-Tet-Empty cells following TGF-β1 treatment using EVOS XL Core microscope with auto-adjusted exposure setting. Fluorescence microscopy for ID8-Tet-iGFP cells imaged at 10X magnification on EVOS M5000.

2.19 Proliferation assay

Transgenic ID8 cells overexpressing *Snai1* ($5x10^4$/well) were seeded into clear 24-well tissue culture plates (Corning) or *Snai2* (1000/well) into 96-well Incucyte® Imagelock tissue culture plates (Sartorius BioScience). Proliferation was assessed by counting viable cells via the IncuCyteS3 analyzer (Sartorius BioScience). Experiments were done in technical triplicate across 3 samples at different days.The results are reported as the mean of the total number of cells per well across three technical replicates every 2 hours until the wells have reached confluence.

2.20 Mouse *in vivo* studies

Animal experiments were carried out using protocols approved by the Animal Care Committee at the University of Ottawa and conforming to the standards defined by the Canadian Council on Animal Care. C57BL/6 mice (for ID8 and derivatives) were purchased from The Jackson Laboratory.

For mouse surgeries involving injection of *Snai1* overexpressing ID8 cells, in an i.b model of ovarian cancer, 1.5 x10^5 cells (ID8-WT, ID8-Tet-Empty, ID8-Tet-iSnail) were injected under the ovarian bursa as described previously. Mice were assessed for survival until humane endpoint, primarily by observing abdominal distension for mice with ovarian tumors. In the murine cohort injected i.b., mice were assessed for survival until humane endpoint to establish an endpoint.

For experiments involving immunodeficient mice, severe combined immunodeficient (SCID) were obtained from The Jackson Laboratory. 1.5 x10^5 STOSE cells were injected i.b as previously described. Animals were monitored for disease progression and euthanized by observing abdominal distension with ascites and tumors collected at that point. Tumors and ascites were snap frozen for RNA or protein analysis.

2.21 Human cancer scRNA-seq dataset

Sixteen high-grade serous ovarian cancer datasets (Hornburg et al., 2021) were obtained with permission from European Genome-Phenom Archive (EGAD00001006974). For the kinase inhibitor-treated time-course experiment, raw

sequencing files and processed UMI count matrices were obtained from the NCBI Gene Expression Omnibus under the accession GSE147405.

Several datasets from droplet-based scRNA-seq studies were collected for this study. In cases where the datasets contained non-tumor data, that data was removed and tumor-only raw UMI count matrices and cell metadata were retained from the sources listed in Table 2.

Table 2: Datasets used for analysis of EMT and MHC machinery gene expression

Cancer origin	Source	Accession
Breast	(S. Z. Wu et al., 2020)	ENA PRJEB35405
Breast	(Qian et al., 2020)	blueprint.lambrechtslab.org
Colorectal	(H.-O. Lee et al., 2020)	GSE144735, GSE132465
Colorectal	(Uhlitz et al., 2021)	GSE166555
Colorectal	(Qian et al., 2020)	blueprint.lambrechtslab.org
Gastric	(Sathe et al., 2020)	dna-discovery.stanford.edu
Lung	(N. Kim et al., 2020)	GSE131907
Lung	(Lambrechts et al., 2018)	E- MTAB-6149, E-MTAB-6653
Lung	(Qian et al., 2020)	blueprint.lambrechtslab.org
Lung	(Laughney et al., 2020)	GSE123904
Ovarian	(Geistlinger et al., 2020)	GSE154600
Ovarian	(Qian et al., 2020)	blueprint.lambrechtslab.org
Pancreatic	(Steele et al., 2020)	GSE155698
Squamous cell	(Ji et al., 2020)	GSE144236

2.22 Human ovarian cancer dataset quality control and processing

Quality control was first performed independently on each 10x Genomics library, and all main processing steps were performed with Seurat v4 (Hao et al., 2021) for the ovarian cancer datasets (Hornburg et al., 2021). Only cells with more than 200 genes detected were retained and cells with a high percentage of mitochondrial gene expression were also removed. Each individual tumor sample matrix was obtained as tables divided into stroma, $CD45^+$, and tumor cell files that we first made into Seurat objects with a minimum of 200 genes per cell and then merged using the 'base::merge()' function prior to processing, yielding 16 individual samples (i.e. 16 tumors). Each sample was processed independently similarly to the OVCA420 cells. Briefly, cells with high percentage mitochondrial genes and low feature number were subset out and cell cycle genes were regressed out for each sample using 'SCTransform' (Choudhary & Satija, 2022; Hafemeister & Satija, 2019). 'SCTransform' was also used to normalize the RNA matrices for each sample using regularized negative binomial regression. PCA was then applied to each individual sample and UMAP embeddings were calculated from the first 30 principal components. We also added metadata such as immune phenotype and patient-ID in each samples' Seurat metadata slot.

2.23 Semi-supervised cell labeling and integration

Cell type labeling was first performed using common markers for cancer cells (*KRT19*, *AMHR2*, *ELF3*, *EPCAM*) and fibroblasts (*COL1A1*, *COL1A2*). We also labeled endothelial cells (*CDH5*, *CLDN5*) and smooth muscle cells (*ACTA2*) to find very small populations (<100 cells) for each, so we removed these populations. To label the $CD45^+$

population we applied Seurat's multimodal reference mapping method (Hao et al., 2021) to each individual sample with their published CITE-Seq reference object of 162,000 PBMCs measured with 228 antibodies. We used all default settings provided by Seurat for this part of the processing pipeline. After mapping the cell populations by the reference object, we merged this with our labels for cancer cells and fibroblasts to finalize the individual sample objects with labels for all clusters.

Seurat's integration (Stuart et al., 2019) was used to align and combine shared populations across the 16 tumors. Briefly, Seurat matches pairs of cells across datasets that share certain biological states, or anchors, based on bulk RNA expression. The corrected data was then scaled and UMAP embeddings were applied to it based on 30 principal components from a PCA run.

2.24 Kaplan-Meier plots

A Kaplan-Meier plot was generated using the Protein Atlas (Uhlen et al., 2017). The plot was obtained by searching for *QSOX1* gene expression and choosing it in the 'Pathology' category. *QSOX1* expression was filtered to include only ovarian cancers with the cut-off for survival analysis automatically chosen by the website software (31.26).

Additional Kaplan-Meier survival plots were generated using https://kmplot.com/ (Lánczky & Győrffy, 2021) with data accessed from bulk RNA-Seq TCGA and microarray datasets. For *LAG3* and *LGALS3*, overall survival of optimally debulked patients with high-grade (3+4), later stage (2+3+4) tumors with *TP53* mutation, were plotted. We chose these settings because they match well with the patient data from

Hornburg et al. (2021) and represent a subset of HGSOC samples from patients with poor expected outcomes.

2.25 Non-negative matrix factorization

Non-negative matrix factorization (NMF) was performed using the 'RcppML' R package (DeBruine et al., 2021). Briefly, 'RcppML' leverages NMF as a machine learning strategy to learn coordinated gene activity in sparse data and present summaries of biological processes as broken into individual vectors of weighted values that contribute to the overall dimensionality in the data.

Chapter 3: Characterization of EMT in human and murine models of ovarian cancer

The results presented in this chapter are the work of the Ph.D. candidate. Some of these results have been **published** in Cancer Research Communications 1 June 2022; 2 (6): 417– 433. https://doi.org/10.1158/2767-9764.CRC-22-0017.

The tumour immune profile of murine ovarian cancer models: An essential tool for ovarian cancer immunotherapy research

Galaxia M. Rodriguez[1,2,†], Kristianne J.C. Galpin[1,2,†], David P. Cook[1,2], **Edward Yakubovich**[1,2], Vincent Maranda[1,2], Elizabeth A. Macdonald[1,2], Juliette Wilson-Sanchez[1,2], Anjali L. Thomas[1,2], Joanna E. Burdette[3], Barbara C. Vanderhyden[1,2,*]

[1]Cancer Therapeutic Program, Ottawa Hospital Research Institute, 501 Smyth Road, Ottawa, Ontario Canada, K1H 8L6.

[2]Department of Cellular and Molecular Medicine, University of Ottawa, 451 Smyth Road, Ottawa, Ontario, Canada, K1H 8M5.

[3]Department of Pharmaceutical Sciences, College of Pharmacy, University of Illinois at Chicago, 900 S. Ashland Ave, Chicago, IL 60607.

[†]These authors contributed equally to this work.

Based on preliminary data showing that certain cytokines, chemokines, and interleukins increase in expression during the EMT of an ovarian cancer cell line (Figure 2) and the previous literature reporting that mesenchymal cells possess certain immunoregulatory capabilities, we first aimed to use single-cell transcriptomics to characterize the EMT in both human ovarian cancers and murine models of ovarian cancer. Before we characterized the potential immunoregulatory capabilities of mesenchymal cancer cells, we confirmed the EMT in our models by assessing expression of known EMT marker genes and comparing them in our models to find which genes can be used to mark mesenchymal cells in cancers. By uncovering the transcriptomic changes that occur in ovarian cancer cells when undergoing EMT, these gene markers could be possibly used in the future to estimate the fraction of mesenchymal cells in bulk techniques such as RNA-seq and quantitative PCR (qPCR). A primary goal here was to characterize EMT in murine models of ovarian cancer as that work has never been attempted before. The characterization efforts included a focus on the immunosuppressive capabilities of mesenchymal cells because the relationship between cancer cells undergoing EMT and immune cells in the TME is yet to be explored in murine models and in human ovarian tumors through single-cell genomics.

3.1 Exploration of the OVCA420 transcriptome following EMT induction with TGFβ-1 reveals QSOX1 is strongly correlated with the EMT

To fully elucidate the changes EMT can induce in the transcriptome of human ovarian cancer cells, we used scRNA-seq to first assess changes in the OVCA420 cell line in response to TGFβ-1 at multiple time points (**Figure 3a**). We began by

constructing a pseudotime continuum for the cells (**Figure 3b**) and from that we derived a list of pseudotime-correlated genes that represent the EMT program for OVCA420 cells treated with TGFβ-1. *ZEB1* was the only canonical EMT gene in the list, suggesting that canonical genes are poor markers of EMT in OVCA420 cells. As another measure of confirming the EMT, we used a previously published list of EMT genes generated by our lab that are specific to cancer cells across many cancer types and contexts to calculate each cells' EMT score (**Figure 3c**), with higher scores indicating cells that are more mesenchymal (Cook & Vanderhyden, 2022). When we correlated pseudotime values with EMT score calculated with the cancer-specific EMT module, we found a positive correlation between the two (**Figure 3d**), suggesting that there is a partial concordance between the two methods used to calculate EMT scores, with the two potentially sharing common genes that may specific to the OVCA420 cells undergoing EMT. We checked whether any genes in the cancer-specific EMT module and genes derived from the pseudotime analysis intersect with another well-known set of EMT genes called the Hallmark EMT module (Liberzon et al., 2015) (**Figure 3e**). We found that one gene, *QSOX1*, was found in all three sets of genes. To confirm that *QSOX1* expression correlates with the EMT, we confirmed its expression in the OVCA420 cells (**Figure 3f**) and found it to be lowest in untreated cells and highest at 7 days after TGFβ-1 treatment. *QSOX1* expression has been previously linked to metastasis in many cancers (Fifield et al., 2020; Geng et al., 2020; Sung et al., 2018; X.-F. Zhang et al., 2019). Taken together, this initial exploration of the transcriptome of ovarian cancer cells undergoing EMT revealed a gene, *QSOX1*, that is highly conserved among different methods and gene lists used to calculate EMT scores on a

transcriptomic level *in silico*. In a potential future experiment to see if *QSOX1* marks mesenchymal cells *in vivo*, expression of the gene in tumor ascites can be compared to expression in the adnexa with the expectation that *QSOX1* will be higher in mesenchymal cell-rich ascites whether by qPCR, bulk RNA-seq, or scRNA-seq.

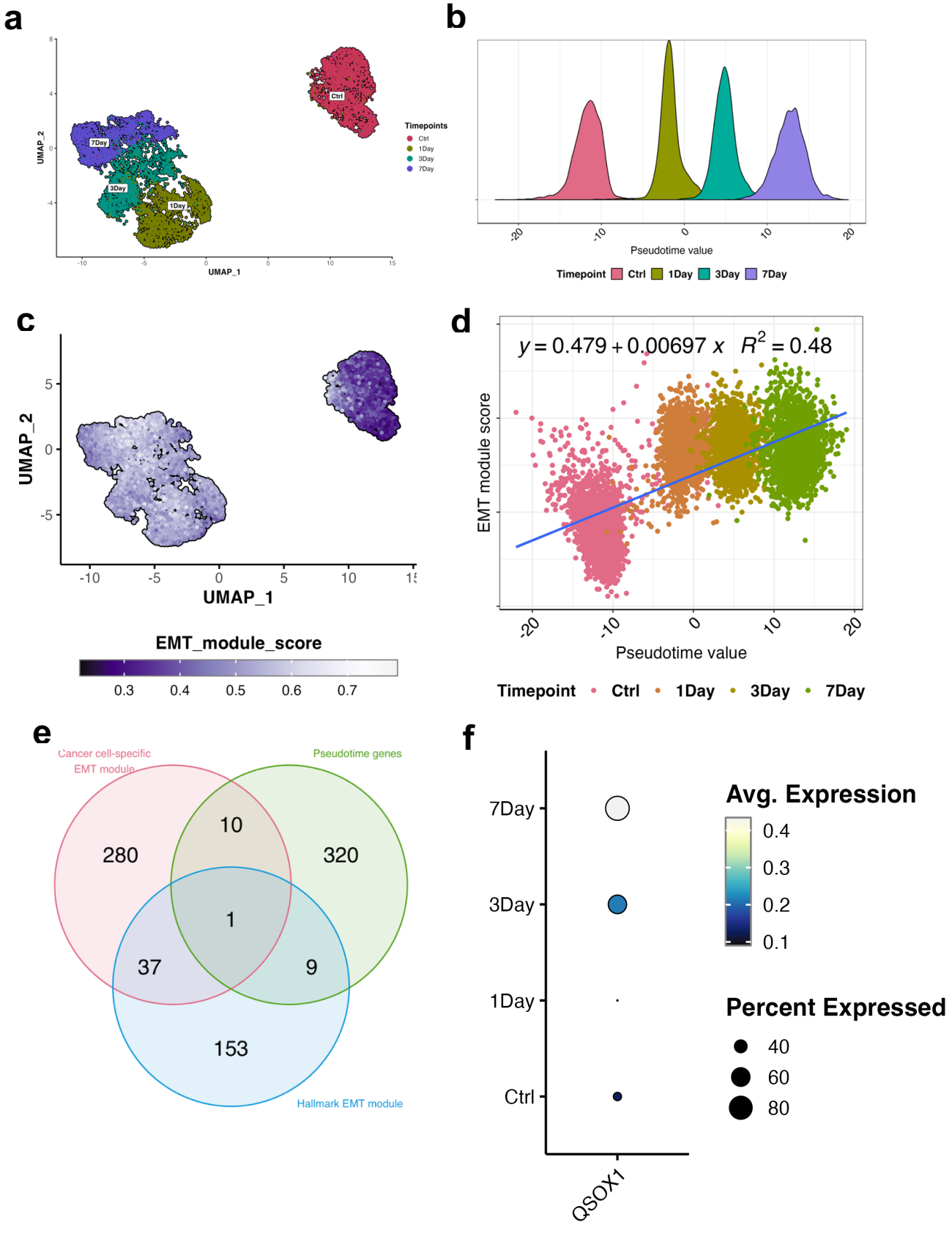
a
UMAP_2
UMAP_1
Ctrl
7Day
3Day
1Day
Timepoints
Ctrl
1Day
3Day
7Day
b
Pseudotime value
Timepoint Ctrl 1Day 3Day 7Day
c
UMAP_2
UMAP_1
EMT_module_score
0.3 0.4 0.5 0.6 0.7
d
$y = 0.479 + 0.00697\ x \quad R^2 = 0.48$
EMT module score
Pseudotime value
Timepoint Ctrl 1Day 3Day 7Day
e
Cancer cell-specific EMT module
Pseudotime genes
Hallmark EMT module
280
10
320
1
37
9
153
f
7Day
3Day
1Day
Ctrl
QSOX1
Avg. Expression
0.4
0.3
0.2
0.1
Percent Expressed
40
60
80

Figure 3. *In vitro* model of EMT correlates in pseudotime with cancer-specific EMT signature scores. (a) UMAP clustering of OVCA420 cells treated with TGF-β1 (10 ng/mL) at four different time points: Ctrl (no treatment), 1-day, 3-day, and 7-day. (b) Density ridge plot showing computed pseudotime scores for all cells, colored by time point. (c) UMAP enrichment plot showing a computed EMT score for each cell based on a set of cancer-specific EMT genes. (d) Positive correlation of computed pseudotime values against cancer-specific EMT scores for all cells (R^2 = 0.48). (e) Venn diagram showing overlap between three different gene sets of EMT: genes derived from the pseudotime calculation of TGFβ-1 treated OVCA420 cells (Pseudotime genes), cancer cell-specific EMT module, Hallmark (MSigDb) EMT module. (F) Average normalized expression of *QSOX1* across different time points in OVCA420 cells treated with TGF-β1.

3.2 QSOX1 and IL32 are highly correlated with EMT in different cell lines treated with different inducers of EMT

Four different cancer cell lines (OVCA420, MCF7, A549, DU145) from ovarian cancer, breast cancer, lung cancer, and prostate cancer were treated with three different EMT inducers for different lengths of time and sequenced via scRNA-seq. For all cell lines and inducers of EMT, *QSOX1* expression gradually increases with EMT and is highest at 7 days post-induction (**Figure 4a**), suggesting that *QSOX1* is a potentially near-universal gene marker for mesenchymal cells, at least *in vitro*. We looked at public RNA-seq data of ovarian cancer patients from the TCGA and compared *QSOX1* gene expression with survival to find that low expression of the gene is associated with longer survival, with the median expression cut-off determined by interquartile range methodology (* p = 0.031; **Figure 4b**), suggesting that having fewer mesenchymal cells in a tumor is associated with better outcomes, possibly due to less metastatic spread given that mesenchymal cells and metastasis in ovarian cancer are closely linked (Rafehi et al., 2016).

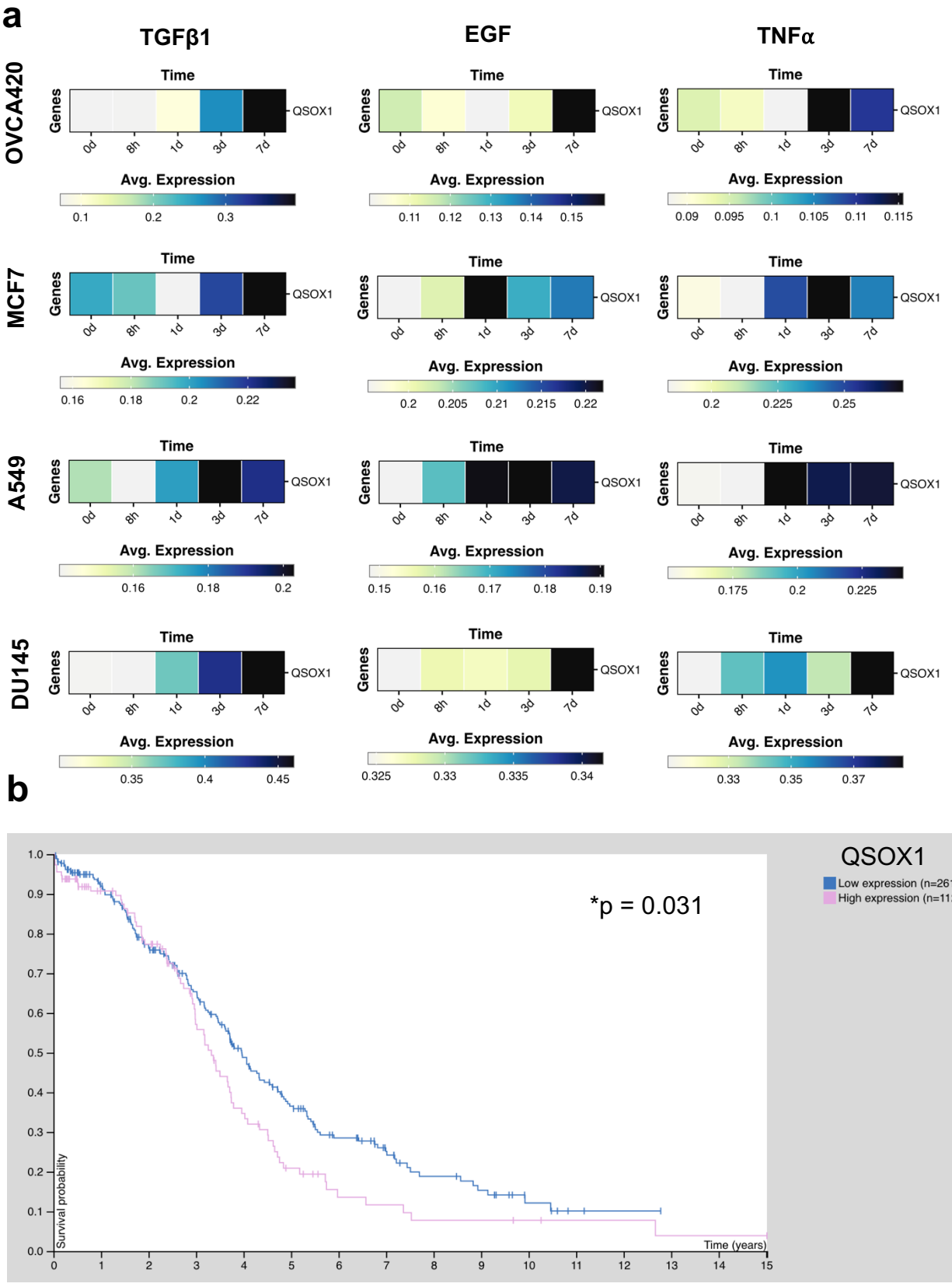
a
TGFβ1
EGF
TNFα
OVCA420
MCF7
A549
DU145
Time
Genes
QSOX1
0d
8h
1d
3d
7d
Avg. Expression
0.1 0.2 0.3
0.11 0.12 0.13 0.14 0.15
0.09 0.095 0.1 0.105 0.11 0.115
0.16 0.18 0.2 0.22
0.2 0.205 0.21 0.215 0.22
0.2 0.225 0.25
0.16 0.18 0.2
0.15 0.16 0.17 0.18 0.19
0.175 0.2 0.225
0.35 0.4 0.45
0.325 0.33 0.335 0.34
0.33 0.35 0.37
b
QSOX1
Low expression (n=261)
High expression (n=112)
*p = 0.031
Survival probability
Time (years)

Figure 4. *QSOX1* is a near-universal marker of EMT and mesenchymal cells in human cancer cells and negatively affects survival in ovarian cancer. (a) Expression heatmaps for *QSOX1* expression in four different cancer cell lines (OVCA420, MCF7, A549, DU145) treated with either TGF-β1 (10 ng/mL), EGF, or TNFα at five different time points: 0d (no treatment), 8 hours (8h), 1-day (1d), 3-day (3d), and 7-day (7d). (b) Kaplan-Meier survival curve for ovarian cancer patients based on bulk *QSOX1* expression from TCGA data of bulk RNA-seq datasets of ovarian tumors. Median expression separating low from high determined by interquartile range methodology.

A model-based analysis of single-cell transcriptomics (MAST) test between untreated OVCA420 cells and cells treated with TGF-β1 for 7 days revealed *IL32* to be one of the most differentially expressed genes in the latter group along with *TGM2*, *LAMC2*, *SERPINA1*, and *SERPINE1* (**Figure 5a**). *IL32* is expressed highest at 7 days after TGF-β1 treatment of OVCA420 ovarian cancer cells (**Figures 5b**), and correlates independently with the pseudotime calculation for that experiment (**Figure 5c**) suggesting *IL32* is a correlate of the EMT in ovarian cancer cells. To determine whether *IL32* expression correlates with EMT in cell lines derived from other cancers, we analyzed the scRNA-seq data from the OVCA420, MCF7, A549, and DU145 cells treated with recombinant TGFβ-1, EGF, or TNFα and noted that expression is highest after 7 days of treatment with TGFβ-1, highest after 1 day of treatment with TNFα, and with no clear trend with EGF (**Figure 5d**). Additionally, we explored expression of either *QSOX1* or *IL32* after removing TGFβ-1 treatment to induce mesenchymal-to-epithelial transition and noted that expression of both begins to decrease, suggesting both are direct correlates of the EMT (**Figure 5e**). Taken together, *IL32* is a strong correlate of the EMT but may be dependent on the type of EMT inducer used, where cell lines from different cancers respond similarly to TGFβ-1 and TNFα treatment.

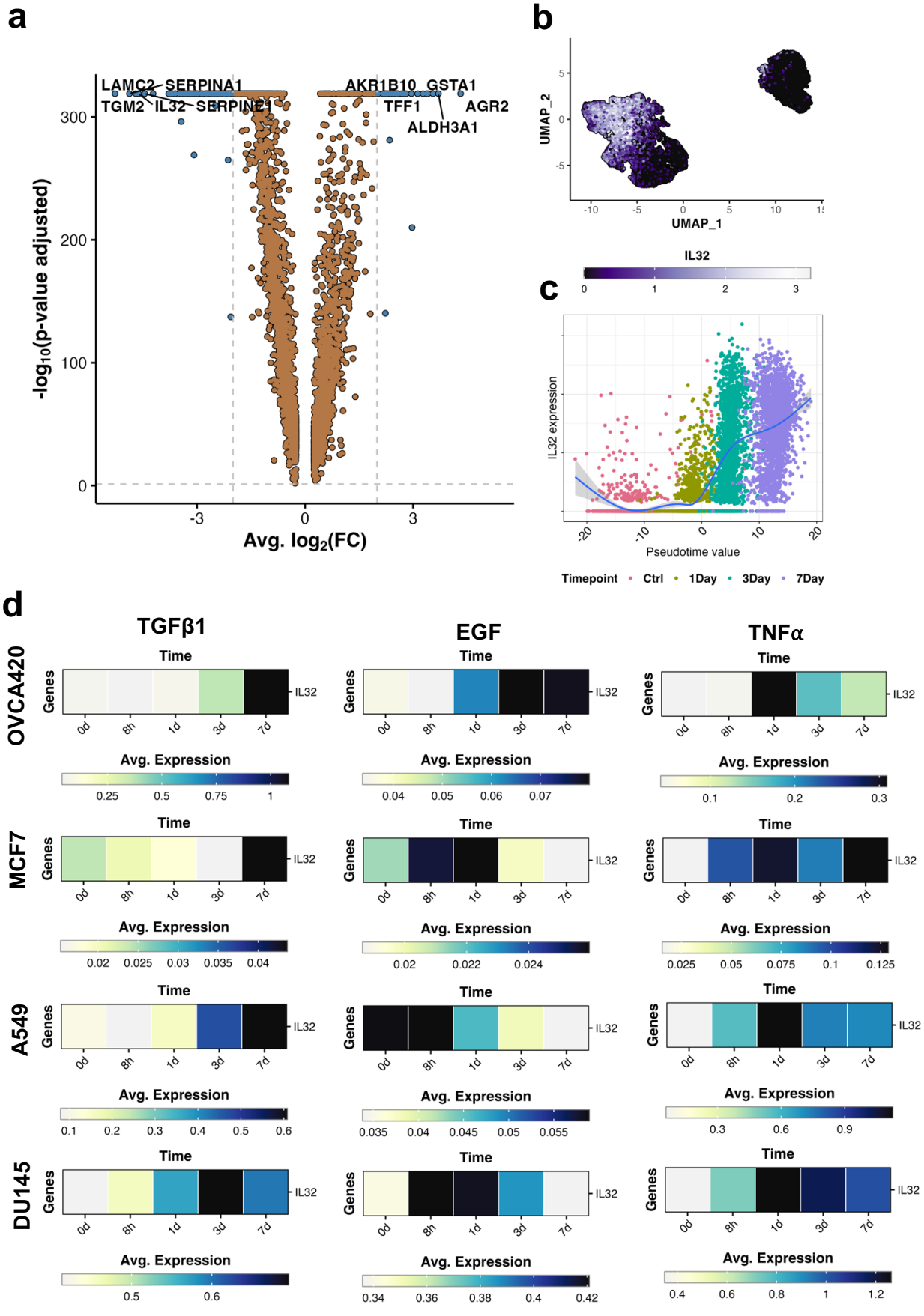
a
LAMC2
SERPINA1
TGM2
IL32
SERPINE1
AKR1B10
GSTA1
TFF1
AGR2
ALDH3A1
-log10(p-value adjusted)
Avg. log2(FC)
b
UMAP_2
UMAP_1
IL32
c
IL32 expression
Pseudotime value
Timepoint
Ctrl
1Day
3Day
7Day
d
TGFβ1
EGF
TNFα
OVCA420
MCF7
A549
DU145
Time
Genes
IL32
0d
8h
1d
3d
7d
Avg. Expression

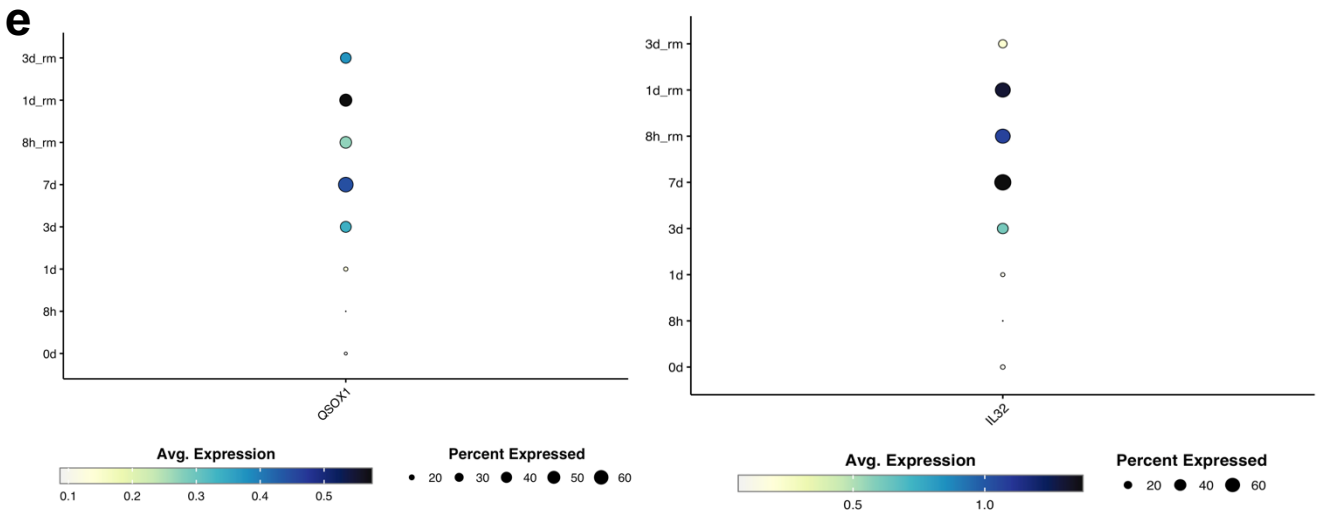

Figure 5. Of all immune regulatory factors, *IL32* correlates the most with EMT progression and is highly expressed in mesenchymal cells. (a) Model-based analysis of single-cell transcriptomics (MAST) between untreated OVCA420 cells and cells treated with TGF-β1 for 7 days. left – higher in treated cells; right – higher in untreated cells. (b) Average expression of *IL32* in all OVCA420 cells treated with TGF-β1 and collected at different time points. (c) General additive model (GAM) of computed pseudotime values against *IL32* expression for all OVCA420 cells treated with TGF-β1 for different lengths of time. (d) Expression heatmaps for *IL32* expression in four different cancer cell lines (OVCA420, MCF7, A549, DU145) treated with either TGF-β1 (10 ng/mL), EGF (30 ng/mL), or TNFα (10 ng/mL) at five different time points: 0d (no treatment), 8 hours (8h), 1-day (1d), 3-day (3d), and 7-day (7d). (e) Dot plots showing expression of either *QSOX1* or *IL32* during EMT induction across time points and after removal of TGF-β1 EMT inducing stimulus after either 8 hours (8h_rm), 1-day (1d_rm), or 3-days (3d_rm) post-removal.

3.3 EMT modulates transcript expression of cytokines, chemokines, and interleukins in ovarian cancer cell lines treated with EMT inducers

Based on the preliminary results in **Figure 2** we determined the RNA expression of a selection of cytokines, chemokines, and interleukins in OVCA420 cells treated with TGF-β1 (**Figure 6a**). Among all the factors examined, there was a positive correlation only between EMT and the chemokines *CCL2*, *CCL5*, *CCL20*, *CXCL1* and the interleukins *IL18*, *IL1A*, and *IL11* where their expression was highest after 7 days of treatment. Because many of these chemokines and interleukins are immunoregulatory and may be secreted from cancer cells undergoing EMT, we measured the abundance of these factors in the media of OVCA420 cells after 4 days of TGFβ-1 treatment. There

were significant protein concentrations for CCL2, CCL5, and IL-1a (** $p < 0.01$) in TGFβ-1 treated cells compared to untreated controls (**Figure 6b**). While the transcripts for many immunoregulatory factors were expressed in OVCA420 cells undergoing EMT, only CCL2, CCL5, and IL-1a were secreted into the media at detectable levels. These chemokines are known to be associated with recruitment of deleterious tumor-associated macrophages (TAMs) (Soria & Ben-Baruch, 2008) and IL-1a is pro-tumorigenic in ovarian cancer (Charbonneau et al., 2014). These findings are consistent with the established knowledge that soluble factors mediate immunosuppression by mesenchymal cells (Ghannam et al., 2010).

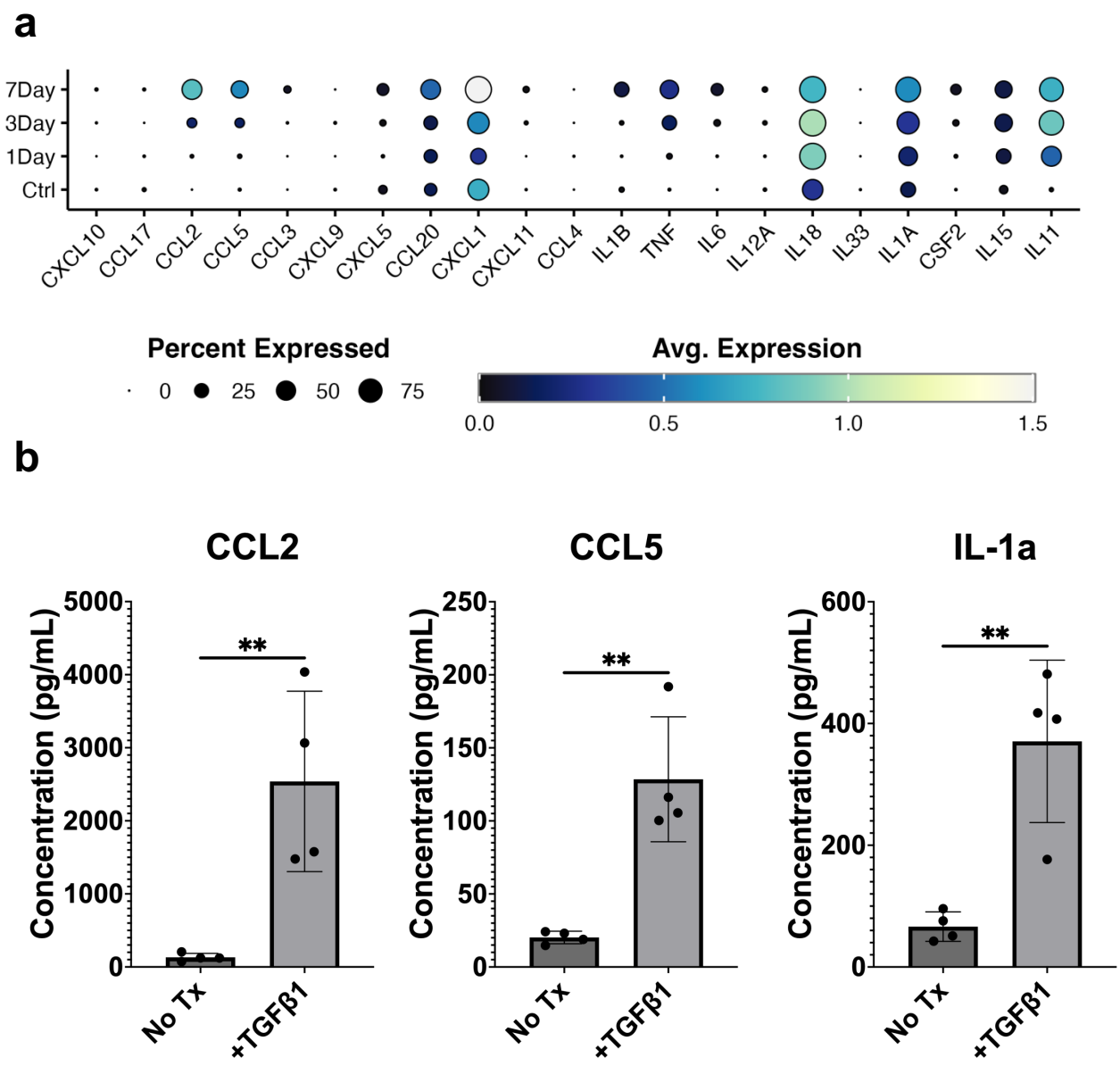

Figure 6. CCL2, CCL5, and IL-1a are secreted from mesenchymal OVCA420 cells. (a) Average RNA expression of cytokines, chemokines, and interleukins in OVCA420 cells treated with TGF-β1 for different lengths of time. (b) Absolute protein concentrations (pg/ml) of cytokines, chemokines, and interleukins measured by multiplexed ELISAs (BioLegend® LEGENDPlex™) of media from OVCA420 cells treated with 10 ng/mL TGF-β1 for 4 days (n = 4).

3.4 TGFβ-1 is the primary immunosuppressor of NK cells in in vitro ovarian cancer EMT model

We decided to determine whether mesenchymal cells affect NK cell cytotoxicity, because both CCL2 and CCL5 bind to receptors (CCR2 and CCR5) on the surface of NK cells (Ozga et al., 2021), which may regulate their cytotoxic potential. To test this, we used an *in vitro* co-culture system of either K562 lymphoblast cells isolated from a chronic leukemia patient (Klein et al., 1976) or OVCA420 cells as target cells and NK92 cells derived from a patient with NK-cell lymphoma (Klingemann, 2023) as effector cells. After pre-treating the NK92 cells for 48 hours with media lifted from either epithelial OVCA420 cells or OVCA420 cells induced to become mesenchymal by treating them with TGFβ-1 for 72 hours, we co-cultured the pre-treated NK-92 cells with either K562 cells or OVCA420 cells for 6 hours. When the NK92 cells were pre-treated with media from mesenchymal cells, there was a marked decrease in the percentage of dead cells for effector-target ratios of 10:1 and 5:1 in both K562-NK92 (**Figure 7a**; * $p < 0.05$) and OVCA420-NK92 (**Figure 7b**; * $p < 0.05$). While this might have suggested that factors secreted by mesenchymal cells, possibly CCL2, CCL5, and IL-1a, suppress the cytotoxic activity of NK cells, the immunosuppressive effect was ameliorated when a neutralizing TGFβ-1 antibody was added (**Figure 7c**). Thus, we concluded that despite the milieu of immunoregulatory factors in mesenchymal factors, the primary immunosuppressive factor was TGFβ-1.

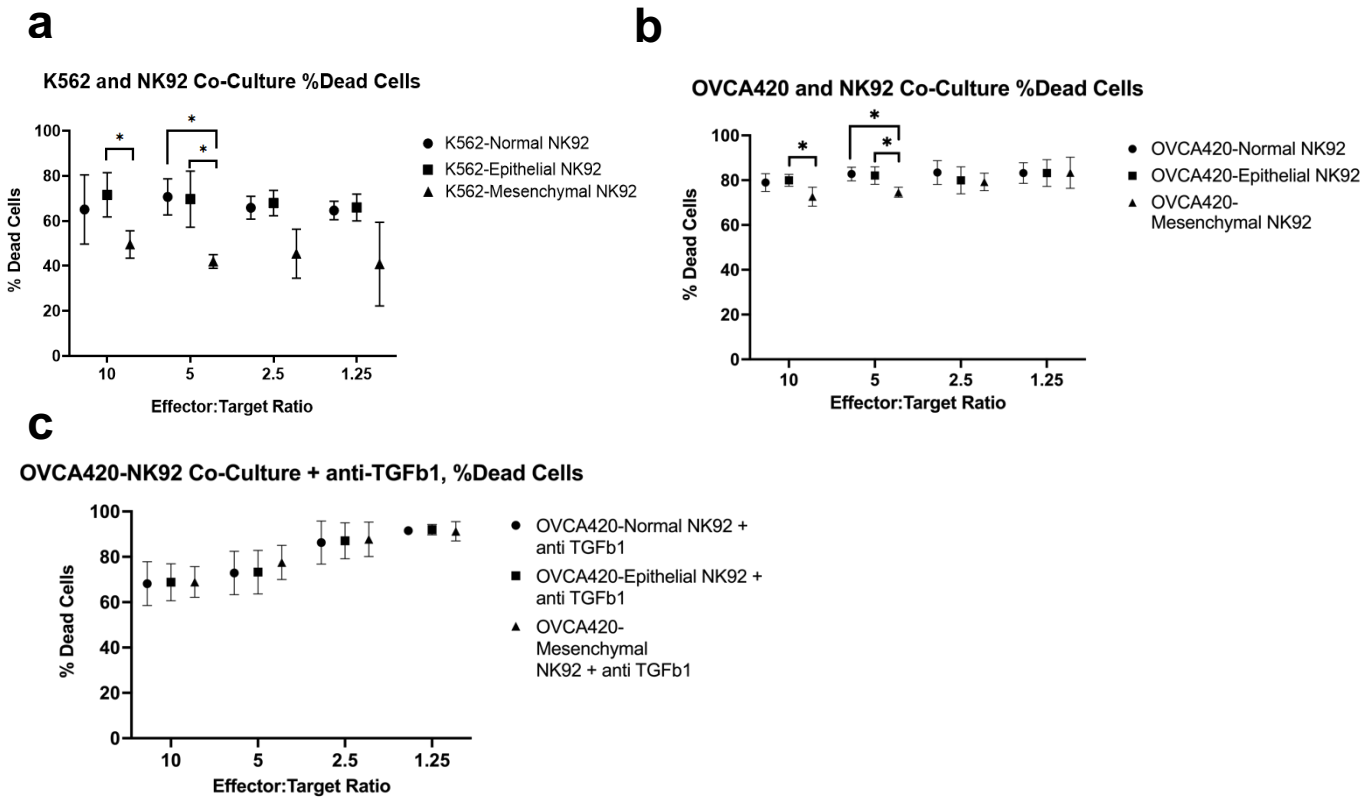

Figure 7. **NK cell cytolytic activity is reduced when pre-treated with media from mesenchymal cells, but effect is alleviated by a TGF-β1 neutralizing antibody**. (a) Reduced killing of K562 cells by NK92 cells pre-treated with media from mesenchymal cells compared with NK92 cells pre-treated with media from epithelial cells at 10:1 (*$p < 0.05$) and 5:1 (*$p < 0.05$) effector-to-target ratios and untreated NK92 cells in the 5:1 effector-to-target ratio group (*$p < 0.05$) in a 6-hour co-culture (n = 4). (b) Reduced killing of OVCA420 cells by NK92 cells pre-treated with media from mesenchymal cells compared with NK92 cells pre-treated with media from epithelial cells at 10:1 (*$p < 0.05$) and 5:1 (*$p < 0.05$) effector-to-target ratios and untreated NK92 cells in the 5:1 effector-to-target ratio group (*$p < 0.05$) in a 6-hour co-culture (n = 4). (c) No difference in killing of OVCA420 cells by NK92 cells pre-treated with media from epithelial or mesenchymal cells when cultured with a TGF-β1 neutralizing antibody (n = 4).

To determine if immunoregulatory factors may exist *in vivo* but are absent specifically from OVCA420 cells, we leveraged an ensemble cell-cell communication algorithm called LIANA and applied it to a scRNA-seq dataset of 6 HGSOC (Geistlinger et al., 2020) (**Figure 8a-c**). We found that expression of *MDK*, *MIF*, *CD59*, *Nectin2* are most correlated with EMT in mesenchymal cells *in vivo* and are most involved in communications with NK cells. Of these identified factors, only CD59 was increased in

expression in OVCA420 cells undergoing EMT *in vitro*. We therefore used recombinant proteins of these factors to pre-treat NK92 cells in additional co-culture experiments.

a

	source	ligand	target	receptor	aggregate_rank
1	EPI	MIF	NK	CXCR4	9.203838e-06
2	EPI	MDK	NK	ITGB2	1.228068e-05
3	EPI	MIF	NK	CD44	2.218576e-05
4	EPI	MDK	NK	ITGB1	1.235128e-05

b

	source	ligand	target	receptor	aggregate_rank
1	FLUX	MIF	NK	CXCR4	2.392979e-05
2	FLUX	MIF	NK	CD44	4.578666e-05
3	FLUX	CD59	NK	CD2	3.357771e-05

c

	source	ligand	target	receptor	aggregate_rank
1	MES	MDK	NK	ITGB2	1.521772e-06
2	MES	MDK	NK	ITGB1	1.536274e-06
3	MES	LGALS3BP	NK	ITGB1	1.877792e-05
4	MES	PLAT	NK	ITGB2	1.534501e-05
5	MES	HLA-B	NK	KLRD1	7.036762e-06
6	MES	TIMP3	NK	CD44	6.181308e-05
7	MES	GRN	NK	TNFRSF1B	2.432681e-05
8	MES	ITGB1BP1	NK	ITGB2	2.956166e-07
9	MES	TNFRSF1A	NK	TNFRSF1B	1.221760e-05
10	MES	BAG6	NK	NCR3	1.203250e-05
11	MES	HLA-E	NK	KLRK1	4.552150e-05
12	MES	NECTIN2	NK	CD96	1.433037e-06

Figure 8. **Snapshot of a list of top-most specific ligands expressed by mesenchymal cells and their likely receptor targets on NK cells**. (a) Table showing different ligands in epithelial cancer cells from a single cell RNA-seq dataset of 6 HGSOC tumors identified by the LIANA cell-cell communication analysis package to be most specific in binding to NK cell receptors. Aggregate rank refers to a weighted average p-value of all cell-cell communication methods' resultant p-value used by LIANA to denote likelihood of an interaction happening. (b) The same analysis as in A, but showing different ligands in partial-EMT cancer cells to be most specific in binding to NK cell receptors. (c) The same analysis as in A, but showing different ligands in mesenchymal cancer cells to be most specific in binding to NK cell receptors.

First, we repeated the previous experiment testing the immunosuppressive potential of conditioned media from mesenchymal cells (**Figure 9a**) and found that NK92 cells pre-treated with mesenchymal conditioned media kill fewer target K562-NL cells with a reduction between 20-30% in dead cells depending on the ratios when NK92 cells are exposed to mesenchymal media. Then, we repeated the same experiment but with the addition of a neutralizing TGFβ-1 antibody to the mesenchymal media prior to NK92 cell conditioning, which resulted in amelioration of the immunosuppressive effect by media from mesenchymal cells (**Figure 9b**). We then treated NK92 cells with recombinant Nectin2, CD59, MIF, MDK, or TGFβ-1 alone, or a combination of TGFβ-1 and neutralizing TGFβ-1 antibody and found that only TGFβ-1 treatment reduced the cytotoxic potential of NK92 cells (**Figures 9c, d**) by 20-50% depending on the ratios used. Taken together, the primary immunosuppressive factor affecting NK cells found in media containing secreted factors from mesenchymal cells is TGFβ-1. This suggests that the four other secreted factors do not directly affect NK cell cytolytic activity. They may, however, contribute to immunosuppression by acting on other cell types, such as TAMs, which are known to be polarized and chemoattracted by factors like CCL2, CCL5, and IL-1a.

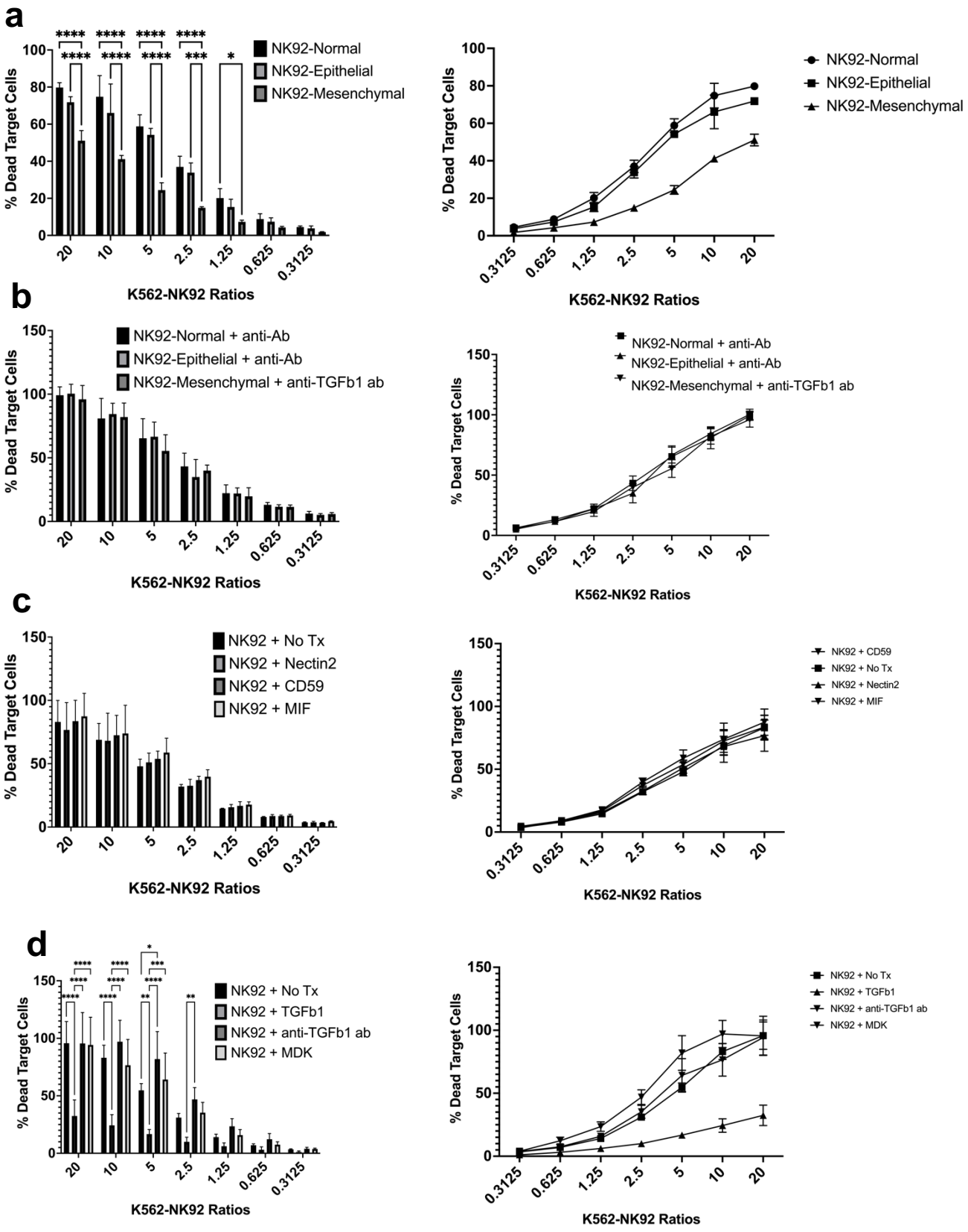
a
NK92-Normal
NK92-Epithelial
NK92-Mesenchymal
% Dead Target Cells
K562-NK92 Ratios
b
NK92-Normal + anti-Ab
NK92-Epithelial + anti-Ab
NK92-Mesenchymal + anti-TGFb1 ab
c
NK92 + No Tx
NK92 + Nectin2
NK92 + CD59
NK92 + MIF
d
NK92 + No Tx
NK92 + TGFb1
NK92 + anti-TGFb1 ab
NK92 + MDK

Figure 9. **NK cell cytolytic activity is unaffected when pre-treated with recombinant ligands associated with mesenchymal cells**. (a) Reduced killing of K562-NL cells by NK92 cells pre-treated with media from mesenchymal cells compared with NK92 cells pre-treated with either media from epithelial cells or normal media at various effector-to-target ratios (**** $p < 0.0001$ for 20:1, 10:1, 5:1, 2.5:1 ratios; *** $p < 0.001$ for 2.5:1 ratio; * $p < 0.05$ for 1.25 ratio) in a 6-hour co-culture of K562-NL and NK92 cells at different effector-to-target ratios (n = 3). (b) No difference in killing of K562-NL cells by NK92 cells pre-treated with media from epithelial or mesenchymal cells, or normal media in combination with TGF-β1 neutralizing antibody in a 6-hour co-culture (n = 3). (c) No difference in killing of K562-NL cells by NK92 cells pre-treated with either recombinant Nectin2, CD59, or MIF in a 6-hour co-culture of K562-NL and NK92 cells at different effector-to-target ratios (n = 3). (d) Reduced killing of K562-NL cells by NK92 cells pre-treated with recombinant TGF-β1 compared with NK92 cells pre-treated with either a solution of TGF-β1 and neutralizing TGF-β1 antibody, recombinant MDK, or untreated at various effector-to-target ratios in a 6-hour co-culture of K562-NL and NK92 cells at different effector-to-target ratios. (**** $p < 0.0001$ for 20:1, 10:1, 5:1, ratios; *** $p < 0.001$ for 5:1 ratio; ** $p < 0.01$ for 5:1 and 2.5:1 ratios; * $p < 0.05$ for 5:1 ratio) (n = 3).

3.5 ID8 and STOSE murine ovarian cancer cell lines undergo EMT when treated with TGFβ-1

Following our results with the human ovarian cancer cells, we sought to determine if EMT-mediated immunosuppression occurs in murine models of ovarian cancer. To this end, we used ID8 and STOSE murine ovarian cancer cells, both of which are established and well-characterized cell lines and tumor models (Rodriguez et al., 2022). Although both originate from spontaneously transformed ovarian epithelial cells, they produce immunologically distinct tumors with ID8 generating “cold” tumors, whereas STOSE are more infiltrated by immune cells. Whether the EMT status of these cell lines plays any role in these distinct phenotypes remains unknown. Induction of EMT in ID8 cells with TGFβ-1 treatment for 7 days resulted in phenotypic changes that suggested that the cells were more mesenchymal, having lost the tight, cobblestone-like epithelial formation and gaining spindle-shaped morphology (**Figure 10a**). We then measured mRNA expression levels of the classic EMT markers *Ncad*, *Slug*, *Vim*, and

Sox4 in ID8 cells treated with TGFβ-1 for 7 days and found significant increases only in *Ncad* and *Slug* (**Figure 10b**) (* $p < 0.05$; ** $p < 0.01$). Additionally, we examined expression of *Il18* and its receptor *Il18r* as it was a strong correlate of EMT in our human OVCA420 ovarian cancer model and it could also be a relevant factor due to its immunosuppressive action together with PD-1 (Terme et al., 2011a; Z. Y. Wang et al., 2002), and found that *Il18* was significantly different (**Figure 10b**) (* $p < 0.05$). We repeated this experiment with another murine ovarian cancer cell line STOSE and found similar results (**Figures 10c-d**) with *Ncad*, *Slug*, *Vim*, and *Il18r* being significantly higher in TGFβ-1 treated cells (* $p < 0.05$). Taken together, these results indicate that both ID8 and STOSE cells can undergo EMT and become mesenchymal when induced with recombinant TGFβ-1. Additionally, *Il18* is correlated with EMT in ID8 cells but not in STOSE, suggesting that the former may use IL18 to regulate the immune environment. IL18 has been previously shown to act as an autocrine factor in tumors (Lebel-Binay et al., 2003), suggesting a possible feedback loop between higher *Il18* expression in mesenchymal cells and enhanced downstream signaling effects of IL18R binding on cancer cells that include NFkB activation and subsequent proinflammatory signals (Wawrocki et al., 2016).

a

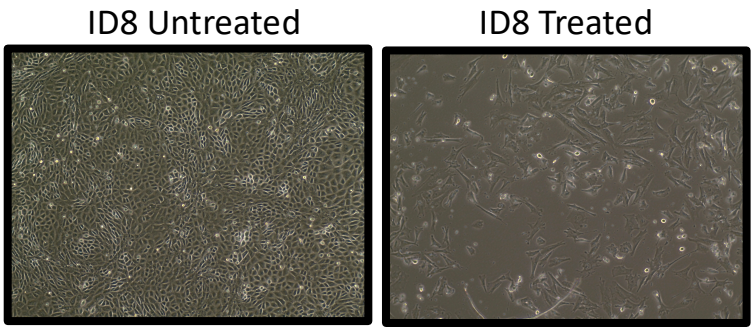
ID8 Untreated
ID8 Treated

b

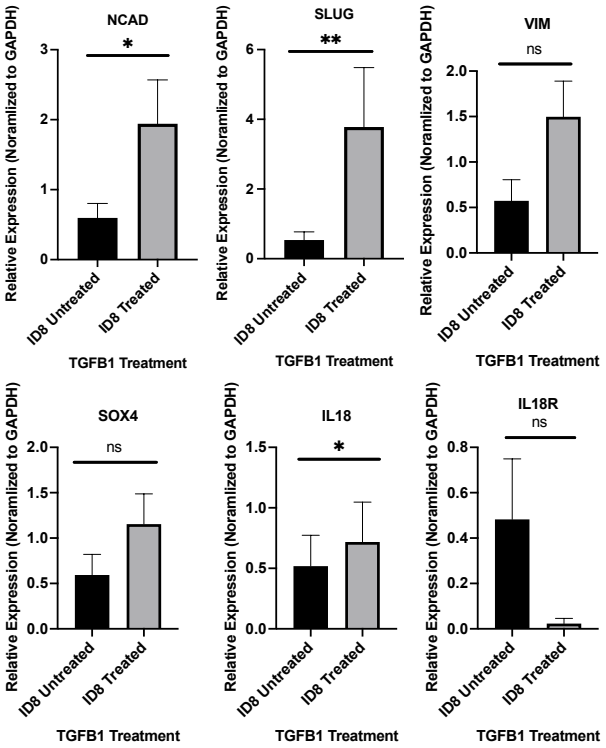
NCAD
*
SLUG
**
VIM
ns
SOX4
ns
IL18
*
IL18R
ns
Relative Expression (Noramlized to GAPDH)
ID8 Untreated
ID8 Treated
TGFB1 Treatment

c

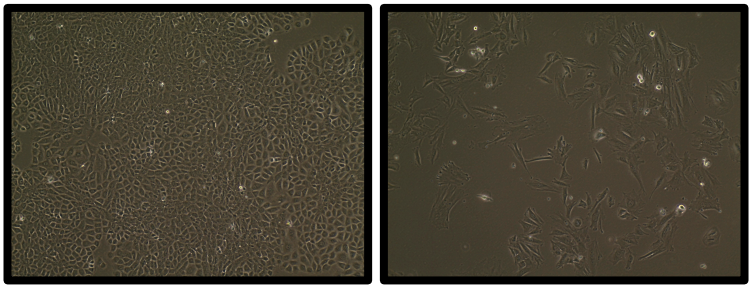
STOSE Untreated
STOSE Treated

d

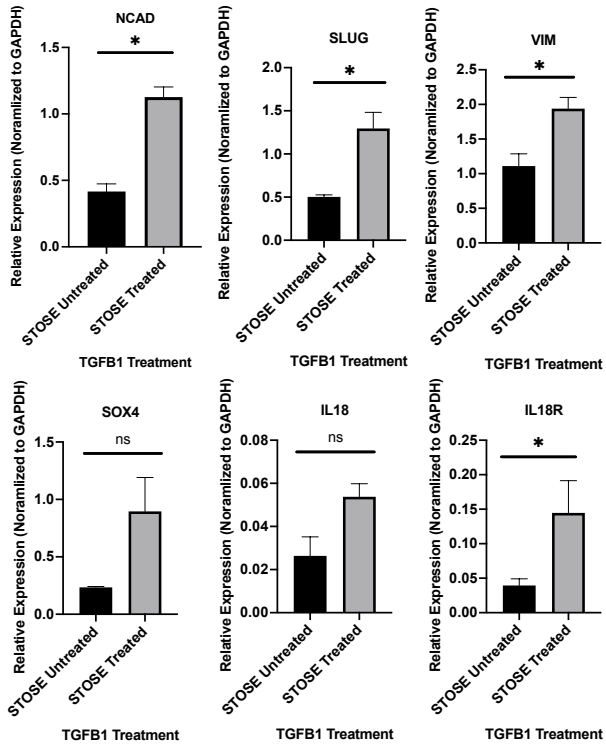
NCAD
*
SLUG
*
VIM
*
SOX4
ns
IL18
ns
IL18R
*
Relative Expression (Noramlized to GAPDH)
STOSE Untreated
STOSE Treated
TGFB1 Treatment

Figure 10. **ID8 and STOSE murine ovarian cancer cell lines morphologically appear mesenchymal and express common EMT genes when treated with TGF-β1 for 7 days**. (a) Widefield microscopy images of untreated and TGF-β1 treated ID8 cells (n = 3). (b) RT-PCR quantification of common EMT genes (* $p < 0.05$ in *NCAD*, *VIM*, *IL18*; ** $p < 0.01$ in *SLUG*) in untreated and TGF-β1 treated ID8 cells (n = 3). (c) Widefield microscopy images of untreated and TGF-β1 treated STOSE cells (n = 3). (d) RT-PCR quantification of common EMT genes (* $p < 0.05$ in *NCAD*, *SLUG*, *VIM*, *IL18R*) in untreated and TGF-β1 treated STOSE cells (n = 3).

To further expand the study of the EMT in the ID8 and STOSE cell lines, we performed a time course treatment of the cell lines with TGFβ-1 and then sequenced the cells via scRNA-seq. Data from the ID8 cells are colored by their length of treatment and we noticed clustering related to the time points (**Figure 11a**). Then, we performed pseudotime analysis on the cells and noted the cells temporally align in pseudotime with their respective time points (**Figure 11b**), suggesting the pseudotime analysis captures EMT progression in these cells after treatment with TGFβ-1. Finally, we correlated values from the pseudotime analysis with EMT scores for each cell generated with a cancer-specific gene module published by our lab (Cook & Vanderhyden, 2022) converted into mouse orthologs (**Figure 11c**) and observed a positive association ($R^2 = 0.15$). When a similar analysis was performed on STOSE cells (**Figures 11d-f**) we noted a similar clustering according to time point, and alignment with pseudotime, but a lack of correlation between the pseudotime analysis and the cancer-specific gene module ($R^2 < 0.01$). Together, these results demonstrate that the cancer-specific gene module, which is based on a pan-cancer analysis of EMT in cancer cells, captures the EM program of the ID8 cells but not the STOSE cells, suggesting that STOSE cells undergo a unique version of the EMT.

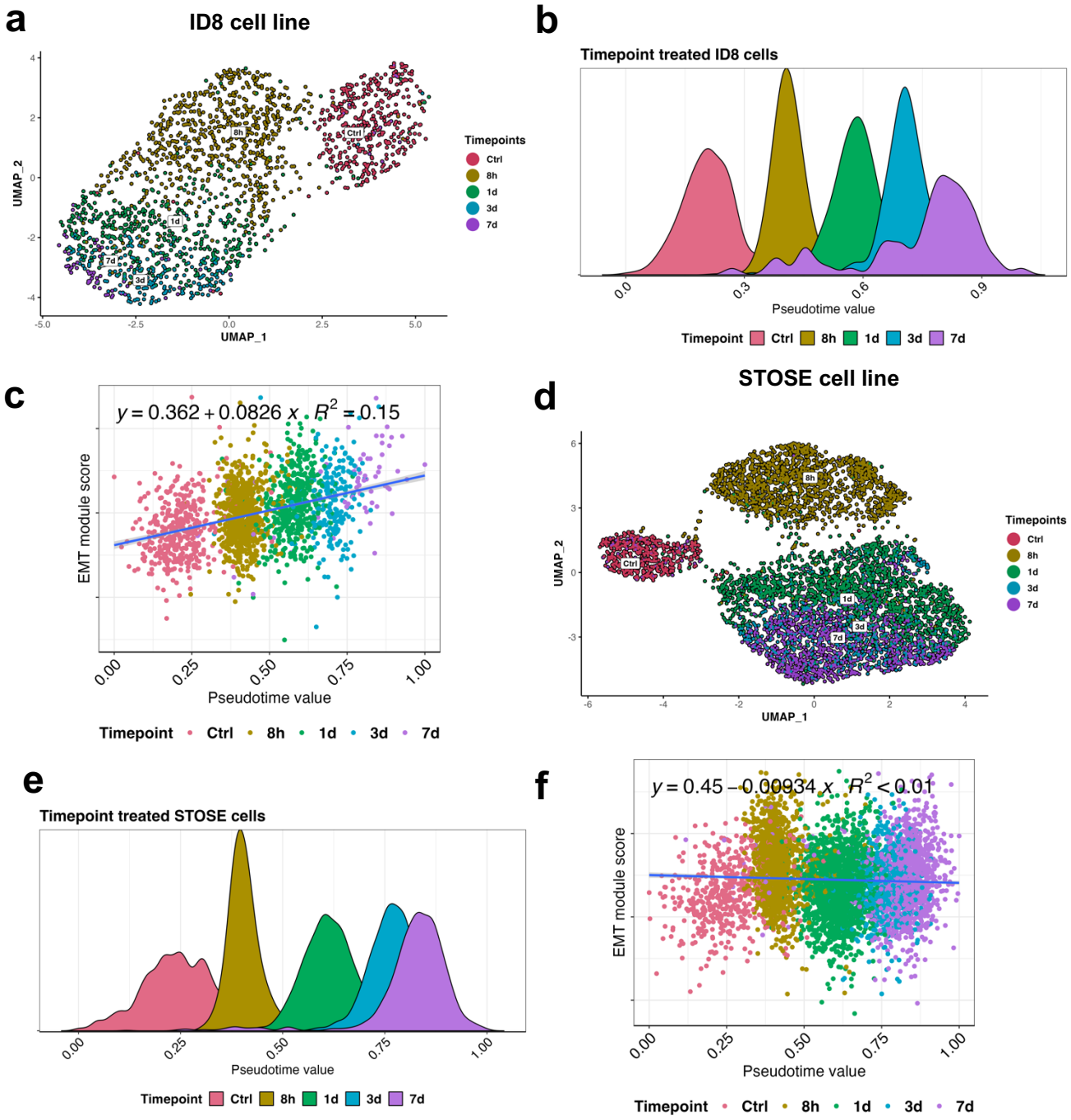

Figure 11. *In vitro* models of EMT using two mouse ovarian cancer cell lines show differing correlations of pseudotime with scores from cancer-specific EMT signature genes. (a) UMAP clustering of murine ID8 cells treated with TGF-β1 (10 ng/mL) at four different time points: Ctrl (no treatment), 8 hours (8h), 1-day (1d), 3-day (3d), and 7-day (7d). (b) Density ridge plot showing computed pseudotime scores for all ID8 cells, colored by time point. (c) Positive correlation of computed pseudotime values in ID8 murine ovarian cancer cells against cancer-specific EMT scores for all cells (R^2 = 0.15). (d-f) Same as a-c, but with STOSE cells, and there is a negative correlation of

computed pseudotime values against cancer-specific EMT scores for all cells ($R^2 < 0.01$).

3.6 Expression of immunoregulatory molecules is not correlated with EMT in murine ovarian cancer cell lines

To determine how the expression of various cytokines, chemokines, and interleukins changes with EMT, we first converted all the immunoregulatory factors from our experiments with human ovarian cancer cell lines to their murine orthologs. Then, we examined the expression of these factors at various time points following TGFβ-1 treatment of ID8 (**Figure 12a**) and STOSE (**Figure 12b**) cell lines. Only one factor increased in expression in correlation with EMT, namely *Il11* in both ID8 and STOSE cell lines, with the rest either remaining unchanged or decreasing in expression with time. Notably, despite *Il18* being a strong correlate of EMT in the human models, it appeared to decrease in expression in the murine cell lines, suggesting that the murine models are potentially unsuitable for testing the immunoregulatory potential of mesenchymal cancer cells. To confirm that *Il18* expression is not positively correlated with EMT in murine cell lines, we performed an ELISA for IL18 in the supernatant of ID8 and STOSE cells treated with TGFβ-1 and compared it to the ascites from mice with syngeneic orthotopic tumors of these cell lines. We included ascites as positive controls for a greater number of mesenchymal cells based on published literature (Rafehi et al., 2016) where we expected to find higher IL18 protein concentrations knowing that IL18 expression is associated with EMT based on our scRNA-seq data. The results indicated that there is no effect of TGFβ-1 on the abundance of IL18 with either cell line (**Figure 12c**). Taken together, our initial aim to study the effects of Il18 and its correlation with EMT on immune cells in the TME of syngeneic orthotopic models of ovarian cancer was

unlikely to succeed due to the lack of a clear relationship between IL18 and EMT in ID8 and STOSE cells.

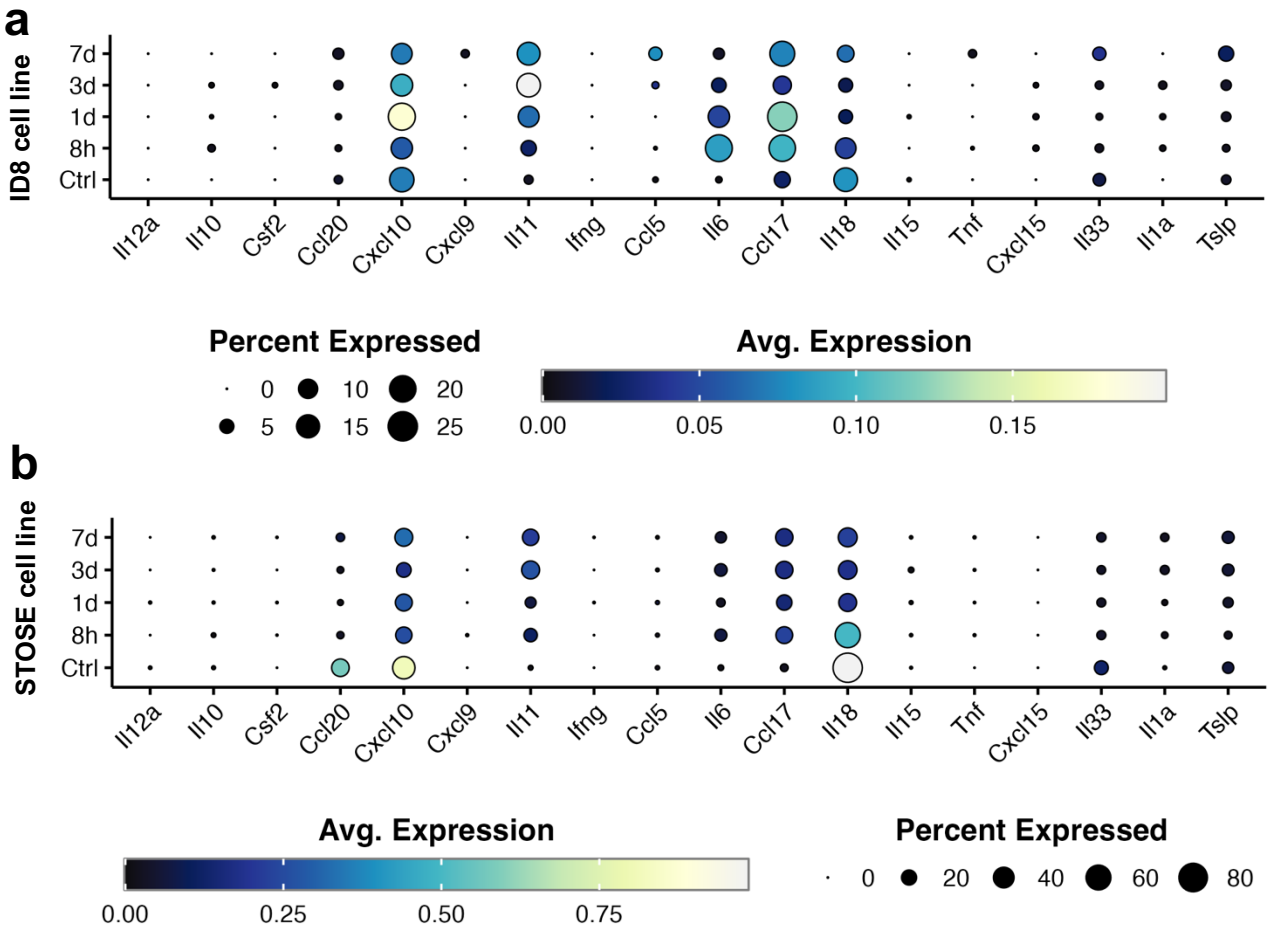
a
ID8 cell line
7d
3d
1d
8h
Ctrl
Il12a
Il10
Csf2
Ccl20
Cxcl10
Cxcl9
Il11
Ifng
Ccl5
Il6
Ccl17
Il18
Il15
Tnf
Cxcl15
Il33
Il1a
Tslp
Percent Expressed
0
5
10
15
20
25
Avg. Expression
0.00
0.05
0.10
0.15
b
STOSE cell line
7d
3d
1d
8h
Ctrl
Il12a
Il10
Csf2
Ccl20
Cxcl10
Cxcl9
Il11
Ifng
Ccl5
Il6
Ccl17
Il18
Il15
Tnf
Cxcl15
Il33
Il1a
Tslp
Avg. Expression
0.00
0.25
0.50
0.75
Percent Expressed
0
20
40
60
80

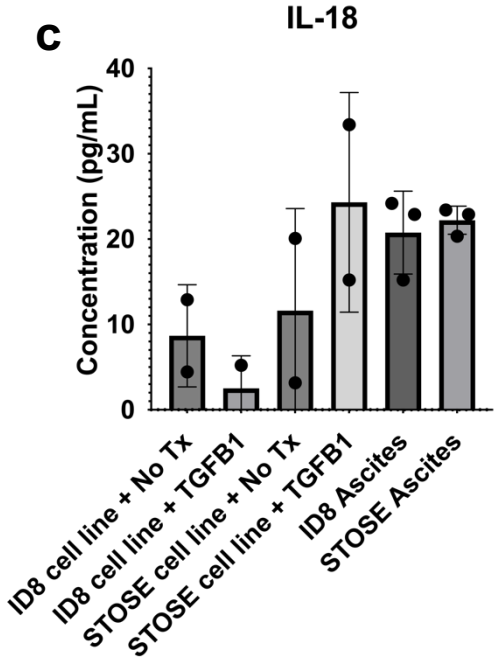
c
IL-18
Concentration (pg/mL)
0
10
20
30
40
ID8 cell line + No Tx
ID8 cell line + TGFB1
STOSE cell line + No Tx
STOSE cell line + TGFB1
ID8 Ascites
STOSE Ascites

Figure 12. Il18 RNA and protein expression is unchanged by EMT in ID8 and STOSE cell lines treated with TGF-β1. (a,b) Average expression levels of cytokines, chemokines, and interleukins in ID8 (a) and STOSE (b) cells treated with TGF-β1 (10 ng/mL) at four different time points: Ctrl (no treatment), 8 hours (8h), 1-day (1d), 3-day (3d), and 7-day (7d). (c) ELISA for IL18 protein abundance in the supernatant from ID8 and STOSE cell lines treated with TGF-β1 (10 ng/mL) for 7 days and in ascites from mice with syngeneic orthotopic ID8 and STOSE tumors (n = 2 for ID8 and STOSE with and without treatments, n = 3 for ID8 and STOSE ascites).

3.7 Orthotopic ID8 and STOSE tumors differentially express classical markers of epithelial ovarian cancer

To delve deeper into the immunoregulatory environment of the syngeneic orthotopic ID8 and STOSE murine ovarian cancer models, we performed scRNA-seq on intrabursal tumors derived from these cell lines and labeled the cell populations according to common cancer cell marker genes for ID8 (**Figure 13a**) and STOSE (**Figure 13b**) tumors. Expression of gene markers of epithelial ovarian cancer in the cancer cell populations revealed heterogeneity in expression of classical markers (**Figure 13c, d**). In particular, classical markers of epithelial cancer cells such as *Krt19* and *Wt1* were predominantly expressed in STOSE cancer cells whereas markers such as *Epcam*, *Amhr2* and *Wt1* were highly expressed in ID8 cancer cells.

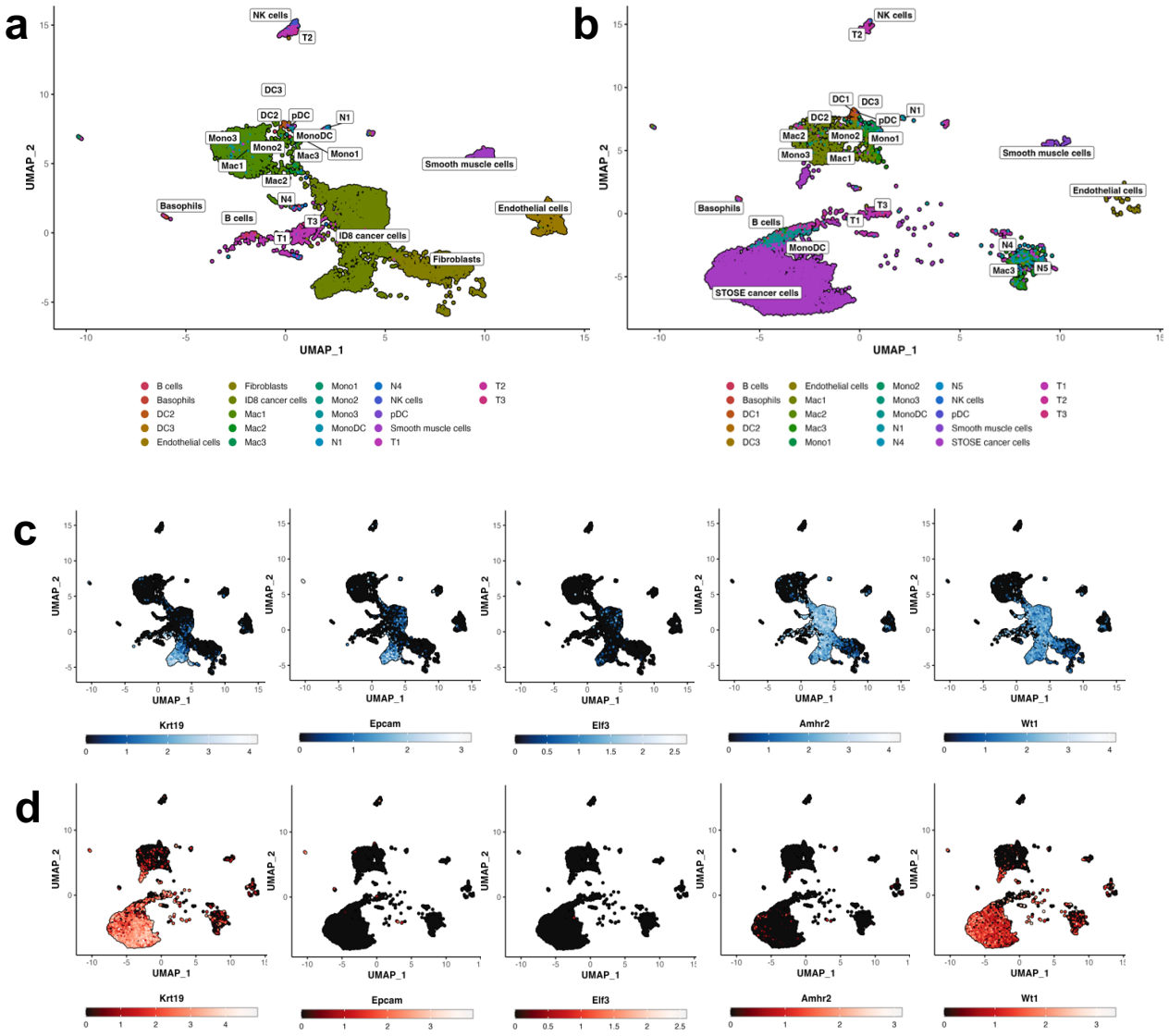

Figure 13. ID8 and STOSE tumors differentially express common cancer cell markers. (a) scRNA-seq UMAP figures depicting cell clusters found in orthotopic ID8 tumor at endpoint. The resultant gene expression matrix contained expression values of 8,104 cells and 20,091 genes and was analyzed using Seurat. (b) scRNA-seq UMAP figures depicting cell clusters found in orthotopic STOSE tumor at endpoint. The resultant gene expression matrix contained expression values of 9,749 cells and 20,091 genes and was analyzed using Seurat. (c,d) UMAP plots showing enrichment of individual cancer cells identified by the expression of common cancer cell genes (*Krt19, Epcam, Elf3, Amhr2, Wt1*) in single cell RNA-seq dataset of ID8 (c) and STOSE (d).

3.8 Orthotopic ID8 and STOSE tumors have unique transcriptional profiles

Based on the differential expression of epithelial ovarian cancer markers between STOSE and ID8 tumors, we decided to look at the unique transcriptional profiles of the cancer cell population in each orthotopic tumor. More specifically, we performed a differential gene expression (DGE) MAST test between the two cancer cell populations in order to generate a unique transcriptional signature for the cancer cell population of each tumor (**Figure 14a**). This analysis revealed that some genes are more strongly expressed in the cancer cells of ID8 tumors than in STOSE tumors, and vice versa (**Figure 14b**). Particularly, we noted that *Sox9* and *Star* (**Figure 14c**) are exclusively expressed by ID8 cancer cells while *Msln*, *Ccl2*, *Il33*, and *Col3a1* are primarily expressed in STOSE cancer cells (**Figure 14d, e**), suggesting that the cancer cells from the two tumors have very different, heterogeneous transcriptomes that could be reflected in the makeup of cells in the TME (**Figure 14a, b**), and have potential impacts on survival, as mice injected orthotopically with STOSE tumors survive for 7 days longer than those injected with ID8 cells, on average (Rodriguez et al., 2022).

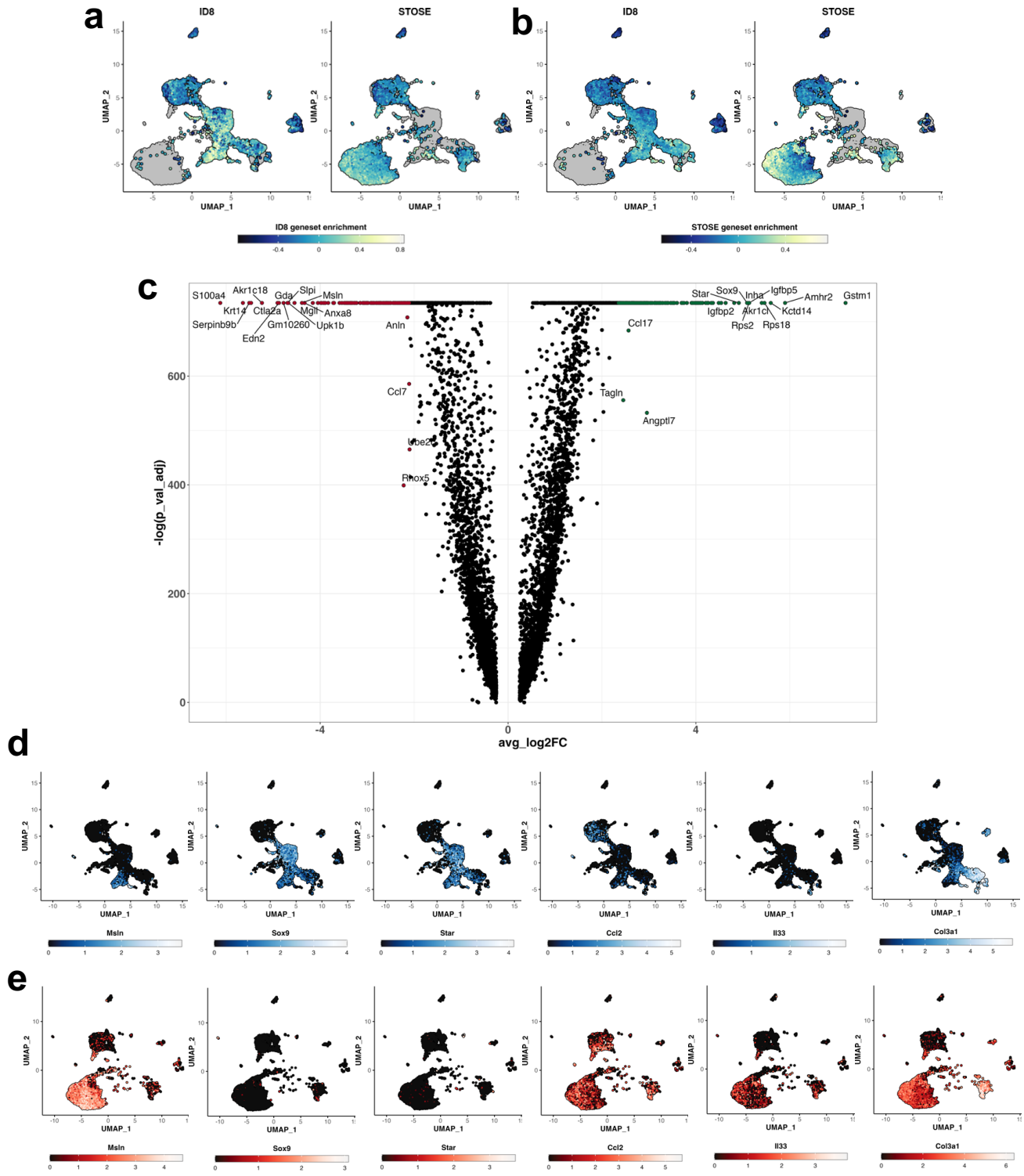
a
ID8
STOSE
UMAP_1
UMAP_2
ID8 geneset enrichment
b
STOSE geneset enrichment
c
S100a4
Akr1c18
Gda
Slpi
Msln
Krt14
Ctla2a
Mgl
Anxa8
Serpinb9b
Gm10260
Upk1b
Edn2
Anln
Ccl7
Ube2c
Rhox5
Star
Sox9
Inha
Igfbp5
Amhr2
Gstm1
Igfbp2
Akr1c6
Kctd14
Rps2
Rps18
Ccl17
Tagln
Angptl7
-log(p_val_adj)
avg_log2FC
d
Msln
Sox9
Star
Ccl2
Il33
Col3a1
e

Figure 14. Cancer cells in orthotopic ID8 and STOSE tumors exclusively express genes that could be used to identify them. (a) UMAP plot showing enrichment of individual cells for average expression of genes from gene set unique to orthotopic ID8 cancer cells generated with a model-base analysis of single-cell transcriptomics (MAST) in orthotopic ID8 and STOSE tumors. (b) UMAP plot similar to (a) but for a gene set unique to STOSE cancer cells. (c) Volcano plot showing differentially expressed genes generated with a MAST test between ID8 and STOSE cancer cells from orthotopic tumors (left – STOSE cancer genes, right – ID8 cancer genes). (d,e) UMAP plots showing enrichment of individual cancer cells for expression of cancer cell genes from MAST differential gene expression test. *Sox9, and Star* are specific to ID8 orthotopic tumors (d) and *Msln, Ccl2, Il33, and Col3a1* are specific to STOSE orthotopic tumors (e).

3.9 Orthotopic ID8 and STOSE tumors differentially regulate many pathways

Following our findings that cancer cells from syngeneic orthotopic ID8 and STOSE tumors possess different transcriptional profiles, we decided to determine which pathways are associated with these differentially expressed genes, and whether these pathways are regulated differently between the two tumors. After performing pathway enrichment analysis of the Hallmark pathways from MSigDb, we found that STOSE cancer cells upregulate pathways related to EMT, cell cycle, and inflammatory immune response while ID8 cancer cells upregulate the Wnt/β-Catenin pathway (**Figure 15a**) suggesting that activity of the EMT pathway may be increased in STOSE tumors and thus there may be more mesenchymal cells in orthotopic STOSE tumors. Additional pathway enrichment analysis with biological pathways from MSigDb revealed that ID8 cancer cells upregulate pathways related to Class II HLA presentation while STOSE cancer cells upregulate pathways related to immune regulation of T cells and lymphocytes in general (**Figure 15b**). Taken together, upregulation of EMT-related pathways and immunoregulatory pathways in STOSE cancer cells is consistent with prior findings of EMT's association with immunoregulation (Datar & Schalper, 2016; Taki et al., 2021). Finally, we scored the cancer cells for EMT using the cancer-specific gene

module after converting the genes to their mouse orthologs and found that there are more mesenchymal cells in STOSE tumors than ID8 tumors (**Figure 15c**), thus supporting the results of the pathway analysis. Taken together, the results suggest that EMT activity in cancer cells is higher in STOSE and there are more mesenchymal cells in STOSE tumors.

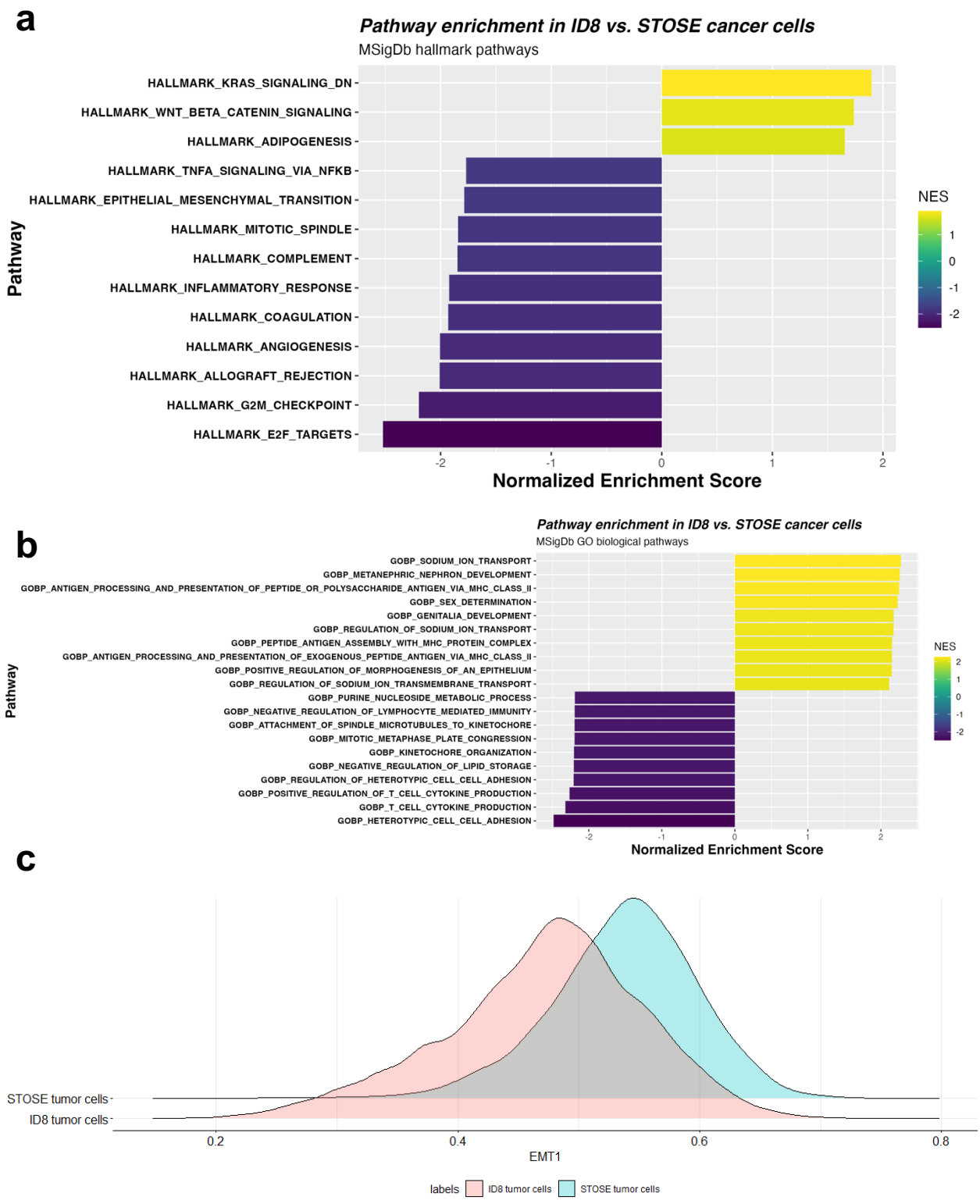
a
Pathway enrichment in ID8 vs. STOSE cancer cells
MSigDb hallmark pathways
HALLMARK_KRAS_SIGNALING_DN
HALLMARK_WNT_BETA_CATENIN_SIGNALING
HALLMARK_ADIPOGENESIS
HALLMARK_TNFA_SIGNALING_VIA_NFKB
HALLMARK_EPITHELIAL_MESENCHYMAL_TRANSITION
HALLMARK_MITOTIC_SPINDLE
HALLMARK_COMPLEMENT
HALLMARK_INFLAMMATORY_RESPONSE
HALLMARK_COAGULATION
HALLMARK_ANGIOGENESIS
HALLMARK_ALLOGRAFT_REJECTION
HALLMARK_G2M_CHECKPOINT
HALLMARK_E2F_TARGETS
Pathway
NES
1
0
-1
-2
-2
-1
0
1
2
Normalized Enrichment Score
b
Pathway enrichment in ID8 vs. STOSE cancer cells
MSigDb GO biological pathways
GOBP_SODIUM_ION_TRANSPORT
GOBP_METANEPHRIC_NEPHRON_DEVELOPMENT
GOBP_ANTIGEN_PROCESSING_AND_PRESENTATION_OF_PEPTIDE_OR_POLYSACCHARIDE_ANTIGEN_VIA_MHC_CLASS_II
GOBP_SEX_DETERMINATION
GOBP_GENITALIA_DEVELOPMENT
GOBP_REGULATION_OF_SODIUM_ION_TRANSPORT
GOBP_PEPTIDE_ANTIGEN_ASSEMBLY_WITH_MHC_PROTEIN_COMPLEX
GOBP_ANTIGEN_PROCESSING_AND_PRESENTATION_OF_EXOGENOUS_PEPTIDE_ANTIGEN_VIA_MHC_CLASS_II
GOBP_POSITIVE_REGULATION_OF_MORPHOGENESIS_OF_AN_EPITHELIUM
GOBP_REGULATION_OF_SODIUM_ION_TRANSMEMBRANE_TRANSPORT
GOBP_PURINE_NUCLEOSIDE_METABOLIC_PROCESS
GOBP_NEGATIVE_REGULATION_OF_LYMPHOCYTE_MEDIATED_IMMUNITY
GOBP_ATTACHMENT_OF_SPINDLE_MICROTUBULES_TO_KINETOCHORE
GOBP_MITOTIC_METAPHASE_PLATE_CONGRESSION
GOBP_KINETOCHORE_ORGANIZATION
GOBP_NEGATIVE_REGULATION_OF_LIPID_STORAGE
GOBP_REGULATION_OF_HETEROTYPIC_CELL_CELL_ADHESION
GOBP_POSITIVE_REGULATION_OF_T_CELL_CYTOKINE_PRODUCTION
GOBP_T_CELL_CYTOKINE_PRODUCTION
GOBP_HETEROTYPIC_CELL_CELL_ADHESION
Pathway
NES
2
1
0
-1
-2
-2
-1
0
1
2
Normalized Enrichment Score
c
STOSE tumor cells
ID8 tumor cells
0.2
0.4
0.6
0.8
EMT1
labels
ID8 tumor cells
STOSE tumor cells

Figure 15. Cancer cells from orthotopic ID8 tumors and STOSE tumors diverge in biological and hallmark pathway activity with STOSE cancer cells exhibiting greater EMT progression than ID8 cancer cells. (a) Pathway enrichment using MSigDb Hallmark pathways based on unique gene signatures of cancer cells from orthotopic ID8 and STOSE tumors generated by differential gene expression MAST test (Left – enriched in STOSE cancer cells; Right – enriched in ID8 cancer cells). (b) Pathway enrichment using MSigDb Gene Ontology (GO) Biological Pathways (BP) based on unique gene signatures of cancer cells from orthotopic ID8 and STOSE tumors generated by differential gene expression MAST test (Left – enriched in STOSE cancer cells; Right – enriched in ID8 cancer cells). (c) Ridge plot showing distribution of murine ortholog cancer-specific EMT module gene scores in ID8 and STOSE cancer cells in orthotopic tumors.

3.10 Upregulation of Snai1/Snail is insufficient to induce an EMT in ID8 cancer cells

To further explore possible links between EMT and presence and/or activity of immune cells in the TME, we sought to generate a more mesenchymal version of an existing epithelial model. Since ID8 cancer cells are low for EMT activity and ID8 tumors have fewer immune cells (i.e., “cold” tumors) than STOSE tumors(Rodriguez et al., 2022) we decided to determine if inducing EMT in these cells by upregulating a known EMT-associated gene *Snai1*/*Snail* would result in a TME with more immune cells (i.e., “hot” tumor). To achieve this, we generated an ID8 cell line with conditional, doxycycline-inducible overexpression of *Snail*, and confirmed the vector generation and infection protocols using GFP overexpression (**Figure 16a**). We then confirmed overexpression of *Snail* by western blot analysis (**Figure 16b**) and qPCR (**Figure 16c**).

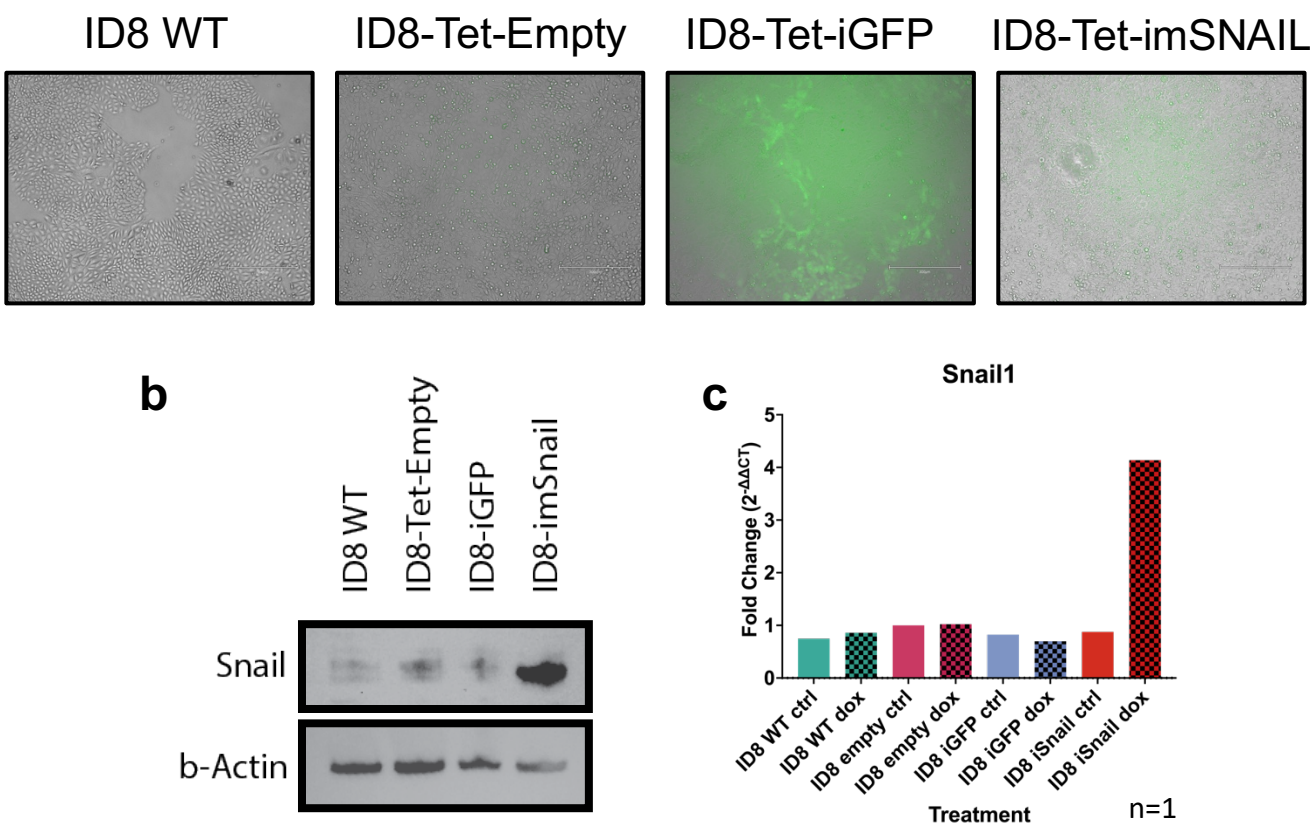

Figure 16. *Snai1* overexpression is driven by rtTA after doxycycline treatment in transgenic ID8 cells. (a) Widefield microscopy images of transgenic ID8 cells with either empty vector (ID8-Tet-Empty), GFP transgene (ID8-Tet-iGFP), or *Snail* overexpression (ID8-Tet-imSnail). Parental ID8 cells (ID8 WT) were used as a control. All cell lines were treated with doxycycline (1 μg/ml) for 3 days. (b) Western blot using *Snai1* antibody on cell lysates from ID8-WT, ID8-Tet-Empty, ID8-Tet-iGFP, and ID8-Tet-imSnail cells after treatment with doxycycline (1 μg/ml) for 3 days. β-actin was used as the loading control (n = 1). (c) Fold change of *Snai1* expression measured by qPCR in ID8 WT, ID8-Tet-Empty, ID8-Tet-iGFP, and ID8-Tet-Snail cells treated with doxycycline (1 μg/ml) for 3 days (n = 1).

To confirm that *Snail* overexpression in ID8 cells initiates EMT, we compared these cells to EMT initiated by TGFβ-1 treatment of the same cells. We treated the cells for 3 days based on previous observations that EMT reaches a maximal transcriptional change at 3 days after treatment of ID8 cells (**Figure 11a-c**). Visual investigation of the cells showed that while the morphology of ID8 cells with an empty or overexpression vector retain phenotypically mesenchymal morphology after TGFβ-1 treatment,

overexpression of *Snail* alone does not result in similar morphology (**Figure 17a, b**). We then probed the different cells for expression of classical EMT markers (*Snai1/Snail*, *Krt19*, *Cdh1*, *Cdh2*, *Sox4*, *Vim*, *Col1a1*, *Col1a2*) and non-classical EMT markers (*Cnn1*, *Actg2*) derived from our scRNA-Seq analysis of the cell lines (**Figure 11a, d**) and found that while doxycycline treatment leads to overexpression of *Snail* (**Figure 17c**), it did not upregulate any EMT-related genes, suggesting that *Snail* overexpression is insufficient for initiation of EMT in ID8 cells.

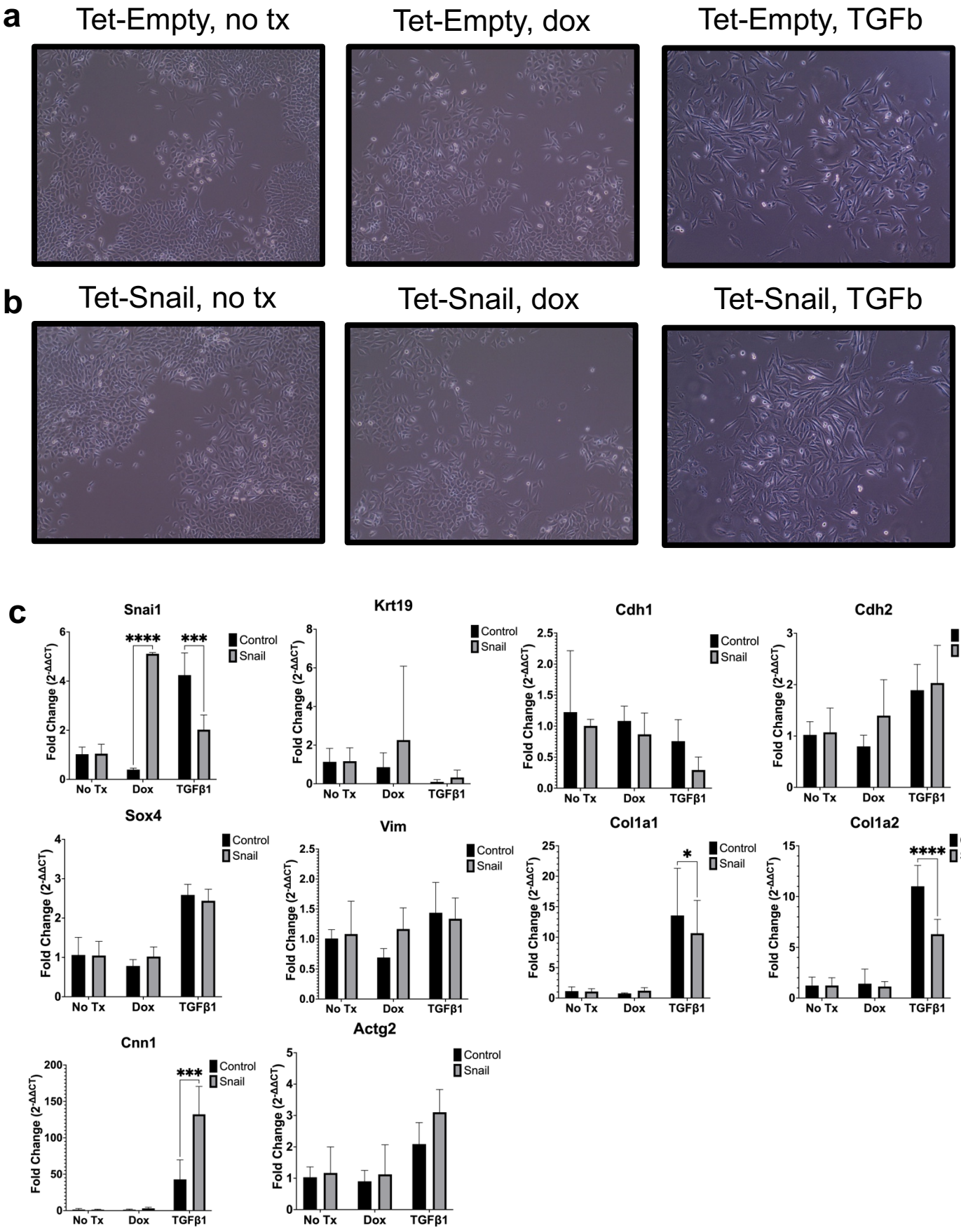
a
Tet-Empty, no tx
Tet-Empty, dox
Tet-Empty, TGFb
b
Tet-Snail, no tx
Tet-Snail, dox
Tet-Snail, TGFb
c
Snai1
Krt19
Cdh1
Cdh2
Sox4
Vim
Col1a1
Col1a2
Cnn1
Actg2
Control
Snail
Fold Change (2-ΔΔCT)
No Tx
Dox
TGFβ1
****
***
*

Figure 17. *Snai1* overexpression in ID8 cells fails to modulate expression of classical and non-classical EMT gene markers. (a, b) Widefield microscopy images of transgenic ID8 cells with either empty vector (Empty), or *Snail* overexpression (Tet-Snail). All cell lines were treated with doxycycline (1 µg/ml) or TGF-β1 (10 ng/mL) for 3 days (n = 3). (c) Log fold change in expression values measured by qPCR of various classical EMT gene markers (*Snai1*, *Krt19*, *Cdh1*, *Cdh2*, *Sox4*, Vim, *Col1a1*, *Col1a2*) and non-classical EMT gene markers (*Cnn1, Actg2*) in ID8-Tet-Empty, ID8-Tet-imSnail cells either untreated or treated with doxycycline (1µg/mL) or TGF-β1 (10 ng/mL) for 3 days (n = 3). Significant differences between Dox and TGF-β1 treated ID8-Snail cells compared to ID-WT control cells (****p < 0.0001; *** p < 0.001) in *Snai1* expression and significant differences in *Col1a1* (*p < 0.05), *Col1a2* (****p < 0.0001), and *Cnn1* (***p < 0.001) in the TGF-β1 treatment group. 1-way ANOVA used as statistical test.

Finally, we performed a proliferation assay and found that *Snail* overexpression failed to affect the proliferation of ID8 cells (**Figure 18**).

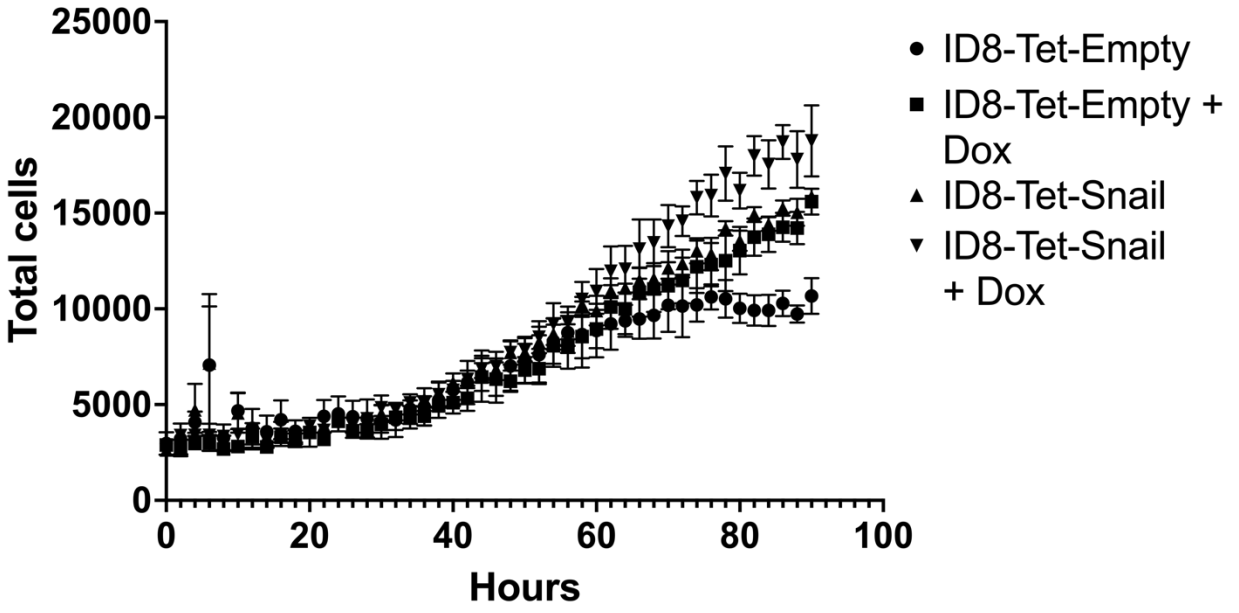

Figure 18. Doxycycline treatment increases proliferation of ID8 cells irrespective of transgene. Growth curve of ID8-Tet-Empty and ID8-Tet-Snail cells treated with doxycycline (1µg/mL) for 3 days, n = 3. Statistics test used is a 2 way ANOVA on each timepoint.

3.11 Upregulation of Snai1 is insufficient to induce an EMT in syngeneic orthotopic ID8 tumors

Despite the lack of EMT response in ID8 cells following *Snail* overexpression, we decided to inject the transgenic cells under the mouse ovarian bursa of C57Bl/6 mice. Two weeks after the injection, overexpression of *Snail* was induced by adding doxycycline to the drinking water. Mice were euthanized at humane endpoint, and there were no differences in survival between tumors generated by the different cell lines (**Figure 19a**). Additionally, there were no differences in mouse weight, tumor weight, ascites volume, and spleen weight at endpoint (**Figure 19b**). Taken together with the results in the previous subsection, *Snai1* overexpression in the cancer cells does not change the ovarian TME sufficiently to affect tumor progression.

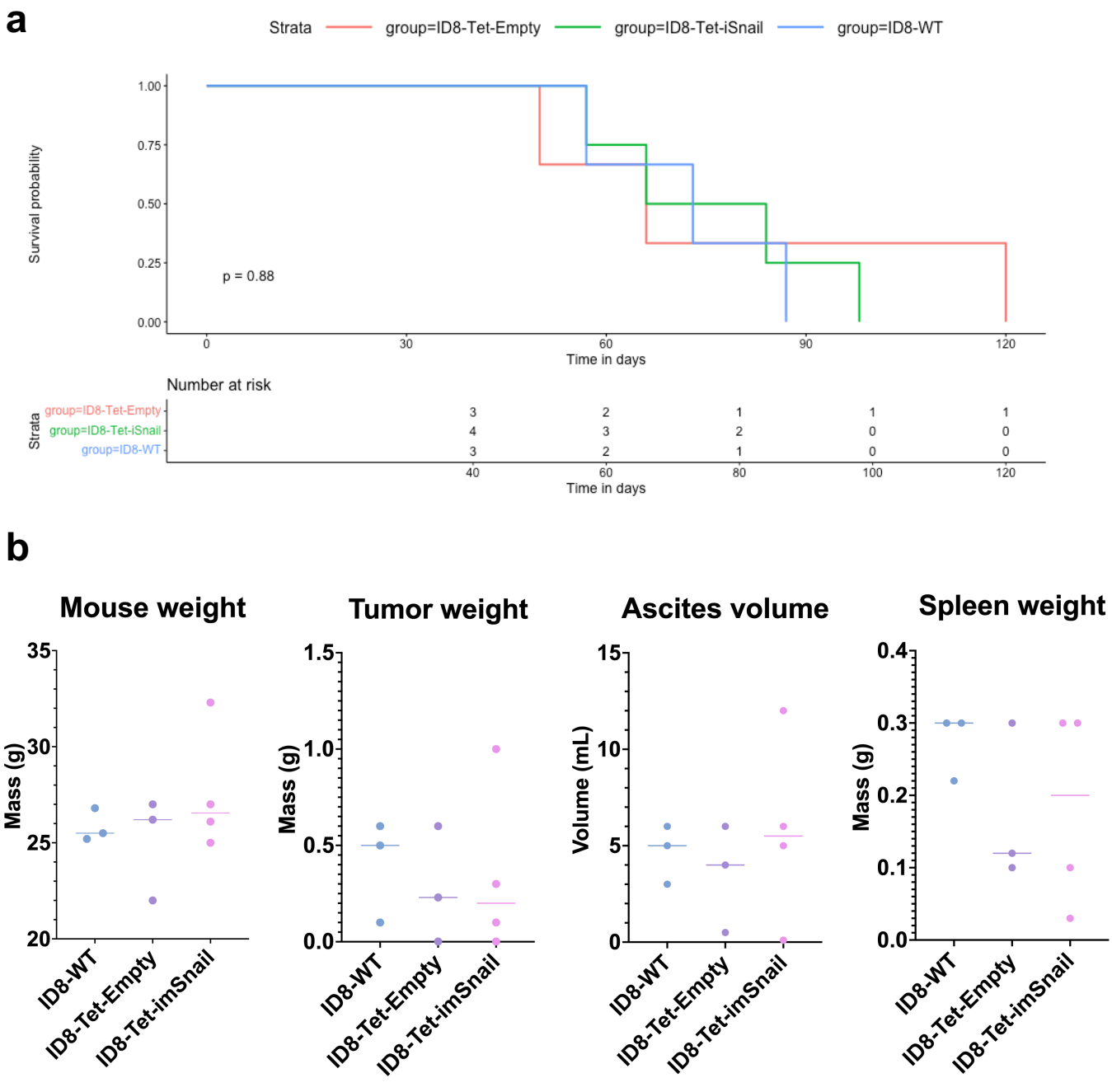

Figure 19. Mice injected orthotopically with Snai1 inducible ID8 cancer cells have no difference in survival compared to mice injected with ID8 parental (WT) cells. (a) Kaplan-Meier survival curves of mice injected under the ovarian bursa with ID8 cells with or without doxycycline-inducible *Snai1* expression. No significant differences (n = 3 for ID8-Tet-Empty and ID8-WT, n = 4 for ID8-Tet-iSnail). (b) Mouse, tumor, and spleen weights and ascites volume collected at endpoint showed no differences among cell lines.

3.12 Upregulation of Snai2/Slug is insufficient to induce an EMT in ID8 cancer cells

A similar counterpart to *Snail* is the sister protein *Slug* which has been shown to induce EMT in some cell lines(Sun et al., 2014; M. Zheng et al., 2015). Similar to our *Snail* experiments, we determined if overexpression of *Slug* in ID8 cells could potentially induce an EMT and turn the canonically “cold” ID8 TME into a “hot” TME. Visual assessment of cellular morphology following doxycycline-driven *Slug* overexpression confirmed that cells treated with doxycycline did not gain mesenchymal cell morphology when compared to cells treated with TGFβ-1 (**Figure 20a, b**). When we probed for classical and non-classical EMT genes when cells bearing the overexpression construct were treated with doxycycline, there was an increase in *Slug* expression, as well as an unexpected increase in *Cdh1* expression (** $p < 0.01$) where a decrease was expected after EMT induction (**Figure 20c**).

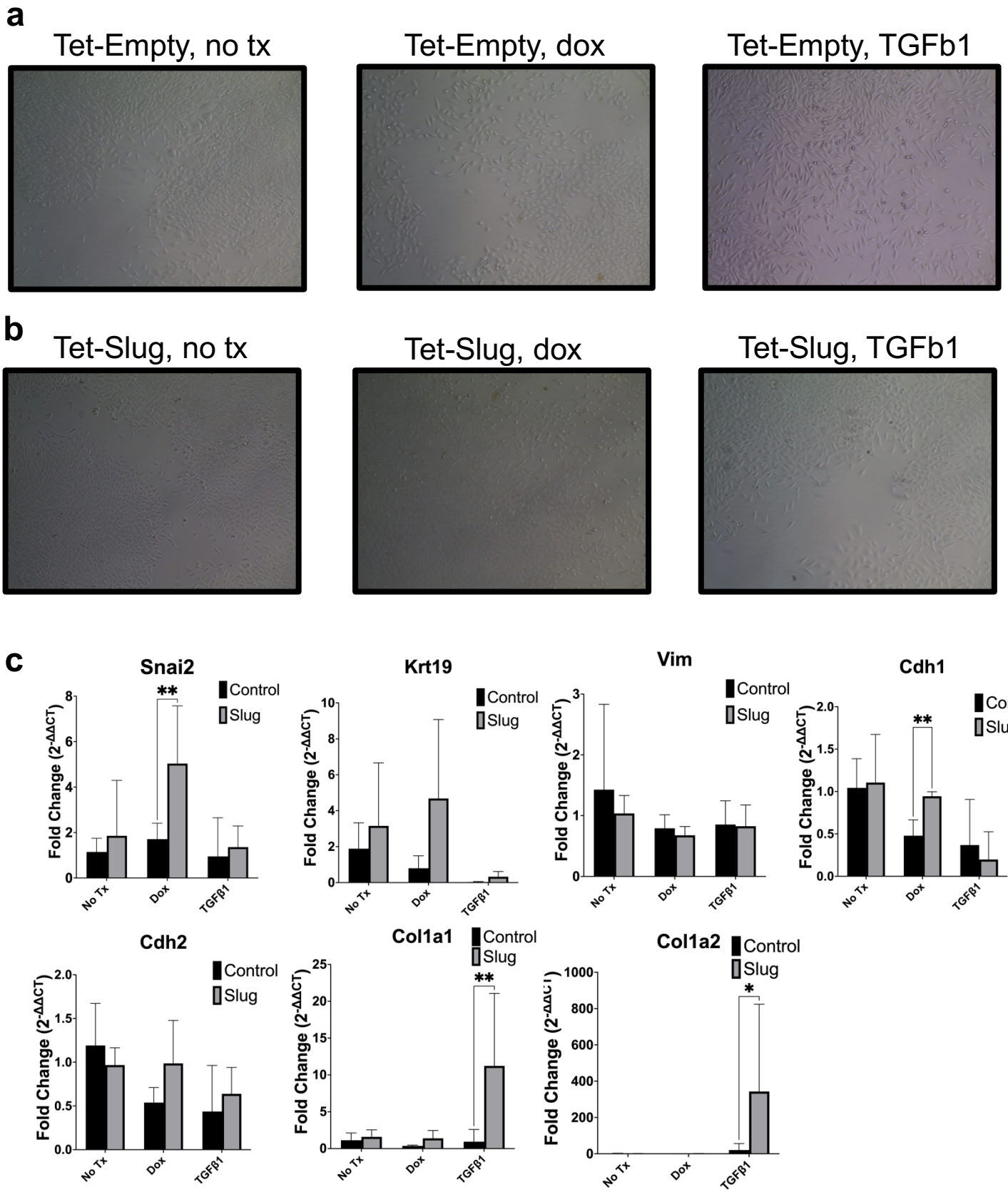
a
Tet-Empty, no tx
Tet-Empty, dox
Tet-Empty, TGFb1
b
Tet-Slug, no tx
Tet-Slug, dox
Tet-Slug, TGFb1
c
Snai2
Krt19
Vim
Cdh1
Cdh2
Col1a1
Col1a2
Control
Slug
Fold Change (2-ΔΔCT)
No Tx
Dox
TGFβ1
**
*

Figure 20. *Snai1* overexpression in ID8 cells fails to change cell morphology or expression of classical EMT markers. (a, b) Representative widefield microscopy images of transgenic ID8 cells with either empty vector (Empty) or *Slug* overexpression (Tet-Slug). All cell lines were treated with doxycycline (1 µg/ml) or TGF-β1 (10 ng/mL) for 3 days (n = 3). (c) Log fold change in gene expression values measured by qPCR of various classical EMT markers (*Snai1*, Vim, *Krt19*, *Cdh1*, *Cdh2*, *Sox4*, *Col1a1*, *Col1a2*) in ID8-Tet-Empty, ID8-Tet-imSnail cells treated with either no treatment, doxycycline (1µg/mL), or TGF-β1 (10 ng/mL) (n = 3). Significant differences between Dox treated ID8-Slug cells compared to ID-WT control cells (** $p < 0.01$) in *Snai2* expression and significant differences in *Col1a1* (**$p < 0.01$) and *Col1a2* (*$p < 0.05$) in the TGF-β1 group, and *Cdh1* (**$p < 0.01$) in the Dox treatment group. 1-way ANOVA used as statistical test.

Finally, we attempted to see if *Slug* overexpression leads to a reduction in the proliferative capacity of cells, as can sometimes be seen in mesenchymal cells, which are slower to proliferate than epithelial cells (Lovisa et al., 2015; Prakash et al., 2019). There were no significant differences in any of the groups when measuring the growth rate of the cells using an Incucyte cell counter (**Figure 21**). Taken together, we concluded that *Slug* overexpression in ID8 cells is insufficient to induce an EMT. Thus, we chose not to attempt to test *in vivo* if overexpression of *Slug* might affect the TME.

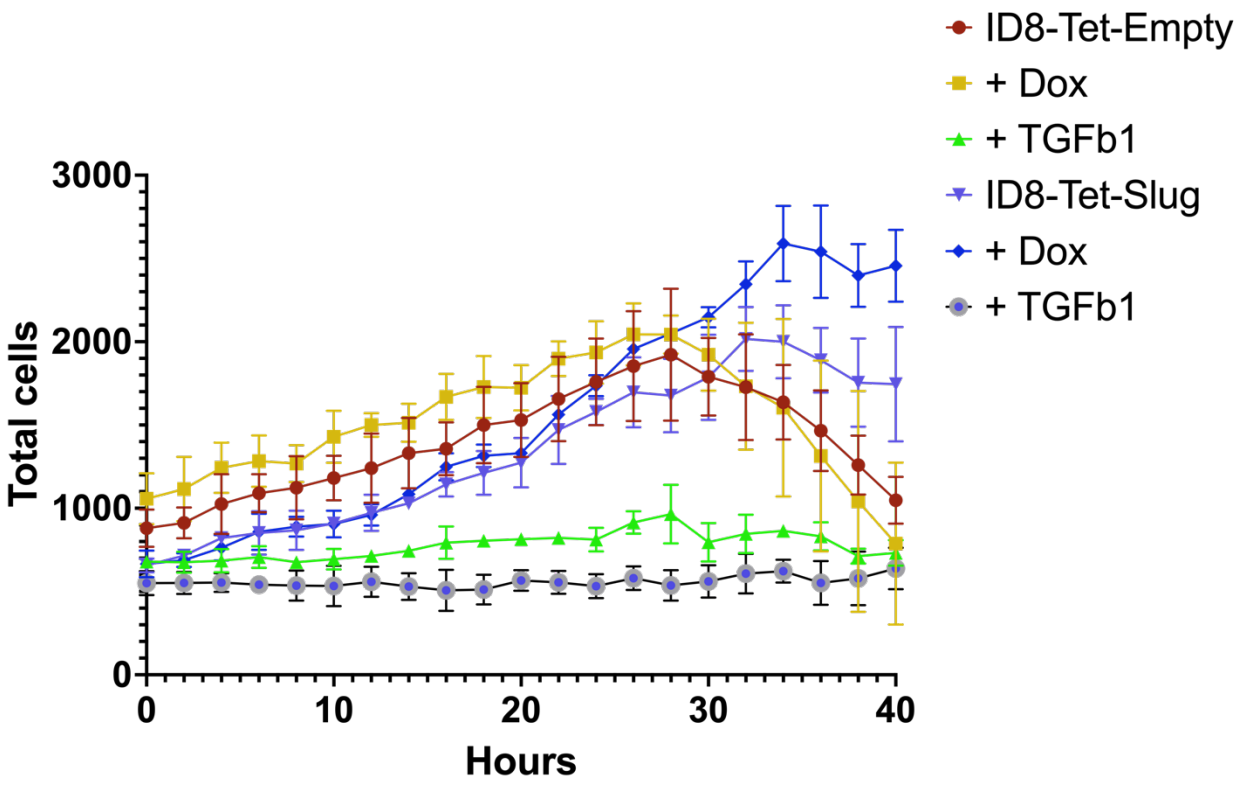

Figure 21. Upregulation of *Slug* does not change proliferation of ID8 cells. Growth curve of ID8-Tet-Empty and ID8-Tet-Slug cells treated with doxycycline (1μg/mL) or TGF-β1 (10 ng/mL) for 3 days (n = 3). Statistics test used is a 2 way ANOVA on each timepoint.

3.13 An immune-infiltrated TME does not confer EMT in cancer cells

With our attempts to turn an immune "cold" TME into a "hot" one by inducing EMT in cancer cells unsuccessful, we decided to explore whether a "reverse" situation is possible where the presence of immune cells in the TME confers a greater number of mesenchymal cells. To do this, we injected STOSE cancer cells under the bursa into either FVB/N mice or SCID mice and hypothesized that in the absence of both B and T lymphocytes in the SCID mice, the STOSE TME will have fewer mesenchymal cells when compared to STOSE tumors from FVB/N mice. Because we would be measuring mesenchymal cell presence in a whole tumor by qPCR, we first had to find markers specific to mesenchymal cells in a robust TME. We leveraged our scRNA-Seq of mouse tumors from **Figure 11a-d** and scored the cells for EMT activity with our cancer-specific

EMT module. Then, we performed a differential gene expression analysis comparing mesenchymal cells to epithelial cells which resulted in a set of mesenchymal cancer cell specific markers *Ifrd1*, *Hbegf*, *Klf4*, *Cxcl1* (**Figure 22a**). We then performed qPCR on whole tumors and found no significant differences in mesenchymal cancer cell markers between wild-type FVB/N and SCID mice (**Figure 22b**). We then refined our differential gene expression analysis to compare the transcriptome of mesenchymal cancer cells to all cell fractions in the TME rather than to just epithelial cancer cells (**Figure 22c**) and selected the markers *Fam162a*, *Higd1a*, *Edn2*, *Pgk1*. We then probed for this new panel of markers and found that while none of the markers were significantly different, *Higd1a* ($p = 0.0527$) and *Edn2* ($p = 0.0599$) trended higher in SCID mice (**Figure 22d**) suggesting that in the absence of immune cells, EMT increases. Hypoxia-inducible gene domain family member 1A (*Higd1a*), a survival factor related to Hypoxia inducible factor 1 (HIF-1), has been previously linked to survival of cancer cells (Ameri et al., 2015) *in vivo* while the role of endothelin 2 (*Edn2*) has yet to be fully elucidated in cancer (X. Wang et al., 2021) though epigenetic silencing of *Edn2* has been noted in colon cancer (R. Wang et al., 2013). Taken together, the initial observation suggesting a correlation between EMT and the presence of immune cells in the TME is yet to be validated in a mouse model and may suggest that ID8 and STOSE murine models of ovarian cancer are inadequate to study the interaction of EMT and immune cell presence.

a

DGE of Mes cells vs. Epi cells

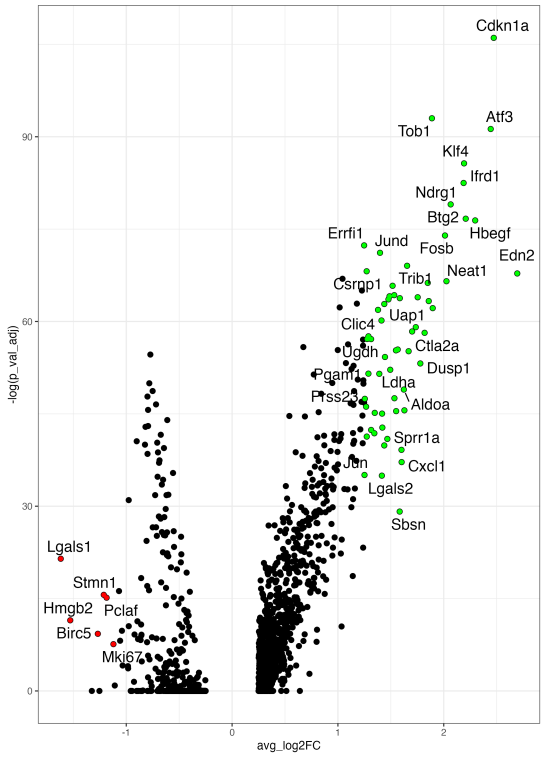

b

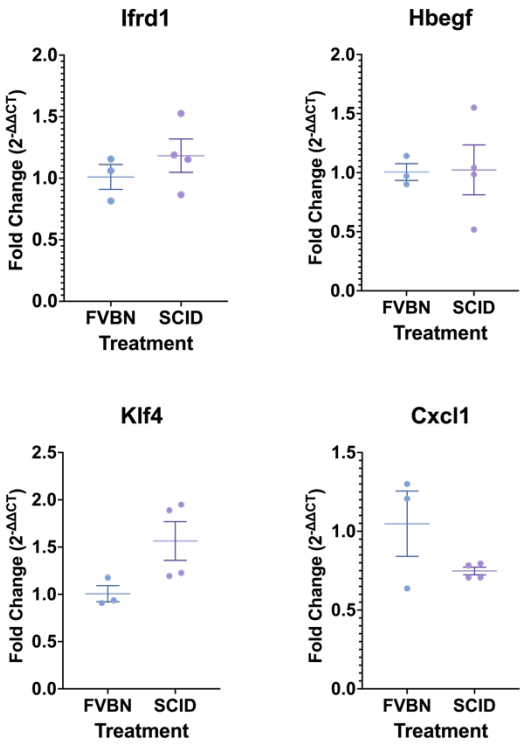

c

DGE of Mes cells vs. whole tumor

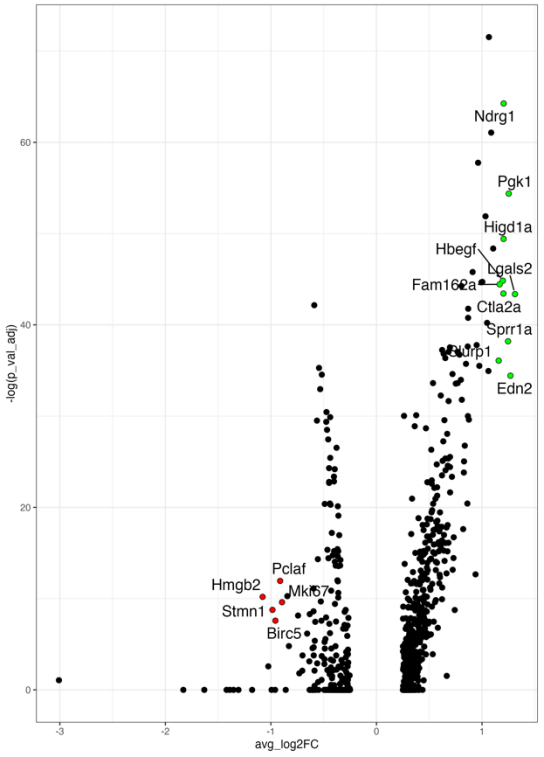

d

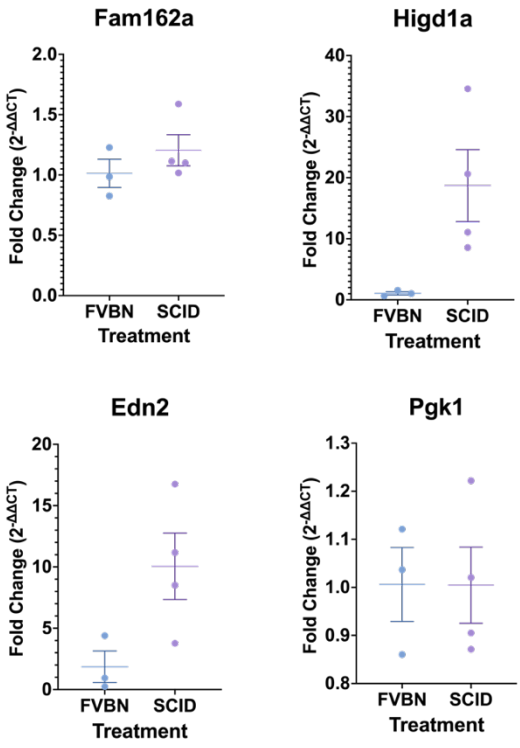

Figure 22. Increased mesenchymal cell presence in STOSE tumors is not driven by immune cells. (a) Volcano plot showing differentially expressed genes generated with a Poisson test between EMT-high and EMT-low cancer cells from orthotopic STOSE tumor (right – genes highest in EMT-high STOSE cancer cells, left – genes highest in EMT-low STOSE cancer cells). (b) Fold change expression levels measured by qPCR of genes chosen from differential gene expression test in bulk orthotopic STOSE tumors from either wild-type FVBN mice or immunocompromised SCID mice (n = 3 FVBN control; n = 4 SCID). (c) Volcano plot showing differentially expressed genes generated with a Poisson test between EMT-high cancer cells and all other cell populations from orthotopic STOSE tumor (right – genes highest in EMT-high STOSE cancer cells, left – genes highest in all other STOSE tumor cell populations). (d) Fold change expression levels measured by qPCR of genes chosen from differential gene expression test in bulk orthotopic STOSE tumors from either wild-type FVB/N mice or immunocompromised SCID mice (n = 3 FVBN control; n = 4 SCID).

Chapter 4: Mesenchymal ovarian cancer cells promote CD8$^+$ T cell exhaustion through the LGALS3-LAG3 axis

These results have been published in *Npj Syst. Biol. Appl.* **9**, 1–17 (2023).

Edward Yakubovich*[1,2,3], David P. Cook[1,2], Galaxia M. Rodriguez[1,2,3], Barbara C. Vanderhyden[1,2,3]

1. Department of Cellular and Molecular Medicine, University of Ottawa, Ottawa, ON, Canada.

2. Cancer Therapeutics Program, Ottawa Hospital Research Institute, Ottawa, ON, Canada.

3. Center for Infection, Immunity and Inflammation, University of Ottawa, ON, Canada

David P. Cook provided the data for the OVCA420 cells treated with TGF-β1 and his expertise in bioinformatics analysis, as well as assistance in editing of the final manuscript draft. Galaxia M. Rodriguez helped with conceptualization and editing of the final manuscript draft.

Given the finding that the increased presence of mesenchymal cells in tumors appears to correlate with the increased presence of immune cells in our mouse models, we continued the characterization of the impact of EMT in ovarian cancer by turning to *in vivo* human tumors. Leveraging single-cell transcriptomic datasets and our successful EMT scoring strategy with the cancer specific EMT module, we performed a cell-cell communication analysis to identify potential vectors of immunosuppression in the ovarian TME. In particular, we explored the receptor-ligand pairs that could underlie immunosuppression by mesenchymal cancer cells against $CD8^+$ T cells, with a specific focus on the phenomenon of T cell exhaustion, something that has only recently been associated with worse prognosis in ovarian cancer patients (K. Wang et al., 2023; Yuan et al., 2023).

4.1 Comparing single-cell profiles of distinct immune phenotypes of HGSOC

To assess how EMT contributes to the activity, immunosuppression and/or exhaustion of $CD8^+$ T cells, we began by accessing a scRNA-Seq dataset of 16 human ovarian cancers (Hornburg et al., 2021). The plan for this data analysis is summarized in **Figure 23a**. We chose this dataset due to its inclusion of immune phenotyping metadata confirmed by histology. We assessed for quality-control and clustered every sample individually by merging the respective $CD45^+$, tumor, and stromal fractions of each individual dataset before using a semi-supervised labeling method to identify the individual cell types comprising each tumor sample, as described in the Methods. The tumor samples analyzed are from a single study where each tumor was processed with an identical protocol (Desbois et al., 2020; Hornburg et al., 2021). Although this protocol

may introduce cell type biases, the assumption is that they are consistent among samples.

First, we overlaid the immune phenotypes of the samples in a UMAP to visualize the grouping of all the cells (**Figure 23b**). Next, we overlaid the results from our semi-supervised labeling method (**Figure 23c-d**) to label the cell types onto the UMAP. While there is some intracellular heterogeneity, most populations group together irrespective of the tumor immune phenotype. This suggests that infiltration status phenotypes minimally contribute to dimensionality reduction and clustering of the cell populations. By examining the population proportion breakdown in the TME by immune phenotype metadata (**Figure 23e, Figure 24**), it was found that semi-supervised labeling of the 16 tumors matches the originally published findings with respect to immune phenotype, where in infiltrated tumors there are the most $CD45^+$ cells relative to cancer cells, fewer $CD45^+$ cells relative to cancer cells in excluded tumors, and fewest $CD45^+$ cells relative to cancer cells in desert tumors. This confirms that our cell labeling method was accurate in correctly identifying $CD45^+$ and $CD45^-$ cells.

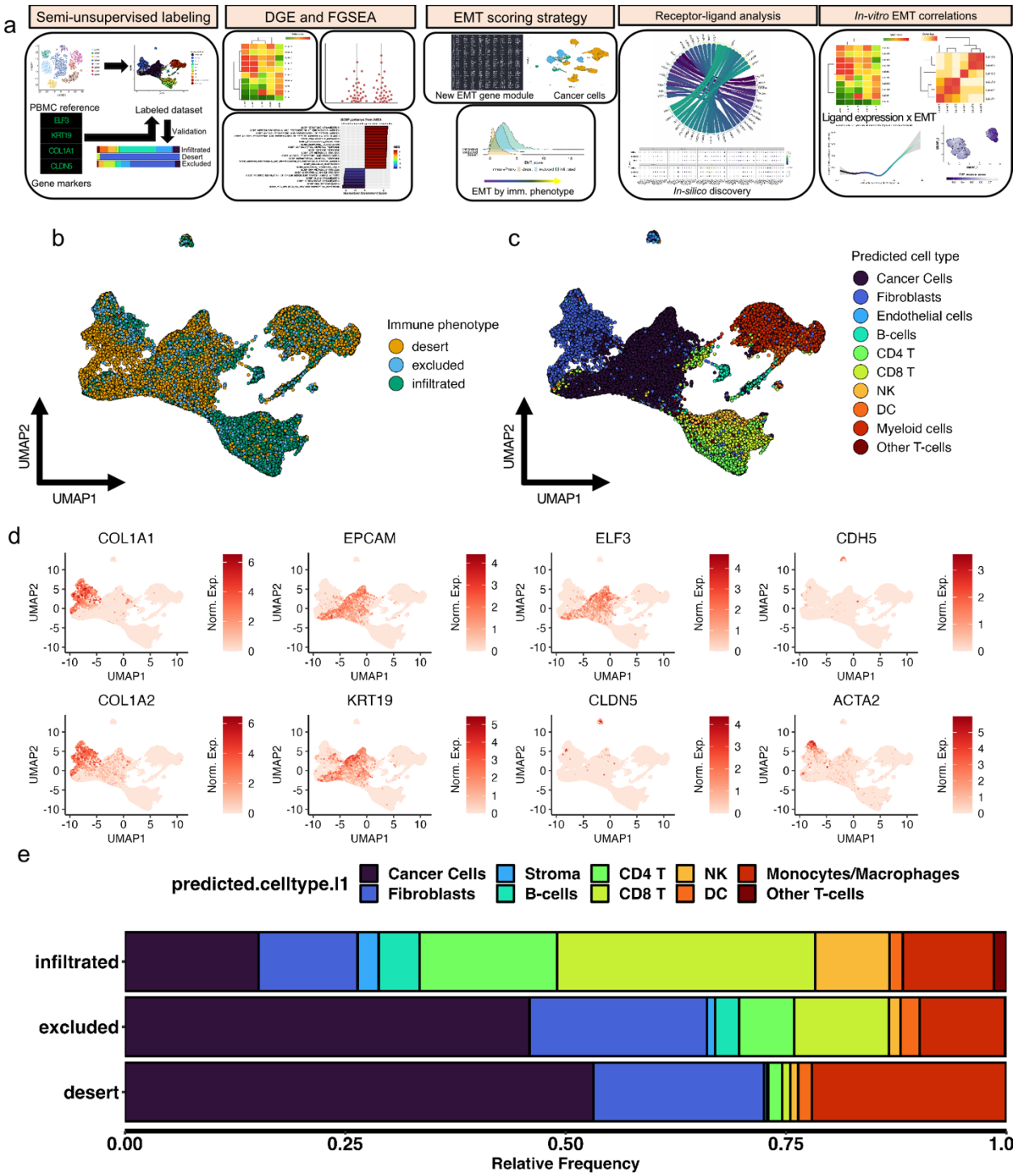

Figure 23. Identification of cell populations from patient-derived tumor cells *in silico* confirms greater immune cell presence in infiltrated tumors compared to excluded and desert tumors. (a) Schematic big-picture overview of analysis and experimental validation procedures. (b) Uniform manifold and approximation projection (UMAP) of patient derived tumor cells colored by tumor immune phenotype. (c) Labeled UMAP from patient derived tumor cells colored by cell population. (d) Series of UMAPs

colored by individual gene expression levels in various cell populations from patient derived tumors: *KRT19, ELF3, EPCAM* for cancer cells; *COL1A1*, *COL1A2* for fibroblasts; *CDH5, CLDN5* for endothelial cells; *ACTA2* for smooth muscle cells. (e) Relative frequency of overall cell populations in patient derived tumor samples separated by immune phenotype and colored by cell population.

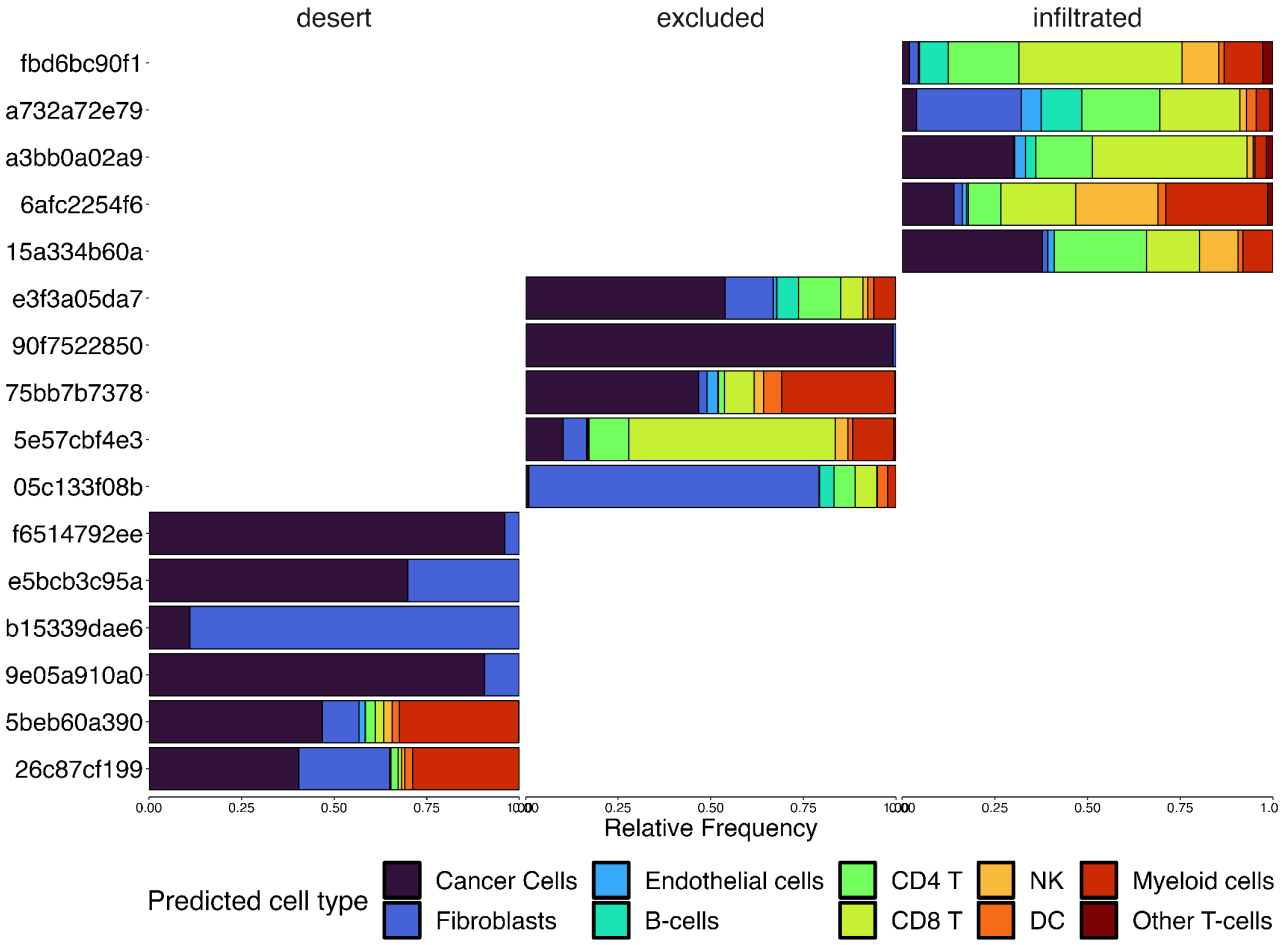

Figure 24. Individual infiltrated tumors have a larger proportion of immune cells compared to excluded or desert tumors. Overall cell population proportions in patient derived tumor cells separated by patient ID and colored by cell population.

To assess the role of cancer cells in contributing to the unique composition of each immune phenotype, we performed DGE analysis to identify the most highly expressed and least expressed genes in the infiltrated TME relative to the desert TME (**Figure 25a**) and excluded TME (**Figure 25b)**. Cancer cells from infiltrated TMEs differentially express genes related to immune regulation within the context of carcinogenesis, such as: *B2M* (H. Zhang et al., 2021), *SLPI* (Nugteren & Samsom, 2021), *HLA-A* (Sabbatino et al., 2020), *ELF3* (H. Xu et al., 2021, p. 3), *MUC1* (David et al., 2016, p. 1), *MDK* (Filippou et al., 2020), *CXCL17* (MacGregor et al., 2019) and others. Based on upregulation of these immune regulatory genes, we performed GSEA

first comparing cancer cells from the infiltrated to the desert TMEs. We discovered that many gene ontology biological pathways (GOBP) related to immune regulation were upregulated in cancer cells from infiltrated TMEs (**Figure 25c-d**). Among the main findings, some pathways were related to chemotaxis and enrichment for processes related to antigen presentation and cytokine activity, suggesting that cancer cells in infiltrated tumors actively participate in modulating the immune response and shape the tumor immune phenotype. Similar results were obtained when investigating the pathway enrichment analyses comparing cancer cells from infiltrated versus excluded TMEs (**Figure 25e**) and excluded to desert TMEs (**Figure 26**) suggesting that pathways related to immune regulation could be “turned on” either as a response to immune infiltration or as a precursor to the arrival of immune cells promoted by cancer cells themselves. These results may be indicative of EMT-related cell-cell signaling driving chemotaxis of various $CD45^+$ cells from different populations to the TME.

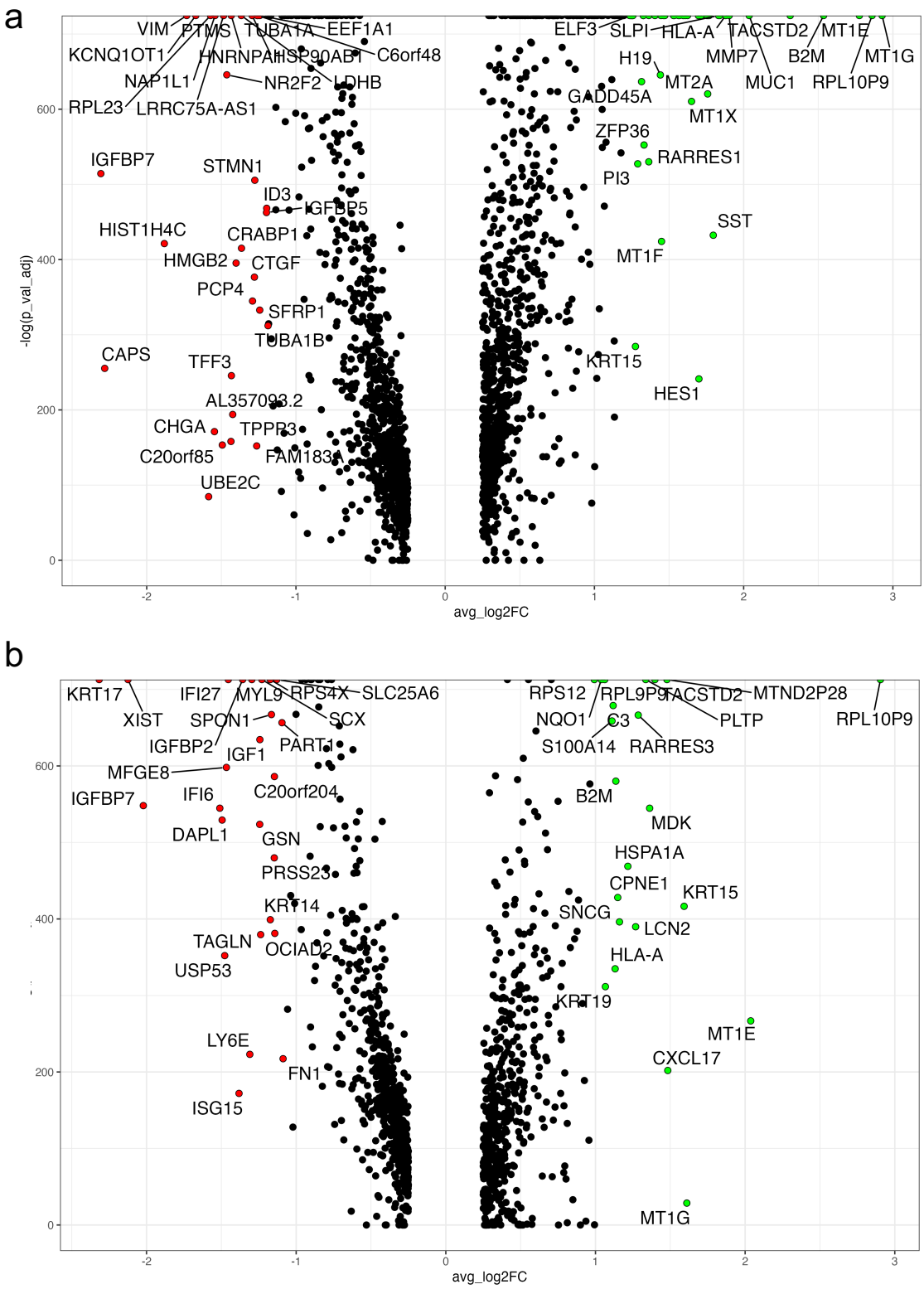
a
VIM
PTMS
TUBA1A
EEF1A1
KCNQ1OT1
HNRNPAB
HSP90AB1
C6orf48
NAP1L1
NR2F2
LDHB
RPL23
LRRC75A-AS1
IGFBP7
STMN1
ID3
IGFBP5
HIST1H4C
CRABP1
HMGB2
CTGF
PCP4
SFRP1
TUBA1B
CAPS
TFF3
AL357093.2
CHGA
TPPP3
C20orf85
FAM183A
UBE2C
ELF3
SLPI
HLA-A
TACSTD2
MT1E
H19
MMP7
B2M
MT1G
MT2A
MUC1
RPL10P9
GADD45A
MT1X
ZFP36
RARRES1
PI3
SST
MT1F
KRT15
HES1
-log(p_val_adj)
avg_log2FC
b
KRT17
IFI27
MYL9
RPS4X
SLC25A6
XIST
SPON1
SCX
IGFBP2
IGF1
PART1
MFGE8
IGFBP7
IFI6
C20orf204
DAPL1
GSN
PRSS23
KRT14
TAGLN
OCIAD2
USP53
LY6E
FN1
ISG15
RPS12
RPL9P9
TACSTD2
MTND2P28
NQO1
C3
PLTP
RPL10P9
S100A14
RARRES3
B2M
MDK
HSPA1A
CPNE1
KRT15
SNCG
LCN2
HLA-A
KRT19
MT1E
CXCL17
MT1G
avg_log2FC

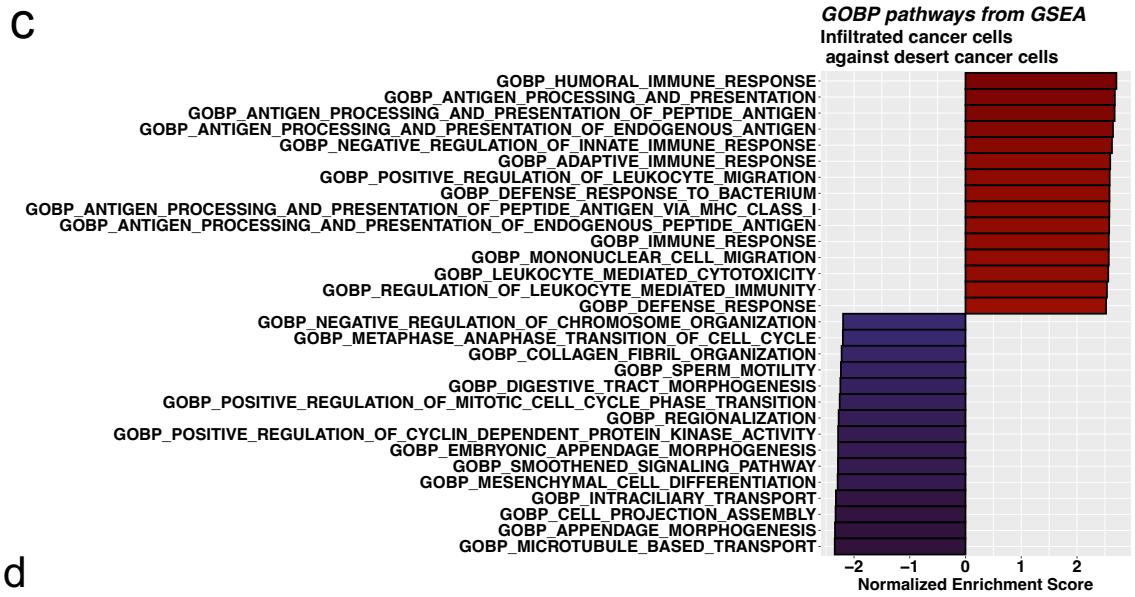
c
GOBP pathways from GSEA
Infiltrated cancer cells
against desert cancer cells
GOBP_HUMORAL_IMMUNE_RESPONSE
GOBP_ANTIGEN_PROCESSING_AND_PRESENTATION
GOBP_ANTIGEN_PROCESSING_AND_PRESENTATION_OF_PEPTIDE_ANTIGEN
GOBP_ANTIGEN_PROCESSING_AND_PRESENTATION_OF_ENDOGENOUS_ANTIGEN
GOBP_NEGATIVE_REGULATION_OF_INNATE_IMMUNE_RESPONSE
GOBP_ADAPTIVE_IMMUNE_RESPONSE
GOBP_POSITIVE_REGULATION_OF_LEUKOCYTE_MIGRATION
GOBP_DEFENSE_RESPONSE_TO_BACTERIUM
GOBP_ANTIGEN_PROCESSING_AND_PRESENTATION_OF_PEPTIDE_ANTIGEN_VIA_MHC_CLASS_I
GOBP_ANTIGEN_PROCESSING_AND_PRESENTATION_OF_ENDOGENOUS_PEPTIDE_ANTIGEN
GOBP_IMMUNE_RESPONSE
GOBP_MONONUCLEAR_CELL_MIGRATION
GOBP_LEUKOCYTE_MEDIATED_CYTOTOXICITY
GOBP_REGULATION_OF_LEUKOCYTE_MEDIATED_IMMUNITY
GOBP_DEFENSE_RESPONSE
GOBP_NEGATIVE_REGULATION_OF_CHROMOSOME_ORGANIZATION
GOBP_METAPHASE_ANAPHASE_TRANSITION_OF_CELL_CYCLE
GOBP_COLLAGEN_FIBRIL_ORGANIZATION
GOBP_SPERM_MOTILITY
GOBP_DIGESTIVE_TRACT_MORPHOGENESIS
GOBP_POSITIVE_REGULATION_OF_MITOTIC_CELL_CYCLE_PHASE_TRANSITION
GOBP_REGIONALIZATION
GOBP_POSITIVE_REGULATION_OF_CYCLIN_DEPENDENT_PROTEIN_KINASE_ACTIVITY
GOBP_EMBRYONIC_APPENDAGE_MORPHOGENESIS
GOBP_SMOOTHENED_SIGNALING_PATHWAY
GOBP_MESENCHYMAL_CELL_DIFFERENTIATION
GOBP_INTRACILIARY_TRANSPORT
GOBP_CELL_PROJECTION_ASSEMBLY
GOBP_APPENDAGE_MORPHOGENESIS
GOBP_MICROTUBULE_BASED_TRANSPORT
−2 −1 0 1 2
Normalized Enrichment Score

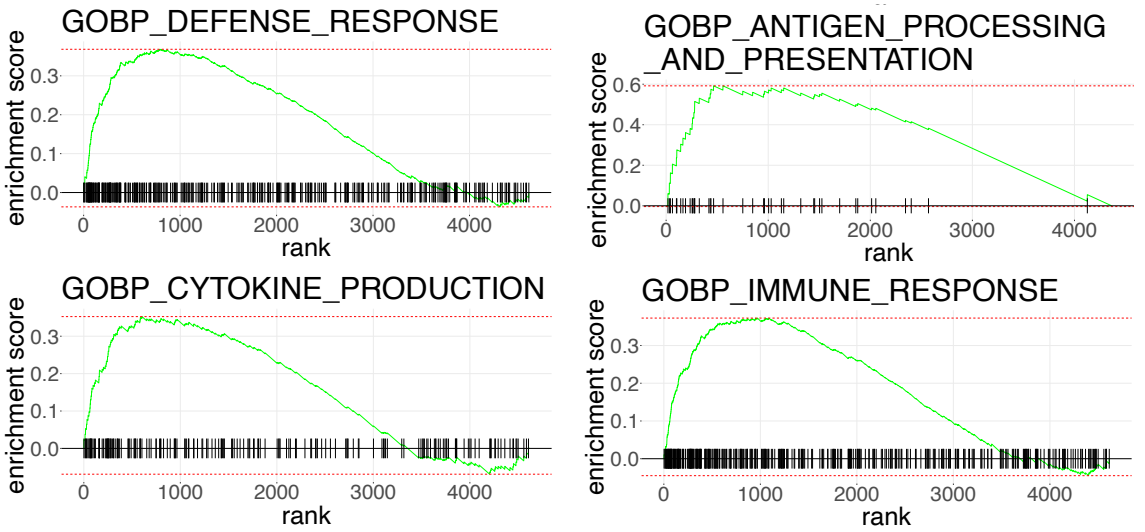
d
GOBP_DEFENSE_RESPONSE
GOBP_ANTIGEN_PROCESSING
_AND_PRESENTATION
GOBP_CYTOKINE_PRODUCTION
GOBP_IMMUNE_RESPONSE
enrichment score
rank
0 1000 2000 3000 4000
0.0 0.1 0.2 0.3
0.0 0.2 0.4 0.6

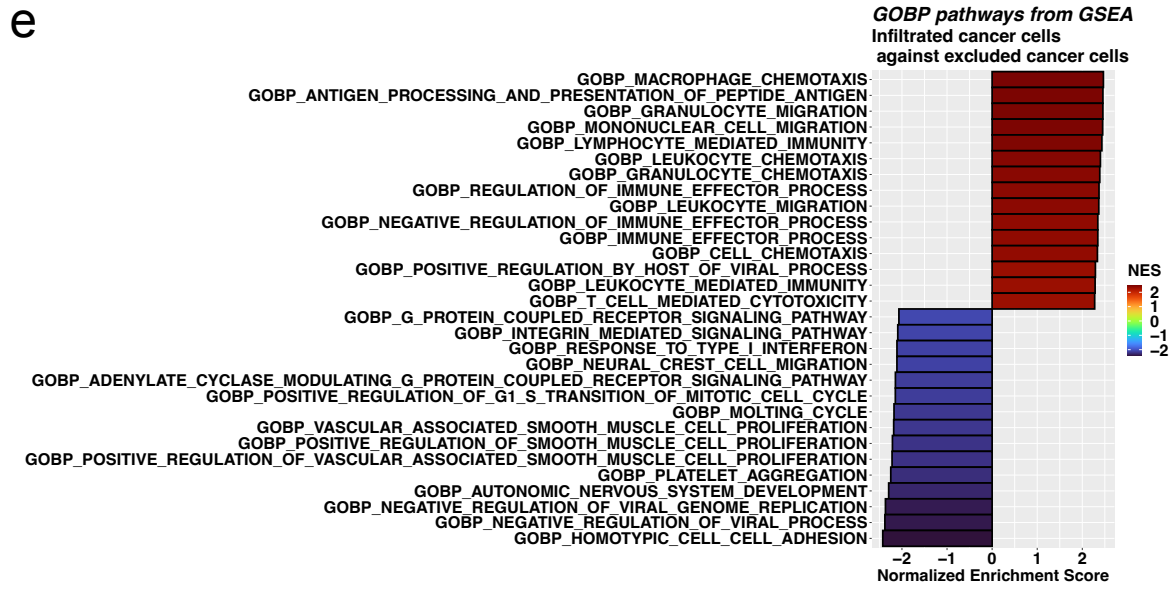
e
GOBP pathways from GSEA
Infiltrated cancer cells
against excluded cancer cells
GOBP_MACROPHAGE_CHEMOTAXIS
GOBP_ANTIGEN_PROCESSING_AND_PRESENTATION_OF_PEPTIDE_ANTIGEN
GOBP_GRANULOCYTE_MIGRATION
GOBP_MONONUCLEAR_CELL_MIGRATION
GOBP_LYMPHOCYTE_MEDIATED_IMMUNITY
GOBP_LEUKOCYTE_CHEMOTAXIS
GOBP_GRANULOCYTE_CHEMOTAXIS
GOBP_REGULATION_OF_IMMUNE_EFFECTOR_PROCESS
GOBP_LEUKOCYTE_MIGRATION
GOBP_NEGATIVE_REGULATION_OF_IMMUNE_EFFECTOR_PROCESS
GOBP_IMMUNE_EFFECTOR_PROCESS
GOBP_CELL_CHEMOTAXIS
GOBP_POSITIVE_REGULATION_BY_HOST_OF_VIRAL_PROCESS
GOBP_LEUKOCYTE_MEDIATED_IMMUNITY
GOBP_T_CELL_MEDIATED_CYTOTOXICITY
GOBP_G_PROTEIN_COUPLED_RECEPTOR_SIGNALING_PATHWAY
GOBP_INTEGRIN_MEDIATED_SIGNALING_PATHWAY
GOBP_RESPONSE_TO_TYPE_I_INTERFERON
GOBP_NEURAL_CREST_CELL_MIGRATION
GOBP_ADENYLATE_CYCLASE_MODULATING_G_PROTEIN_COUPLED_RECEPTOR_SIGNALING_PATHWAY
GOBP_POSITIVE_REGULATION_OF_G1_S_TRANSITION_OF_MITOTIC_CELL_CYCLE
GOBP_MOLTING_CYCLE
GOBP_VASCULAR_ASSOCIATED_SMOOTH_MUSCLE_CELL_PROLIFERATION
GOBP_POSITIVE_REGULATION_OF_SMOOTH_MUSCLE_CELL_PROLIFERATION
GOBP_POSITIVE_REGULATION_OF_VASCULAR_ASSOCIATED_SMOOTH_MUSCLE_CELL_PROLIFERATION
GOBP_PLATELET_AGGREGATION
GOBP_AUTONOMIC_NERVOUS_SYSTEM_DEVELOPMENT
GOBP_NEGATIVE_REGULATION_OF_VIRAL_GENOME_REPLICATION
GOBP_NEGATIVE_REGULATION_OF_VIRAL_PROCESS
GOBP_HOMOTYPIC_CELL_CELL_ADHESION
−2 −1 0 1 2
Normalized Enrichment Score
NES
2
1
0
−1
−2

Figure 25. Cancer cells from infiltrated tumors upregulate signaling pathways related to immune cell chemotaxis, immune modulation, and antigen presentation compared to cancer cells from excluded or desert tumors. (a, b) Volcano plots of differentially expressed genes (DGE) between cancer cells of desert and infiltrated tumors and excluded and infiltrated tumors. (c) Enrichment plot of infiltrated GOBP terms from GSEA of a selection of significant (*p-adjusted < 0.05) pathways between cancer cells of infiltrated (red) and desert tumors (blue). (d) GSEA enrichment ranks of significantly upregulated (*p-adjusted < 0.05) pathways related to immune regulation in cancer cells from infiltrated tumors. (e) Enrichment plot of infiltrated GOBP terms from GSEA of a selection of significant (*p-adjusted < 0.05) pathways between cancer cells of infiltrated (red) and excluded tumors (blue).

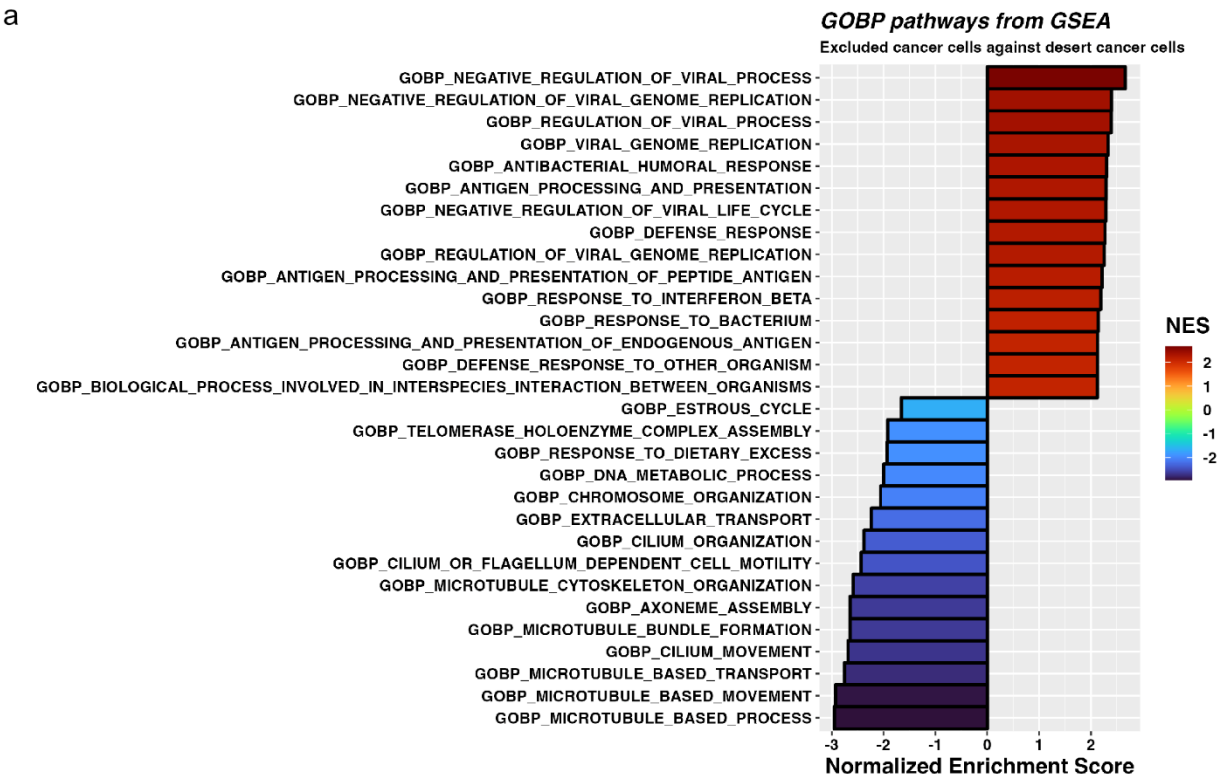

Figure 26. Fast gene set enrichment (FGSEA) analysis of enriched biological pathways in DEGs between cancer cells of infiltrated and excluded TMEs, and of excluded and desert TMEs. FGSEA analysis of biological pathways enriched by DEGs overexpressed in cancer cells from excluded TMEs compared to cancer cells from desert TMEs.

4.2 Cancer cells from infiltrated tumors are more mesenchymal compared to cancer cells from other immune phenotypes

Our discovery that cancer cells in infiltrated TMEs activate immune regulatory pathways prompted us to assess the EMT status of cancer cells given that cells in partial or fully mesenchymal states are known for their immunoregulatory capabilities (Rivera-Cruz et al., 2017; Trivanović et al., 2016; Weiss & Dahlke, 2019). Hornburg et al. (2021) (Hornburg et al., 2021) showed that desert TMEs contain malignant cells with higher expression of EMT-associated genes using the MSigDB Hallmark gene set (Liberzon et al., 2015). Our gene set scoring using the subset of 58 Hallmark genes they found associated with the desert tumors reproduced their findings (**Figure 27a-b**). However,

when we performed gene set scoring on the cells with the complete 200-gene Hallmark gene set, no difference was found between tumor immune phenotypes (**Figure 27c-d**). By applying GSEA enrichment analysis of either the Hallmark gene module, the Hornburg gene subset, or our cancer-specific gene module, we also found the Hornburg subset enriched in DEGs from desert-derived cancer cells, whereas applying both the full Hallmark EMT gene set and our cancer-specific EMT gene signature yielded negative enrichment scores (**Figure 27e**).

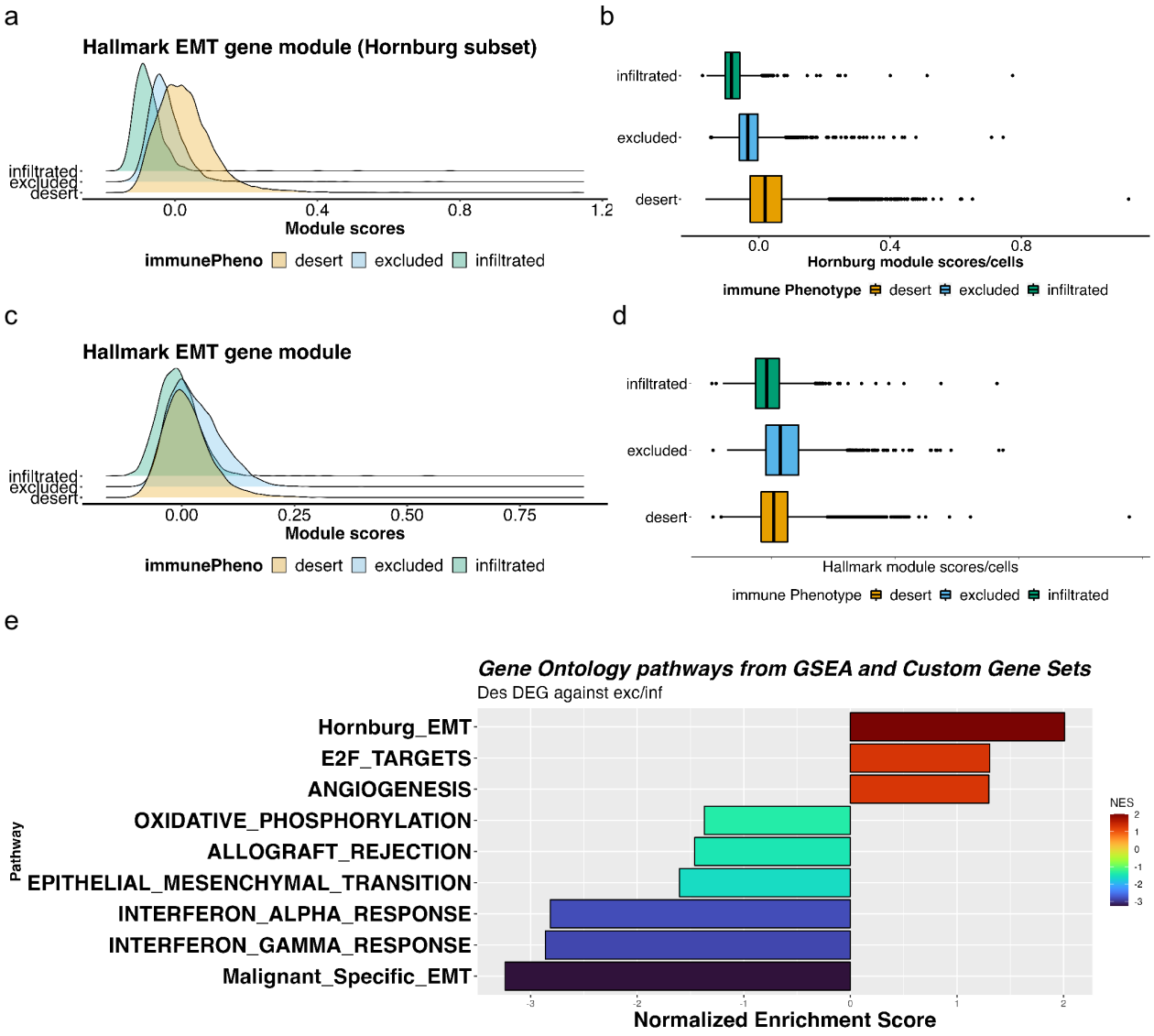

Figure 27. A comparison of different EMT gene module scores on cancer cells from TMEs with different immune phenotypes. (a) Ridge plot of Hornburg EMT module scores (derivative of Hallmark EMT module) split by immune phenotypes (b) Boxplot of Hornburg EMT module scores split by immune phenotypes. (c) Ridge plot of Hallmark EMT module scores split by immune phenotypes (d) Boxplot of EMT Hallmark scores split by immune phenotypes. (e) GSEA enrichment analysis for three different EMT modules: select Hallmark EMT module from Hornburg et al. (2021) (Hornburg_EMT), our cancer-specific EMT module (Malignant_Specific_EMT), and Hallmark EMT module (EPITHELIAL_MESENCHYMAL_TRANSITION) and other pathways either significantly enriched for in desert DEGs (red) or in excluded/infiltrated DEGs (green/blue).

Based on this analysis, it is unclear if scores calculated using the Hallmark EMT gene set are sufficient to indicate a mesenchymal phenotype. Signature activity among malignant cells from different tumor immune phenotypes revealed some key differences in the cancer cell population (**Figure 28a**). The score distribution was then evaluated across the malignant cells derived from the 16 tumors (**Figure 28b**) revealing a notably higher EMT activity score of infiltrated tumors compared to excluded and desert tumors (**Figure 28c-d; Figure 29**).

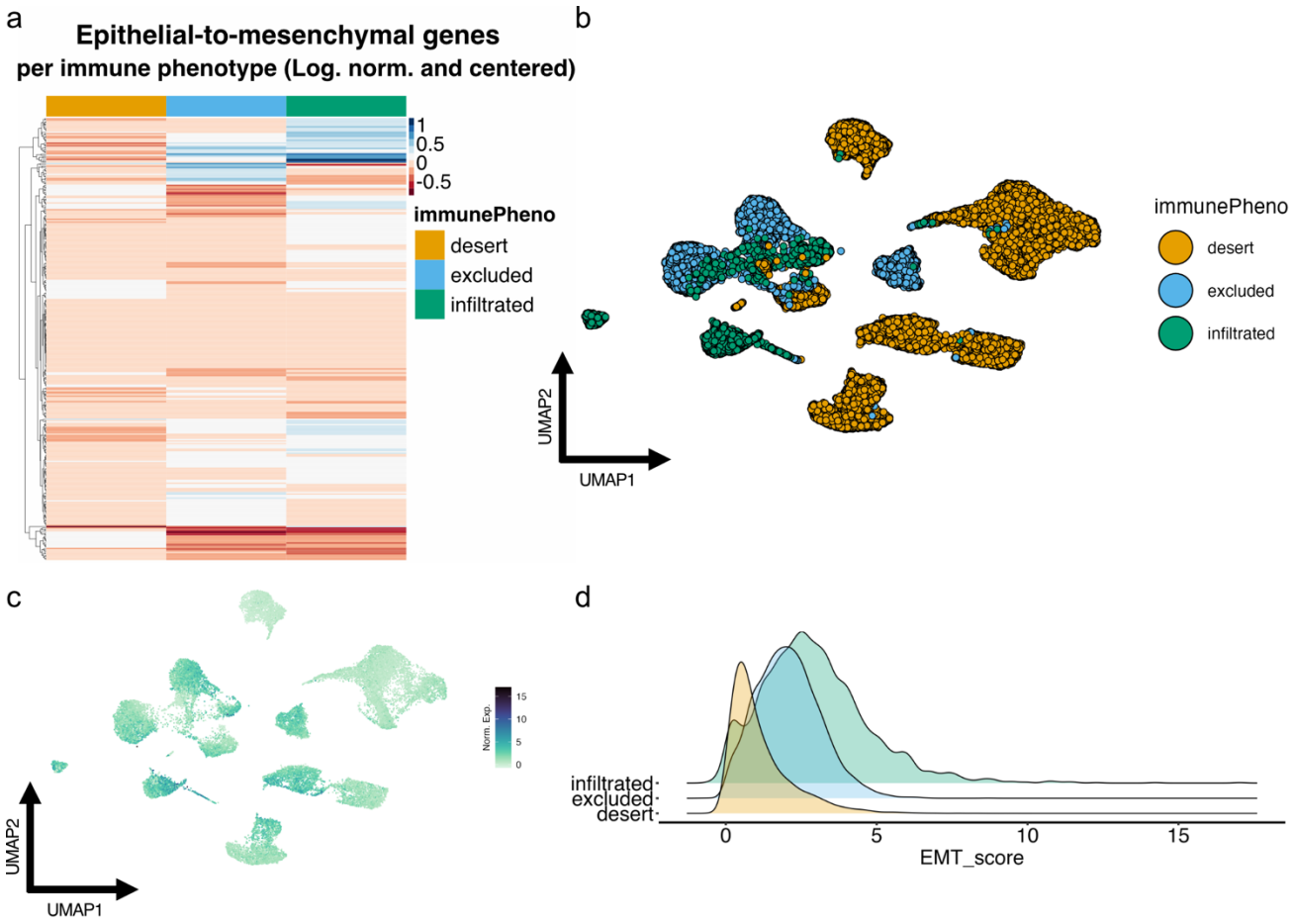

Figure 28. Cancer cells from infiltrated tumors have higher cancer-specific EMT signature scores compared to cancer cells from excluded and desert tumors. (a) Quantile scaled heatmap of cancer-specific EMT signature genes arrayed by immune phenotype. (b) UMAP clustering of cancer cell compartment of scRNA-seq dataset of 16 HGSOC tumors colored by the immune phenotype of the specific source tumor. (c) Enrichment UMAP plot for the cancer-specific EMT signature scores in the clustered cancer cell compartment. (d) Ridge plot of individual cancer-specific EMT signature module scores in the cancer cell compartment of each tumor's immune phenotype.

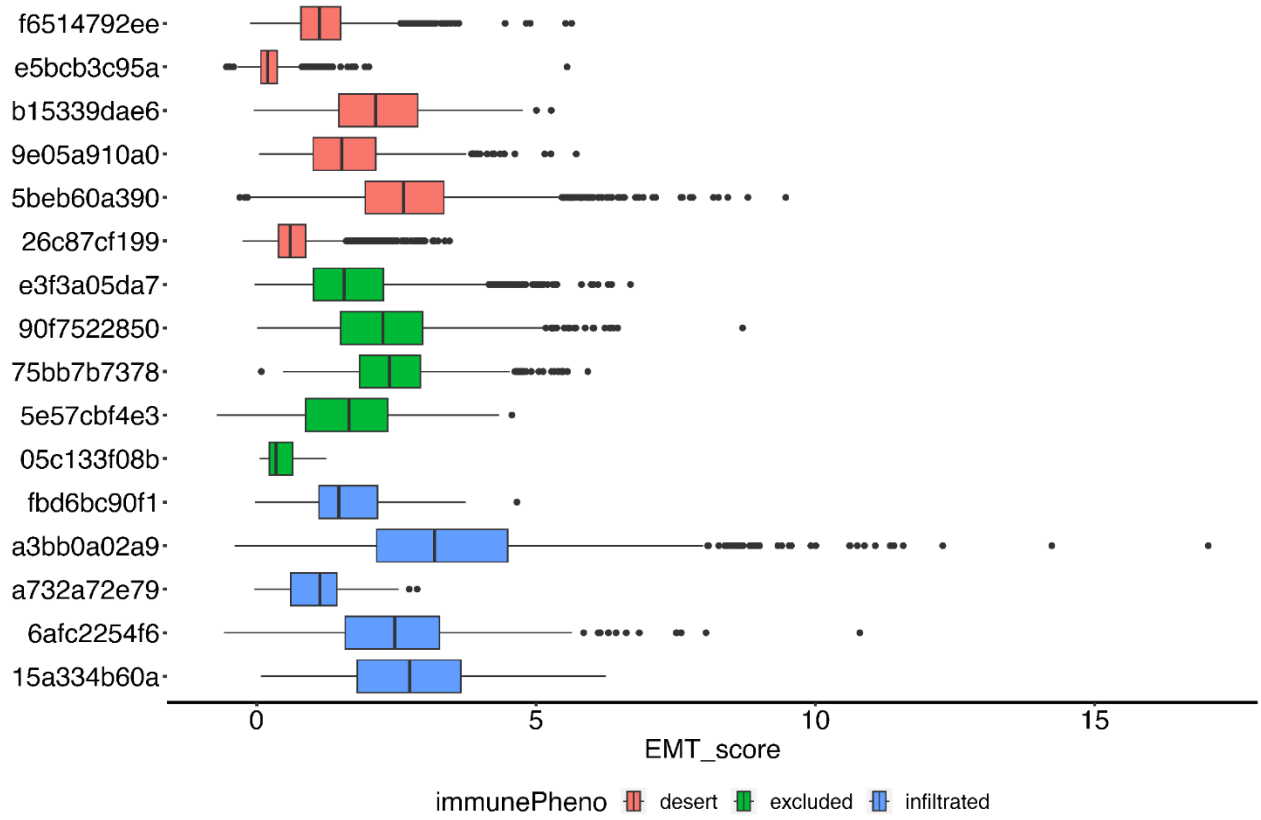

Figure 29. Individual infiltrated tumors contain cancer cells further along the EMT program compared to excluded or desert tumors. Boxplot of cancer-specific EMT signature scores' dispersion in cancer cells arrayed by TME immune phenotype.

This result was surprising as desert TMEs have been previously linked to higher EMT signatures in the cancer cells of HGSOC (Bou-Tayeh & Miller, 2021; Hornburg et al., 2021; L. Zhang et al., 2003). Consistent with our finding, individual cancer-specific EMT signature genes such as *PDIA3*, *HLA-A*, *BCAM*, *B2M*, *LGALS3BP*, and *HLA-C* were highly expressed in cancer cells from infiltrated and excluded TMEs (**Figure 30**). Importantly, none of the tumor samples was found as an obvious outlier for cancer-specific EMT signature scores (**Figure 29**). Interestingly, cancer cells from infiltrated TMEs appeared to be more heterogeneous in their EMT scoring and skewed towards mesenchymal phenotypes.

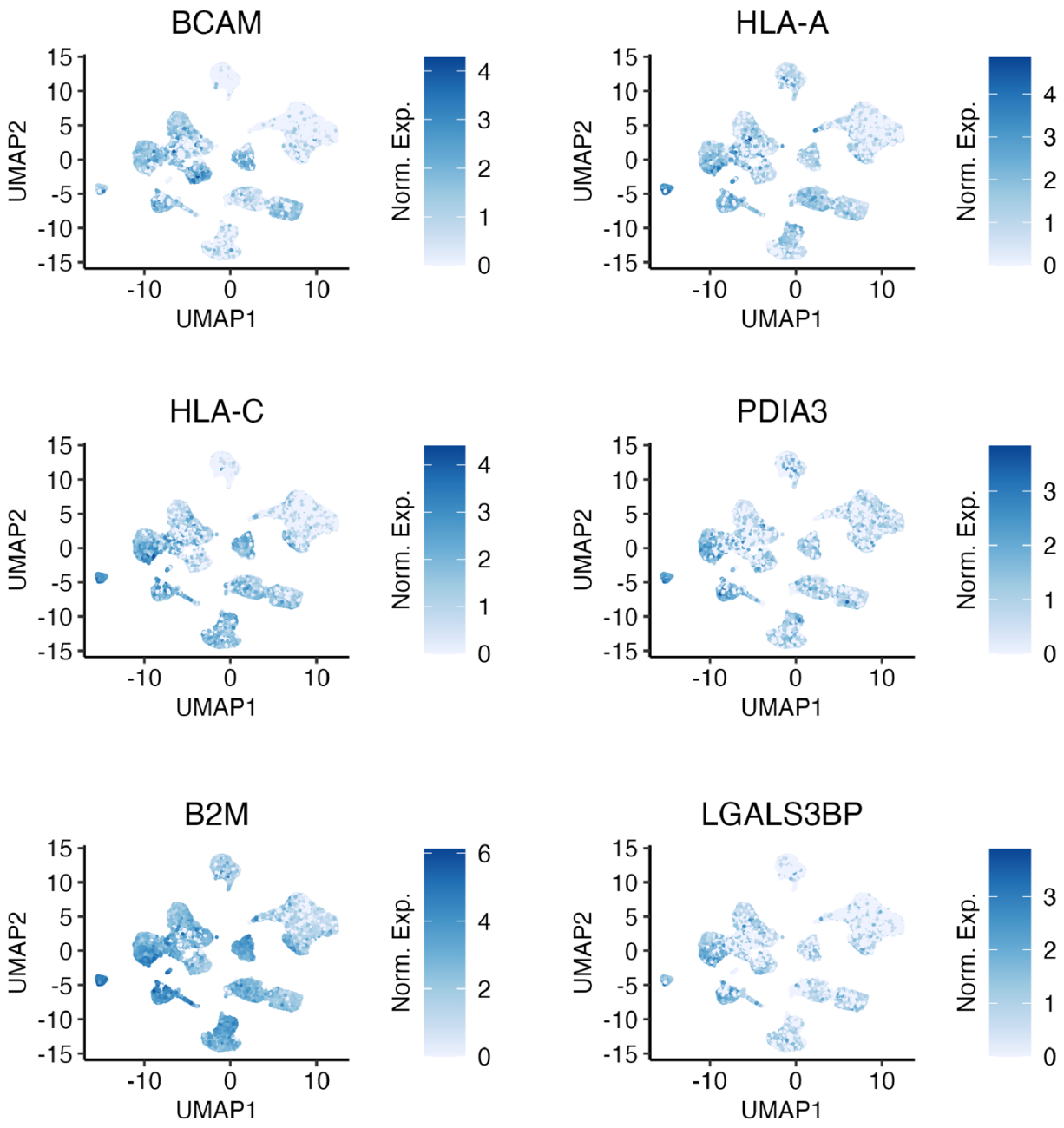

Figure 30. Cancer cells from infiltrated tumors have greater enrichment for select genes from the cancer-specific EMT module. Enrichment UMAP plots for a subset of genes from the cancer-specific EMT signature module in the re-clustered cancer cell compartment.

To validate the cancer-specific EMT signature's fidelity in determining EMT, we leveraged an EOC cell line that we had previously shown to undergo transcriptional changes associated with EMT when treated with TGF-β1 (Cook & Vanderhyden, 2020). OVCA420 cells were treated with TGF-β1 to induce EMT and the cells were collected at three different time-points to perform scRNA-seq (**Figure 31a**). We modelled a continuous pseudotemporal EMT trajectory from the data (**Figure 31b**) and found that scores from the EMT signature increase throughout EMT progression as expected, alongside pseudotime values (**Figure 31c**). Furthermore, the OVCA420 *in vitro* model of EMT involved activation of classical EMT genes such *SOX4*, *SNAI2*, *COL1A1*, and *FN1* (**Figure 31d**).

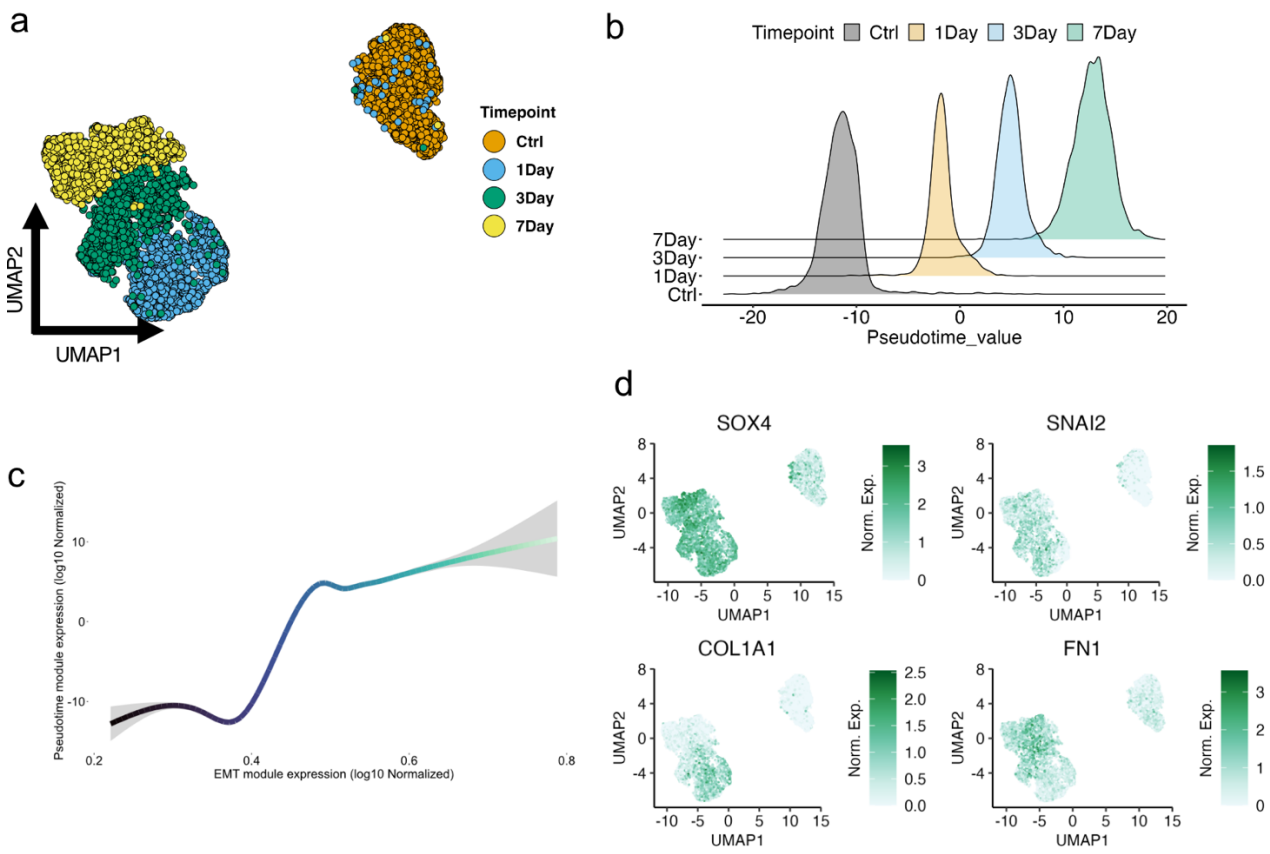

Figure 31. *in vitro* EMT model in OVCA420 ovarian cancer cells shows high expression of EMT markers after treatment and correlates with the cancer-specific EMT module based on pseudotime analysis. (a) UMAP clustering of OVCA420 cells treated with TGF-β1 for 4 lengths of time: Ctrl (control, no treatment), 1-day, 3-day, and 7-day. (b) Pseudotime value density for each individual time point in OVCA420 cells treated with TGF-β1. (c) Generalized additive model (GAM) fitted line correlating pseudotime values and cancer-specific EMT signature scores. (d) Enrichment UMAP plot of classical EMT markers *Sox4*, *Snai2*, *Col1a1*, and *FN1* in OVCA420 cells treated with TGF-β1.

We then leveraged non-negative matrix factorization (NMF), a technique which enables the investigation of coordinated gene expression sources of heterogeneity in the data in a semi-supervised manner with machine learning. Using the data from the OVCA420 cells treated with TGF-β1, we generated a list of 10 possible cell state programs (**Figure 32**) representing the inherent expression of unique sub-groups of cells throughout the time course (**Figure 31a**). Of all the NMF-derived programs, programs 2 and 10 were most consistent with an EMT program by observing which cells are the most enriched for those programs and cross-referencing that with the individual clusters in **Figure 31a** by observation. Program 10 (**Figure 32**) enriches the cell cluster located at the final time point of 7-days after TGF-β1 treatment, where we expect a 'maximal' mesenchymal state. Conversely, Program 2 enriches cells at the 3- and 7-day time points suggesting that genes associated with that particular NMF are expressed in partial or fully mesenchymal cells, respectfully.

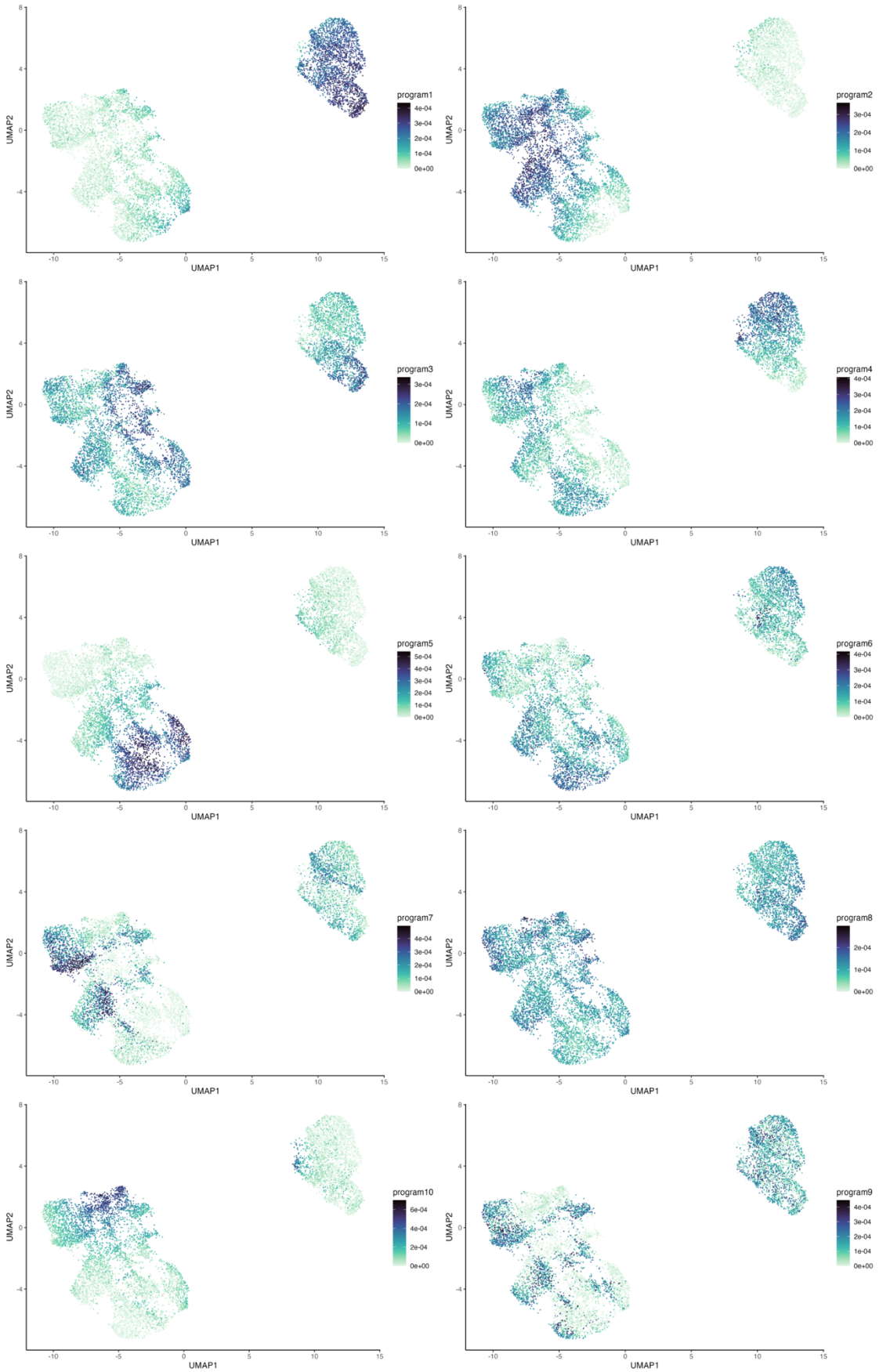
program1
4e-04
3e-04
2e-04
1e-04
0e+00
program2
3e-04
2e-04
1e-04
0e+00
program3
3e-04
2e-04
1e-04
0e+00
program4
4e-04
3e-04
2e-04
1e-04
0e+00
program5
5e-04
4e-04
3e-04
2e-04
1e-04
0e+00
program6
4e-04
3e-04
2e-04
1e-04
0e+00
program7
4e-04
3e-04
2e-04
1e-04
0e+00
program8
2e-04
1e-04
0e+00
program10
6e-04
4e-04
2e-04
0e+00
program9
4e-04
3e-04
2e-04
1e-04
0e+00
UMAP1
UMAP2

Figure 32. Enrichment of OVCA420 cells treated with TGF-β1 by 10 different programs generated through machine learning by application of NMF to the data. All plots represent the 'h' coefficient of the NMF generated programs.

To further explore program 10, we took the top 500 most-weighted genes in the program and ran an Enrichr analysis (**Figure 33a**). We discovered that program 10 enriches for Hallmark gene modules related to immunoregulatory pathways such as 'TNF-alpha signaling via NF-kB' (***p < 0.001), and others to 'p53 pathway' (***p < 0.001), and 'mTORC1 signalling' (***p < 0.001) while also enriching the Hallmark EMT gene module. When we performed the same analysis for program 2 (**Figure 32**), we found reduced enrichment for the 'TNF-alpha signaling via NF-kB' pathway as well as 'p53 pathway' (**Figure 33b**). These results suggest that a distinct immunoregulatory program is activated upon TGF-β1 induced-EMT and may not be well represented by the Hallmark EMT gene set.

a

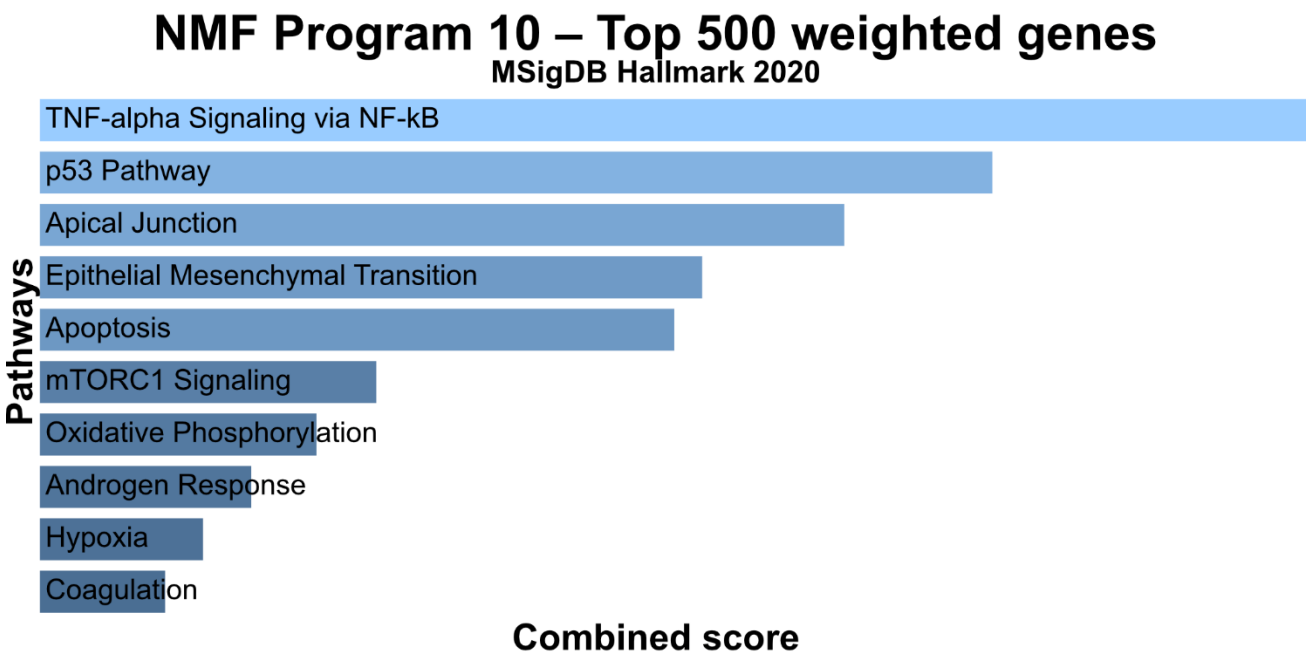

b

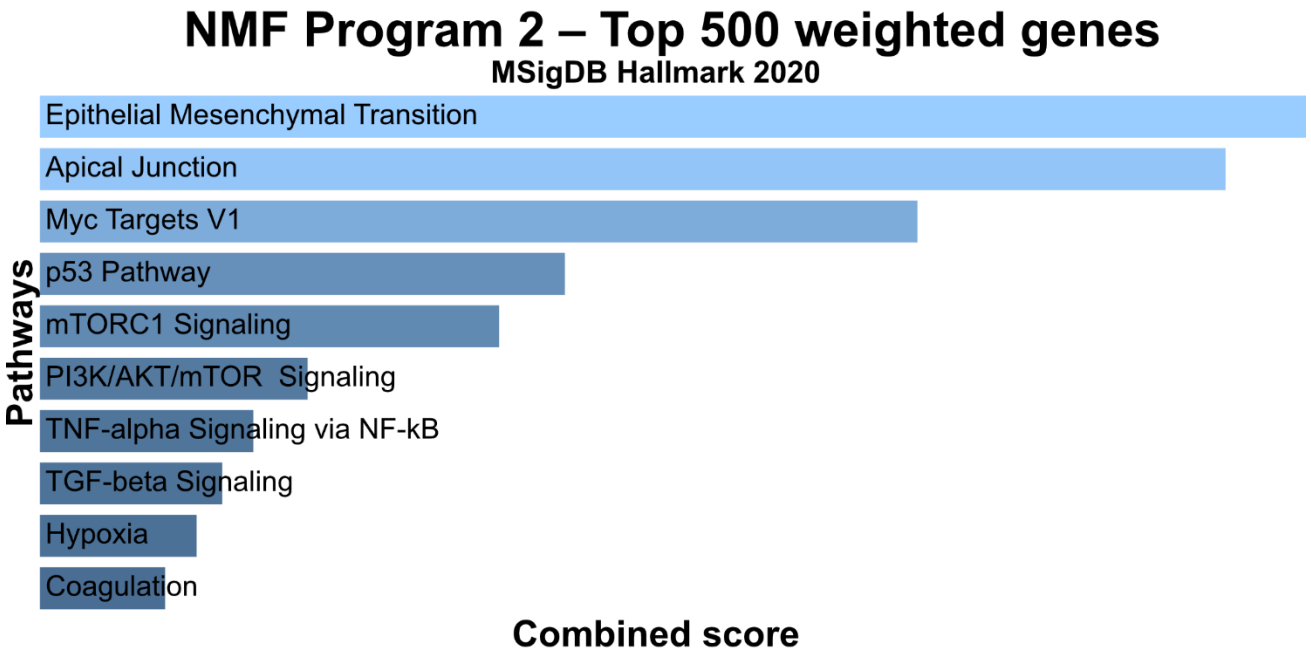

Figure 33. NMF Program 10 enriches for immunoregulatory signaling pathways. (a) Enrichr analysis of top 500 genes, by weight, identified by NMF program 10 enriching for pathways in MSigDB Hallmark 2020 database. (b) Enrichr analysis of top 500 genes, by weight, identified by NMF program 2 enriching for pathways in MSigDB Hallmark 2020 database.

Analysis of the enrichment of cancer cells in the dataset of 16 HGSOC for genes encapsulated in our *in vitro*-derived NMF program 10 (**Figure 34**) revealed a greater overall presence of mesenchymal cells in the cancer cell population derived from the infiltrated tumors, followed by cancer cells from excluded and then desert tumors. Scoring the tumors with this defined NMF signature showed enrichment in infiltrated tumors consistent with the distribution of scores from the cancer-specific EMT signature. These findings suggest that program 10 identifies genes related to an immunoregulatory program activated by EMT in HGSOC cancer cells, that is most prevalent in mesenchymal cancer cells from infiltrated tumors. We therefore sought next to determine whether the EMT program could have a direct role in shaping the tumor immune phenotypes.

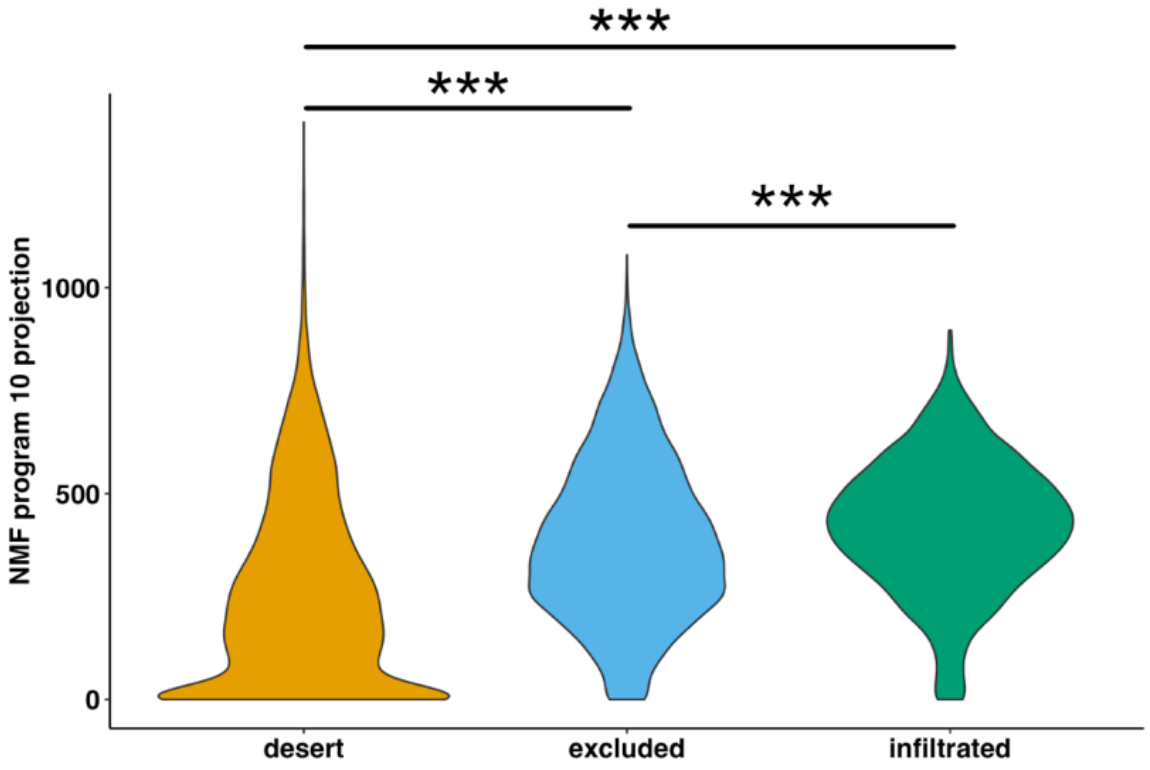

Figure 34. Mesenchymal phenotype-related NMF program 10 genes are most expressed in cancer cells from infiltrated tumors. Violin plot of NMF program 10 'h' coefficient values for cancer cells *in vivo* in 16 HGSOC arrayed by immune phenotype. A one-way ANOVA test with Tukey's multiple comparisons performed on program 10 'h' coefficient values reveals significant differences among all immune subtypes (***p < 0.001).

4.3 EMT is linked to $CD8^+$ T cell activity and exhaustion through the LAG3 receptor

Since our findings indicate that EMT in cancer cells correlates with the presence of immune cells (**Figure 28d, Figure 30, Figure 34**), we dissected the inter-cellular communications in each tumor immune phenotype by evaluating the unique expression of ligands in malignant cells and their cognate receptors in $CD8^+$ T cells. $CD8^+$ T cells are very abundant in infiltrated tumors (**Figure 23e, Figure 24**), and we were interested in assessing whether EMT influences antitumor immunity in infiltrated and excluded cancers. The ligand-receptor interactome analysis of communication between cancer cells from infiltrated and excluded tumors to $CD8^+$ T-cell receptors revealed that most interactions are borne from mesenchymal cancer cells towards $CD8^+$ T cells in both immune phenotypes (**Figure 35a-b**).

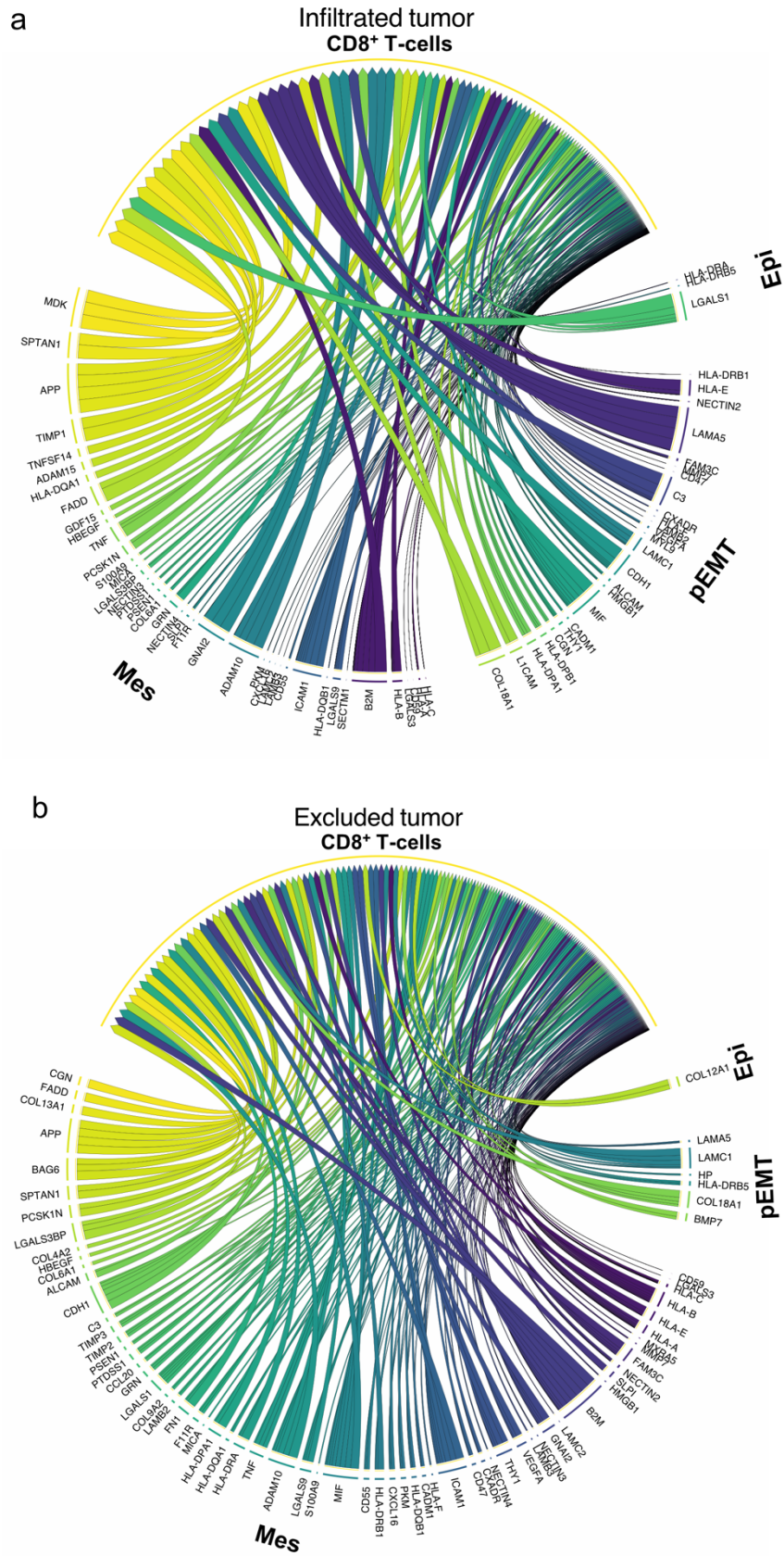
a
Infiltrated tumor
CD8⁺ T-cells
Epi
pEMT
Mes
b
Excluded tumor
CD8⁺ T-cells
Epi
pEMT
Mes

Figure 35. Most ligands targeting CD8⁺ T-cells in the TME originate from the mesenchymal cancer cells. (a,b) Circle plot of ligands originating from cancer cells arrayed by delineated EMT status and interacting with recipient CD8⁺ T-cells in infiltrated (a) and excluded tumors (b). Order and color of ligands corresponds to p-value aggregate rank reflecting specificity of interactions (most specific – purple color, clockwise). The number of tracks per ligand corresponds to the number of overall interactions the ligand has with different receptors. Track width corresponds to p-value aggregate rank within a ligand if the ligand has multiple receptor targets.

We then assessed the top cancer cell to CD8⁺ T cell receptor-ligand interactions with the former arrayed by EMT status (**Figure 36a**). Heterogeneity in signaling between different immune phenotypes is evident, where receptor-ligand pairs such as *SECTM1 - CD7* appear to be unique to infiltrated tumors (**Figure 36a**). The top five ligands targeting CD8⁺ T-cells by mesenchymal cancer cells from infiltrated tumors were *HLA-C*, *HLA-A*, *CD59*, *LGALS3*, and *B2M* (**Figure 36a, b**). We found similar gene patterns in mesenchymal cells' ligands in excluded tumors with *CD59*, *LGALS3*, *HLA-C*, *HLA-B*, and *HLA-E* (**Figure 36a, c**). The finding of classic MHC I molecule expression by cancer cells was not surprising as HLA I expressing tumors have been previously linked to TIL frequency, with TILs eventually inducing HLA allotype selection, consequently enabling cancer cells to evade antitumoral immunity (Aptsiauri et al., 2018, p.; Kooi et al., 1996). Nonetheless, we were expecting to find other dominant inhibitory ligands such as PD-L1 promoting immunosuppression, but *LGALS3* (Galectin-3, Gal-3) emerged as a top ligand, highlighting its potential role in the EMT driven immunosuppression in EOC (Alsuliman et al., 2015; Fei et al., 2019, p. 1; Loret et al., 2019; Nhokaew et al., 2019; Whitehair et al., 2020, p. 1).

Further investigation of the specific receptors targeted by *LGALS3* showed that the *LAG3* complex on CD8⁺ T cells is the primary recipient of *LGALS3*, as well as MHC

II molecules, matching previous literature findings (Graydon et al., 2021; Kouo et al., 2015; Zhai et al., 2020) (**Figure 36a-c; Figure 37a-b)**. In fact, *LAG3* appears to be one of the most targeted receptor complexes by rank in both infiltrated and excluded tumors, suggesting the possible exhaustion of these cells. The observation linking the LGALS3-LAG3 interaction to EMT prompted us to further investigate $CD8^+$ T cell exhaustion as a possible consequence of the EMT process in primary HGSOC.

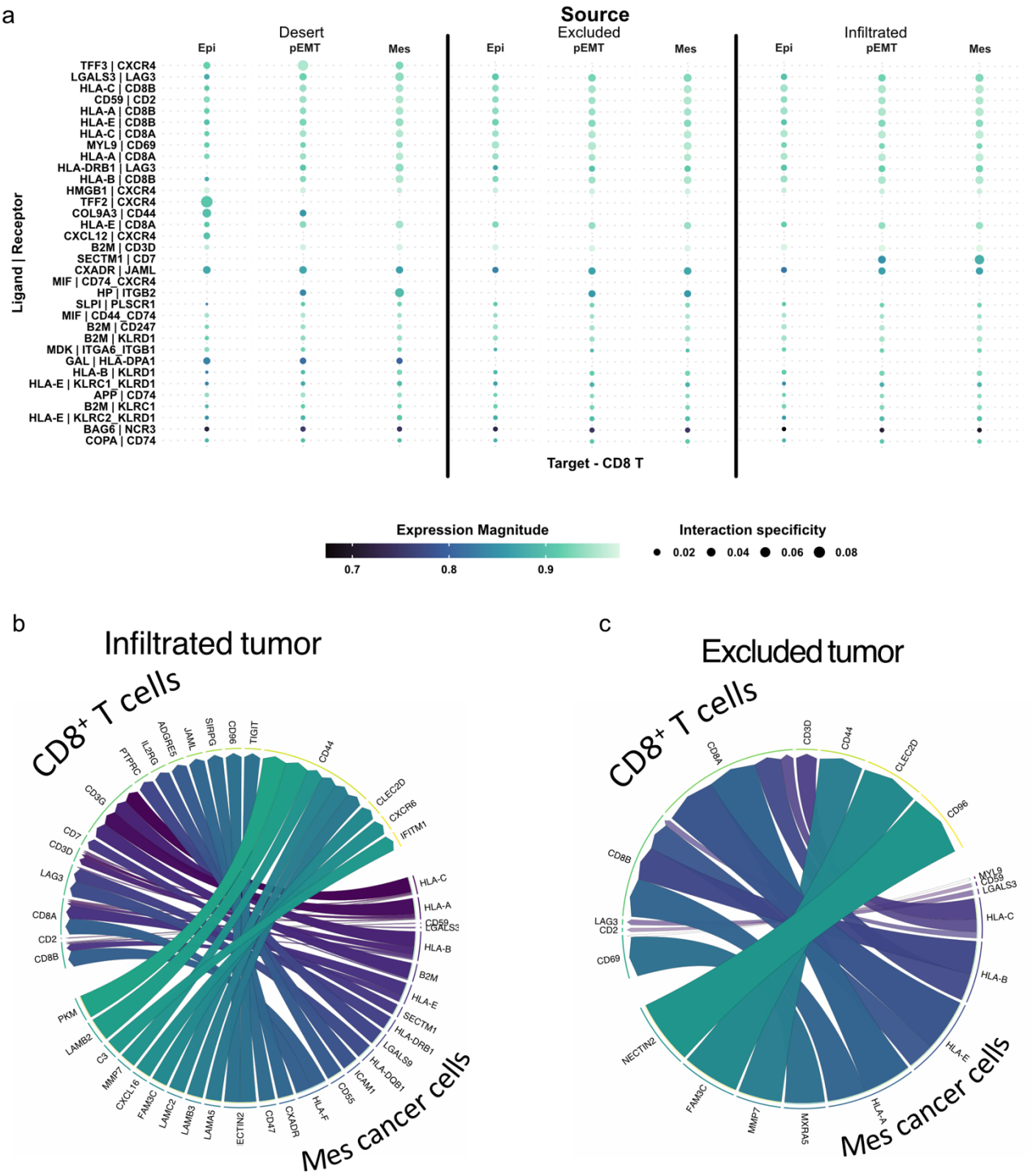

Figure 36. Top-most ligands targeting CD8⁺ T-cells in the TME originating from the mesenchymal cancer cells. (a) Cell-cell communication analysis of top-most ligand-receptor pairs from cancer cells from 16 HGSOC samples arrayed by infiltration phenotype of tumors and EMT to CD8⁺ T-cells. 'Expression magnitude' is a measure of expression levels of a certain interaction. 'Specificity' is a measure of the specificity of interactions across all cell types. Interactions are ordered by p-value where top-most receptor-ligand pair has lowest p-value. (b,c) Circle plot of ligands originating from

mesenchymal cancer cells in infiltrated tumors (b) and excluded tumors (c), and the receptors targeted on recipient $CD8^+$ T-cells. Order and color of ligands corresponds to p-value aggregate rank reflecting specificity of interactions (most specific – purple color, clockwise). The number of tracks per ligand corresponds to the number of overall interactions the ligand has with different receptors. Track width corresponds to p-value aggregate rank within a ligand if the ligand has multiple receptor targets.

a

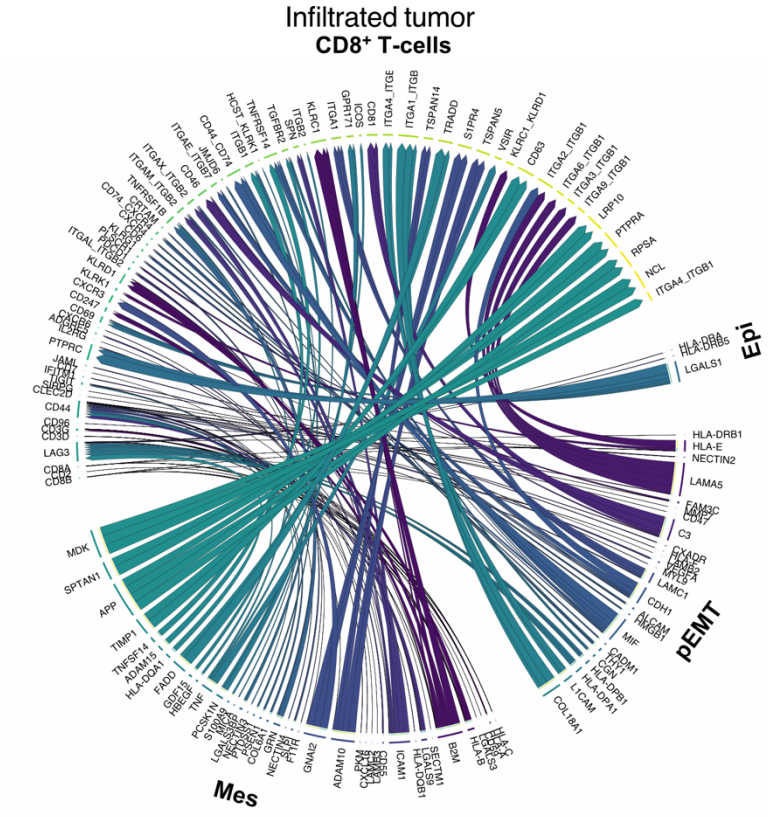
Infiltrated tumor
CD8+ T-cells
Epi
pEMT
Mes
HLA-DRB5
LGALS1
HLA-DRB1
HLA-E
NECTIN2
LAMA5
C3
LAMC1
CDH1
MIF
COL18A1
MDK
SPTAN1
APP
TIMP1
TNFSF14
ADAM15
HLA-DQA1
FADD
GDF15
TNF
ADAM10
GNAI2
ICAM1
SECTM1
HLA-DQB1
B2M
HLA-B

b

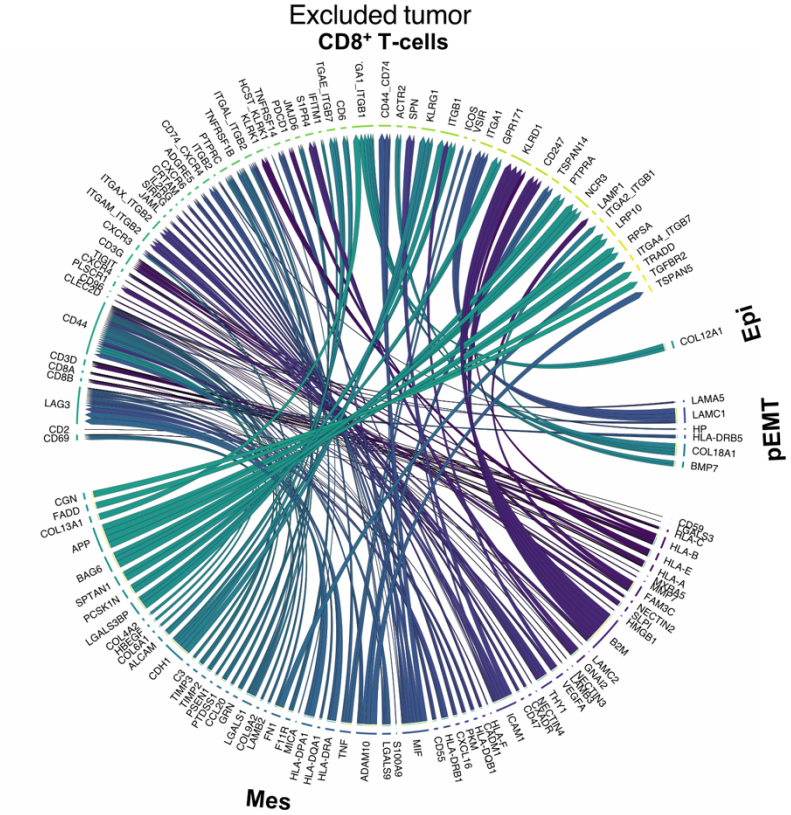
Excluded tumor
CD8+ T-cells
Epi
pEMT
Mes
COL12A1
LAMA5
LAMC1
HP
HLA-DRB5
COL18A1
BMP7
CD55
HLA-C
HLA-B
HLA-E
HLA-A
NECTIN2
B2M
ICAM1
MIF
ADAM10
TNF
HLA-DRA
HLA-DQA1
FADD
COL13A1
APP
BAG6
SPTAN1
PCSK1N
LGALS3BP
CDH1
C3
LGALS1
CD44
CD3D
CD8A
CD8B
LAG3
CD2
CD69
CXCR3
CD3G
TIGIT
CLEC2B
ITGAX_ITGB2
ITGAM_ITGB2
CD74_CXCR4
TNFRSF1B
ITGAL_ITGB2
HCST_KLRK1
TNFRSF14_KLRK1
ITGB1
CD8
ITGAE_ITGB7
CD44_CD74
ACTR2
SPN
KLRG1
ICOS
VSIR
ITGA1
GPR171
KLRD1
CD247
TSPAN14
PTPRA
NCR3
LAMP1
ITGA2_ITGB1
LRP10
RPSA
ITGA4_ITGB7
TRADD
TGFBR2
TSPAN5

Figure 37. Cell-cell communication map between cancer cells' ligands arrayed by EMT and their binding partner receptors on CD8$^+$ T cells. (a,b) Circle plot of ligands originating from cancer cells arrayed by delineated EMT status in infiltrated tumors (a) and excluded tumors (b), and the receptors targeted on recipient CD8$^+$ T-cells.

Common exhaustion markers or checkpoint inhibitors of CD8$^+$ T-cells include *BTLA*, *CD160*, *CD244*, *CTLA4*, *HAVCR2*, *LAG3*, *TIGIT, and PD1,* the *NFAT* family *(NFAT5*, *NFATC1-4)* of transcription factors involved in promoting T cell exhaustion*,* and *IRF4, BATF, VSIR, and CIITA,* a master regulator of MHC II expression which is known to interact with LAG3 (Maruhashi et al., 2018). Of these markers, *LAG3* and *TIGIT* are most active in CD8$^+$ T cells in infiltrated tumors (**Figure 38a**). In fact, high *LAG3* and *TIGIT* expression in infiltrated tumors could be indicative of a specific inflammatory milieu triggering *LAG3* upon CD8$^+$ T cell infiltration and sensitizing these cells to exhaustion signals from mesenchymal cancer cells. A breakdown of all the ligands targeting the *LAG3* receptor on CD8$^+$ T cells, regardless of cancer cell EMT status or tumor immune phenotype, showed that most ligands for *LAG3* are HLA II molecules, with *LGALS3* being the only non-MHC related ligand (**Figure 38b**). Despite HLA II ligands making up the bulk of interactions between cancer cells and *LAG3* on CD8$^+$ T-cells, we did not find any associations between EMT and HLA II expression (data not shown). Additionally, NECTINs 2, 3, and 4 are the major interacting partner with TIGIT between cancer cells and CD8$^+$ T-cells, suggesting another possible vector for T cell exhaustion by mesenchymal cancer cells.

GSEA of the DEGs between LAG3$^+$ and LAG3$^-$ CD8 T cells revealed enrichment for molecular pathways related to decreased cytotoxic T cell cytolysis (MP:0005079) and abnormal CD8$^+$ T cell morphology (MP:0002436) (**Figure 38c**), suggesting that

there is a significant contingent of $CD8^+$ T cells in infiltrated tumors that are cytolytically non-functional as a result of LAG3-related signaling. Fibrinogen-like protein 1 (FGL1) has been shown recently to be a ligand of LAG3, also potentially influencing T cell exhaustion (J. Wang et al., 2019). Interestingly, we found FGL1 is expressed only by mesenchymal cancer cells in infiltrated tumors (**Figure 38d**). As these findings show that there is a significant proportion of $LAG3^+$ $CD8^+$ T-cell targeted by ligand $LGALS3^+$ originating from mesenchymal cancer cells, we sought to further explore the link between *LGALS3* and EMT to better elucidate how EMT could modulate $CD8^+$ T-cell exhaustion.

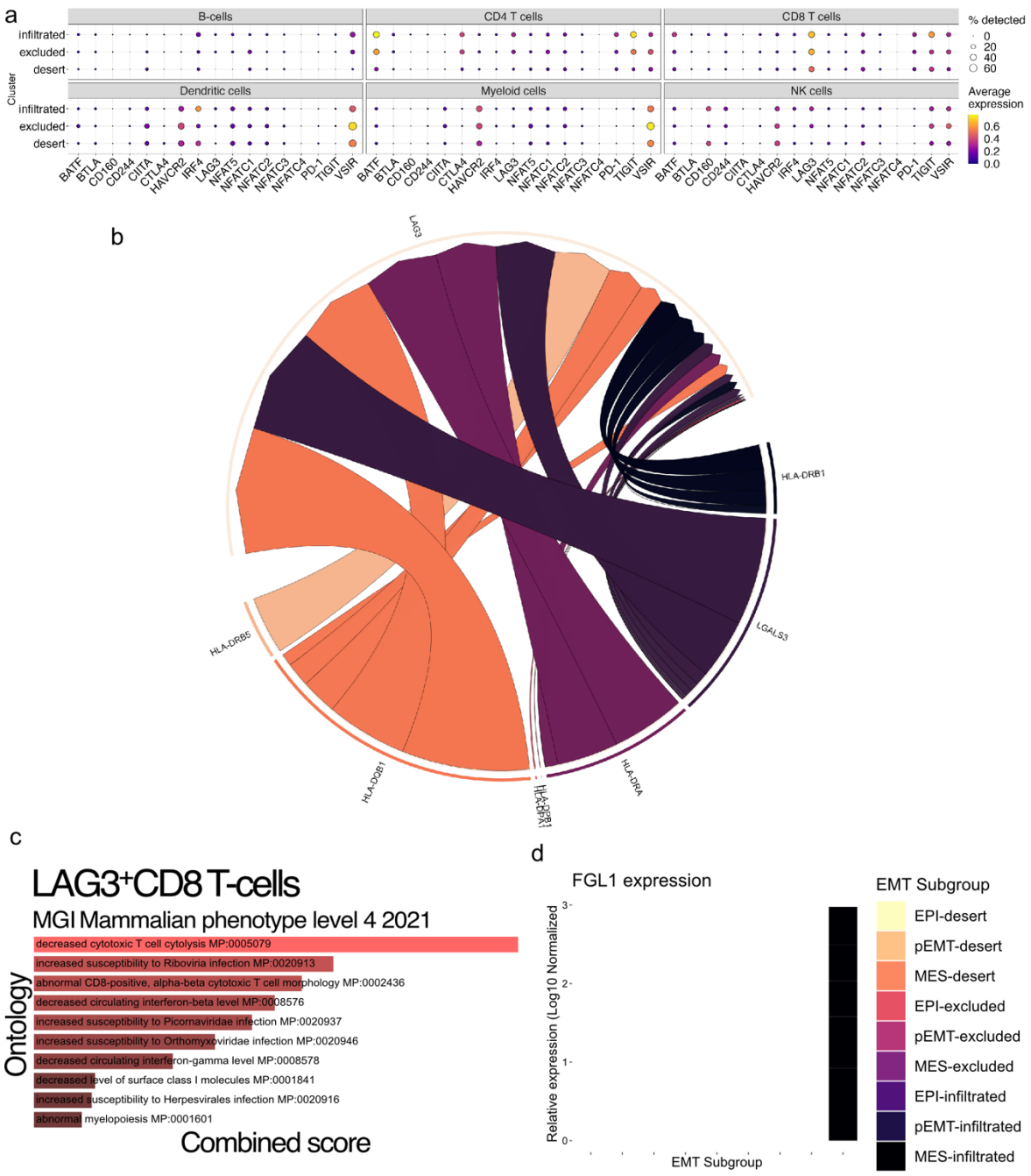

Figure 38. Most CD8⁺ T-cells in HGSOC express *LAG3*, a marker of T cell exhaustion. (a) Dot plot showing expression levels and frequency of common markers of T-cell exhaustion in the entire CD45⁺ cell compartment. (b) Circle plot of CD8⁺ T-cell LAG3 receptor complex and all the ligands that target it. (c) Analysis of enriched pathways from a DEG analysis of LAG3⁺ CD8 T-cells compared to LAG3⁻ T-cells in the

Mouse Genome Informatics (MGI) database. (d) Log-normalized expression of FGL1 in the EMT-delineated compartment of cancer cells from each tumor immune phenotype.

4.4 LGALS3 is linked with EMT in both in vivo and in vitro contexts

To determine whether *LGALS3* has any association with EMT, we examined its expression across cancer cells arrayed by both tumor immune phenotype and EMT status. We also assessed LGALS3 Binding Protein (*LGALS3BP*) as it is known to synergize with *LGALS3* in certain contexts (He et al., 2019, p. 3). Both *LGALS3* and *LGALS3BP* appear to have higher expression in mesenchymal cancer cells, regardless of the tumor immune phenotype (**Figure 39a**). We fitted expression of *LGALS3* (**Figure 39b**) and *LGALS3BP* (**Figure 39c**) against EMT score and arrayed by tumor immune phenotype to find that *LGALS3* expression increases alongside the cancer-specific EMT signature expression in every tumor immune phenotype and every delineated EMT phase (i.e. EPI, pEMT, and MES). By contrast, *LGALS3BP* increases most in earlier, epithelial phases in all tumor immune phenotypes, and then plateaus, suggesting it is more important in earlier phases of the EM program. To determine whether *LGALS3* correlates with survival in HGSOC, we analyzed the TCGA data and found that low *LGALS3* expression in bulk RNA-Seq of HGSOC is associated with longer survival (*p = 0.013) (**Figure 39d**). These findings suggest that *LGALS3* expression correlates with EMT in cancer cells and contributes to reduced survival of ovarian cancer patients. Finally, we checked the expression of *LGALS3* in OVCA420 and MCF7 cells that were treated first with TGF-β1 to induce EMT and then the stimulus was removed to induce MET, to find *LGALS3* expression remained consistent after removal.

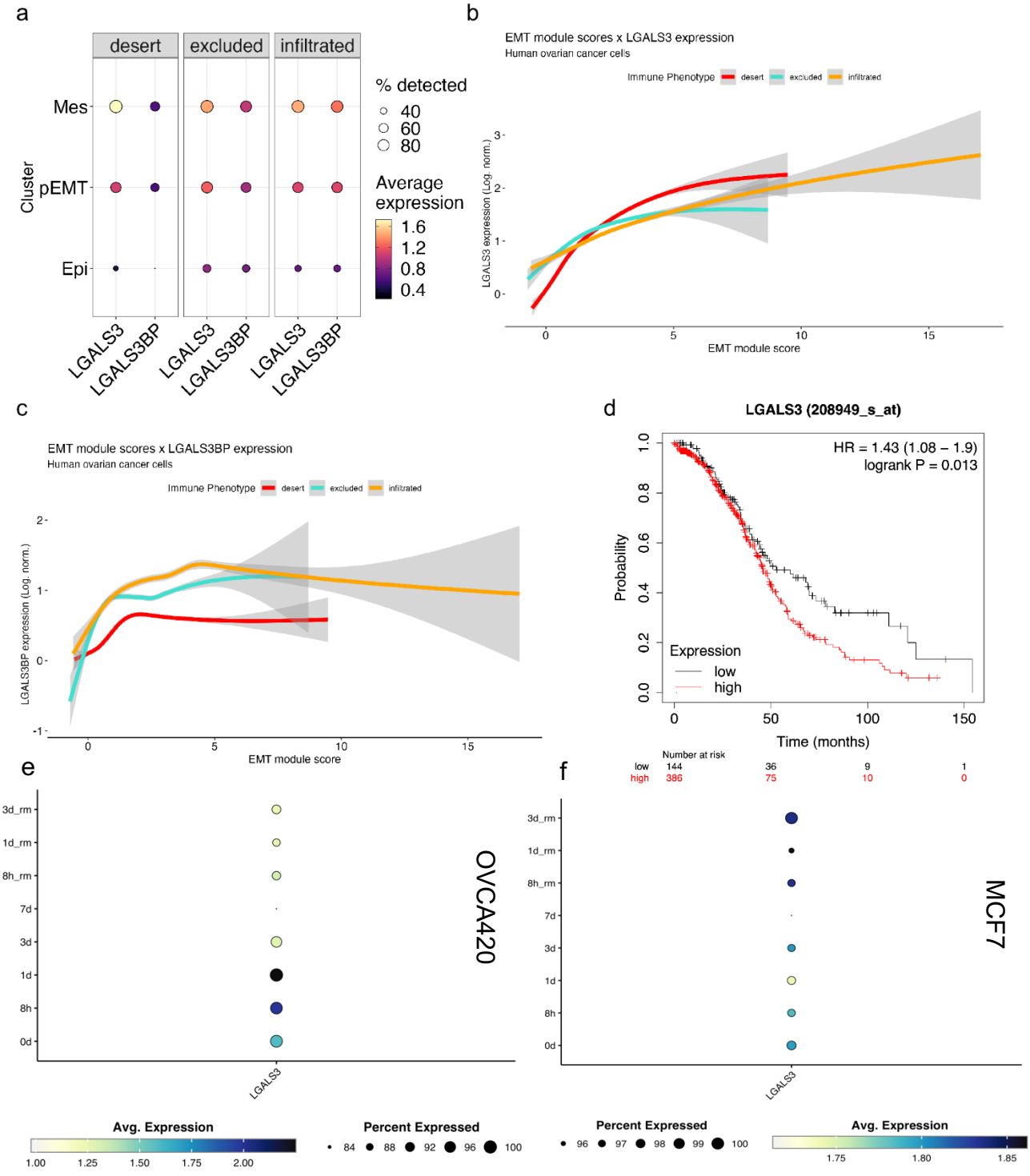

Figure 39. *LGALS3* and *LGALS3BP* expression in cancer cells correlates with EMT *in vivo*. (a) Dot plot showing *LGALS3* and *LGALS3BP* in the cancer cell compartment arrayed by EMT status and the percentage of cells that express these

genes in each immune phenotype. (b,c) Log-normalized *LGALS3* (b) and *LGALS3BP* (c) expression fitted via generalized linear model against cancer-specific EMT signature scores in cancer cells, segregated by tumor immune phenotype. (d) Kaplan-Meier curve comparing patient overall survival in *LGALS3*-high and *LGALS3*-low expressing ovarian tumors from TCGA data. (e,f) Dot plot showing *LGALS3* expression in a model of EMT *in vitro* where TGF-β1 was removed (8 hour post-removal – 8h_rm, 1 day post-removal – 1d_rm, 3 days post-removal – 3d_rm) as an EMT stimulus from OVCA420 cells (e) and MCF7 cells (f) prior to sequencing.

To elucidate if *LGALS3* is associated with the EMT in other model systems and under different conditions, we referred to our TGF-β1 treated OVCA420 cancer cells and correlated expression of *LGALS3* with the cancer-specific EMT signature scores (**Figure 40a**). We fitted a generalized linear model (GLM) and noted a modest positive association ($R^2 = 0.01$) between *LGALS3* and cancer-specific EMT signature scores (**Figure 40b**). We also noted that, as EMT progresses, the cells appear to separate into two populations of mesenchymal cells where *LGALS3* is expressed in one but not the other. To determine if *LGALS3* is consistently implicated in EMT rather than simply a consequence of TGF-β1 treatment, we accessed our previously published data (Cook & Vanderhyden, 2020) where multiple cell lines of different cancer types (ovarian, OVCA420; breast, MCF7; prostate, DU145; and lung, A549) were each treated with EMT inducers (TGF-β1, TNFα, EGF). While these proteins were chosen for their ability to induce EMT through different receptors and pathways, in certain cancers they can be secreted by immune cells, such as TNFα by $CD8^+$ T cells (Kearney et al., 2018), thus mimicking the immune response to cancer cells. We found a similar positive correlation

between *LGALS3* and cancer-specific EMT signature scores in OVCA420 cells treated with either EGF (R^2 = 0.01) or TNF-α (R^2 = 0.02) (**Figure 40c-d**). Other cancer cell types also showed positive correlations: MCF7 cells (TGF-β1, R^2 = 0.24; TNF-α, R^2 = 0.21, EGF, R^2 = 0.22) (**Figure 40e-g**), DU145 (TGF-β1, R^2 = 0.1; TNF-α, R^2 = 0.11, EGF, R^2 = 0.11) (**Figure 41a-c**), and A549 (TGF-β1, R^2 = 0.05; TNF-α, R^2 = 0.1, EGF, R^2 = 0.12) (**Figure 41d-f**), with breast cancer cells showing the strongest correlations between *LGALS3* expression and EMT. Taken together, our findings indicate that *LGALS3* expression is correlated with the EMT of cancer cells *in vivo* and *in vitro*, and that EMT drives expression of *LGALS3* in HGSOC cells. Additionally, *LGALS3* expression is a “core” gene in the EMT program that is activated under a variety of EMT inducers through TGF-β1-, or TNF-α-, or EGF-induced signaling. Mesenchymal cancer cells in turn exert inhibitory antitumoral signaling on $CD8^+$ T cell promoting a dysfunctional cytotoxic state and exhaustion by binding to the *LAG3* receptor complex.

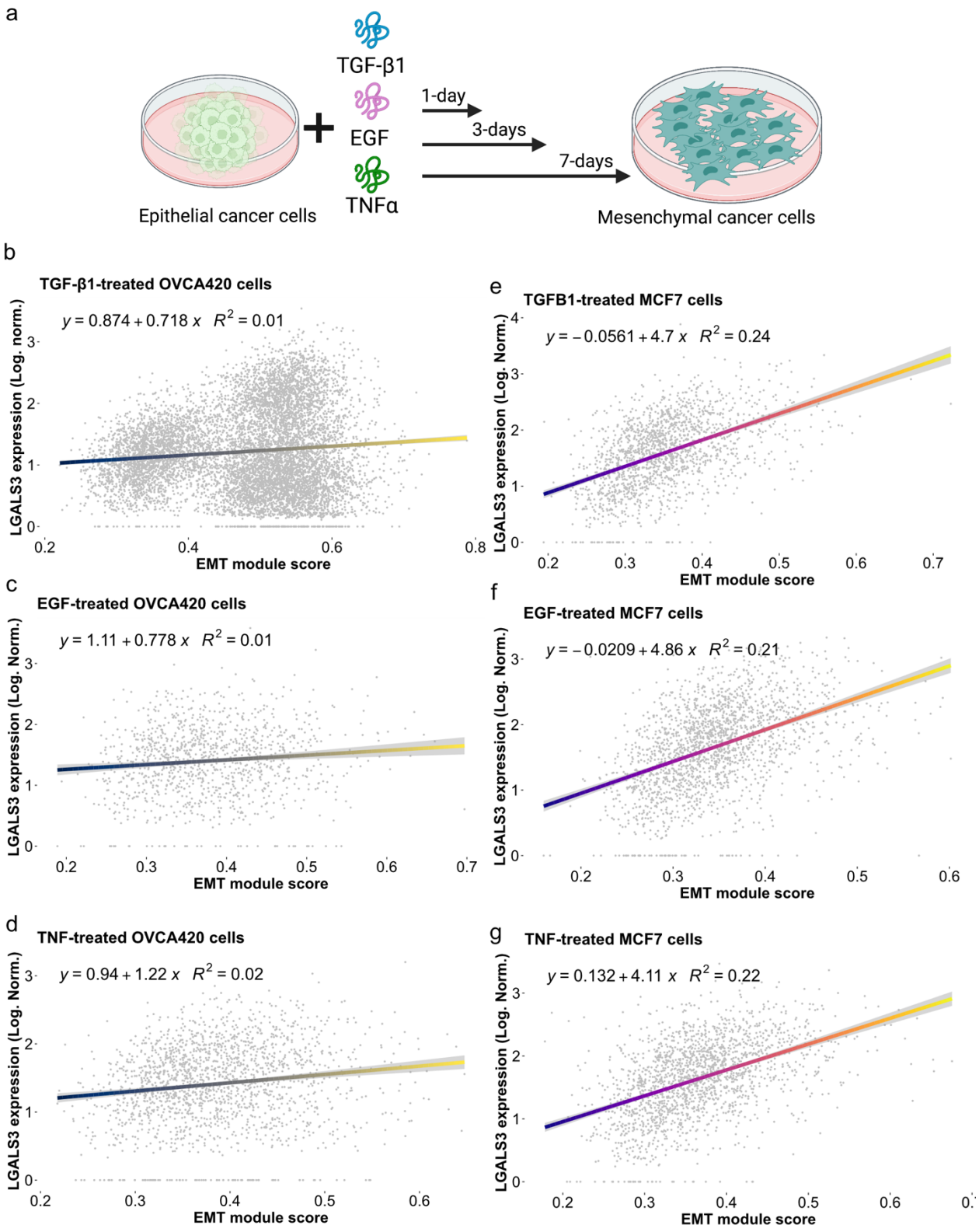

Figure 40. LGALS3 is directly correlated with the EMT *in vitro* in ovarian and breast cancer cell lines. (a) Schematic of cell line treatment (b-d) Log-normalized

expression of LGALS3 as generalized linear model against cancer-specific EMT signature scores in OVCA420 ovarian cancer cells treated with TGF-β1 (b), TNFα (c), and EGF (d). (e-g) Log-normalized expression of LGALS3 GLM-correlated against cancer-specific EMT signature scores in breast cancer MCF7 cells treated with TGF-β1 (e), TNFα (f), and EGF (g).

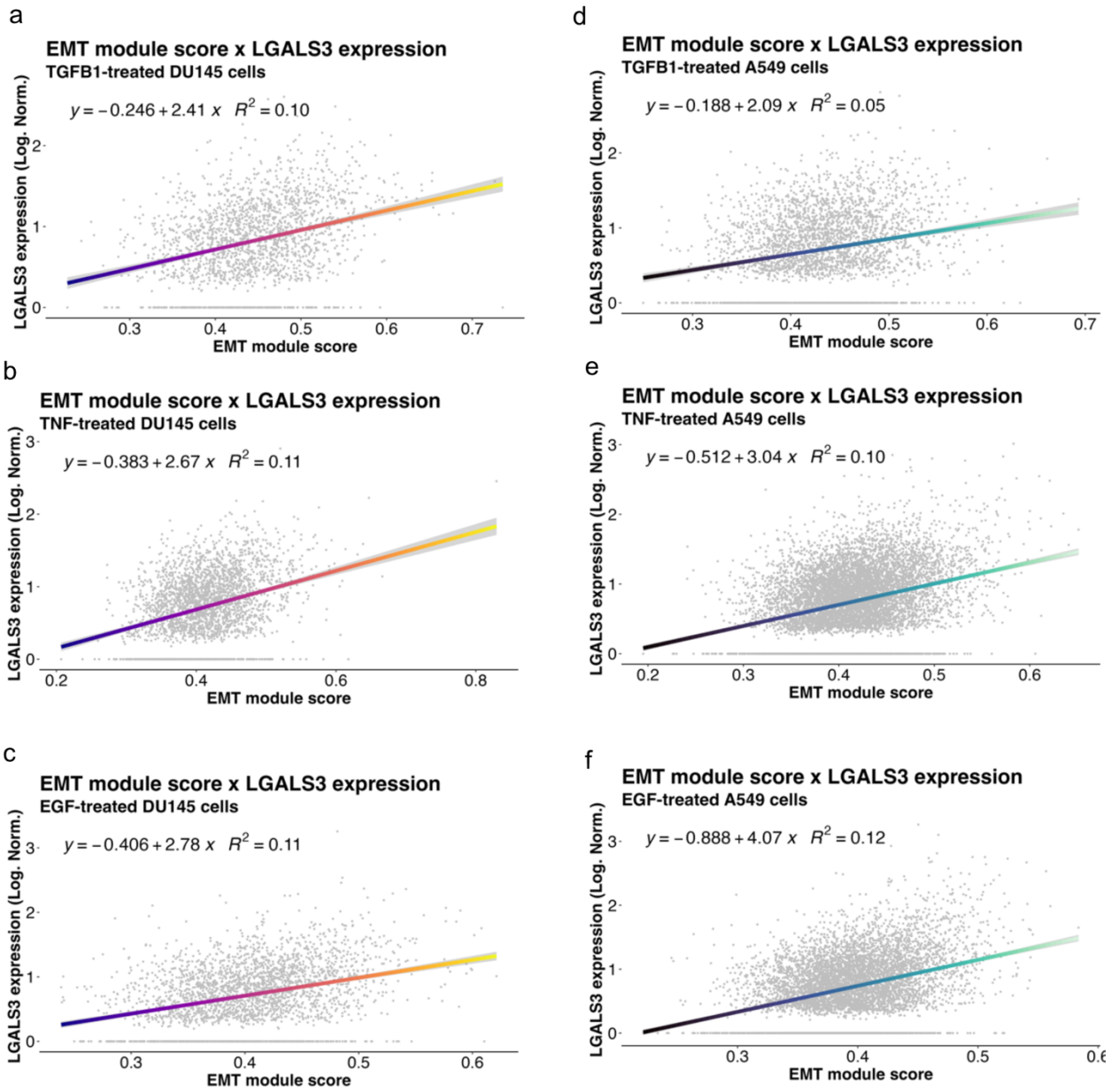

Figure 41. LGALS3 is directly correlated with the EMT *in vitro* in prostate and lung cancer cell lines. (a-c) Log-normalized expression of LGALS3 GLM-correlated against cancer-specific EMT signature scores in DU145 prostate cancer cells treated with TGF-β1 (a), TNFα (b), and EGF (c). (d-f) Log-normalized expression of LGALS3 GLM-correlated against cancer-specific EMT signature scores in A549 lung cancer cells treated with TGF-β1 (d), TNFα (e), and EGF (f).

4.5 GSK3 and Aurora-A kinase inhibitors attenuate LGALS3 expression

To determine the possible pathways linking EMT and *LGALS3* expression we referred to a kinase inhibitor screen previously published by this lab that elucidated

some of the signaling dependencies of the EMT (Cook & Vanderhyden, 2020). Particularly, the modularity of the EMT spectrum was revealed to be a core part of the process where some TGF-β1R-independent kinases attenuated the EMT despite treatment with various inducers (TGF-β1, TNFα, and EGF). In the original screen it was discovered that both RIP1 kinase inhibitor Necrostatin-5 and TGF-β1R inhibitor LY364947 abrogated EMT in all treatment conditions. When we explored this screen further (**Figure 42a-c**), we noted that two kinase inhibitors produced the most consistent reduction in *LGALS3* expression across cell lines and treatments: CHIR99021, a GSK3 kinase inhibitor and phthalazinone pyrazole, an Aurora kinase A inhibitor (**Figure 42d**), suggesting *LGALS3* expression is potentially dependent on activation of the Wnt and NF-kB pathways, or the β-catenin pathway during EMT. Finally, when we explored the effects of these two kinase inhibitors on pseudotime values as a measure of EMT and LGALS3 expression, we found that neither CHIR99021 nor phthalazinone pyrazole appear to attenuate the EMT, suggesting that blocking LGALS3 upregulation is not sufficient to prevent EMT (**Figure 43**).

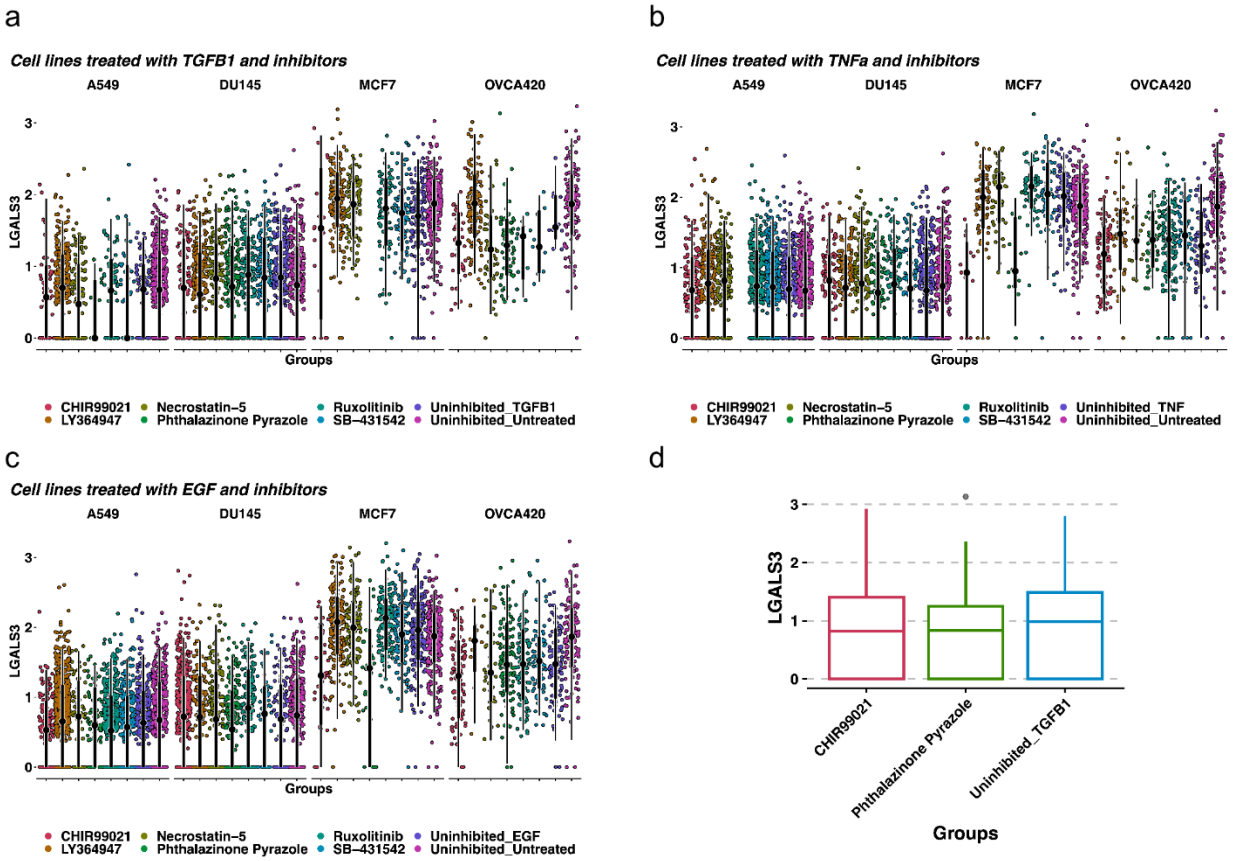

Figure 42. Kinase inhibitor screen shows GSK3 and Aurora-A kinase inhibitors attenuate EMT and LGALS3 expression. (a-c) Log-normalized expression of LGALS3 in A549, DU145, MCF7, or OVCA420 cell lines either treated either with EMT inducers TGF-β1 (a), TNFα (b), EGF (c) or EMT inducers and kinase inhibitors: RIP1 kinase inhibitor Necrostatin5, TGFβR1 kinase inhibitor LY364947, JAK1/2 kinase inhibitor Ruxolitinib, TGFβ/ALK kinase inhibitor SB-431542, GSK3 kinase inhibitor CHIR99021, or TGF-β1 and Aurora kinase A inhibitor phthalazinone pyrazole. (d) LGALS3 expression in OVCA420 cells treated with TGF-β1, TGF-β1 and GSK3 kinase inhibitor CHIR99021, or TGF-β1 and Aurora kinase A inhibitor phthalazinone pyrazole.

a

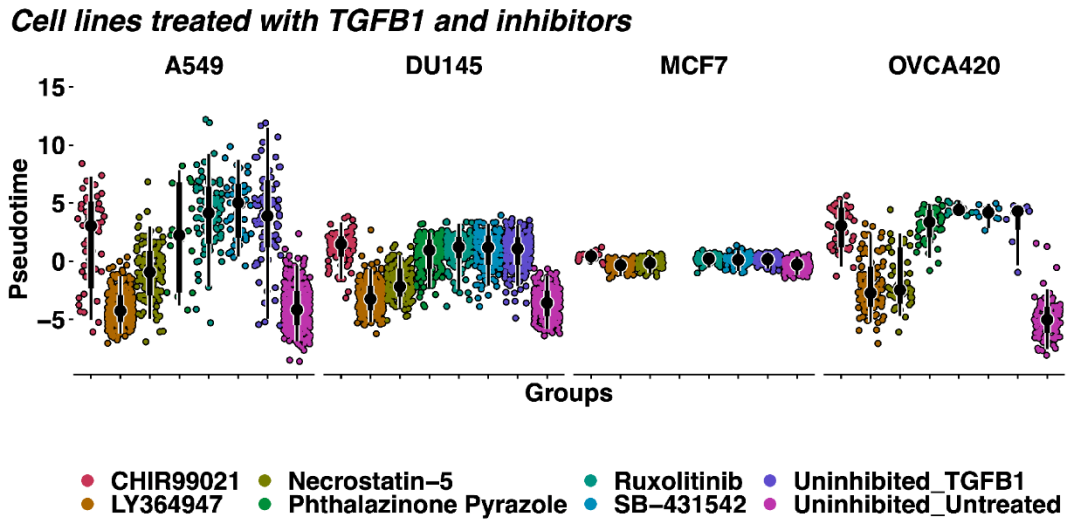
Cell lines treated with TGFB1 and inhibitors
A549
DU145
MCF7
OVCA420
Pseudotime
15
10
5
0
−5
Groups
CHIR99021
LY364947
Necrostatin−5
Phthalazinone Pyrazole
Ruxolitinib
SB−431542
Uninhibited_TGFB1
Uninhibited_Untreated

b

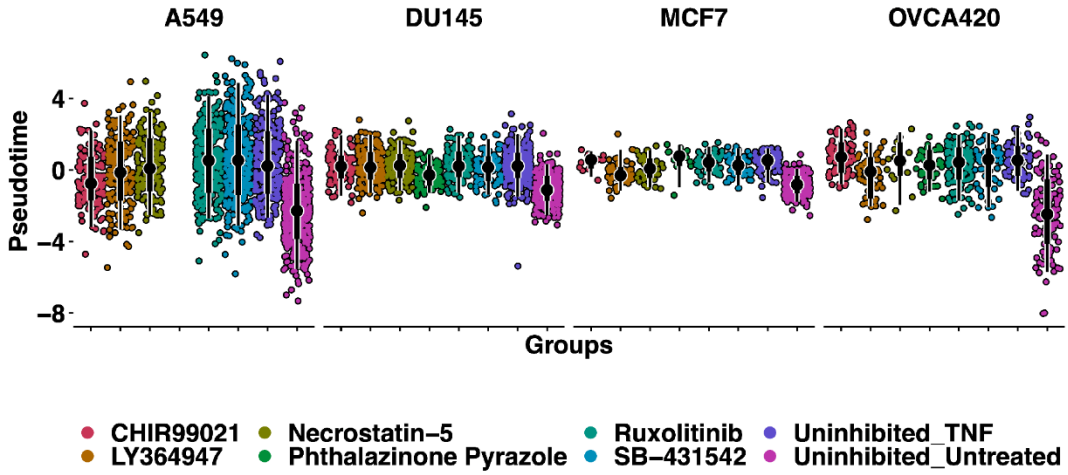
Cell lines treated with TNFa and inhibitors
A549
DU145
MCF7
OVCA420
Pseudotime
4
0
−4
−8
Groups
CHIR99021
LY364947
Necrostatin−5
Phthalazinone Pyrazole
Ruxolitinib
SB−431542
Uninhibited_TNF
Uninhibited_Untreated

c

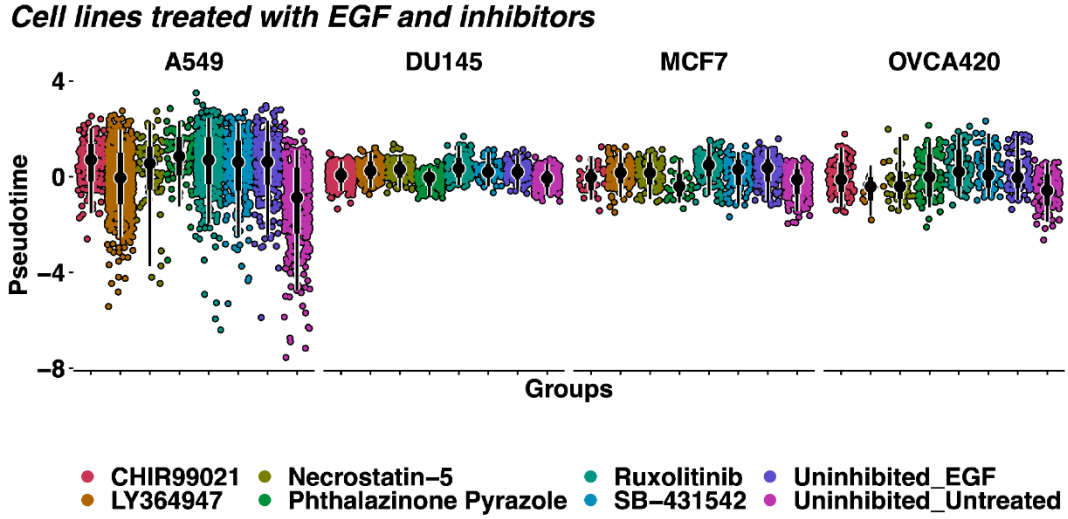
Cell lines treated with EGF and inhibitors
A549
DU145
MCF7
OVCA420
Pseudotime
4
0
−4
−8
Groups
CHIR99021
LY364947
Necrostatin−5
Phthalazinone Pyrazole
Ruxolitinib
SB−431542
Uninhibited_EGF
Uninhibited_Untreated

Figure 43. Pseudotime values across time-pointed treated cell lines of different origins treated with different EMT inducers. (a-c) Pseudotime values of A549, DU145, MCF7, or OVCA420 cell lines either treated either with EMT inducers TGF-β1 (a), TNFα (b), EGF (c) or EMT inducers and kinase inhibitors: RIP1 kinase inhibitor Necrostatin5, TGFβR1 kinase inhibitor LY364947, JAK1/2 kinase inhibitor Ruxolitinib, TGFβ/ALK kinase inhibitor SB-431542, GSK3 kinase inhibitor CHIR99021, or TGF-β1 and Aurora kinase A inhibitor phthalazinone pyrazole.

Chapter 5: scRNA-seq analysis reveals classical and non-classical HLA I allotype expression positively associates with EMT in cancer

These results presented in this chapter contributed to a review article published in *Cancers* **15**, 5694 (2023).

Unveiling the Immunogenicity of Ovarian Tumors as the Crucial Catalyst for Therapeutic Success

Galaxia M. Rodriguez[1,2†], **Edward Yakubovich**[1,2†], and Barbara C. Vanderhyden[1,2*].

[1]Cancer Therapeutic Program, Ottawa Hospital Research Institute, 501 Smyth Road, Ottawa, Ontario Canada, K1H 8L6.

[2]Department of Cellular and Molecular Medicine, University of Ottawa, 451 Smyth Road, Ottawa, Ontario, Canada, K1H 8M5.

[†]These authors contributed equally to this work.

Keywords: Classic HLA I, non-classic HLA I, ovarian cancer, tumor immunogenicity, EMT, tumor-associated antigens.

5.1 EMT is associated with expression of Class I HLA molecules

Results in the previous chapter showed that there is a correlation between EMT and presence of immune cells in the TME, where a greater proportion of mesenchymal cells in the TME is associated with a higher proportion of cytotoxic immune cells in the TME. From that analysis, we discovered links between EMT and the regulation of immune cell activity, with the LAG3-LGALS3 axis being one of them. Furthermore, individual cancer-specific EMT signature genes that were highly expressed in cancer cells from infiltrated and excluded TMEs included HLA-A and HLA-C. Tumor immunogenicity is largely dependent on the expression of HLA complexes (Shiina et al., 2009). HLA complexes are essential proteins that present foreign antigens and self-peptides for detection by T lymphocytes (Shiina et al., 2009). The HLA gene in humans is the most complex and polymorphic in the human genome, and has been associated with over a 100 different diseases (Cruz-Tapias et al., 2013; Shiina et al., 2009). Class I HLA molecules are polymorphic and ubiquitously expressed HLA-A, -B, and -C allotypes and non-classical HLA-E, -F, -G, -H, -J, -K, and -L allotypes. HLAs are involved in immunosurveillance and, for that reason, tumors tend to downregulate these genes as a means of immune escape (B. C. Taylor & Balko, 2022), a common hallmark of EOC (Aust et al., 2017; Dholakia et al., 2022; Garrido, 2019). We therefore decided to delve deeper and explore the link between antigen presenting machinery (APM) and EMT. Published evidence indicates that there is an inverse correlation between the two (Mullins et al., 2022; Terry et al., 2017) in various animal and cell line models of cancer, using a variety of *in vivo*, *in vitro*, and *in silico* methods (Antony & Huang, 2017; Dongre et al., 2021; Tripathi et al., 2016). We began our exploration by obtaining scRNA-seq

datasets from a variety of cancer types (breast cancer, colorectal cancer, gastric cancer, lung cancer, nasopharyngeal cancer, ovarian cancer, pancreatic ductal adenocarcinoma, squamous cell carcinoma) and examining aggregate expression of all Class I HLA molecules (HLA A-G) against either the Hallmark EMT module or scoring using our cancer-specific EMT module. The results revealed positive correlations between the averaged expression of HLAs and the cancer-specific EMT module score in cancer cells from all tumor types analyzed, (**Figure 44a**) or using the Hallmark EMT module (**Figure 44b**) where there were similar trends, albeit weaker R^2 coefficient of determination values, in almost all cancers except nasopharyngeal cancer.

a

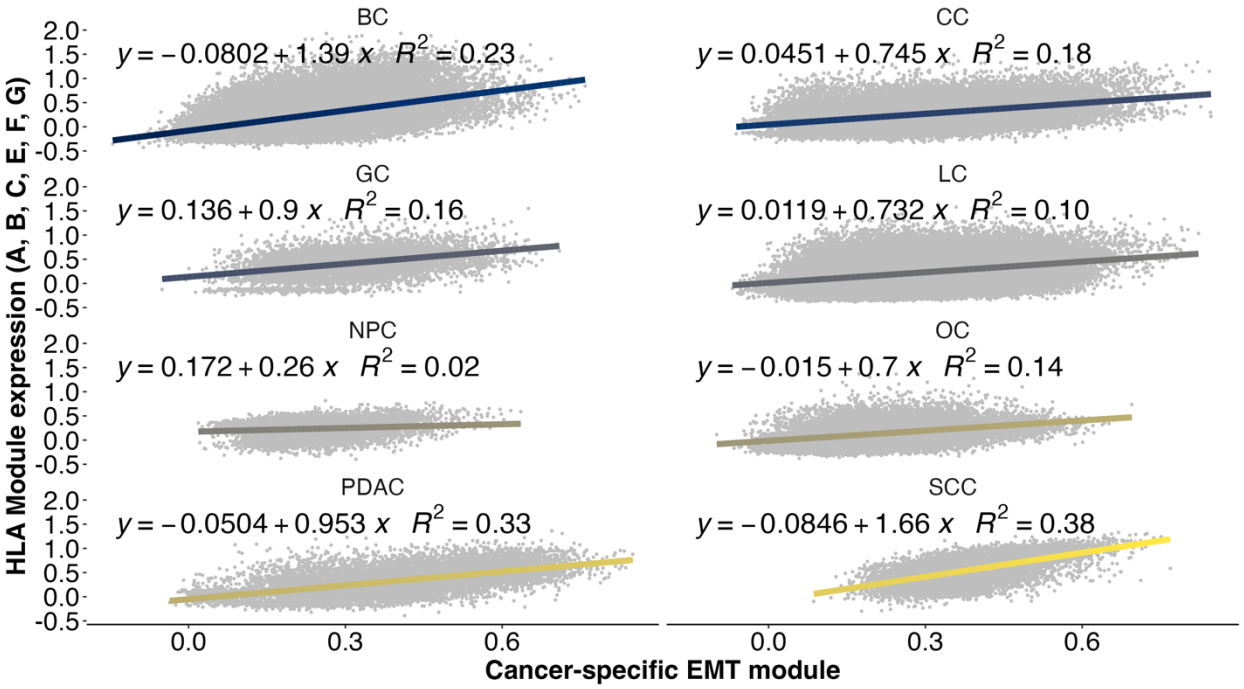
BC
y = −0.0802 + 1.39 x R² = 0.23
CC
y = 0.0451 + 0.745 x R² = 0.18
GC
y = 0.136 + 0.9 x R² = 0.16
LC
y = 0.0119 + 0.732 x R² = 0.10
NPC
y = 0.172 + 0.26 x R² = 0.02
OC
y = −0.015 + 0.7 x R² = 0.14
PDAC
y = −0.0504 + 0.953 x R² = 0.33
SCC
y = −0.0846 + 1.66 x R² = 0.38
HLA Module expression (A, B, C, E, F, G)
Cancer-specific EMT module

b

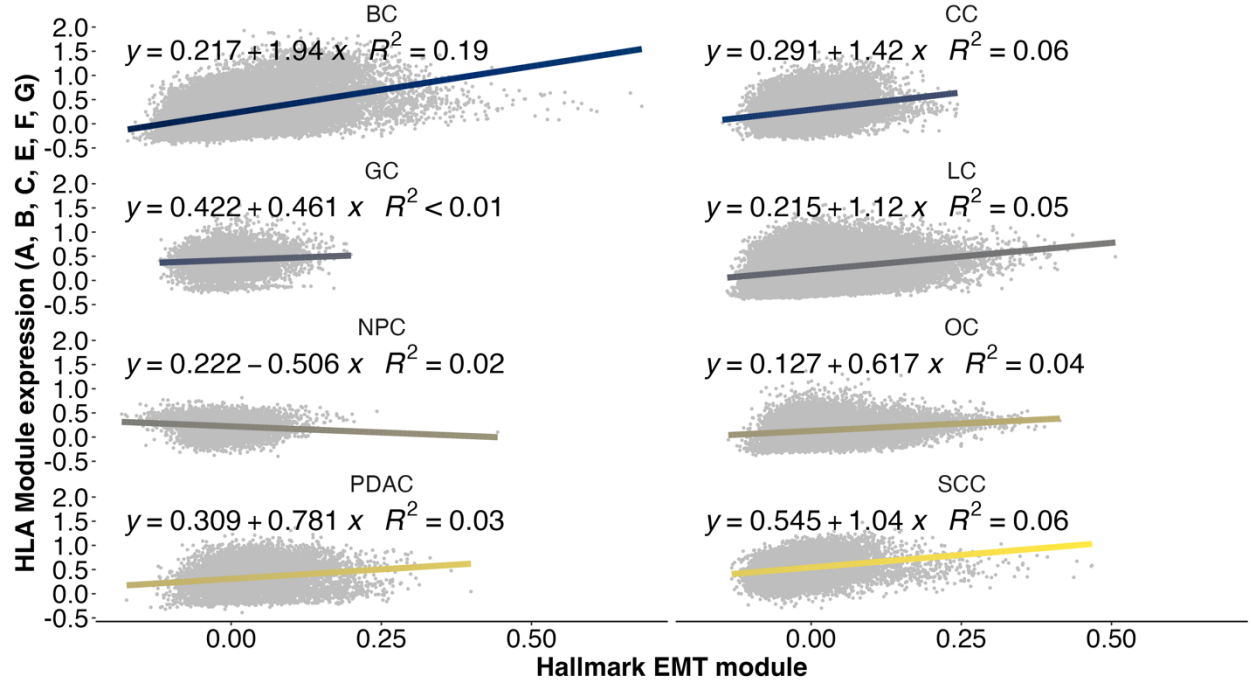
BC
y = 0.217 + 1.94 x R² = 0.19
CC
y = 0.291 + 1.42 x R² = 0.06
GC
y = 0.422 + 0.461 x R² < 0.01
LC
y = 0.215 + 1.12 x R² = 0.05
NPC
y = 0.222 − 0.506 x R² = 0.02
OC
y = 0.127 + 0.617 x R² = 0.04
PDAC
y = 0.309 + 0.781 x R² = 0.03
SCC
y = 0.545 + 1.04 x R² = 0.06
HLA Module expression (A, B, C, E, F, G)
Hallmark EMT module

Figure 44. Average gene expression of MHC-I related HLA allotypes correlates with EMT in various cancer types. Expression of MHC-I related HLA allotypes (HLA A-G) scored in the cancer cell compartment of a variety of tumors (BC – Breast Cancer, CC – Colon Cancer, GC – Gastric Cancer, LC – Lung Cancer, NPC – Nasopharyngeal Cancer, OC – Ovarian Cancer, PDAC – Pancreatic Ductal Adenocarcinoma, SCC – Squamous Cell Carcinoma). HLA expression was correlated with EMT scores of those cells based on either (a) a cancer-specific EMT module published by Cook and Vanderhyden (2022) or (b) the Hallmark EMT module from MSigDb.

The association between individual HLA I molecules and EMT in ovarian cancer cells specifically was then investigated to find that *HLA-A*, *HLA-B*, *HLA-C*, and *HLA-E* show a correlation ($R^2 = 0.19$, $R^2 = 0.15$, $R^2 = 0.16$, $R^2 = 0.09$) with cancer-specific EMT module scores (**Figure 45a**). We also found an association between *HLA-A*, *HLA-B*, *HLA-C* ($R^2 = 0.07$, $R^2 = 0.03$, $R^2 = 0.0.4$) and Hallmark EMT module scores (**Figure 45b**). Taken together, these findings suggest that, in contrast to published evidence for an inverse correlation (Mullins et al., 2022; Terry et al., 2017), the mesenchymal state of ovarian cancer cells is associated with an increase in expression of classical HLA I molecules (HLA-A, HLA-B, HLA-C) but not non-classical HLA I molecules (HLA-E, HLA-F, HLA-G).

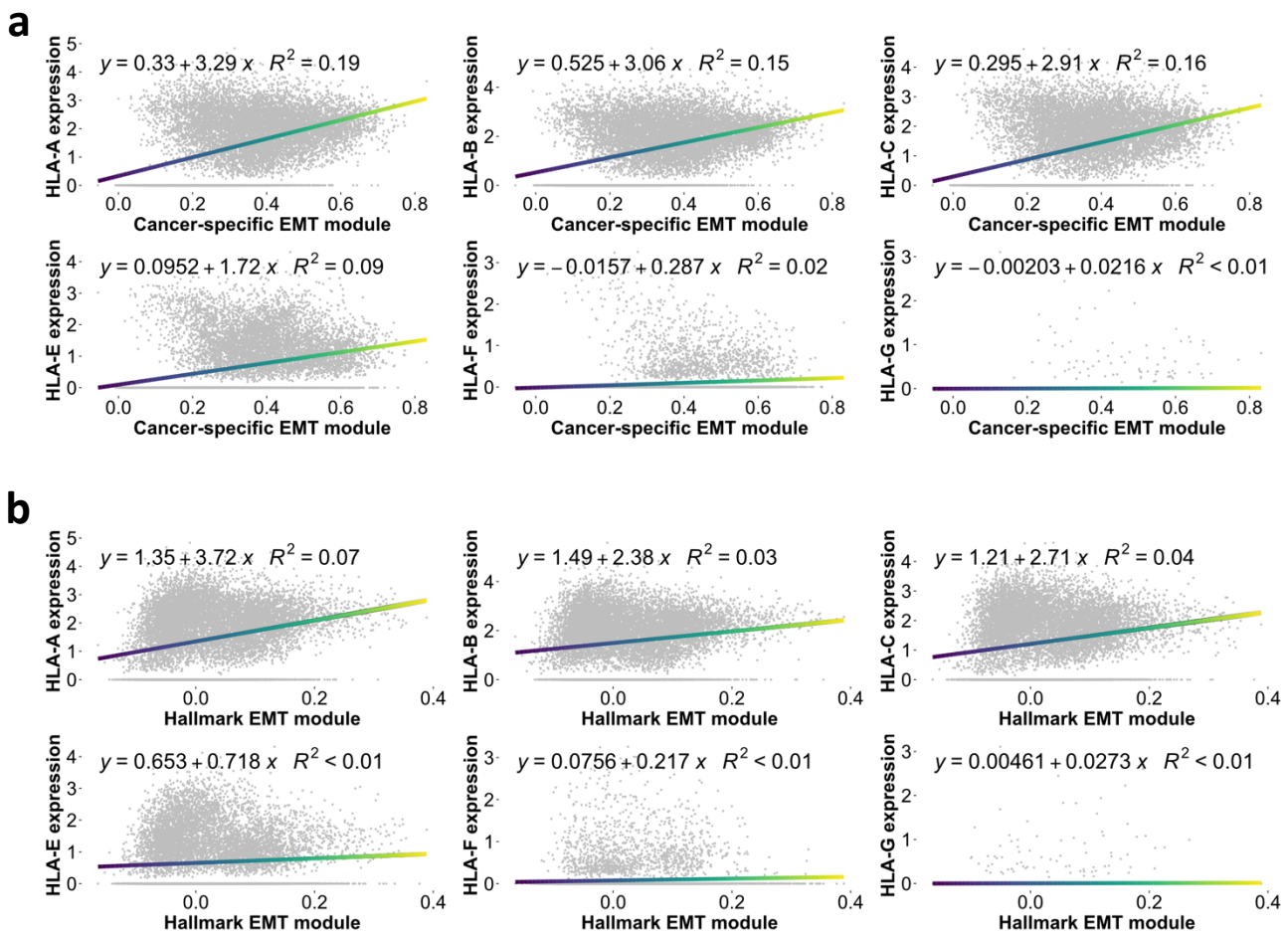

Figure 45. Average gene expression of specific HLA I allotypes increases in correlation with the average EMT gene expression in ovarian cancer cells. Gene expression of HLA I allotypes in ovarian cancer cells using the cancer-specific EMT module (a) or the Hallmark EMT module (b).

5.2 Activation of EMT pathways is associated with an increased expression of HLA molecules in vitro in cancer cells from different cancer types

Based on the observation that there is an association between EMT and HLA I allotype expression *in vivo*, we decided to explore the link further by treating three different cancer cell lines with three EMT inducers *in vitro* and sequencing the cells over five different time points. HLA expression was examined, as well as the expression of MHC machinery genes *TAP1*, *TAP2*, and *PSMB9*. We previously confirmed that all three inducers indeed promote EMT in these cell lines (Cook & Vanderhyden, 2020). In

TGFβ-1 treated OVCA420 cells, there was a small increase in *HLA-A* expression and a modest increase in *HLA-C* expression, while in both MCF7 and A549 cells there was a modest increase in expression of *HLA-A*, *HLA-B*, *HLA-C*, and *HLA-E* (**Figure 46a**). There was also an increase in expression of *TAP1* in OVCA420, MCF7, and A549 cell lines. The results suggest that TGFβ-1 treatment increases the expression of HLA I allotypes and related machinery in cell lines from different cancer types.

When we examined HLA I allotypes and related machinery after EGF treatment of the different cell lines we did not notice any consistent changes in expression in any of the targets (**Figure 46b**). However, examination of these targets in TNFα treated cells revealed similar trends to TGFβ-1 treatment where *HLA-A* and *HLA-C* slightly increased in OVCA420 cells. while *HLA-A*, *HLA-B*, *HLA-C*, *HLA-E*, *TAP1*, and *PSMB9* increased in MCF7 and A549 cells following TNFα treatment (**Figure 46c**). Taken together, the results indicate that TGFβ-1 and TNFα upregulate expression of both classical and non-classical HLA I allotypes as well related machinery in MCF7 and A549 cells in correlation with the EMT. It remains unknown whether upregulation of these genes is a consequence of the EMT or happens in parallel with the EMT.

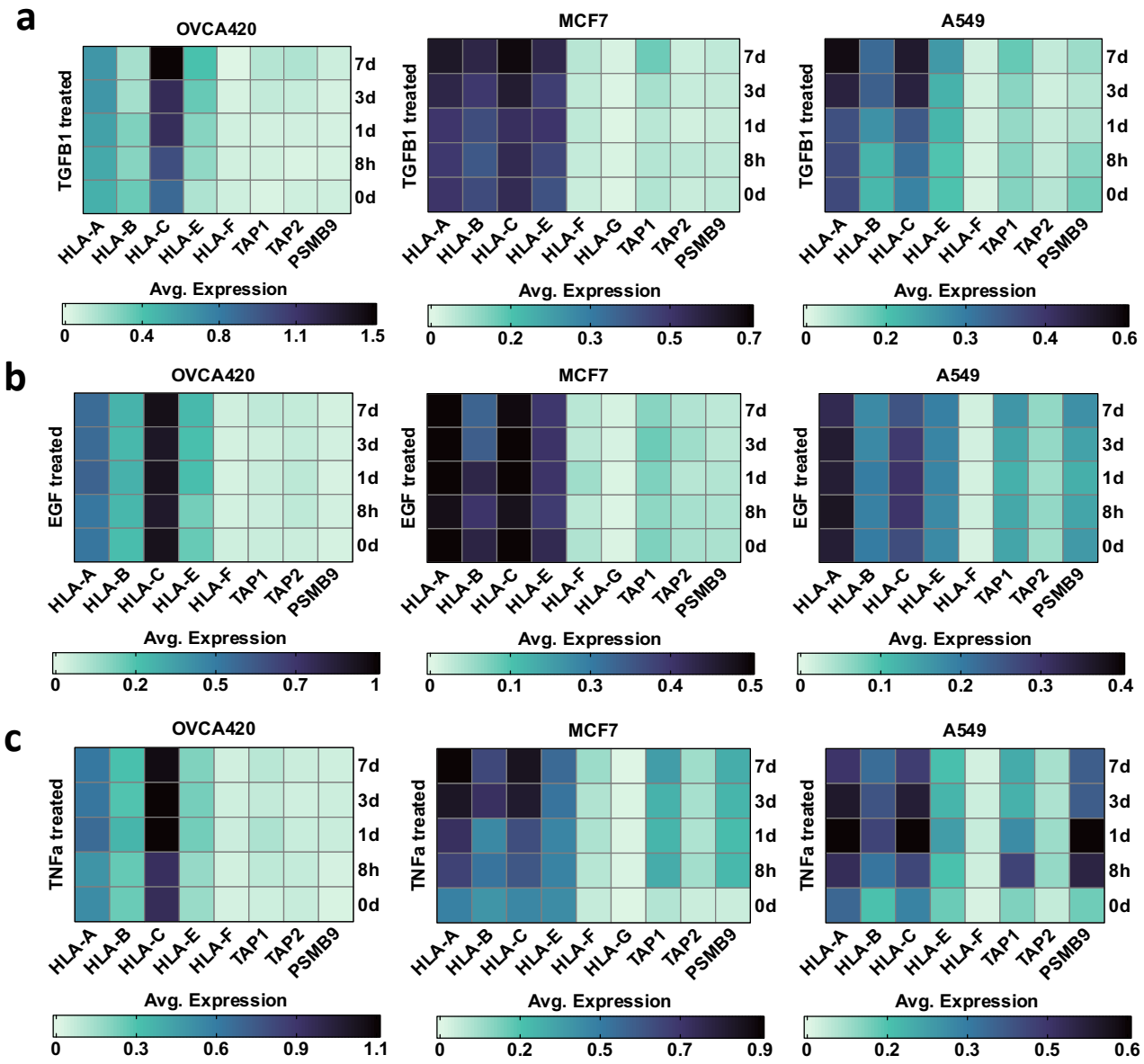

Figure 46. Average gene expression of HLA I allotypes and some APM components correlate with EMT in cancer cell lines. Heat map showing expression levels of transcripts for MHC-I related HLA allotypes (*HLA A-G*) and machinery (*TAP1, TAP2, PSMB9*) in ovarian (OVCA420), breast (MCF7) and lung (A549) cancer cell lines in response to treatment with (a) TGF-β1, (b) EGF, and (c) TNFα for 0 and 8 hours, and 1, 3, and 7 days. Data were extracted from single-cell RNA-seq datasets published by Cook and Vanderhyden, 2022.

5.3 RIP1 kinase inhibitor Necrostatin-5 reduces the expression level of some HLA I components

Given that EMT and HLA I expression appears to be correlated in our *in vivo* and *in vitro* model systems, we next explored whether a panel of kinase inhibitors previously

shown to attenuate EMT(Cook & Vanderhyden, 2020) can also attenuate expression of HLA I machinery. To do this, we leveraged a scRNA-Seq dataset(Cook & Vanderhyden, 2020) of MCF7 cells treated with a wide variety of kinase inhibitors. As per previous sections, we had already demonstrated that TNFα treatment in MCF7 cells increases per-cell EMT scores calculated using the cancer-specific EMT module. In this analysis, Necrostatin-5 appeared to modulate TNFα-induced expression of *HLA-A*, *HLA-C*, and *PSMB9* (**Figure 47**), suggesting that while Necrostatin-5 may affect the pathways activated by TNFα treatment that led to HLA I upregulation. This result implicates the RIP1 kinase pathway in upregulation of HLA I related molecules and machinery. While these results are specific to the breast cancer cell line MCF7, this does not necessarily mean that Necrostatin-5 is unable to attenuate HLA expression in ovarian cancer. Indeed, the analysis of ovarian cancer cells, specifically the OVCA420 cell line used for the kinase inhibitor experiment, was impeded by the low number of cells sequenced per sample, thus preventing us from making conclusions about the effects of Necrostatin-5 on OVCA420 cells as it relates to EMT. Nevertheless, as seen in ovarian cancer and indeed other cancer types, there is a correlation between EMT and HLA expression that is contrary to previous findings (X.-H. Chen et al., 2015; Y. Gu et al., 2023; Mullins et al., 2022; G. Wang et al., 2021), suggesting that this topic is not a foregone conclusion and requires future experimentation with single-cell methods.

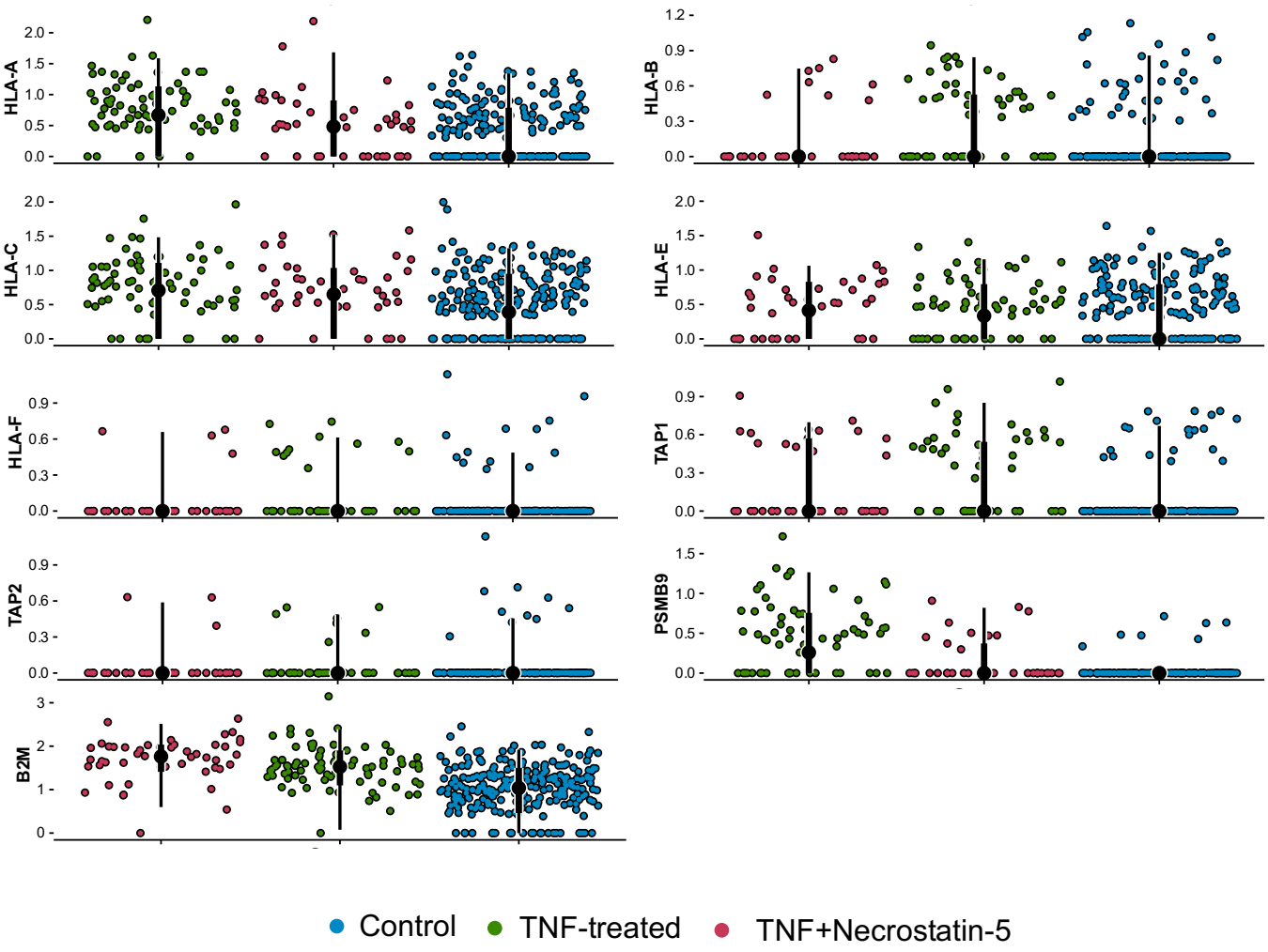

Figure 47. Average gene expression of classical HLA I allotypes and APM components is abrogated by RIP1 kinase inhibitor in TNFα treated MCF7 cells. Gene expression of MHC-I related HLA allotypes (*HLA A-F*) and machinery (*PSMB9*, *TAP1*, *TAP2*, *PSMB9*, *B2M*) in MCF7 cancer cells treated with TNFα with or without the addition of the RIP1 kinase inhibitor necrostatin-5.

Chapter 6: Discussion

6.1 Characterization of EMT in human and murine models of ovarian cancer

Results from this section have shown that there is a possible link between immune infiltration and EMT, where a greater presence of mesenchymal cells in the TME correlates with a greater number and variety of immune cells. Furthermore, we identified factors *CCL2*, *CCL5*, and *IL1a* that are possibly linked to some kind of regulation of NK cells, though immunosuppression of NK cells was primarily achieved by exposure to TGF-β1. Finally, we discovered *QSOX1* and *IL32* as markers of mesenchymal cells in human ovarian cancer.

6.1.1 Detecting EMT and classifying cells using RNA-level data

Historically, there have been a handful of markers used to identify EMT. Broadly speaking, they are Snail, Slug, Zeb1/2, Twist1/2, N-cadherin, E-cadherin, Vimentin. Based on all the information known about EMT, it is natural to assume that using these markers to identify mesenchymal cells would be the gold standard. However, several key issues must be considered to address this notion: First, modalities matter when discussing EMT, where protein expression and gene expression of EMT markers is often inconsistent when trying to classify cells on an epithelial versus mesenchymal axis (Subhadarshini et al., 2023; Zeisberg & Neilson, 2009). One reason for this disconnect could be related to post-translational modifications of the proteins that regulate EMT (J. Yang et al., 2020). In fact, it has been suggested that biological markers are inadequate to describe cells undergoing EMT or the reverse MET process (J. Yang et al., 2020). Rather, it was proposed that in addition to the classical set of biomarkers, researchers

should strive to describe functional changes in the cells that are consistent with EMT, like changes to the cell-cycle and protein production, on top of utilizing the biomarker suite (J. Yang et al., 2020).

Second, further complications are expected when considering the context specificity of the EMT such that both the biomarker and functional profile of cells undergoing the transition depends on the context, i.e., healthy vs. disease type, *in vitro* or *in vivo* investigations, and organism (Cook & Vanderhyden, 2020). For example, clinical investigations of the EMT (Z. Huang et al., 2022), therapeutic considerations that take EMT into account (Z. Huang et al., 2022), research-based investigations of the EMT (Cook & Vanderhyden, 2022), and cell types (Malagoli Tagliazucchi et al., 2023) are all important contexts that can dictate which EMT markers to use. In another example, while the classical EMT markers have been associated with EMT and mesenchymal cells in some cancer contexts, not all of them faithfully capture mesenchymal cells across all cancer contexts (Cook & Vanderhyden, 2022; Liberzon et al., 2015).

Third, some classical EMT markers fail to capture intermediate states, the so-called partial-EMT (pEMT), likely because discovery of these markers hails from developmental contexts which are not fully analogous, transcriptionally speaking, to cancer contexts (Tyler & Tirosh, 2021). Last of all, EMT markers can be associated with non-cancer cells in some *in vivo* contexts, making them suboptimal for characterizing metastasis in tumor tissues if the technique used cannot distinguish cancer cells from other cell types in the TME (McCorry et al., 2018; Tyler & Tirosh, 2021). Taken together, it is becoming clear that finding a catch-all biomarker or a set of markers for EMT will be

difficult, especially on the RNA level where transcripts can be subject to many modifications prior to and after translation.

Recent attempts have been made to establish a set of genes or a module that can adequately capture the entire spectrum of EMT, that is both pEMT states and fully mesenchymal states, with a simple score based strategy where a higher “score” would indicate a “more mesenchymal” cell (Cook & Vanderhyden, 2022). Thus, we set out to characterize the EMT using single-cell cancer data from models in which EMT was induced in a time course. Because the use of a gene module requires, at the very least, RNA-level data on a single-cell level, we decided to try and distill this strategy to some single genes that could be reliable at detecting EMT for bulk RNA-seq or qPCR purposes. Our attempts to do so are not novel (Liberzon et al., 2015; Yetkin & Alotaibi, 2023), and our intention was to highlight the complexity of EMT rather than to add to the milieu of EMT biomarkers in the field. We discovered through cross-referencing multiple gene modules against scRNA-seq data that *QSOX1* emerges as the most consistent single gene for an EMT scoring strategy where higher levels of *QSOX1* expression are associated with increasingly more mesenchymal cells. QSOX1, an enzyme crucial in protein folding, has previously been linked to metastasis in glioblastoma (Geng et al., 2020), renal cell carcinoma (Fifield et al., 2020), lung cancer (Sung et al., 2018), and liver cancer (X.-F. Zhang et al., 2019). Moreover, recent work has shown that *QSOX1* promotes invasion and migration of cancer cells in glioblastoma through the PI3K/AKT pathway (Geng et al., 2020), which has previously been established as an EMT-related pathway that promotes Snail expression and repression of E-cad (W. Xu et al., 2015). Interestingly, we also found that low *QSOX1* expression in bulk RNA-seq data from the

Protein Atlas is associated with greater survival of ovarian cancer patients, suggesting that *QSOX1* may indeed be associated with metastasis, an obvious complication of progressing cancer that lowers the chances of survival. However, in breast cancer, high *QSOX1* expression has been associated with better outcomes (Pernodet et al., 2012), despite our finding that high *QSOX1* expression in breast cancer-derived MCF7 cells is associated with mesenchymal cells. Taken together, we found that *QSOX1* can reliably be used in *in vitro* contexts to trace the EMT in ovarian cancer cells, where higher expression values are associated with increasingly mesenchymal phenotypes.

In our attempts to characterize the EMT, we also discovered *IL32* transcripts to be highly correlated with EMT. Interestingly, IL32 has recently been at the forefront of EMT and cancer research (L. Gong et al., 2020b; Khawar et al., 2016; Wen et al., 2019). Little is known about its correlation with EMT, since researchers have had to contend with the fact that it has opposite effects in different cancer contexts (Shim et al., 2022). Indeed, results from our *in vitro* time course of cancer cells undergoing EMT show that *IL32* is a marker in very specific contexts that depend on the inducer used and the origin of the cancer cell line. One possible reason for these differences could be the fact that IL32 was found to trigger the MAPK signalling cascade through integrin β3 receptor on the plasma membrane in MCF7 cells (Wen et al., 2019), a receptor that synergistically promotes EMT together with TGF-β1 (Kariya et al., 2021). Not surprisingly, *IL32* shows the highest expression in MCF7 cells treated with TGF-β1 for 7 days in our models.

Taken together, our efforts to characterize EMT in mesenchymal ovarian cancer cells revealed that expression of two genes, *QSOX1* and *IL32,* have a positive

correlation, where higher expression correlates with more mesenchymal cells. Of course, one drawback of our experiments is that both genes were investigated using *in vitro* models, so future experiments should be expanded to include *in vivo* datasets. Another drawback of these findings is generalizability, where using these markers for single-cell data could prove useful in both *in vitro* and *in vivo* data, but other RNA-based assays like qPCR may be restricted to *in vitro* data as the presence of *QSOX1* in cell types other than cancer may confound analysis of EMT in bulk material like total RNA from whole tumors.

6.1.2 The immunosuppressive effects of mesenchymal cancer cells on NK cells

It is a well-established fact that EMT, and more specifically mesenchymal cells, possess a very intense immunosuppressive potential in cancer (Dongre et al., 2020; Rodriguez et al., 2023; Taki et al., 2021). Based on preliminary data showing high expression of many chemokines, cytokines, and interleukins in OVCA420 ovarian cancer cells following TGF-β1 treatment, we explored the immunosuppressive correlates of EMT using *in vitro* and *in silico* techniques. Particularly, we honed in on NK cells as these are cytotoxic cells capable of cancer clearing (S.-Y. Wu et al., 2020). There is relatively sparse literature on the effects of EMT directly on NK cells' immunosurveillance ability (Okita et al., 2018) specifically when compared to the vast literature on EMT-mediated immunosuppression of $CD8^+$ T-cells.

NK cells are innate lymphoid cells possessing the ability to rapidly detect cells that are either infected or transformed and eliminate them (Kiessling et al., 1975; Spits et al., 2016). Importantly, infiltration of NK cells into the tumor microenvironment (TME)

has been associated with longer survival in many cancers, including ovarian cancer (K. Imai et al., 2000).The capability of NK cells to enact cytotoxic action and immunosurveillance against cancer cells is tightly regulated by activating ligands that are expressed by tumor cells and interact with NK cell receptors, such as NK cell group 2 member D (NKG2D), or inhibitory ligands such as killer lectin-like receptor G1 (KLRG1) and major histocompatibility complex I (MHC I) (Bauer et al., 1999; Cerwenka et al., 2001; Cosman et al., 2001; Martinet & Smyth, 2015). It is the integration of these signals that determines whether an NK cell will activate against the cell by recognizing it as a non-self-interaction or permit cell survival by recognizing it as a self-interaction, that is a healthy cell that is of that organism. Interestingly, E-cad is an inhibitory signal of NK cell activity through the KLRG1 receptor (Schwartzkopff et al., 2007) while cell adhesion molecules 1 (CADM1), a factor often upregulated during EMT, activates NK cells through the cytotoxic and regulatory T cell-associated (CRTAM) receptor on NK cells (Boles et al., 2005; Chockley et al., 2018). Other effectors of NK cell function and chemotaxis include chemokines CCL2, CCL3, CCL4, CCL5, interleukins IL-2, IL-8, IL-15, IL-18 and a milieu of other receptor-ligand combinations (Ran et al., 2022). Taken together, there are a myriad of factors that could affect NK cell cytotoxicity in cancer.

When we first set out to determine which possible factors expressed and secreted during EMT could affect NK cell function or trafficking, we cast a wide net with our screen to find factors secreted by OVCA420 ovarian cancer cells undergoing EMT in response to TGF-β1 treatment. Unfortunately, very few factors were present at detectable levels in the media of mesenchymal cells that were absent from epithelial media, but there were three notable factors, namely CCL2, CCL5, and IL1a. The role of

these factors in regulating the activity of NK has already been extensively characterized. CCL2 and CCL5 are involved in trafficking and recruitment of NK cells to where they are expressed (Ran et al., 2022) while the role of IL1a is to promote NK cell production of IFNγ (Conti et al., 1991; Cooper et al., 2001). IFNγ in turn plays a role in regulating tumor growth and apoptosis of cancer (Cui et al., 2020), similar to when it is secreted by other cytotoxic cells like $CD8^+$ T-cells.

Bearing in mind that we were looking for any novel factors that could be involved in immunosuppression of NK cells, it was disappointing to discover that the factors found in our assays had already been well characterized for their effects on NK cells. Regardless, when we sought to determine if mesenchymal media have any immunosuppressive effects on NK cells, we discovered that the main factor involved in repressing the cytotoxic ability of NK cells was TGF-β1, a not unexpected result (Castriconi et al., 2003). While it is true that we treated the cells with TGF-β1 to induce EMT which could account for the immunosuppressive effect that was observed, even if EMT was induced by other means that did not involve an exogenous signal (i.e*. Snai1 or Snal2 overexpression*), the cells would still produce TGF-β1 and self-regulate using autocrine mechanisms once mesenchymal (DAROQUI et al., 2012; Yeh et al., 2018). Even after we leveraged a novel cell-cell communication algorithm on our scRNA-seq data, none of the ligands identified there (CD59, Nectin2, MIF, MDK) successfully had any immunosuppressive effect on NK cells.

Based on all the available evidence, we made the following conclusions. First, the main immunosuppressive force behind repression of NK cell cytotoxicity is likely

TGF-β1, which is to be expected considering the TGF-β pathway is a key EMT pathway. Second, it is well-established that the factors identified in our multiplexed ELISA screens are involved in chemotaxis of NK cells. This is consistent with previous evidence that NK cells' activation is regulated by a very tightly conserved set of receptors and ligands as outlined earlier, none of which are CCL2, CCL5, and IL1a. Rather, these factors are involved in chemotaxis of other immunosuppressive cells such as TAMs, T regs, and MDSCs. Third, while our scRNA-seq cell-cell communication screen did identify some novel factors that interact with NK cells, it is likely that they either require some adjuvant to activate NK cells (Deuss et al., 2017; Marcenaro et al., 2003) or work in combination or are also involved in trafficking of the cells. Fourth, our model system relied on the effector function of NK92 cells which could be different from healthy NK cells considering that NK92 cells are immortalized lymphoma cells (J. H. Gong et al., 1994) and may have different sets of receptors and different signaling pathways compared to healthy NK cells.

Regardless of the potential technical issues involved with the biology of NK92 cells, it is apparent the main driving immunosuppressive force on these cells is TGF-β1. As such, future experiments could investigate the roles of factors such as MDK, MIF, Nectin2, CCL2, CCL5, and IL1a in chemotaxis of NK92 cells as a function of EMT using two-chamber migration and invasion assays, for example.

6.1.3 Characterization of EMT in murine ID8 and STOSE models

After characterizing the EMT in human *in vitro* models of cancer, we decided to do the same in the murine syngeneic ovarian cancer models ID8 and STOSE.

Extensive characterization of these cells (Cook et al., 2023) and the tumors they generate (Cook et al., 2023; Rodriguez et al., 2022) showed that while they are both models of ovarian cancer resulting from spontaneous transformation of ovarian surface epithelial cells, they are not without their differences, such as greater presence and variety of immune cells in the TME. Based on these differences, we aimed to characterize the EMT in these cells and the tumors they generate, as potential models in which the immunosuppressive actions could be manipulated and studied in vivo. The initial analysis using our cancer-specific EMT module showed that the module's scores correlated with our independent pseudotime analysis in ID8 cells but not STOSE cells, suggesting that the cancer-specific module marks the EMT continuum in ID8 cells but is inadequate to mark EMT in STOSE cells, *in vitro*. Bearing in mind that this cancer-specific EMT module was context-agnostic in human cancers (Cook & Vanderhyden, 2022), we were surprised to learn that its scores did not correlate with pseudotime values in the STOSE cells. While this does not necessarily mean that the EMT module should not be used here, it does suggest there is a better module composed of different genes that can better classify mesenchymal cells in STOSE cells after being induced to undergo EMT.

We were curious to see if the correlations between chemokines, cytokines, and interleukins found in the human *in vitro* models are also reflected in the murine models. In the multiplexed ELISA screens, we found no discernible trend of any factor that correlated with EMT. Despite this, we assessed if IL18, a well-known PD-1-dependent immunosuppressor in cancer (H. X. Lim et al., 2014; Nakamura et al., 2018; Terme et al., 2011b), has a significant presence in mesenchymal ID8 and STOSE cells or in

ascites derived from syngeneic orthotopic ID8 and STOSE tumors to find that it does not. However, we did note a trend where the ascites from either ID8 or STOSE tumors had double the concentration of IL18 compared to the supernatant of cell lines that are fully mesenchymal, though it may also have come from non-cancer cells such as CAFs, also present in the ascitic fluid.

While attempting to identify immunosuppressive factors produced by the murine cancer cell lines, we also found some genetic differences between ID8 and STOSE cancer cells. For example, the classical epithelial cancer cell marker *Epcam* can be used as a biomarker for cancer cells in ID8 tumors but not STOSE tumors, suggesting that the two cell lines and tumor microenvironments they generate are vastly different despite having the same tissue of origin. We therefore generated unique gene signatures for ID8 and STOSE cancer cells within tumors and found that each respective cancer cell population has unique genetic markers that distinguish it from the other, once again highlighting the heterogeneity between them. For example, while *Sox9* and *Star* are unique to ID8 cancer cells, *Slpi* and *Krt14* are unique to STOSE cancer cells. In addition to being used to mark cancer cells in each respective model, these markers can be used to compare to similar analyses of DEGs in the different subtypes of HGSOC, which would enable the selection of a model best suited to future experiments on that subtype. We also found that these signatures enrich for different biological pathways in each disease, suggesting that the underlying genetic differences between the two models lead to very different TMEs.

Finally, after converting the cancer specific EMT module to its murine orthologs and using it to score the cancer cells from each tumor, we found that STOSE cancer

cells have higher EMT scores compared to ID8 cancer cells. Curiously, STOSE TMEs also have more immune infiltration when compared to ID8 TMEs (Rodriguez et al., 2022), suggesting a possible link between cancer cell EMT and greater infiltration by immune cells.

6.1.4 Exploring links between EMT and immune infiltration

Knowing that an ID8 TME is immune poor, or "colder" than a STOSE TME, and also has fewer mesenchymal cells, we further explored the possible correlation between ID8, STOSE EMT scores and immune infiltration. Specifically, we sought to determine if upregulation of an EMT-TF to induce an EMT would be sufficient to increase immune infiltration. We targeted upregulation of either *Snail* and *Slug* as they have been established to be sufficient induce an EMT and promote invasion and dissemination of cancer cells in breast cancer (Dongre et al., 2017). Unfortunately, when we treated the cells with doxycycline to induce *Snail* expression, we saw no differences in the qPCR analysis of either classical EMT markers or non-classical markers derived from the scRNA-seq dataset of the cell lines. We also saw no visual changes reminiscent of mesenchymal phenotypes and no decrease in cellular proliferation, a common feature of mesenchymal cells. Mice that were injected orthotopically with these cells and then fed doxycycline also showed no differences in survival, tumor weight, and ascites volume after *Snail* was overexpressed. A lack of any discernible EMT was also seen with *Slug* overexpression, leading us to conclude that neither *Snail* nor *Slug* are sufficient to induce an EMT in ID8 cells. We had expected some changes to the cells based on other experiments where normal mouse ovarian surface epithelial cells

(mOSE) did acquire EMT-dependent stemness phenotypes seen in mesenchymal cells when *Snail* was overexpressed (Carter et al., 2021). Based on these observations, we concluded that the spontaneous transformation into ID8 cells has caused the cells to lose their responsiveness to *Snail* as an inducer of EMT. In future experiments, it may be required to upregulate both *Snail* and *Slug* in the same cells to achieve EMT, or perhaps different EMT-TFs such as Zeb1/2 and Twist1/2, alone or in combination, could be tested.

Because we were unsuccessful in our attempts to link EMT and immune infiltration in murine models of ovarian cancer, the remainder of the work in this thesis returned to human ovarian cancers to explore similar links using *in silico* techniques.

6.2 Mesenchymal ovarian cancer cells promote $CD8^+$ T cell exhaustion through the LGALS3-LAG3 axis

In this chapter, we discovered that there is a positive correlation between infiltration of immune cells in the ovarian TME and EMT in cancer cells. Additionally, we found that mesenchymal cells expressing *LGALS3* may exhaust $CD8^+$ T cells through the *LAG3* receptor, suggesting that there is another mechanism deployed by mesenchymal cells to avoid immunosurveillance.

6.2.1 LAG3 is a druggable target for ovarian cancer therapy

In this study, we explored whether the epithelial-mesenchymal state of the cancer cells in human ovarian cancers have different interactions with the immune cells of the TME. We showed that the EMT, a complex cellular process underpinning metastasis,

associates with *LGALS3* expression, which may act as a ligand for *LAG3* in $CD8^+$ T cells, promoting T cell exhaustion and dampening antitumor immunity. Additionally, we showed that infiltrated TMEs in HGSOC have cancer cells that are, on average, more mesenchymal than those found in the excluded or desert phenotypes, with the potential implication that a greater chance for metastasis and immunosuppression is possible in those tumors. Given that infiltrated and excluded tumors have been correlated with better survival among HGSOC patients compared to desert tumors, and the presence of $CD8^+$ T cells in these tumors, there is great potential for treating these patients with LAG3 checkpoint blockade therapy combined with other immune checkpoint inhibitors as it has been demonstrated in the mouse IE9mp1 EOC model by Huang et al. (2015). Because HGSOC patients with infiltrated TMEs have the best survival of the three subtypes of tumor infiltration, and that there is a readily available, albeit exhausted pool of $CD8^+$ T cells, there is potential to leverage therapy against the LGALS3-LAG3 axis to provide even better chances of survival despite the increased risk of metastasis. Recently, the US Food and Drug administration (FDA) approved the second-generation checkpoint inhibitor 'Opdualag', an anti-LAG3 and anti-PD1 combination drug that targets metastatic or unresectable melanoma ("FDA Approves Anti-LAG3 Checkpoint," 2022). Additionally, the development of new peptides, such as C25, that block LAG3 binding to MHC II has been proven to activate $CD8^+$ T cells (Zhai et al., 2020; Zhao et al., 2022, p. 3). LAG3 blockade therapies have been shown to have therapeutic benefit for patients with chronic lymphocytic leukemia, melanoma, and pancreatic adenocarcinoma (Chocarro et al., 2022; Sordo-Bahamonde et al., 2021). In *BRCA*-mutated HGSOC patients, LAG3 was positively correlated with PD-L1; however,

combination immunotherapies in human HGSOC to block the activity of both inhibitory checkpoints were found to have negligible efficacy, suggesting other underlying mechanisms governing the immunosuppressive TME of HGSOC in the context of *LAG3* expression (Whitehair et al., 2020).

6.2.2 EMT-linked LGALS3 is implicated in CD8⁺ T cell exhaustion in ovarian cancer

Recent scRNA-seq investigations on BRCA1/2 mutated HGSOCs have shown a potential link between EMT and $CD8^+$ T-cell exhaustion (Launonen et al., 2022). As well, EMT and T cells found in malignant ascites from EOC express high levels of LAG3 and PD-1 (Y. Imai et al., 2018; Rådestad et al., 2018). This latter observation is of particular interest as it has been previously suggested that EOC ascites contain a significant mesenchymal cancer cell population (Capellero et al., 2022; Rafehi et al., 2016). As well, mesenchymal and pEMT cancer cell states have been linked to higher PD-L1 expression in breast cancer (Sahoo et al., 2021) suggesting that even a partial EMT state is correlated with immunosuppression. Similar relationships between LGALS3 and T cell exhaustion in TGF-β1 induced fibrotic disease (MacKinnon et al., 2012) have been uncovered, where LGALS3 inhibitors (Humphries et al., 2022; Slack et al., 2021) were proven to be effective in treating the disease. In cancer contexts where TGF-β1 plays a major role in initiation and maintenance of EMT, patients may also benefit from LGALS3 inhibitors. For example, LGALS3 has a strong proinflammatory role when expressed by fibroblasts (Filer et al., 2009), eliciting secretion of IL-6, CXCL8, CCL2, and CCL5 all of which are factors that play a role in carcinogenesis and immunosuppression. Anti-TIGIT therapy has also shown mixed success in treating a

variety of solid tumors, including ovarian cancer (Mettu et al., 2022) with other clinical trials demonstrating better clinical benefits in tumors with high *TIGIT* expression (Sarikonda et al., 2022). Curiously, $CD8^+$ T cells infiltrated ovarian tumors have high *TIGIT* expression as shown in this study, which may suggest ovarian tumors are a potential target for a combination of anti-LAG3 and anti-TIGIT therapy. Moreover, combination therapies including anti-TIGIT and anti-PD-L1 synergize to enhance cytolytic $CD8^+$ T cell activity (Chauvin et al., 2015; Johnston et al., 2014) which could be used to target ovarian tumors of the infiltrated subtype to alleviate exhaustion and immunosuppression.

Galectin-3 (Gal-3/LGALS3), encoded by the *LGALS3* gene, is a lectin that can be both expressed on the cell surface (Farhad et al., 2018) and secreted (Krześlak & Lipińska, 2004, p. 3), and is expressed by the majority of human cells. It exhibits several immune-regulatory functions such as reducing the affinity of TCR for its cognate MHC I-peptide ligand by sequestering the TCR from its $CD8^+$ co-receptor (Demotte et al., 2010), causing apoptosis (Fukumori et al., 2003), and internalization of the TCR (H.-Y. Chen et al., 2009), leading to decreased IFN-γ production upon LAG3 engagement on $CD8^+$ T cells (Kouo et al., 2015). *LGALS3* has been linked to poor prognosis in EOC (Luk et al., 2020) with the assertion that it may be activating the Wnt/β-Catenin pathway to effect cancer stemness mechanisms (Y. Liu et al., 2018). Additionally, overexpression of Galectin-1 (*LGALS1*), a protein similar to *LGALS3*, promotes EMT in fibroblasts through TGF-β signalling pathways (T. Wu et al., 2018, p. 3). *LGALS3* has also been linked to the EMT previously (Priglinger et al., 2016) and has been suggested as a T cell-directed immunotherapy to increase efficacy of current immune checkpoint

inhibitors. Interestingly, some of our *in vitro* results demonstrate there could be two different EMT trajectories where *LGALS3* is expressed in one but not the other, suggesting that the EMT can lead to heterogenous populations of mesenchymal cells.

The potential to rescue CD8+ T-cells from exhaustion has been shown, notably in studies where anti-PD1 therapy improved the function of exhausted tumor-infiltrating $CD8^+$ T cells in ovarian cancer (Leem et al., 2020). Whether targeting LGALS3-LAG3 axis has similar potential to rescue CD8+ T cell function alone or in combination with other immunotherapies such as anti-PD1, anti-CTLA4, and anti-TIGIT, requires further investigation. The *LGALS3* inhibitor GB0139 has shown promise in acute lung injury where its mechanism of action involves reducing IL-6, TNF-α, and MIP-1α (Humphries et al., 2022), and thus may also prove efficacious in ovarian cancer where TNF-α plays a role in EMT initiation and maintenance. Galectin-3C, a dominant-negative inhibitor of *LGALS3,* reduces the metastatic potential of ovarian cancer either in combination with Paclitaxel or alone (Mirandola et al., 2014).

It should be noted that the suggestion to target infiltrated ovarian tumors with checkpoint therapy is based on our interpretation of data from primary tumors. Indeed, the immune environment in the ascites or metastases may be different where $CD8^+$ T cells may not be exhausted and could clear cancer cells, thus reducing metastatic spread and contributing to the positive survival prognosis of infiltrated tumors. In these cases, checkpoint therapy may be less effective depending on the TME, but could still assist the immune system in clearing the primary tumor site.

In our screen of various kinase inhibitors, the highly selective and potent GSK3 inhibitor CHIR99021 reduced expression levels of *LGALS3* while not affecting EMT

signature scores, suggesting it may be suitable for therapeutic investigation due to its possible specificity to *LGALS3*. GSK3 inhibition or downregulation can potentiate the cytotoxicity of CD8+ T cells against lymphoma cells (A. Taylor & Rudd, 2017), gastric cancer cells (J.-Y. Zhang et al., 2018), and melanoma cells, with the latter also showing a blockage of LAG3 because of GSK3 targeting by small molecule inhibitors (Rudd et al., 2020).

6.2.3 The link between tumor infiltration and EMT

A surprising finding in this study was the correlation between EMT and tumor immune cell infiltration, since previous studies have reported greater EMT in desert tumors. Certain immune cells, such as $CD4^+$ $CD25^+$ T_{reg} cells, tumor-associated macrophages, and MDSCs can induce EMT in cancer cells (Taki et al., 2021) and our study shows upregulation of chemotactic signals during EMT. Consequently, we propose the existence of a positive feedback loop between immune cells and cancer cells, based on their EMT status. In this scenario, initial signals favoring EMT are propagated through the TME, perhaps from the stroma and fibroblasts (Bulle & Lim, 2020; Hussain et al., 2020; Zvaifler, 2006), or the result of hypoxic conditions (Hapke & Haake, 2020; Misra et al., 2012; Tam et al., 2020). Cancer cells receiving those signals undergo EMT and upregulate pathways related to leukocyte and lymphoid chemotaxis by secreting relevant interleukins and chemokines, as predicted by our findings. Tumor infiltration by activated immune cells promote secretion of factors such as TGF-β1, TNF-α, and ADAM17 intensifying EMT signals and further driving EMT progression in the cancer cell population, resulting in a tumor-promoting positive feedback loop. This

would ultimately lead to T cell exhaustion through elevated LAG3 stimulation, among other coinhibitory markers, such as TIGIT. The validity of this feedback loop hypothesis warrants further investigation, for example, by assessing the tumor immune cell composition in mouse models of ovarian cancer that express a sufficient number of inducible EMT signals in conjunction, such as *SNAIL*, *SLUG*, and *ZEB1*.

Our results do not eliminate the possibility that active $CD8^+$ T cells select for survival of pro-exhaustion mesenchymal cells by successfully attacking the less immunosuppressive epithelial cells. However, this still leaves a question about the origin of signals that promote EMT, whether they originate from another population of cells such as fibroblasts secreting TGF-β1. Our results demonstrate that while desert tumors have a large fibroblast population, there are fewer mesenchymal cancer cells in them than infiltrated tumors, further suggesting that EMT signals likely originate from a different cell population, such as immune cells. Therefore, even if $CD8^+$ T cells and other immune cells select for mesenchymal cells, the trigger for EMT may also originate in those cells. Interestingly, based on the analysis in section 3.13, the results suggested that an immune infiltrated environment does not correlate with EMT. However, the analysis of human tumors in this chapter indicate that several refinements to that conclusion are needed: First, the technique used in our murine analysis of the EMT-immune infiltration link targeted a bulk sample with a handful of transcriptional probes, albeit generated via single-cell analysis. To make a strong conclusion about the EMT-immune infiltration link, the use of more transcriptionally comprehensive techniques such as single cell RNA-seq may be required. There always exists a certain level of ambiguity when attempting to impute a phenomenon, such as EMT, from a single

population of cells in a bulk sample of many cell types and this can be alleviated using single cell technology. Additionally, the use of robust gene modules instead of single probes would provide a more comprehensive assessment of transcriptional programs such as the EMT. Second, while it is true that STOSE tumors are more infiltrated by immune cells than ID8 tumors, it would appear that the majority of the infiltrating cells are myeloid cells rather than cytotoxic T or NK cells as occurs in the human samples (Rodriguez et al., 2022). As the type of infiltrating cells are different than what is observed in the human context, it may be the case that myeloid cells do not pressure cancer cells to undergo EMT as cytotoxic T cells do, resulting in a less mesenchymal TME, assuming there may be a bidirectional relationship between EMT and tumor infiltration. Nevertheless, we believe the link between EMT and immune infiltration is worthy of further investigation in a syngeneic mouse model of ovarian cancer that better resembles the immune infiltration seen in human tumors.

Our results indicating that there are more mesenchymal cells in infiltrated TMEs as opposed to desert TMEs likely differ from Hornburg et al. (Hornburg et al., 2021) for a few reasons. First, we used a cancer-specific EMT signature that can capture the intra-tumoral heterogeneity of the epithelial/mesenchymal program and states. The Hallmark EMT gene set, when combined with classical EMT markers (i.e. *SNAI1/2, ZEB1/2, TWIST1*) captures mostly pEMT states (Tyler & Tirosh, 2021) and is based on founder gene sets, some of which are not from a cancer context (Cook & Vanderhyden, 2022; Liberzon et al., 2015). Second, the Hallmark EMT gene set enriches in stromal compartments (McCorry et al., 2018) and also in cancer-associated fibroblasts (Tyler & Tirosh, 2021) suggesting it may be poorly optimized to capture malignant mesenchymal

cells at all, at least on a single-cell RNA level. Only 58 out of 200 genes in the Hallmark EMT gene set were enriched in Hornburg et al.'s analysis of desert tumors and were on the cusp of significance. Third, our scoring strategy to compute EMT scores differs from their enrichment analysis in that our strategy provides valuable single-cell level scoring compared to bulk sample averages. Pseudo-bulking scoring methods have difficulty accounting for cell-to-cell variability (Hou et al., 2020) which could impact EMT calculations where different cell states exist even within the same cell type. We believe that as the cancer-specific EMT signature was derived from scRNA-Seq datasets, it may be best used in single-cell contexts using analysis algorithms best-suited to the technology.

6.3 Unveiling the Immunogenicity of Ovarian Tumors as the Crucial Catalyst for Therapeutic Success

Here, we found that a correlation exists between classical and non-classical HLA I allotypes and machinery, and EMT in cancer disease, at least on the RNA level, by leveraging single-cell genomics and carefully curating a scRNA-seq of various cancers.

6.3.1 EMT and HLA I expression are inversely correlated in cancer

The findings that mesenchymal cells could be instrumental in exhaustion of $CD8^+$ T cells through the LGALS3-LAG3 axis prompted further investigation into the immunogenicity of ovarian tumors. Specifically, we explored the correlation between EMT and expression of MHC machinery in ovarian cancer knowing that the majority of EOC downregulate MHC I expression like other cancers (Aust et al., 2017; Dholakia et al., 2022; Garrido, 2019). As mentioned above, infiltration of cytotoxic immune cells has

a positive effect on survival (S. D. Brown et al., 2014; Hamanishi et al., 2007; Sato et al., 2005; Vitale et al., 2005; L. Zhang et al., 2003) with increased expression of MHC I genes predictive of greater infiltration (Han et al., 2008; Santoiemma et al., 2016). Ultimately, HLA I expression and diversity of allotypes is lost as tumors progress (Garrido, 2019; Han et al., 2008; Vitale et al., 2005), with a correlation between loss of APM and stage of disease in ovarian cancer, colorectal cancer, melanoma, non-small cell lung cancer, esophageal squamous cell cancer, and other cancers (Hazini et al., 2021; Lin et al., 2013; Menon et al., 2002; Rutten et al., 2014). It was for that reason that we were very surprised to find that classical HLA I allotypes correlated with EMT, with high expression in the cancer cell fraction of many tumors.

6.3.2 EMT and HLA I expression appear positively linked in ovarian cancer

Despite the strong evidence for an association between EMT and the loss of MHC I/APM expression, this inverse correlation is not universal. In a mesenchymal breast cancer cell line, a mesenchymal-to-epithelial reversion induced by upregulation of an EMT suppressor microRNA miR-200 (Chockley & Keshamouni, 2016) also suppressed PD-L1 expression and led to greater CD8+ T cell cytotoxicity. However, in a bioinformatic analysis of microRNAs affecting APM expression, high levels of expression of miR-200a-5p suppressed TAP1 expression in melanoma (Lazaridou et al., 2020). Another analysis revealed that transgenic knock-in of miR-200c increased MHC I expression in the murine mammary cancer cell line EO771 (Camp et al., 2022). Thus, while the roles of these individual miR-200 molecules in suppressing EMT are well-established (Cavallari et al., 2021), they appear to have differing roles in the

regulation of HLA and APM expression, which warrants further investigation. Based on our results, it is possible that this altered association between EMT and HLA expression is because these are data from human tumors rather than from cell lines in vitro or mouse models reportedly previously, which suggests that the TME may well influence this relationship. It is also possible that when epithelial cells undergo EMT, they acquire some phenotypes of mesenchymal stem cells (Pradella et al., 2017; S. Wang et al., 2015), including the ability to modulate expression of MHC I molecules as a way to avoid targeting by NK cells that rely on self- and non-self detection methodology (Machado et al., 2013; Ryan et al., 2005). Taking this into consideration, it is possible that cancer cells acquire MHC I expression to avoid killing by NK cells in another method of immune evasion when undergoing EMT. Additionally, the disconnect between RNA and protein expression could also account for this correlation, where RNA expression of HLA I allotypes increases though protein expression remains stable or decreases through various post-translational mechanisms.

Taken together, these findings suggest that the presence of HLA I molecules in cancer cells is associated with the presence of mesenchymal cells, and the EMT may promote the expression of HLA I molecules in certain cancers.

6.4 Significance and Future directions

Based on the differences in correlation between EMT and HLA across different cancers, further characterization of this possible phenomenon is required. Usage of new techniques such as CITE-seq (Stoeckius et al., 2017) could bridge the gap between RNA and protein expression that stands in the way of making conclusions based on

scRNA-seq data. This can be applied to both *in vitro* and *in vivo* experiments, though would be ideally targeted towards *in vivo* tumors to decipher the proteome of EMT and HLA I by leveraging the cancer-specific EMT module to categorize cells into EMT bins. Additionally, a multiplexed experiment looking at protein expression of MHC I machinery from a variety of cancer cell lines after treatment with different EMT inducers *in vitro* could further shed light on the connection between EMT and HLA I expression. Experiments involving mouse models could also be leveraged where orthotopic tumors can be harvested at different time points prior to endpoint and then sequenced with scRNA-seq or CITE-seq to determine whether levels of HLA I increase or decrease with tumor progression. In this case, it may also be possible to use the cancer-specific EMT module to score the murine cancer cells for EMT and impute the fraction of mesenchymal cells across the time points. To conclude, the positive link between EMT and HLA I expression is a finding that contradicts some well-established research, though other research has shown this to be possible. Further experimentation is required to unravel why HLA I and EMT are correlated in our models of EMT in ovarian cancer.

With single-cell sequencing technologies still rapidly improving in both capability and fidelity, there is tremendous potential to expand the study of cell-cell interactomes with tumors either through advances in technology or improved algorithm design. For example, technologies such as CITE-Seq can be leveraged to supplement genomic sequencing data with cell surface-level protein expression data combined with established receptor-ligand algorithms to generate a clearer picture of the interactome of the TME (H. J. Kim et al., 2020). Future exploration of the interactome that we have

generated could reveal novel interactions between cancer cells and other immune cell types, or further delve into subtypes of T cells such as T_{reg} cells, to paint a more complete picture of the receptor-ligand interactions in the TME of HGSOC. To conclude, ovarian mesenchymal cancer cells suppress $CD8^+$ T cell activity through the pro-exhaustion LAG3-LGALS3 pathway. There is a therapeutic opportunity to target HGSOC that are already infiltrated by $CD8^+$ T cells and relieve them of barriers that dampen antitumoral activity, such as T cell exhaustion. Other than targeting the LAG3-LGALS3 pathway itself, it may be possible to attenuate the EMT to prevent pathway activity specifically and remove a possible source of immunosuppression.

Chapter 7: Conclusion

The epithelial-mesenchymal transition contributes to metastasis of cancer cells and immunosuppression of immune cells in the TME. There is already a well-established link between mesenchymal cells and immunosuppression in the TME: attraction of immunosuppressive cell types like MDSCs and Tregs, downregulation of APM, and upregulation of immune checkpoint inhibitors like PD-L1 and CTLA-4. As it stands, researchers are looking for an ever-expanding set of links between EMT and immune cells in the TME in an effort to combat cancer cell immune evasion and assist patients in clearing the tumor. Perhaps in the future, countering the immunosuppression mediated by mesenchymal cancer cells will also lead to uncovering ways to prevent those cells from facilitating migration and invasion into other tissues.

The work presented here attempted to assist in that effort to characterize EMT-driven immunosuppression in ovarian cancer. First, we characterized the EMT *in vitro*

and *in vivo* in murine models of ovarian cancer. Our findings show that mesenchymal cancer cells in mouse cell lines upregulate chemokine, cytokine, and interleukin factor genes that are known to chemoattract immunosuppressive cell types such as TAMs and Tregs. Additionally, we have found that the main immunosuppressive force behind attenuation of NK cells' cytolytic activity is TGF-β1, which can be secreted from cells undergoing EMT. We also found a positive correlation between EMT and infiltration of immune cells into the TME of orthotopic ovarian tumors in mice, suggesting that the two phenomena may be intertwined. Based on this finding, we characterized the relationship between EMT and immune cells *in silico* using a scRNA-seq dataset of human HGSOC, finding that there is a positive correlation between EMT and immune infiltration in HGSOC. We interpret this as a possible presence of immune cells either driving or being driven by EMT; the directionality of this relationship is still unknown and should be considered for future studies. We have attempted to decipher this relationship using mouse models but have so far been unsuccessful, as the models we were using seem resistant to undergoing EMT. However, we found that mesenchymal cancer cells in human tumors may contribute to exhaustion of $CD8^+$ T cells by upregulating *LGALS3* and binding to the LAG3 receptor. Finally, we noted that there is a positive correlation between MHC I genes and EMT, suggesting there is more to the immunogenicity of mesenchymal cells than previously described.

Taken together, this work further expands on the association between EMT and cancer immunogenicity and contributes some new and surprising findings that, in some cases, challenge conventions. Future research using next-generation sequencing and other *in silico* techniques could help further bridge the gap in knowledge of how

mesenchymal cells contribute to TME immunosuppression while also explaining some of the surprising findings in this thesis.

Bibliography

Aghajani, M. J., Yang, T., Schmitz, U., James, A., McCafferty, C. E., de Souza, P., Niles, N., & Roberts, T. L. (2020). Epithelial-to-mesenchymal transition and its association with PD-L1 and CD8 in thyroid cancer. *Endocrine Connections*, *9*(10), 1028–1041. https://doi.org/10.1530/EC-20-0268

Agnihotri, N., Kumar, S., & Mehta, K. (2013). Tissue transglutaminase as a central mediator in inflammation-induced progression of breast cancer. *Breast Cancer Research*, *15*(1), 202. https://doi.org/10.1186/bcr3371

Akalay, I., Janji, B., Hasmim, M., Noman, M. Z., Thiery, J. P., Mami-Chouaib, F., & Chouaib, S. (2013). EMT impairs breast carcinoma cell susceptibility to CTL-mediated lysis through autophagy induction. *Autophagy*, *9*(7), 1104–1106. https://doi.org/10.4161/auto.24728

Alsop, K., Fereday, S., Meldrum, C., deFazio, A., Emmanuel, C., George, J., Dobrovic, A., Birrer, M. J., Webb, P. M., Stewart, C., Friedlander, M., Fox, S., Bowtell, D., & Mitchell, G. (2012). BRCA mutation frequency and patterns of treatment response in BRCA mutation-positive women with ovarian cancer: A report from the Australian Ovarian Cancer Study Group. *Journal of Clinical Oncology: Official Journal of the American Society of Clinical Oncology*, *30*(21), 2654–2663. https://doi.org/10.1200/JCO.2011.39.8545

Alsuliman, A., Colak, D., Al-Harazi, O., Fitwi, H., Tulbah, A., Al-Tweigeri, T., Al-Alwan, M., & Ghebeh, H. (2015). Bidirectional crosstalk between PD-L1 expression and epithelial to mesenchymal transition: Significance in claudin-low breast cancer cells. *Molecular Cancer*, *14*, 149. https://doi.org/10.1186/s12943-015-0421-2

Ameri, K., Jahangiri, A., Rajah, A. M., Tormos, K. V., Nagarajan, R., Pekmezci, M., Nguyen, V., Wheeler, M. L., Murphy, M. P., Sanders, T. A., Jeffrey, S. S., Yeghiazarians, Y., Rinaudo, P. F., Costello, J. F., Aghi, M. K., & Maltepe, E. (2015). HIGD1A Regulates Oxygen Consumption, ROS Production, and AMPK Activity during Glucose Deprivation to Modulate Cell Survival and Tumor Growth. *Cell Reports*, *10*(6), 891–899. https://doi.org/10.1016/j.celrep.2015.01.020

Andrews, L. P., Marciscano, A. E., Drake, C. G., & Vignali, D. A. A. (2017). LAG3 (CD223) as a Cancer Immunotherapy Target. *Immunological Reviews*, *276*(1), 80–96. https://doi.org/10.1111/imr.12519

Antony, J., & Huang, R. Y.-J. (2017). AXL-Driven EMT State as a Targetable Conduit in Cancer. *Cancer Research*, *77*(14), 3725–3732. https://doi.org/10.1158/0008-5472.CAN-17-0392

Aptsiauri, N., Ruiz-Cabello, F., & Garrido, F. (2018). The transition from HLA-I positive to HLA-I negative primary tumors: The road to escape from T-cell responses. *Current Opinion in Immunology*, *51*, 123–132. https://doi.org/10.1016/j.coi.2018.03.006

Aust, S., Felix, S., Auer, K., Bachmayr-Heyda, A., Kenner, L., Dekan, S., Meier, S. M., Gerner, C., Grimm, C., & Pils, D. (2017). Absence of PD-L1 on tumor cells is associated with reduced MHC I expression and PD-L1 expression increases in recurrent serous ovarian cancer. *Scientific Reports*, *7*(1), Article 1. https://doi.org/10.1038/srep42929

Bachmayr-Heyda, A., Aust, S., Heinze, G., Polterauer, S., Grimm, C., Braicu, E. I., Sehouli, J., Lambrechts, S., Vergote, I., Mahner, S., Pils, D., Schuster, E.,

Thalhammer, T., Horvat, R., Denkert, C., Zeillinger, R., & Castillo-Tong, D. C. (2013). Prognostic impact of tumor infiltrating CD8+ T cells in association with cell proliferation in ovarian cancer patients—A study of the OVCAD consortium. *BMC Cancer*, *13*(1), 422. https://doi.org/10.1186/1471-2407-13-422

Banerjee, A., Gordon, S. M., Intlekofer, A. M., Paley, M. A., Mooney, E. C., Lindsten, T., Wherry, E. J., & Reiner, S. L. (2010). Cutting Edge: The Transcription Factor Eomesodermin Enables CD8+ T Cells To Compete for the Memory Cell Niche. *The Journal of Immunology*, *185*(9), 4988–4992. https://doi.org/10.4049/jimmunol.1002042

Barberà, M. J., Puig, I., Domínguez, D., Julien-Grille, S., Guaita-Esteruelas, S., Peiró, S., Baulida, J., Francí, C., Dedhar, S., Larue, L., & García de Herreros, A. (2004). Regulation of Snail transcription during epithelial to mesenchymal transition of tumor cells. *Oncogene*, *23*(44), Article 44. https://doi.org/10.1038/sj.onc.1207990

Bard, L., Boscher, C., Lambert, M., Mège, R.-M., Choquet, D., & Thoumine, O. (2008). A Molecular Clutch between the Actin Flow and N-Cadherin Adhesions Drives Growth Cone Migration. *The Journal of Neuroscience*, *28*(23), 5879–5890. https://doi.org/10.1523/JNEUROSCI.5331-07.2008

Barrallo-Gimeno, A., & Nieto, M. A. (2005). The Snail genes as inducers of cell movement and survival: Implications in development and cancer. *Development*, *132*(14), 3151–3161. https://doi.org/10.1242/dev.01907

Bates, R. C., & Mercurio, A. M. (2003). Tumor Necrosis Factor-α Stimulates the Epithelial-to-Mesenchymal Transition of Human Colonic Organoids. *Molecular Biology of the Cell*, *14*(5), 1790–1800. https://doi.org/10.1091/mbc.E02-09-0583

Batlle, E., Sancho, E., Francí, C., Domínguez, D., Monfar, M., Baulida, J., & García de Herreros, A. (2000). The transcription factor Snail is a repressor of E-cadherin gene expression in epithelial tumour cells. *Nature Cell Biology*, *2*(2), Article 2. https://doi.org/10.1038/35000034

Bauer, S., Groh, V., Wu, J., Steinle, A., Phillips, J. H., Lanier, L. L., & Spies, T. (1999). Activation of NK Cells and T Cells by NKG2D, a Receptor for Stress-Inducible MICA. *Science*, *285*(5428), 727–729. https://doi.org/10.1126/science.285.5428.727

Berx, G., Becker, K. F., Höfler, H., & van Roy, F. (1998). Mutations of the human E-cadherin (CDH1) gene. *Human Mutation*, *12*(4), 226–237. https://doi.org/10.1002/(SICI)1098-1004(1998)12:4<226::AID-HUMU2>3.0.CO;2-D

Berx, G., Cleton-Jansen, A. M., Nollet, F., de Leeuw, W. J., van de Vijver, M., Cornelisse, C., & van Roy, F. (1995). E-cadherin is a tumour/invasion suppressor gene mutated in human lobular breast cancers. *The EMBO Journal*, *14*(24), 6107–6115.

Blackburn, S. D., Shin, H., Haining, W. N., Zou, T., Workman, C. J., Polley, A., Betts, M. R., Freeman, G. J., Vignali, D. A. A., & Wherry, E. J. (2009). Coregulation of CD8+ T cell exhaustion by multiple inhibitory receptors during chronic viral infection. *Nature Immunology*, *10*(1), 29–37. https://doi.org/10.1038/ni.1679

Blanco, M. J., Moreno-Bueno, G., Sarrio, D., Locascio, A., Cano, A., Palacios, J., & Nieto, M. A. (2002). Correlation of Snail expression with histological grade and

lymph node status in breast carcinomas. *Oncogene*, *21*(20), 3241–3246. https://doi.org/10.1038/sj.onc.1205416

Bloch-Zupan, A., Hunter, N., Manthey, A., & Gibbins, J. (2001). R-twist gene expression during rat palatogenesis. *The International Journal of Developmental Biology*, *45*(2), 397–404.

Boles, K. S., Barchet, W., Diacovo, T., Cella, M., & Colonna, M. (2005). The tumor suppressor TSLC1/NECL-2 triggers NK-cell and CD8+ T-cell responses through the cell-surface receptor CRTAM. *Blood*, *106*(3), 779–786. https://doi.org/10.1182/blood-2005-02-0817

Bolger, A. M., Lohse, M., & Usadel, B. (2014). Trimmomatic: A flexible trimmer for Illumina sequence data. *Bioinformatics*, *30*(15), 2114–2120. https://doi.org/10.1093/bioinformatics/btu170

Bou-Tayeh, B., & Miller, M. L. (2021). Ovarian tumors orchestrate distinct cellular compositions. *Immunity*, *54*(6), 1107–1109. https://doi.org/10.1016/j.immuni.2021.05.014

Brabletz, T., Kalluri, R., Nieto, M. A., & Weinberg, R. A. (2018). EMT in cancer. *Nature Reviews Cancer*, *18*(2), Article 2. https://doi.org/10.1038/nrc.2017.118

Brown, K. A., Aakre, M. E., Gorska, A. E., Price, J. O., Eltom, S. E., Pietenpol, J. A., & Moses, H. L. (2004). Induction by transforming growth factor-beta1 of epithelial to mesenchymal transition is a rare event in vitro. *Breast Cancer Research: BCR*, *6*(3), R215-231. https://doi.org/10.1186/bcr778

Brown, S. D., Warren, R. L., Gibb, E. A., Martin, S. D., Spinelli, J. J., Nelson, B. H., & Holt, R. A. (2014). Neo-antigens predicted by tumor genome meta-analysis

correlate with increased patient survival. *Genome Research*, *24*(5), 743–750. https://doi.org/10.1101/gr.165985.113

Bulle, A., & Lim, K.-H. (2020). Beyond just a tight fortress: Contribution of stroma to epithelial-mesenchymal transition in pancreatic cancer. *Signal Transduction and Targeted Therapy*, *5*(1), Article 1. https://doi.org/10.1038/s41392-020-00341-1

Burstin, J. von, Eser, S., Paul, M. C., Seidler, B., Brandl, M., Messer, M., Werder, A. von, Schmidt, A., Mages, J., Pagel, P., Schnieke, A., Schmid, R. M., Schneider, G., & Saur, D. (2009). E-Cadherin Regulates Metastasis of Pancreatic Cancer In Vivo and Is Suppressed by a SNAIL/HDAC1/HDAC2 Repressor Complex. *Gastroenterology*, *137*(1), 361-371.e5. https://doi.org/10.1053/j.gastro.2009.04.004

Camp, F. A., Brunetti, T. M., Williams, M. M., Christenson, J. L., Sreekanth, V., Costello, J. C., Hay, Z. L. Z., Kedl, R. M., Richer, J. K., & Slansky, J. E. (2022). Antigens Expressed by Breast Cancer Cells Undergoing EMT Stimulate Cytotoxic CD8+ T Cell Immunity. *Cancers*, *14*(18), Article 18. https://doi.org/10.3390/cancers14184397

Canadian Cancer Statistics. (2023, November 11). *Canadian Cancer Statistics 2023*. Canadian Cancer Society. https://cancer.ca/en/cancer-information/resources/publications/canadian-cancer-statistics-2023

Cancer Genome Atlas Research Network. (2011). Integrated genomic analyses of ovarian carcinoma. *Nature*, *474*(7353), 609–615. https://doi.org/10.1038/nature10166

Cano, A., Pérez-Moreno, M. A., Rodrigo, I., Locascio, A., Blanco, M. J., del Barrio, M. G., Portillo, F., & Nieto, M. A. (2000). The transcription factor Snail controls epithelial–mesenchymal transitions by repressing E-cadherin expression. *Nature Cell Biology*, *2*(2), Article 2. https://doi.org/10.1038/35000025

Capellero, S., Erriquez, J., Battistini, C., Porporato, R., Scotto, G., Borella, F., Di Renzo, M. F., Valabrega, G., & Olivero, M. (2022). Ovarian Cancer Cells in Ascites Form Aggregates That Display a Hybrid Epithelial-Mesenchymal Phenotype and Allows Survival and Proliferation of Metastasizing Cells. *International Journal of Molecular Sciences*, *23*(2), 833. https://doi.org/10.3390/ijms23020833

Caramel, J., Papadogeorgakis, E., Hill, L., Browne, G. J., Richard, G., Wierinckx, A., Saldanha, G., Osborne, J., Hutchinson, P., Tse, G., Lachuer, J., Puisieux, A., Pringle, J. H., Ansieau, S., & Tulchinsky, E. (2013). A Switch in the Expression of Embryonic EMT-Inducers Drives the Development of Malignant Melanoma. *Cancer Cell*, *24*(4), 466–480. https://doi.org/10.1016/j.ccr.2013.08.018

Carter, L. E., Cook, D. P., McCloskey, C. W., Grondin, M. A., Landry, D. A., Dang, T., Collins, O., Gamwell, L. F., Dempster, H. A., & Vanderhyden, B. C. (2021). Transcriptional heterogeneity of stemness phenotypes in the ovarian epithelium. *Communications Biology*, *4*(1), Article 1. https://doi.org/10.1038/s42003-021-02045-w

Casas, E., Kim, J., Bendesky, A., Ohno-Machado, L., Wolfe, C. J., & Yang, J. (2011). Snail2 is an essential mediator of Twist1-induced epithelial-mesenchymal transition and metastasis. *Cancer Research*, *71*(1), 245–254. https://doi.org/10.1158/0008-5472.CAN-10-2330

Castriconi, R., Cantoni, C., Della Chiesa, M., Vitale, M., Marcenaro, E., Conte, R., Biassoni, R., Bottino, C., Moretta, L., & Moretta, A. (2003). Transforming growth factor β1 inhibits expression of NKp30 and NKG2D receptors: Consequences for the NK-mediated killing of dendritic cells. *Proceedings of the National Academy of Sciences*, *100*(7), 4120–4125. https://doi.org/10.1073/pnas.0730640100

Cavallari, I., Ciccarese, F., Sharova, E., Urso, L., Raimondi, V., Silic-Benussi, M., D'Agostino, D. M., & Ciminale, V. (2021). The miR-200 Family of microRNAs: Fine Tuners of Epithelial-Mesenchymal Transition and Circulating Cancer Biomarkers. *Cancers*, *13*(23), 5874. https://doi.org/10.3390/cancers13235874

Cerwenka, A., Baron, J. L., & Lanier, L. L. (2001). Ectopic expression of retinoic acid early inducible-1 gene (RAE-1) permits natural killer cell-mediated rejection of a MHC class I-bearing tumor in vivo. *Proceedings of the National Academy of Sciences*, *98*(20), 11521–11526. https://doi.org/10.1073/pnas.201238598

Chaffer, C. L., Brueckmann, I., Scheel, C., Kaestli, A. J., Wiggins, P. A., Rodrigues, L. O., Brooks, M., Reinhardt, F., Su, Y., Polyak, K., Arendt, L. M., Kuperwasser, C., Bierie, B., & Weinberg, R. A. (2011). Normal and neoplastic nonstem cells can spontaneously convert to a stem-like state. *Proceedings of the National Academy of Sciences of the United States of America*, *108*(19), 7950–7955. https://doi.org/10.1073/pnas.1102454108

Chakrabarty, A., Chakraborty, S., Bhattacharya, R., & Chowdhury, G. (2021). Senescence-Induced Chemoresistance in Triple Negative Breast Cancer and Evolution-Based Treatment Strategies. *Frontiers in Oncology*, *11*. https://www.frontiersin.org/articles/10.3389/fonc.2021.674354

Chang, C.-J., Chao, C.-H., Xia, W., Yang, J.-Y., Xiong, Y., Li, C.-W., Yu, W.-H., Rehman, S. K., Hsu, J. L., Lee, H.-H., Liu, M., Chen, C.-T., Yu, D., & Hung, M.-C. (2011). P53 regulates epithelial–mesenchymal transition and stem cell properties through modulating miRNAs. *Nature Cell Biology*, *13*(3), Article 3. https://doi.org/10.1038/ncb2173

Charbonneau, B., Block, M. S., Bamlet, W. R., Vierkant, R. A., Kalli, K. R., Fogarty, Z., Rider, D. N., Sellers, T. A., Tworoger, S. S., Poole, E., Risch, H. A., Salvesen, H. B., Kiemeney, L. A., Baglietto, L., Giles, G. G., Severi, G., Trabert, B., Wentzensen, N., Chenevix-Trench, G., … Goode, E. L. (2014). Risk of Ovarian Cancer and the NF-κB Pathway: Genetic association with IL1A and TNFSF10. *Cancer Research*, *74*(3), 852–861. https://doi.org/10.1158/0008-5472.CAN-13-1051

Chauvin, J.-M., Pagliano, O., Fourcade, J., Sun, Z., Wang, H., Sander, C., Kirkwood, J. M., Chen, T. T., Maurer, M., Korman, A. J., & Zarour, H. M. (2015). TIGIT and PD-1 impair tumor antigen-specific $CD8^+$ T cells in melanoma patients. *The Journal of Clinical Investigation*, *125*(5), 2046–2058. https://doi.org/10.1172/JCI80445

Chen, H.-Y., Fermin, A., Vardhana, S., Weng, I.-C., Lo, K. F. R., Chang, E.-Y., Maverakis, E., Yang, R.-Y., Hsu, D. K., Dustin, M. L., & Liu, F.-T. (2009). Galectin-3 negatively regulates TCR-mediated CD4+ T-cell activation at the immunological synapse. *Proceedings of the National Academy of Sciences of the United States of America*, *106*(34), 14496–14501. https://doi.org/10.1073/pnas.0903497106

Chen, L., Xiong, Y., Li, J., Zheng, X., Zhou, Q., Turner, A., Wu, C., Lu, B., & Jiang, J. (2017). PD-L1 Expression Promotes Epithelial to Mesenchymal Transition in

Human Esophageal Cancer. *Cellular Physiology and Biochemistry*, *42*(6), 2267–2280. https://doi.org/10.1159/000480000

Chen, X.-H., Liu, Z.-C., Zhang, G., Wei, W., Wang, X.-X., Wang, H., Ke, H.-P., Zhang, F., Wang, H.-S., Cai, S.-H., & Du, J. (2015). TGF-β and EGF induced HLA-I downregulation is associated with epithelial-mesenchymal transition (EMT) through upregulation of snail in prostate cancer cells. *Molecular Immunology*, *65*(1), 34–42. https://doi.org/10.1016/j.molimm.2014.12.017

Cheng, F., Shen, Y., Mohanasundaram, P., Lindström, M., Ivaska, J., Ny, T., & Eriksson, J. E. (2016). Vimentin coordinates fibroblast proliferation and keratinocyte differentiation in wound healing via TGF-β–Slug signaling. *Proceedings of the National Academy of Sciences of the United States of America*, *113*(30), E4320–E4327. https://doi.org/10.1073/pnas.1519197113

Chihara, N., Madi, A., Kondo, T., Zhang, H., Acharya, N., Singer, M., Nyman, J., Marjanovic, N. D., Kowalczyk, M. S., Wang, C., Kurtulus, S., Law, T., Etminan, Y., Nevin, J., Buckley, C. D., Burkett, P. R., Buenrostro, J. D., Rozenblatt-Rosen, O., Anderson, A. C., … Kuchroo, V. K. (2018). Induction and transcriptional regulation of the co-inhibitory gene module in T cells. *Nature*, *558*(7710), Article 7710. https://doi.org/10.1038/s41586-018-0206-z

Chocarro, L., Blanco, E., Arasanz, H., Fernández-Rubio, L., Bocanegra, A., Echaide, M., Garnica, M., Ramos, P., Fernández-Hinojal, G., Vera, R., Kochan, G., & Escors, D. (2022). Clinical landscape of LAG-3-targeted therapy. *Immuno-Oncology Technology*, *14*, 100079. https://doi.org/10.1016/j.iotech.2022.100079

Chockley, P. J., Chen, J., Chen, G., Beer, D. G., Standiford, T. J., & Keshamouni, V. G. (2018). Epithelial-mesenchymal transition leads to NK cell-mediated metastasis-specific immunosurveillance in lung cancer. *The Journal of Clinical Investigation*, *128*(4), 1384–1396. https://doi.org/10.1172/JCI97611

Chockley, P. J., & Keshamouni, V. G. (2016). Immunological Consequences of Epithelial–Mesenchymal Transition in Tumor Progression. *The Journal of Immunology*, *197*(3), 691–698. https://doi.org/10.4049/jimmunol.1600458

Choudhary, S., & Satija, R. (2022). Comparison and evaluation of statistical error models for scRNA-seq. *Genome Biology*, *23*(1), 27. https://doi.org/10.1186/s13059-021-02584-9

Cocks, M. M., & Mills, A. M. (2022). The Immune Checkpoint Inhibitor LAG-3 and Its Ligand GAL-3 in Vulvar Squamous Neoplasia. *International Journal of Gynecological Pathology: Official Journal of the International Society of Gynecological Pathologists*, *41*(2), 113–121. https://doi.org/10.1097/PGP.0000000000000782

Colomiere, M., Ward, A. C., Riley, C., Trenerry, M. K., Cameron-Smith, D., Findlay, J., Ackland, L., & Ahmed, N. (2009). Cross talk of signals between EGFR and IL-6R through JAK2/STAT3 mediate epithelial–mesenchymal transition in ovarian carcinomas. *British Journal of Cancer*, *100*(1), Article 1. https://doi.org/10.1038/sj.bjc.6604794

Comijn, J., Berx, G., Vermassen, P., Verschueren, K., van Grunsven, L., Bruyneel, E., Mareel, M., Huylebroeck, D., & van Roy, F. (2001). The two-handed E box

binding zinc finger protein SIP1 downregulates E-cadherin and induces invasion. *Molecular Cell*, *7*(6), 1267–1278. https://doi.org/10.1016/s1097-2765(01)00260-x

Comunale, F., Causeret, M., Favard, C., Cau, J., Taulet, N., Charrasse, S., & Gauthier-Rouvière, C. (2007). Rac1 and RhoA GTPases have antagonistic functions during N-cadherin-dependent cell—Cell contact formation in C2C12 myoblasts. *Biology of the Cell*, *99*(9), 503–517. https://doi.org/10.1042/BC20070011

Conti, P., Dempsey, R. A., Reale, M., Barbacane, R. C., Panara, M. R., Bongrazio, M., & Mier, J. W. (1991). Activation of human natural killer cells by lipopolysaccharide and generation of interleukin-1 alpha, beta, tumour necrosis factor and interleukin-6. Effect of IL-1 receptor antagonist. *Immunology*, *73*(4), 450–456.

Control of Cell Behavior During Vertebrate Development by Slug, a Zinc Finger Gene | *Science*. (n.d.). Retrieved November 27, 2023, from https://www.science.org/doi/10.1126/science.7513443?url_ver=Z39.88-2003&rfr_id=ori:rid:crossref.org&rfr_dat=cr_pub%20%200pubmed

Cook, D. P., Galpin, K. J. C., Rodriguez, G. M., Shakfa, N., Wilson-Sanchez, J., Echaibi, M., Pereira, M., Matuszewska, K., Haagsma, J., Murshed, H., Cudmore, A. O., MacDonald, E., Tone, A., Shepherd, T. G., Petrik, J. J., Koti, M., & Vanderhyden, B. C. (2023). Comparative analysis of syngeneic mouse models of high-grade serous ovarian cancer. *Communications Biology*, *6*(1), Article 1. https://doi.org/10.1038/s42003-023-05529-z

Cook, D. P., & Vanderhyden, B. C. (2020). Context specificity of the EMT transcriptional response. *Nature Communications*, *11*(1), Article 1. https://doi.org/10.1038/s41467-020-16066-2

Cook, D. P., & Vanderhyden, B. C. (2022). Transcriptional census of epithelial-mesenchymal plasticity in cancer. *Science Advances*, *8*(1), eabi7640. https://doi.org/10.1126/sciadv.abi7640

Cooper, M. A., Fehniger, T. A., Ponnappan, A., Mehta, V., Wewers, M. D., & Caligiuri, M. A. (2001). Interleukin-1β costimulates interferon-γ production by human natural killer cells. *European Journal of Immunology*, *31*(3), 792–801. https://doi.org/10.1002/1521-4141(200103)31:3<792::AID-IMMU792>3.0.CO;2-U

Cosman, D., Müllberg, J., Sutherland, C. L., Chin, W., Armitage, R., Fanslow, W., Kubin, M., & Chalupny, N. J. (2001). ULBPs, Novel MHC Class I–Related Molecules, Bind to CMV Glycoprotein UL16 and Stimulate NK Cytotoxicity through the NKG2D Receptor. *Immunity*, *14*(2), 123–133. https://doi.org/10.1016/S1074-7613(01)00095-4

Cruz-Tapias, P., Castiblanco, J., & Anaya, J.-M. (2013). HLA Association with Autoimmune Diseases. In *Autoimmunity: From Bench to Bedside [Internet]*. El Rosario University Press. https://www.ncbi.nlm.nih.gov/books/NBK459459/

Cui, F., Qu, D., Sun, R., Zhang, M., & Nan, K. (2020). NK cell-produced IFN-γ regulates cell growth and apoptosis of colorectal cancer by regulating IL-15. *Experimental and Therapeutic Medicine*, *19*(2), 1400–1406. https://doi.org/10.3892/etm.2019.8343

DAROQUI, M. C., VAZQUEZ, P., DE KIER JOFFÉ, E. B., BAKIN, A. V., & PURICELLI, L. I. (2012). TGF-β autocrine pathway and MAPK signaling promote cell invasiveness and in vivo mammary adenocarcinoma tumor progression. *Oncology Reports*, *28*(2), 567–575. https://doi.org/10.3892/or.2012.1813

Datar, I., & Schalper, K. A. (2016). Epithelial–Mesenchymal Transition and Immune Evasion during Lung Cancer Progression: The Chicken or the Egg? *Clinical Cancer Research : An Official Journal of the American Association for Cancer Research*, *22*(14), 3422–3424. https://doi.org/10.1158/1078-0432.CCR-16-0336

David, J. M., Hamilton, D. H., & Palena, C. (2016). MUC1 upregulation promotes immune resistance in tumor cells undergoing brachyury-mediated epithelial-mesenchymal transition. *OncoImmunology*, *5*(4), e1117738. https://doi.org/10.1080/2162402X.2015.1117738

DeBruine, Z. J., Melcher, K., & Triche, T. J. (2021). *Fast and robust non-negative matrix factorization for single-cell experiments* (p. 2021.09.01.458620). bioRxiv. https://doi.org/10.1101/2021.09.01.458620

Demotte, N., Wieërs, G., Van Der Smissen, P., Moser, M., Schmidt, C., Thielemans, K., Squifflet, J.-L., Weynand, B., Carrasco, J., Lurquin, C., Courtoy, P. J., & van der Bruggen, P. (2010). A galectin-3 ligand corrects the impaired function of human CD4 and CD8 tumor-infiltrating lymphocytes and favors tumor rejection in mice. *Cancer Research*, *70*(19), 7476–7488. https://doi.org/10.1158/0008-5472.CAN-10-0761

Derynck, R., & Feng, X.-H. (1997). TGF-β receptor signaling. *Biochimica et Biophysica Acta (BBA) - Reviews on Cancer*, *1333*(2), F105–F150. https://doi.org/10.1016/S0304-419X(97)00017-6

Desbois, M., Udyavar, A. R., Ryner, L., Kozlowski, C., Guan, Y., Dürrbaum, M., Lu, S., Fortin, J.-P., Koeppen, H., Ziai, J., Chang, C.-W., Keerthivasan, S., Plante, M., Bourgon, R., Bais, C., Hegde, P., Daemen, A., Turley, S., & Wang, Y. (2020).

Integrated digital pathology and transcriptome analysis identifies molecular mediators of T-cell exclusion in ovarian cancer. *Nature Communications*, *11*, 5583. https://doi.org/10.1038/s41467-020-19408-2

Deuss, F. A., Gully, B. S., Rossjohn, J., & Berry, R. (2017). Recognition of nectin-2 by the natural killer cell receptor T cell immunoglobulin and ITIM domain (TIGIT). *The Journal of Biological Chemistry*, *292*(27), 11413. https://doi.org/10.1074/jbc.M117.786483

Dhasarathy, A., Phadke, D., Mav, D., Shah, R. R., & Wade, P. A. (2011). The Transcription Factors Snail and Slug Activate the Transforming Growth Factor-Beta Signaling Pathway in Breast Cancer. *PLOS ONE*, *6*(10), e26514. https://doi.org/10.1371/journal.pone.0026514

Dholakia, J., Scalise, C. B., Katre, A. A., Goldsberry, W. N., Meza-Perez, S., Randall, T. D., Norian, L. A., Novak, L., & Arend, R. C. (2022). Sequential modulation of the Wnt/β-catenin signaling pathway enhances tumor-intrinsic MHC I expression and tumor clearance. *Gynecologic Oncology*, *164*(1), 170–180. https://doi.org/10.1016/j.ygyno.2021.09.026

Dimitrov, D., Türei, D., Garrido-Rodriguez, M., Burmedi, P. L., Nagai, J. S., Boys, C., Ramirez Flores, R. O., Kim, H., Szalai, B., Costa, I. G., Valdeolivas, A., Dugourd, A., & Saez-Rodriguez, J. (2022). Comparison of methods and resources for cell-cell communication inference from single-cell RNA-Seq data. *Nature Communications*, *13*(1), Article 1. https://doi.org/10.1038/s41467-022-30755-0

Dong, C., Wu, Y., Yao, J., Wang, Y., Yu, Y., Rychahou, P. G., Evers, B. M., & Zhou, B. P. (2012). G9a interacts with Snail and is critical for Snail-mediated E-cadherin

repression in human breast cancer. *The Journal of Clinical Investigation*, *122*(4), 1469–1486. https://doi.org/10.1172/JCI57349

Dongre, A., Rashidian, M., Eaton, E. N., Reinhardt, F., Thiru, P., Zagorulya, M., Nepal, S., Banaz, T., Martner, A., Spranger, S., & Weinberg, R. A. (2021). Direct and Indirect Regulators of Epithelial–Mesenchymal Transition–Mediated Immunosuppression in Breast Carcinomas. *Cancer Discovery*, *11*(5), 1286–1305. https://doi.org/10.1158/2159-8290.CD-20-0603

Dongre, A., Rashidian, M., Reinhardt, F., Bagnato, A., Keckesova, Z., Ploegh, H. L., & Weinberg, R. A. (2017). Epithelial-to-mesenchymal Transition contributes to Immunosuppression in Breast Carcinomas. *Cancer Research*, *77*(15), 3982–3989. https://doi.org/10.1158/0008-5472.CAN-16-3292

Dongre, A., & Weinberg, R. A. (2019). New insights into the mechanisms of epithelial–mesenchymal transition and implications for cancer. *Nature Reviews Molecular Cell Biology*, *20*(2), Article 2. https://doi.org/10.1038/s41580-018-0080-4

Dongre, A., Weinberg, R., Rashidian, M., Eaton, E., Reinhardt, F., Thiru, P., Zagorulya, M., Nepal, S., Banaz, T., Martner, A., & Spranger, S. (2020). 232 The epithelial-to-mesenchymal transition (EMT) contributes to immunosuppression in breast carcinomas and regulates their response to immune checkpoint blockade. *Journal for ImmunoTherapy of Cancer*, *8*(Suppl 3). https://doi.org/10.1136/jitc-2020-SITC2020.0232

Du, D., Katsuno, Y., Meyer, D., Budi, E. H., Chen, S., Koeppen, H., Wang, H., Akhurst, R. J., & Derynck, R. (2018). Smad3-mediated recruitment of the methyltransferase SETDB1/ESET controls Snail1 expression and epithelial–

mesenchymal transition. *EMBO Reports*, *19*(1), 135–155. https://doi.org/10.15252/embr.201744250

Etemadmoghadam, D., George, J., Cowin, P. A., Cullinane, C., Kansara, M., Australian Ovarian Cancer Study Group, Gorringe, K. L., Smyth, G. K., & Bowtell, D. D. L. (2010). Amplicon-dependent CCNE1 expression is critical for clonogenic survival after cisplatin treatment and is correlated with 20q11 gain in ovarian cancer. *PloS One*, *5*(11), e15498. https://doi.org/10.1371/journal.pone.0015498

Farhad, M., Rolig, A. S., & Redmond, W. L. (2018). The role of Galectin-3 in modulating tumor growth and immunosuppression within the tumor microenvironment. *OncoImmunology*, *7*(6), e1434467. https://doi.org/10.1080/2162402X.2018.1434467

FDA approves anti-LAG3 checkpoint. (2022). *Nature Biotechnology*, *40*(5), Article 5. https://doi.org/10.1038/s41587-022-01331-0

Fei, Z., Deng, Z., Zhou, L., Li, K., Xia, X., & Xie, R. (2019). PD-L1 Induces Epithelial–Mesenchymal Transition in Nasopharyngeal Carcinoma Cells Through Activation of the PI3K/AKT Pathway. *Oncology Research*, *27*(7), 801–807. https://doi.org/10.3727/096504018X15446984186056

Fifield, A. L., Hanavan, P. D., Faigel, D. O., Sergienko, E., Bobkov, A., Meurice, N., Petit, J. L., Polito, A., Caulfield, T. R., Castle, E. P., Copland, J. A., Mukhopadhyay, D., Pal, K., Dutta, S. K., Luo, H., Ho, T. H., & Lake, D. F. (2020). Molecular Inhibitor of QSOX1 Suppresses Tumor Growth in vivo. *Molecular Cancer Therapeutics*, *19*(1), 112–122. https://doi.org/10.1158/1535-7163.MCT-19-0233

Filer, A., Bik, M., Parsonage, G. N., Fitton, J., Trebilcock, E., Howlett, K., Cook, M., Raza, K., Simmons, D. L., Thomas, A. M. C., Salmon, M., Scheel-Toellner, D., Lord, J. M., Rabinovich, G. A., & Buckley, C. D. (2009). Galectin 3 induces a distinctive pattern of cytokine and chemokine production in rheumatoid synovial fibroblasts via selective signaling pathways. *Arthritis & Rheumatism*, *60*(6), 1604–1614. https://doi.org/10.1002/art.24574

Filippou, P. S., Karagiannis, G. S., & Constantinidou, A. (2020). Midkine (MDK) growth factor: A key player in cancer progression and a promising therapeutic target. *Oncogene*, *39*(10), Article 10. https://doi.org/10.1038/s41388-019-1124-8

Fondrevelle, M. E., Kantelip, B., Reiter, R. E., Chopin, D. K., Thiery, J. P., Monnien, F., Bittard, H., & Wallerand, H. (2009). The expression of Twist has an impact on survival in human bladder cancer and is influenced by the smoking status. *Urologic Oncology: Seminars and Original Investigations*, *27*(3), 268–276. https://doi.org/10.1016/j.urolonc.2007.12.012

Franco, H. L., Casasnovas, J., Rodríguez-Medina, J. R., & Cadilla, C. L. (2011). Redundant or separate entities?—Roles of Twist1 and Twist2 as molecular switches during gene transcription. *Nucleic Acids Research*, *39*(4), 1177–1186. https://doi.org/10.1093/nar/gkq890

Friedman, L. A., Ring, K. L., & Mills, A. M. (2020). LAG-3 and GAL-3 in Endometrial Carcinoma: Emerging Candidates for Immunotherapy. *International Journal of Gynecological Pathology: Official Journal of the International Society of Gynecological Pathologists*, *39*(3), 203–212. https://doi.org/10.1097/PGP.0000000000000608

Fucikova, J., Coosemans, A., Orsulic, S., Cibula, D., Vergote, I., Galluzzi, L., & Spisek, R. (2021). Immunological configuration of ovarian carcinoma: Features and impact on disease outcome. *Journal for ImmunoTherapy of Cancer*, *9*(10), e002873. https://doi.org/10.1136/jitc-2021-002873

Fucikova, J., Rakova, J., Hensler, M., Kasikova, L., Belicova, L., Hladikova, K., Truxova, I., Skapa, P., Laco, J., Pecen, L., Praznovec, I., Halaska, M. J., Brtnicky, T., Kodet, R., Fialova, A., Pineau, J., Gey, A., Tartour, E., Ryska, A., … Spisek, R. (2019). TIM-3 Dictates Functional Orientation of the Immune Infiltrate in Ovarian Cancer. *Clinical Cancer Research*, *25*(15), 4820–4831. https://doi.org/10.1158/1078-0432.CCR-18-4175

Fukuda, S., Nishida-Fukuda, H., Nanba, D., Nakashiro, K., Nakayama, H., Kubota, H., & Higashiyama, S. (2016). Reversible interconversion and maintenance of mammary epithelial cell characteristics by the ligand-regulated EGFR system. *Scientific Reports*, *6*(1), Article 1. https://doi.org/10.1038/srep20209

Fukumori, T., Takenaka, Y., Yoshii, T., Kim, H.-R. C., Hogan, V., Inohara, H., Kagawa, S., & Raz, A. (2003). CD29 and CD7 Mediate Galectin-3-Induced Type II T-Cell Apoptosis. *Cancer Research*, *63*(23), 8302–8311.

Galván, J. A., Zlobec, I., Wartenberg, M., Lugli, A., Gloor, B., Perren, A., & Karamitopoulou, E. (2015). Expression of E-cadherin repressors SNAIL, ZEB1 and ZEB2 by tumour and stromal cells influences tumour-budding phenotype and suggests heterogeneity of stromal cells in pancreatic cancer. *British Journal of Cancer*, *112*(12), Article 12. https://doi.org/10.1038/bjc.2015.177

Garrido, F. (2019). HLA Class-I Expression and Cancer Immunotherapy. In F. Garrido (Ed.), *MHC Class-I Loss and Cancer Immune Escape* (pp. 79–90). Springer International Publishing. https://doi.org/10.1007/978-3-030-17864-2_3

Gavrilović, J., Moens, G., Thiery, J. P., & Jouanneau, J. (1990). Expression of transfected transforming growth factor alpha induces a motile fibroblast-like phenotype with extracellular matrix-degrading potential in a rat bladder carcinoma cell line. *Cell Regulation*, *1*(13), 1003–1014.

Geistlinger, L., Oh, S., Ramos, M., Schiffer, L., LaRue, R. S., Henzler, C. M., Munro, S. A., Daughters, C., Nelson, A. C., Winterhoff, B. J., Chang, Z., Talukdar, S., Shetty, M., Mullaney, S. A., Morgan, M., Parmigiani, G., Birrer, M. J., Qin, L.-X., Riester, M., … Waldron, L. (2020). Multi-omic analysis of subtype evolution and heterogeneity in high-grade serous ovarian carcinoma. *Cancer Research*, *80*(20), 4335–4345. https://doi.org/10.1158/0008-5472.CAN-20-0521

Geng, Y., Xu, C., Wang, Y., & Zhang, L. (2020). Quiescin Sulfhydryl Oxidase 1 Regulates the Proliferation, Migration and Invasion of Human Glioblastoma Cells via PI3K/Akt Pathway. *OncoTargets and Therapy*, *13*, 5721–5729. https://doi.org/10.2147/OTT.S255941

Ghannam, S., Bouffi, C., Djouad, F., Jorgensen, C., & Noël, D. (2010). Immunosuppression by mesenchymal stem cells: Mechanisms and clinical applications. *Stem Cell Research & Therapy*, *1*(1), 2. https://doi.org/10.1186/scrt2

Ghosh, R. D., Ghuwalewala, S., Das, P., Mandloi, S., Alam, S. K., Chakraborty, J., Sarkar, S., Chakrabarti, S., Panda, C. K., & Roychoudhury, S. (2016). MicroRNA profiling of cisplatin-resistant oral squamous cell carcinoma cell lines enriched

with cancer-stem-cell-like and epithelial-mesenchymal transition-type features. *Scientific Reports*, *6*, 23932. https://doi.org/10.1038/srep23932

Gilboa, L., Nohe, A., Geissendörfer, T., Sebald, W., Henis, Y. I., & Knaus, P. (2000). Bone Morphogenetic Protein Receptor Complexes on the Surface of Live Cells: A New Oligomerization Mode for Serine/Threonine Kinase Receptors. *Molecular Biology of the Cell*, *11*(3), 1023–1035.

Gong, J. H., Maki, G., & Klingemann, H. G. (1994). Characterization of a human cell line (NK-92) with phenotypical and functional characteristics of activated natural killer cells. *Leukemia*, *8*(4), 652–658.

Gong, L., Liu, G., Zhu, H., Li, C., Li, P., Liu, C., Tang, H., Wu, K., Wu, J., Liu, D., & Tang, X. (2020a). IL-32 induces epithelial-mesenchymal transition by triggering endoplasmic reticulum stress in A549 cells. *BMC Pulmonary Medicine*, *20*(1), 278. https://doi.org/10.1186/s12890-020-01319-z

Gong, L., Liu, G., Zhu, H., Li, C., Li, P., Liu, C., Tang, H., Wu, K., Wu, J., Liu, D., & Tang, X. (2020b). IL-32 induces epithelial-mesenchymal transition by triggering endoplasmic reticulum stress in A549 cells. *BMC Pulmonary Medicine*, *20*(1), 278. https://doi.org/10.1186/s12890-020-01319-z

Gonzalez, D. M., & Medici, D. (2014). Signaling mechanisms of the epithelial-mesenchymal transition. *Science Signaling*, *7*(344), re8–re8. https://doi.org/10.1126/scisignal.2005189

Grande, M. T., Sánchez-Laorden, B., López-Blau, C., De Frutos, C. A., Boutet, A., Arévalo, M., Rowe, R. G., Weiss, S. J., López-Novoa, J. M., & Nieto, M. A. (2015). Snail1-induced partial epithelial-to-mesenchymal transition drives renal

fibrosis in mice and can be targeted to reverse established disease. *Nature Medicine*, *21*(9), Article 9. https://doi.org/10.1038/nm.3901

Graydon, C. G., Mohideen, S., & Fowke, K. R. (2021). LAG3's Enigmatic Mechanism of Action. *Frontiers in Immunology*, *11*, 615317. https://doi.org/10.3389/fimmu.2020.615317

Greaves, D., & Calle, Y. (2022). Epithelial Mesenchymal Transition (EMT) and Associated Invasive Adhesions in Solid and Haematological Tumours. *Cells*, *11*(4), 649. https://doi.org/10.3390/cells11040649

Grebinoski, S., Zhang, Q., Cillo, A. R., Manne, S., Xiao, H., Brunazzi, E. A., Tabib, T., Cardello, C., Lian, C. G., Murphy, G. F., Lafyatis, R., Wherry, E. J., Das, J., Workman, C. J., & Vignali, D. A. A. (2022). Autoreactive CD8+ T cells are restrained by an exhaustion-like program that is maintained by LAG3. *Nature Immunology*, *23*(6), 868–877. https://doi.org/10.1038/s41590-022-01210-5

Greenburg, G., & Hay, E. D. (1982). Epithelia suspended in collagen gels can lose polarity and express characteristics of migrating mesenchymal cells. *The Journal of Cell Biology*, *95*(1), 333–339. https://doi.org/10.1083/jcb.95.1.333

Gressner, A. M., Weiskirchen, R., Breitkopf, K., & Dooley, S. (2002). Roles of TGF-beta in hepatic fibrosis. *Frontiers in Bioscience: A Journal and Virtual Library*, *7*, d793-807. https://doi.org/10.2741/A812

Grigore, A. D., Jolly, M. K., Jia, D., Farach-Carson, M. C., & Levine, H. (2016). Tumor Budding: The Name is EMT. Partial EMT. *Journal of Clinical Medicine*, *5*(5), Article 5. https://doi.org/10.3390/jcm5050051

Grigorian, A., & Demetriou, M. (2010). Manipulating cell surface glycoproteins by targeting N-glycan-galectin interactions. *Methods in Enzymology*, *480*, 245–266. https://doi.org/10.1016/S0076-6879(10)80012-6

Gu, Y., Zhang, Z., & ten Dijke, P. (2023). Harnessing epithelial-mesenchymal plasticity to boost cancer immunotherapy. *Cellular & Molecular Immunology*, *20*(4), Article 4. https://doi.org/10.1038/s41423-023-00980-8

Gu, Z., Gu, L., Eils, R., Schlesner, M., & Brors, B. (2014). Circlize implements and enhances circular visualization in R. *Bioinformatics*, *30*(19), 2811–2812. https://doi.org/10.1093/bioinformatics/btu393

Gudey, S. K., Sundar, R., Heldin, C.-H., Bergh, A., & Landström, M. (2017). Pro-invasive properties of Snail1 are regulated by sumoylation in response to TGFβ stimulation in cancer. *Oncotarget*, *8*(58), 97703–97726. https://doi.org/10.18632/oncotarget.20097

Guilford, P., Hopkins, J., Harraway, J., McLeod, M., McLeod, N., Harawira, P., Taite, H., Scoular, R., Miller, A., & Reeve, A. E. (1998). E-cadherin germline mutations in familial gastric cancer. *Nature*, *392*(6674), Article 6674. https://doi.org/10.1038/32918

Guillon, J., Petit, C., Toutain, B., Guette, C., Lelièvre, E., & Coqueret, O. (2019). Chemotherapy-induced senescence, an adaptive mechanism driving resistance and tumor heterogeneity. *Cell Cycle*, *18*(19), 2385–2397. https://doi.org/10.1080/15384101.2019.1652047

Guo, W., Keckesova, Z., Donaher, J. L., Shibue, T., Tischler, V., Reinhardt, F., Itzkovitz, S., Noske, A., Zürrer-Härdi, U., Bell, G., Tam, W. L., Mani, S. A., van

Oudenaarden, A., & Weinberg, R. A. (2012). Slug and Sox9 Cooperatively Determine the Mammary Stem Cell State. *Cell*, *148*(5), 1015–1028. https://doi.org/10.1016/j.cell.2012.02.008

Hafemeister, C., & Satija, R. (2019). Normalization and variance stabilization of single-cell RNA-seq data using regularized negative binomial regression. *Genome Biology*, *20*(1), 296. https://doi.org/10.1186/s13059-019-1874-1

Hamanishi, J., Mandai, M., Iwasaki, M., Okazaki, T., Tanaka, Y., Yamaguchi, K., Higuchi, T., Yagi, H., Takakura, K., Minato, N., Honjo, T., & Fujii, S. (2007). Programmed cell death 1 ligand 1 and tumor-infiltrating CD8+ T lymphocytes are prognostic factors of human ovarian cancer. *Proceedings of the National Academy of Sciences*, *104*(9), 3360–3365. https://doi.org/10.1073/pnas.0611533104

Han, L. Y., Fletcher, M. S., Urbauer, D. L., Mueller, P., Landen, C. N., Kamat, A. A., Lin, Y. G., Merritt, W. M., Spannuth, W. A., Deavers, M. T., De Geest, K., Gershenson, D. M., Lutgendorf, S. K., Ferrone, S., & Sood, A. K. (2008). HLA Class I Antigen Processing Machinery Component Expression and Intratumoral T-Cell Infiltrate as Independent Prognostic Markers in Ovarian Carcinoma. *Clinical Cancer Research*, *14*(11), 3372–3379. https://doi.org/10.1158/1078-0432.CCR-07-4433

Hannigan, G., Troussard, A. A., & Dedhar, S. (2005). Integrin-linked kinase: A cancer therapeutic target unique among its ILK. *Nature Reviews Cancer*, *5*(1), Article 1. https://doi.org/10.1038/nrc1524

Hansen, S. M., Berezin, V., & Bock, E. (2008). Signaling mechanisms of neurite outgrowth induced by the cell adhesion molecules NCAM and N-Cadherin.

Cellular and Molecular Life Sciences, *65*(23), 3809–3821. https://doi.org/10.1007/s00018-008-8290-0

Hao, Y., Hao, S., Andersen-Nissen, E., Mauck, W. M., Zheng, S., Butler, A., Lee, M. J., Wilk, A. J., Darby, C., Zager, M., Hoffman, P., Stoeckius, M., Papalexi, E., Mimitou, E. P., Jain, J., Srivastava, A., Stuart, T., Fleming, L. M., Yeung, B., … Satija, R. (2021). Integrated analysis of multimodal single-cell data. *Cell*, *184*(13), 3573-3587.e29. https://doi.org/10.1016/j.cell.2021.04.048

Hapke, R. Y., & Haake, S. M. (2020). Hypoxia-induced epithelial to mesenchymal transition in cancer. *Cancer Letters*, *487*, 10–20. https://doi.org/10.1016/j.canlet.2020.05.012

Hay, E. D., & Zuk, A. (1995). Transformations between epithelium and mesenchyme: Normal, pathological, and experimentally induced. *American Journal of Kidney Diseases: The Official Journal of the National Kidney Foundation*, *26*(4), 678–690. https://doi.org/10.1016/0272-6386(95)90610-x

Hazan, R. B., Phillips, G. R., Qiao, R. F., Norton, L., & Aaronson, S. A. (2000). Exogenous expression of N-cadherin in breast cancer cells induces cell migration, invasion, and metastasis. *The Journal of Cell Biology*, *148*(4), 779–790. https://doi.org/10.1083/jcb.148.4.779

Hazini, A., Fisher, K., & Seymour, L. (2021). Deregulation of HLA-I in cancer and its central importance for immunotherapy. *Journal for Immunotherapy of Cancer*, *9*(8), e002899. https://doi.org/10.1136/jitc-2021-002899

He, X., Zhang, S., Chen, J., & Li, D. (2019). Increased LGALS3 expression independently predicts shorter overall survival in patients with the proneural

subtype of glioblastoma. *Cancer Medicine*, *8*(5), 2031–2040. https://doi.org/10.1002/cam4.2075

Heldin, C.-H., Östman, A., & Rönnstrand, L. (1998). Signal transduction via platelet-derived growth factor receptors. *Biochimica et Biophysica Acta (BBA) - Reviews on Cancer*, *1378*(1), F79–F113. https://doi.org/10.1016/S0304-419X(98)00015-8

Hirohashi, S. (1998). Inactivation of the E-Cadherin-Mediated Cell Adhesion System in Human Cancers. *The American Journal of Pathology*, *153*(2), 333–339. https://doi.org/10.1016/S0002-9440(10)65575-7

Hobson, J., Gummadidala, P., Silverstrim, B., Grier, D., Bunn, J., James, T., & Rincon, M. (2013). Acute Inflammation induced by the biopsy of mouse mammary tumors promotes the development of metastasis. *Breast Cancer Research and Treatment*, *139*(2), 391–401. https://doi.org/10.1007/s10549-013-2575-1

Hornburg, M., Desbois, M., Lu, S., Guan, Y., Lo, A. A., Kaufman, S., Elrod, A., Lotstein, A., DesRochers, T. M., Munoz-Rodriguez, J. L., Wang, X., Giltnane, J., Mayba, O., Turley, S. J., Bourgon, R., Daemen, A., & Wang, Y. (2021). Single-cell dissection of cellular components and interactions shaping the tumor immune phenotypes in ovarian cancer. *Cancer Cell*, *39*(7), 928-944.e6. https://doi.org/10.1016/j.ccell.2021.04.004

Hosono, S., Kajiyama, H., Terauchi, M., Shibata, K., Ino, K., Nawa, A., & Kikkawa, F. (2007). Expression of Twist increases the risk for recurrence and for poor survival in epithelial ovarian carcinoma patients. *British Journal of Cancer*, *96*(2), 314–320. https://doi.org/10.1038/sj.bjc.6603533

Hou, W., Ji, Z., Ji, H., & Hicks, S. C. (2020). A systematic evaluation of single-cell RNA-sequencing imputation methods. *Genome Biology*, *21*(1), 218. https://doi.org/10.1186/s13059-020-02132-x

Hsu, D. S.-S., Wang, H.-J., Tai, S.-K., Chou, C.-H., Hsieh, C.-H., Chiu, P.-H., Chen, N.-J., & Yang, M.-H. (2014). Acetylation of snail modulates the cytokinome of cancer cells to enhance the recruitment of macrophages. *Cancer Cell*, *26*(4), 534–548. https://doi.org/10.1016/j.ccell.2014.09.002

Huang, R.-Y., Eppolito, C., Lele, S., Shrikant, P., Matsuzaki, J., & Odunsi, K. (2015). LAG3 and PD1 co-inhibitory molecules collaborate to limit CD8+ T cell signaling and dampen antitumor immunity in a murine ovarian cancer model. *Oncotarget*, *6*(29), 27359–27377.

Huang, Y., Hong, W., & Wei, X. (2022). The molecular mechanisms and therapeutic strategies of EMT in tumor progression and metastasis. *Journal of Hematology & Oncology*, *15*(1), 129. https://doi.org/10.1186/s13045-022-01347-8

Huang, Z., Zhang, Z., Zhou, C., Liu, L., & Huang, C. (2022). Epithelial–mesenchymal transition: The history, regulatory mechanism, and cancer therapeutic opportunities. *MedComm*, *3*(2), e144. https://doi.org/10.1002/mco2.144

Huels, D. J., Ridgway, R. A., Radulescu, S., Leushacke, M., Campbell, A. D., Biswas, S., Leedham, S., Serra, S., Chetty, R., Moreaux, G., Parry, L., Matthews, J., Song, F., Hedley, A., Kalna, G., Ceteci, F., Reed, K. R., Meniel, V. S., Maguire, A., … Sansom, O. J. (2015). E-cadherin can limit the transforming properties of activating β-catenin mutations. *The EMBO Journal*, *34*(18), 2321–2333. https://doi.org/10.15252/embj.201591739

Hultgren, N. W., Fang, J. S., Ziegler, M. E., Ramirez, R. N., Phan, D. T. T., Hatch, M. M. S., Welch-Reardon, K. M., Paniagua, A. E., Kim, L. S., Shon, N. N., Williams, D. S., Mortazavi, A., & Hughes, C. C. W. (2020). Slug regulates the Dll4-Notch-VEGFR2 axis to control endothelial cell activation and angiogenesis. *Nature Communications*, *11*, 5400. https://doi.org/10.1038/s41467-020-18633-z

Humphries, D. C., Mills, R., Boz, C., McHugh, B. J., Hirani, N., Rossi, A. G., Pedersen, A., Schambye, H. T., Slack, R. J., Leffler, H., Nilsson, U. J., Wang, W., Sethi, T., & Mackinnon, A. C. (2022). Galectin-3 inhibitor GB0139 protects against acute lung injury by inhibiting neutrophil recruitment and activation. *Frontiers in Pharmacology*, *13*, 949264. https://doi.org/10.3389/fphar.2022.949264

Hüsemann, Y., Geigl, J. B., Schubert, F., Musiani, P., Meyer, M., Burghart, E., Forni, G., Eils, R., Fehm, T., Riethmüller, G., & Klein, C. A. (2008). Systemic Spread Is an Early Step in Breast Cancer. *Cancer Cell*, *13*(1), 58–68. https://doi.org/10.1016/j.ccr.2007.12.003

Hussain, S., Peng, B., Cherian, M., Song, J. W., Ahirwar, D. K., & Ganju, R. K. (2020). The Roles of Stroma-Derived Chemokine in Different Stages of Cancer Metastases. *Frontiers in Immunology*, *11*, 598532. https://doi.org/10.3389/fimmu.2020.598532

Imai, K., Matsuyama, S., Miyake, S., Suga, K., & Nakachi, K. (2000). Natural cytotoxic activity of peripheral-blood lymphocytes and cancer incidence: An 11-year follow-up study of a general population. *The Lancet*, *356*(9244), 1795–1799. https://doi.org/10.1016/S0140-6736(00)03231-1

Imai, Y., Hasegawa, K., Matsushita, H., Fujieda, N., Sato, S., Miyagi, E., Kakimi, K., & Fujiwara, K. (2018). Expression of multiple immune checkpoint molecules on T cells in malignant ascites from epithelial ovarian carcinoma. *Oncology Letters*, *15*(5), 6457–6468. https://doi.org/10.3892/ol.2018.8101

Ji, A. L., Rubin, A. J., Thrane, K., Jiang, S., Reynolds, D. L., Meyers, R. M., Guo, M. G., George, B. M., Mollbrink, A., Bergenstråhle, J., Larsson, L., Bai, Y., Zhu, B., Bhaduri, A., Meyers, J. M., Rovira-Clavé, X., Hollmig, S. T., Aasi, S. Z., Nolan, G. P., … Khavari, P. A. (2020). Multimodal Analysis of Composition and Spatial Architecture in Human Squamous Cell Carcinoma. *Cell*, *182*(2), 497-514.e22. https://doi.org/10.1016/j.cell.2020.05.039

Johnston, R. J., Comps-Agrar, L., Hackney, J., Yu, X., Huseni, M., Yang, Y., Park, S., Javinal, V., Chiu, H., Irving, B., Eaton, D. L., & Grogan, J. L. (2014). The immunoreceptor TIGIT regulates antitumor and antiviral CD8(+) T cell effector function. *Cancer Cell*, *26*(6), 923–937. https://doi.org/10.1016/j.ccell.2014.10.018

Kajiyama, H., Hosono, S., Terauchi, M., Shibata, K., Ino, K., Yamamoto, E., Nomura, S., Nawa, A., & Kikkawa, F. (2007). Twist Expression Predicts Poor Clinical Outcome of Patients with Clear Cell Carcinoma of the Ovary. *Oncology*, *71*(5–6), 394–401. https://doi.org/10.1159/000107108

Kalluri, R., & Neilson, E. G. (2003). Epithelial-mesenchymal transition and its implications for fibrosis. *Journal of Clinical Investigation*, *112*(12), 1776–1784. https://doi.org/10.1172/JCI200320530

Kalluri, R., & Weinberg, R. A. (2009). The basics of epithelial-mesenchymal transition. *The Journal of Clinical Investigation*, *119*(6), 1420–1428. https://doi.org/10.1172/JCI39104

Kandalaft, L. E., Dangaj Laniti, D., & Coukos, G. (2022). Immunobiology of high-grade serous ovarian cancer: Lessons for clinical translation. *Nature Reviews Cancer*, *22*(11), Article 11. https://doi.org/10.1038/s41568-022-00503-z

Karin, M., & Greten, F. R. (2005). NF-κB: Linking inflammation and immunity to cancer development and progression. *Nature Reviews Immunology*, *5*(10), Article 10. https://doi.org/10.1038/nri1703

Kariya, Y., Oyama, M., Suzuki, T., & Kariya, Y. (2021). Avβ3 Integrin induces partial EMT independent of TGF-β signaling. *Communications Biology*, *4*(1), Article 1. https://doi.org/10.1038/s42003-021-02003-6

Kearney, C. J., Vervoort, S. J., Hogg, S. J., Ramsbottom, K. M., Freeman, A. J., Lalaoui, N., Pijpers, L., Michie, J., Brown, K. K., Knight, D. A., Sutton, V., Beavis, P. A., Voskoboinik, I., Darcy, P. K., Silke, J., Trapani, J. A., Johnstone, R. W., & Oliaro, J. (2018). Tumor immune evasion arises through loss of TNF sensitivity. *Science Immunology*, *3*(23), eaar3451. https://doi.org/10.1126/sciimmunol.aar3451

Khawar, M. B., Abbasi, M. H., & Sheikh, N. (2016). IL-32: A Novel Pluripotent Inflammatory Interleukin, towards Gastric Inflammation, Gastric Cancer, and Chronic Rhino Sinusitis. *Mediators of Inflammation*, *2016*, e8413768. https://doi.org/10.1155/2016/8413768

Kiessling, R., Klein, E., Pross, H., & Wigzell, H. (1975). „Natural" killer cells in the mouse. II. Cytotoxic cells with specificity for mouse Moloney leukemia cells.

Characteristics of the killer cell. *European Journal of Immunology*, *5*(2), 117–121. https://doi.org/10.1002/eji.1830050209

Kim, H. J., Lin, Y., Geddes, T. A., Yang, J. Y. H., & Yang, P. (2020). CiteFuse enables multi-modal analysis of CITE-seq data. *Bioinformatics*, *36*(14), 4137–4143. https://doi.org/10.1093/bioinformatics/btaa282

Kim, J., Kong, J., Chang, H., Kim, H., & Kim, A. (2016). EGF induces epithelial-mesenchymal transition through phospho-Smad2/3-Snail signaling pathway in breast cancer cells. *Oncotarget*, *7*(51), 85021. https://doi.org/10.18632/oncotarget.13116

Kim, N., Kim, H. K., Lee, K., Hong, Y., Cho, J. H., Choi, J. W., Lee, J.-I., Suh, Y.-L., Ku, B. M., Eum, H. H., Choi, S., Choi, Y.-L., Joung, J.-G., Park, W.-Y., Jung, H. A., Sun, J.-M., Lee, S.-H., Ahn, J. S., Park, K., … Lee, H.-O. (2020). Single-cell RNA sequencing demonstrates the molecular and cellular reprogramming of metastatic lung adenocarcinoma. *Nature Communications*, *11*(1), Article 1. https://doi.org/10.1038/s41467-020-16164-1

Klein, E., Vánky, F., Ben-Bassat, H., Neumann, H., Ralph, P., Zeuthen, J., & Polliack, A. (1976). Properties of the K562 cell line, derived from a patient with chronic myeloid leukemia. *International Journal of Cancer*, *18*(4), 421–431. https://doi.org/10.1002/ijc.2910180405

Klingemann, H. (2023). The NK-92 cell line—30 years later: Its impact on natural killer cell research and treatment of cancer. *Cytotherapy*, *25*(5), 451–457. https://doi.org/10.1016/j.jcyt.2022.12.003

Konecny, G. E., Wang, C., Hamidi, H., Winterhoff, B., Kalli, K. R., Dering, J., Ginther, C., Chen, H.-W., Dowdy, S., Cliby, W., Gostout, B., Podratz, K. C., Keeney, G., Wang, H.-J., Hartmann, L. C., Slamon, D. J., & Goode, E. L. (2014). Prognostic and Therapeutic Relevance of Molecular Subtypes in High-Grade Serous Ovarian Cancer. *JNCI Journal of the National Cancer Institute*, *106*(10). https://doi.org/10.1093/jnci/dju249

Kong, D., Wang, Z., Sarkar, S. H., Li, Y., Banerjee, S., Saliganan, A., Kim, H.-R. C., Cher, M. L., & Sarkar, F. H. (2008). Platelet-Derived Growth Factor-D Overexpression Contributes to Epithelial-Mesenchymal Transition of PC3 Prostate Cancer Cells. *Stem Cells (Dayton, Ohio)*, *26*(6), 1425–1435. https://doi.org/10.1634/stemcells.2007-1076

Kooi, S., Zhang, H. Z., Patenia, R., Edwards, C. L., Platsoucas, C. D., & Freedman, R. S. (1996). HLA class I expression on human ovarian carcinoma cells correlates with T-cell infiltration in vivo and T-cell expansion in vitro in low concentrations of recombinant interleukin-2. *Cellular Immunology*, *174*(2), 116–128. https://doi.org/10.1006/cimm.1996.0301

Korotkevich, G., Sukhov, V., Budin, N., Shpak, B., Artyomov, M. N., & Sergushichev, A. (2021). *Fast gene set enrichment analysis* (p. 060012). bioRxiv. https://doi.org/10.1101/060012

Kouo, T., Huang, L., Pucsek, A. B., Cao, M., Solt, S., Armstrong, T., & Jaffee, E. (2015). Galectin-3 shapes antitumor immune responses by suppressing CD8+ T cells via LAG-3 and inhibiting expansion of plasmacytoid dendritic cells. *Cancer*

Immunology Research, *3*(4), 412–423. https://doi.org/10.1158/2326-6066.CIR-14-0150

Kroeger, P. T., & Drapkin, R. (2017). Pathogenesis and heterogeneity of ovarian cancer. *Current Opinion in Obstetrics & Gynecology*, *29*(1), 26–34. https://doi.org/10.1097/GCO.0000000000000340

Krześlak, A., & Lipińska, A. (2004). Galectin-3 as a multifunctional protein. *Cellular & Molecular Biology Letters*, *9*(2), 305–328.

Kudo-Saito, C., Shirako, H., Ohike, M., Tsukamoto, N., & Kawakami, Y. (2013). CCL2 is critical for immunosuppression to promote cancer metastasis. *Clinical & Experimental Metastasis*, *30*(4), 393–405. https://doi.org/10.1007/s10585-012-9545-6

Kudo-Saito, C., Shirako, H., Takeuchi, T., & Kawakami, Y. (2009). Cancer metastasis is accelerated through immunosuppression during Snail-induced EMT of cancer cells. *Cancer Cell*, *15*(3), 195–206. https://doi.org/10.1016/j.ccr.2009.01.023

Kurachi, M. (2019). CD8+ T cell exhaustion. *Seminars in Immunopathology*, *41*(3), 327–337. https://doi.org/10.1007/s00281-019-00744-5

Lachat, C., Peixoto, P., & Hervouet, E. (2021). Epithelial to Mesenchymal Transition History: From Embryonic Development to Cancers. *Biomolecules*, *11*(6), 782. https://doi.org/10.3390/biom11060782

Lambert, A. W., Pattabiraman, D. R., & Weinberg, R. A. (2017). Emerging Biological Principles of Metastasis. *Cell*, *168*(4), 670–691. https://doi.org/10.1016/j.cell.2016.11.037

Lambrechts, D., Wauters, E., Boeckx, B., Aibar, S., Nittner, D., Burton, O., Bassez, A., Decaluwé, H., Pircher, A., Van den Eynde, K., Weynand, B., Verbeken, E., De Leyn, P., Liston, A., Vansteenkiste, J., Carmeliet, P., Aerts, S., & Thienpont, B. (2018). Phenotype molding of stromal cells in the lung tumor microenvironment. *Nature Medicine*, *24*(8), Article 8. https://doi.org/10.1038/s41591-018-0096-5

Lamouille, S., Xu, J., & Derynck, R. (2014). Molecular mechanisms of epithelial–mesenchymal transition. *Nature Reviews Molecular Cell Biology*, *15*(3), Article 3. https://doi.org/10.1038/nrm3758

Lánczky, A., & Győrffy, B. (2021). Web-Based Survival Analysis Tool Tailored for Medical Research (KMplot): Development and Implementation. *Journal of Medical Internet Research*, *23*(7), e27633. https://doi.org/10.2196/27633

Latifi, A., Luwor, R. B., Bilandzic, M., Nazaretian, S., Stenvers, K., Pyman, J., Zhu, H., Thompson, E. W., Quinn, M. A., Findlay, J. K., & Ahmed, N. (2012). Isolation and Characterization of Tumor Cells from the Ascites of Ovarian Cancer Patients: Molecular Phenotype of Chemoresistant Ovarian Tumors. *PLoS ONE*, *7*(10), e46858. https://doi.org/10.1371/journal.pone.0046858

Laughney, A. M., Hu, J., Campbell, N. R., Bakhoum, S. F., Setty, M., Lavallée, V.-P., Xie, Y., Masilionis, I., Carr, A. J., Kottapalli, S., Allaj, V., Mattar, M., Rekhtman, N., Xavier, J. B., Mazutis, L., Poirier, J. T., Rudin, C. M., Pe'er, D., & Massagué, J. (2020). Regenerative lineages and immune-mediated pruning in lung cancer metastasis. *Nature Medicine*, *26*(2), Article 2. https://doi.org/10.1038/s41591-019-0750-6

Launonen, I.-M., Lyytikäinen, N., Casado, J., Anttila, E. A., Szabó, A., Haltia, U.-M., Jacobson, C. A., Lin, J. R., Maliga, Z., Howitt, B. E., Strickland, K. C., Santagata, S., Elias, K., D'Andrea, A. D., Konstantinopoulos, P. A., Sorger, P. K., & Färkkilä, A. (2022). Single-cell tumor-immune microenvironment of BRCA1/2 mutated high-grade serous ovarian cancer. *Nature Communications*, *13*(1), Article 1. https://doi.org/10.1038/s41467-022-28389-3

Lazaridou, M.-F., Gonschorek, E., Massa, C., Friedrich, M., Handke, D., Mueller, A., Jasinski-Bergner, S., Dummer, R., Koelblinger, P., & Seliger, B. (2020). Identification of miR-200a-5p targeting the peptide transporter TAP1 and its association with the clinical outcome of melanoma patients. *OncoImmunology*, *9*(1), 1774323. https://doi.org/10.1080/2162402X.2020.1774323

Lebel-Binay, S., Thiounn, N., De Pinieux, G., Vieillefond, A., Debré, B., Bonnefoy, J.-Y., Fridman, W.-H., & Pagès, F. (2003). IL-18 is produced by prostate cancer cells and secreted in response to interferons. *International Journal of Cancer*, *106*(6), 827–835. https://doi.org/10.1002/ijc.11285

Lee, H.-O., Hong, Y., Etlioglu, H. E., Cho, Y. B., Pomella, V., Van den Bosch, B., Vanhecke, J., Verbandt, S., Hong, H., Min, J.-W., Kim, N., Eum, H. H., Qian, J., Boeckx, B., Lambrechts, D., Tsantoulis, P., De Hertogh, G., Chung, W., Lee, T., … Park, W.-Y. (2020). Lineage-dependent gene expression programs influence the immune landscape of colorectal cancer. *Nature Genetics*, *52*(6), Article 6. https://doi.org/10.1038/s41588-020-0636-z

Lee, P. P., Yee, C., Savage, P. A., Fong, L., Brockstedt, D., Weber, J. S., Johnson, D., Swetter, S., Thompson, J., Greenberg, P. D., Roederer, M., & Davis, M. M.

(1999). Characterization of circulating T cells specific for tumor-associated antigens in melanoma patients. *Nature Medicine*, *5*(6), 677–685. https://doi.org/10.1038/9525

Leem, G., Park, J., Jeon, M., Kim, E.-S., Kim, S. W., Lee, Y. J., Choi, S. J., Choi, B., Park, S., Ju, Y. S., Jung, I., Kim, S., Shin, E.-C., Lee, J. Y., & Park, S.-H. (2020). 4-1BB co-stimulation further enhances anti-PD-1-mediated reinvigoration of exhausted CD39+ CD8 T cells from primary and metastatic sites of epithelial ovarian cancers. *Journal for ImmunoTherapy of Cancer*, *8*(2), e001650. https://doi.org/10.1136/jitc-2020-001650

Leng, Z., Li, Y., Zhou, G., Lv, X., Ai, W., Li, J., & Hou, L. (2020). Krüppel-like factor 4 regulates stemness and mesenchymal properties of colorectal cancer stem cells through the TGF-β1/Smad/snail pathway. *Journal of Cellular and Molecular Medicine*, *24*(2), 1866–1877. https://doi.org/10.1111/jcmm.14882

Lheureux, S., Braunstein, M., & Oza, A. M. (2019). Epithelial ovarian cancer: Evolution of management in the era of precision medicine. *CA: A Cancer Journal for Clinicians*, *69*(4), 280–304. https://doi.org/10.3322/caac.21559

Li, C.-W., Xia, W., Huo, L., Lim, S.-O., Wu, Y., Hsu, J. L., Chao, C.-H., Yamaguchi, H., Yang, N.-K., Ding, Q., Wang, Y., Lai, Y.-J., LaBaff, A. M., Wu, T.-J., Lin, B.-R., Yang, M.-H., Hortobagyi, G. N., & Hung, M.-C. (2012). Epithelial-mesenchyme transition induced by TNF-α requires NF-κB-mediated transcriptional upregulation of Twist1. *Cancer Research*, *72*(5), 1290–1300. https://doi.org/10.1158/0008-5472.CAN-11-3123

Li, X., Deng, W., Nail, C. D., Bailey, S. K., Kraus, M. H., Ruppert, J. M., & Lobo-Ruppert, S. M. (2006). Snail induction is an early response to Gli1 that determines the efficiency of epithelial transformation. *Oncogene*, *25*(4), Article 4. https://doi.org/10.1038/sj.onc.1209077

Liberzon, A., Birger, C., Thorvaldsdóttir, H., Ghandi, M., Mesirov, J. P., & Tamayo, P. (2015). The Molecular Signatures Database (MSigDB) hallmark gene set collection. *Cell Systems*, *1*(6), 417–425. https://doi.org/10.1016/j.cels.2015.12.004

Lim, H. X., Hong, H.-J., Cho, D., & Kim, T. S. (2014). IL-18 Enhances Immunosuppressive Responses by Promoting Differentiation into Monocytic Myeloid-Derived Suppressor Cells. *The Journal of Immunology*, *193*(11), 5453–5460. https://doi.org/10.4049/jimmunol.1401282

Lim, S., Becker, A., Zimmer, A., Lu, J., Buettner, R., & Kirfel, J. (2013). SNAI1-Mediated Epithelial-Mesenchymal Transition Confers Chemoresistance and Cellular Plasticity by Regulating Genes Involved in Cell Death and Stem Cell Maintenance. *PLoS ONE*, *8*(6), e66558. https://doi.org/10.1371/journal.pone.0066558

Lin, A., Xu, H.-H., Xu, D.-P., Zhang, X., Wang, Q., & Yan, W.-H. (2013). Multiple steps of HLA-G in ovarian carcinoma metastasis: Alter NK cytotoxicity and induce matrix metalloproteinase-15 (MMP-15) expression. *Human Immunology*, *74*(4), 439–446. https://doi.org/10.1016/j.humimm.2012.11.021

Liu, M., Yang, J., Zhang, Y., Zhou, Z., Cui, X., Zhang, L., Fung, K.-M., Zheng, W., Allard, F. D., Yee, E. U., Ding, K., Wu, H., Liang, Z., Zheng, L., Fernandez-Zapico, M. E.,

Li, Y.-P., Bronze, M. S., Morris, K. T., Postier, R. G., … Li, M. (2018). ZIP4 Promotes Pancreatic Cancer Progression by Repressing ZO-1 and Claudin-1 through a ZEB1-Dependent Transcriptional Mechanism. *Clinical Cancer Research*, *24*(13), 3186–3196. https://doi.org/10.1158/1078-0432.CCR-18-0263

Liu, Y., Xie, L., Wang, D., Li, D., Xu, G., Wang, L., Zhou, H., Yu, Y., Lin, Z., & Lu, H. (2018). Galectin-3 and β-catenin are associated with a poor prognosis in serous epithelial ovarian cancer. *Cancer Management and Research*, *10*, 3963–3971. https://doi.org/10.2147/CMAR.S171146

Lo, H.-W., Hsu, S.-C., Xia, W., Cao, X., Shih, J.-Y., Wei, Y., Abbruzzese, J. L., Hortobagyi, G. N., & Hung, M.-C. (2007). Epidermal Growth Factor Receptor Cooperates with Signal Transducer and Activator of Transcription 3 to Induce Epithelial-Mesenchymal Transition in Cancer Cells via Up-regulation of TWIST Gene Expression. *Cancer Research*, *67*(19), 9066–9076. https://doi.org/10.1158/0008-5472.CAN-07-0575

Loret, N., Denys, H., Tummers, P., & Berx, G. (2019). The Role of Epithelial-to-Mesenchymal Plasticity in Ovarian Cancer Progression and Therapy Resistance. *Cancers*, *11*(6), 838. https://doi.org/10.3390/cancers11060838

Lovisa, S., LeBleu, V. S., Tampe, B., Sugimoto, H., Vadnagara, K., Carstens, J. L., Wu, C.-C., Hagos, Y., Burckhardt, B. C., Pentcheva-Hoang, T., Nischal, H., Allison, J. P., Zeisberg, M., & Kalluri, R. (2015). Epithelial-to-mesenchymal transition induces cell cycle arrest and parenchymal damage in renal fibrosis. *Nature Medicine*, *21*(9), 998–1009. https://doi.org/10.1038/nm.3902

Luk, H.-M., Wang, D.-Y., Xie, L.-L., Liu, X.-Y., Xu, G.-C., & Lu, H.-W. (2020). Expression and clinical significance of Gal-3 and NFκB pathway-related factors in epithelial ovarian carcinoma. *International Journal of Clinical and Experimental Pathology*, *13*(5), 1197–1205.

Luo, J.-L., Kamata, H., & Karin, M. (2005). IKK/NF-κB signaling: Balancing life and death – a new approach to cancer therapy. *Journal of Clinical Investigation*, *115*(10), 2625–2632. https://doi.org/10.1172/JCI26322

MacGregor, H. L., Garcia-Batres, C., Sayad, A., Elia, A., Berman, H. K., Toker, A., Katz, S. R., Shaw, P. A., Clarke, B. A., Crome, S. Q., Robert-Tissot, C., Bernardini, M. Q., Nguyen, L. T., & Ohashi, P. S. (2019). Tumor cell expression of B7-H4 correlates with higher frequencies of tumor-infiltrating APCs and higher CXCL17 expression in human epithelial ovarian cancer. *Oncoimmunology*, *8*(12), e1665460. https://doi.org/10.1080/2162402X.2019.1665460

Machado, C. de V., Telles, P. D. da S., & Nascimento, I. L. O. (2013). Immunological characteristics of mesenchymal stem cells. *Revista Brasileira de Hematologia e Hemoterapia*, *35*(1), 62–67. https://doi.org/10.5581/1516-8484.20130017

Macintyre, G., Goranova, T. E., De Silva, D., Ennis, D., Piskorz, A. M., Eldridge, M., Sie, D., Lewsley, L.-A., Hanif, A., Wilson, C., Dowson, S., Glasspool, R. M., Lockley, M., Brockbank, E., Montes, A., Walther, A., Sundar, S., Edmondson, R., Hall, G. D., … Brenton, J. D. (2018). Copy-number signatures and mutational processes in ovarian carcinoma. *Nature Genetics*, *50*(9), 1262–1270. https://doi.org/10.1038/s41588-018-0179-8

MacKinnon, A. C., Gibbons, M. A., Farnworth, S. L., Leffler, H., Nilsson, U. J., Delaine, T., Simpson, A. J., Forbes, S. J., Hirani, N., Gauldie, J., & Sethi, T. (2012). Regulation of Transforming Growth Factor-β1–driven Lung Fibrosis by Galectin-3. *American Journal of Respiratory and Critical Care Medicine*, *185*(5), 537–546. https://doi.org/10.1164/rccm.201106-0965OC

Macnair, W., Gupta, R., & Claassen, M. (2022). psupertime: Supervised pseudotime analysis for time-series single-cell RNA-seq data. *Bioinformatics*, *38*(Supplement_1), i290–i298. https://doi.org/10.1093/bioinformatics/btac227

Malagoli Tagliazucchi, G., Wiecek, A. J., Withnell, E., & Secrier, M. (2023). Genomic and microenvironmental heterogeneity shaping epithelial-to-mesenchymal trajectories in cancer. *Nature Communications*, *14*, 789. https://doi.org/10.1038/s41467-023-36439-7

Mani, S. A., Guo, W., Liao, M.-J., Eaton, E. N., Ayyanan, A., Zhou, A. Y., Brooks, M., Reinhard, F., Zhang, C. C., Shipitsin, M., Campbell, L. L., Polyak, K., Brisken, C., Yang, J., & Weinberg, R. A. (2008). The epithelial-mesenchymal transition generates cells with properties of stem cells. *Cell*, *133*(4), 704–715. https://doi.org/10.1016/j.cell.2008.03.027

Marcenaro, E., Augugliaro, R., Falco, M., Castriconi, R., Parolini, S., Sivori, S., Romeo, E., Millo, R., Moretta, L., Bottino, C., & Moretta, A. (2003). CD59 is physically and functionally associated with natural cytotoxicity receptors and activates human NK cell-mediated cytotoxicity. *European Journal of Immunology*, *33*(12), 3367–3376. https://doi.org/10.1002/eji.200324425

Martinet, L., & Smyth, M. J. (2015). Balancing natural killer cell activation through paired receptors. *Nature Reviews. Immunology*, *15*(4), 243–254. https://doi.org/10.1038/nri3799

Maruhashi, T., Okazaki, I., Sugiura, D., Takahashi, S., Maeda, T. K., Shimizu, K., & Okazaki, T. (2018). LAG-3 inhibits the activation of CD4+ T cells that recognize stable pMHCII through its conformation-dependent recognition of pMHCII. *Nature Immunology*, *19*(12), Article 12. https://doi.org/10.1038/s41590-018-0217-9

McCloskey, C. W., Goldberg, R. L., Carter, L. E., Gamwell, L. F., Al-Hujaily, E. M., Collins, O., Macdonald, E. A., Garson, K., Daneshmand, M., Carmona, E., & Vanderhyden, B. C. (2014). A new spontaneously transformed syngeneic model of high-grade serous ovarian cancer with a tumor-initiating cell population. *Frontiers in Oncology*, *4*, 53. https://doi.org/10.3389/fonc.2014.00053

McCorry, A. M., Loughrey, M. B., Longley, D. B., Lawler, M., & Dunne, P. D. (2018). Epithelial-to-mesenchymal transition signature assessment in colorectal cancer quantifies tumour stromal content rather than true transition. *The Journal of Pathology*, *246*(4), 422–426. https://doi.org/10.1002/path.5155

McGinnis, C. S., Patterson, D. M., Winkler, J., Conrad, D. N., Hein, M. Y., Srivastava, V., Hu, J. L., Murrow, L. M., Weissman, J. S., Werb, Z., Chow, E. D., & Gartner, Z. J. (2019). MULTI-seq: Sample multiplexing for single-cell RNA sequencing using lipid-tagged indices. *Nature Methods*, *16*(7), Article 7. https://doi.org/10.1038/s41592-019-0433-8

McNiven, M. A. (2013). Breaking away: Matrix remodeling from the leading edge. *Trends in Cell Biology*, *23*(1), 16–21. https://doi.org/10.1016/j.tcb.2012.08.009

Medici, D., Hay, E. D., & Goodenough, D. A. (2006). Cooperation between Snail and LEF-1 Transcription Factors Is Essential for TGF-β1-induced Epithelial-Mesenchymal Transition. *Molecular Biology of the Cell*, *17*(4), 1871–1879. https://doi.org/10.1091/mbc.e05-08-0767

Mehlen, P., & Puisieux, A. (2006). Metastasis: A question of life or death. *Nature Reviews. Cancer*, *6*(6), 449–458. https://doi.org/10.1038/nrc1886

Mendonsa, A., Na, T.-Y., & Gumbiner, B. M. (2018). E-cadherin in Contact Inhibition and Cancer. *Oncogene*, *37*(35), 4769–4780. https://doi.org/10.1038/s41388-018-0304-2

Menon, A. G., Morreau, H., Tollenaar, R. A. E. M., Alphenaar, E., Puijenbroek, M. van, Putter, H., Rhijn, C. M. J., Velde, C. J. H. van de, Fleuren, G. J., & Kuppen, P. J. K. (2002). Down-Regulation of HLA-A Expression Correlates with a Better Prognosis in Colorectal Cancer Patients. *Laboratory Investigation*, *82*(12), 1725–1733. https://doi.org/10.1097/01.LAB.0000043124.75633.ED

Mercado-Pimentel, M. E., & Runyan, R. B. (2007). Multiple Transforming Growth Factor-β Isoforms and Receptors Function during Epithelial-Mesenchymal Cell Transformation in the Embryonic Heart. *Cells Tissues Organs*, *185*(1–3), 146–156. https://doi.org/10.1159/000101315

Mettu, N. B., Ulahannan, S. V., Bendell, J. C., Garrido-Laguna, I., Strickler, J. H., Moore, K. N., Stagg, R., Kapoun, A. M., Faoro, L., & Sharma, S. (2022). A Phase 1a/b Open-Label, Dose-Escalation Study of Etigilimab Alone or in Combination with Nivolumab in Patients with Locally Advanced or Metastatic Solid Tumors. *Clinical*

Cancer Research, *28*(5), 882–892. https://doi.org/10.1158/1078-0432.CCR-21-2780

Mirandola, L., Yu, Y., Cannon, M. J., Jenkins, M. R., Rahman, R. L., Nguyen, D. D., Grizzi, F., Cobos, E., Figueroa, J. A., & Chiriva-Internati, M. (2014). Galectin-3 inhibition suppresses drug resistance, motility, invasion and angiogenic potential in ovarian cancer. *Gynecologic Oncology*, *135*(3), 573–579. https://doi.org/10.1016/j.ygyno.2014.09.021

Misra, A., Pandey, C., Sze, S. K., & Thanabalu, T. (2012). Hypoxia Activated EGFR Signaling Induces Epithelial to Mesenchymal Transition (EMT). *PLOS ONE*, *7*(11), e49766. https://doi.org/10.1371/journal.pone.0049766

Miyoshi, A., Kitajima, Y., Sumi, K., Sato, K., Hagiwara, A., Koga, Y., & Miyazaki, K. (2004). Snail and SIP1 increase cancer invasion by upregulating MMP family in hepatocellular carcinoma cells. *British Journal of Cancer*, *90*(6), Article 6. https://doi.org/10.1038/sj.bjc.6601685

Morel, A.-P., Lièvre, M., Thomas, C., Hinkal, G., Ansieau, S., & Puisieux, A. (2008). Generation of breast cancer stem cells through epithelial-mesenchymal transition. *PloS One*, *3*(8), e2888. https://doi.org/10.1371/journal.pone.0002888

Mullins, R., Pal, A., Barrett, T. F., Neal, M. E. H., & Puram, S. V. (2022). Epithelial-mesenchymal plasticity in tumor immune evasion. *Cancer Research*, *82*(13), 2329–2343. https://doi.org/10.1158/0008-5472.CAN-21-4370

Murakami, R., Matsumura, N., Mandai, M., Yoshihara, K., Tanabe, H., Nakai, H., Yamanoi, K., Abiko, K., Yoshioka, Y., Hamanishi, J., Yamaguchi, K., Baba, T., Koshiyama, M., Enomoto, T., Okamoto, A., Murphy, S. K., Mori, S., Mikami, Y.,

Minamiguchi, S., & Konishi, I. (2016). Establishment of a Novel Histopathological Classification of High-Grade Serous Ovarian Carcinoma Correlated with Prognostically Distinct Gene Expression Subtypes. *The American Journal of Pathology*, *186*(5), 1103–1113. https://doi.org/10.1016/j.ajpath.2015.12.029

Muralidharan, S., Sehgal, M., Soundharya, R., Mandal, S., Majumdar, S. S., Yeshwanth, M., Saha, A., & Jolly, M. K. (2022). PD-L1 Activity Is Associated with Partial EMT and Metabolic Reprogramming in Carcinomas. *Current Oncology*, *29*(11), 8285–8301. https://doi.org/10.3390/curroncol29110654

Nakamura, K., Kassem, S., Cleynen, A., Chrétien, M.-L., Guillerey, C., Putz, E. M., Bald, T., Förster, I., Vuckovic, S., Hill, G. R., Masters, S. L., Chesi, M., Bergsagel, P. L., Avet-Loiseau, H., Martinet, L., & Smyth, M. J. (2018). Dysregulated IL-18 Is a Key Driver of Immunosuppression and a Possible Therapeutic Target in the Multiple Myeloma Microenvironment. *Cancer Cell*, *33*(4), 634-648.e5. https://doi.org/10.1016/j.ccell.2018.02.007

Nath, A., Oak, A., Chen, K. Y., Li, I., Splichal, R. C., Portis, J., Foster, S., Walton, S. P., & Chan, C. (2021). Palmitate-induced IRE1-XBP1-ZEB signaling represses desmoplakin expression and promotes cancer cell migration. *Molecular Cancer Research : MCR*, *19*(2), 240–248. https://doi.org/10.1158/1541-7786.MCR-19-0480

Nawshad, A., & Hay, E. D. (2003). TGFβ3 signaling activates transcription of the LEF1 gene to induce epithelial mesenchymal transformation during mouse palate development. *Journal of Cell Biology*, *163*(6), 1291–1301. https://doi.org/10.1083/jcb.200306024

Nawshad, A., LaGamba, D., & Hay, E. D. (2004). Transforming growth factor β (TGFβ) signalling in palatal growth, apoptosis and epithelial mesenchymal transformation (EMT). *Archives of Oral Biology*, *49*(9), 675–689. https://doi.org/10.1016/j.archoralbio.2004.05.007

Nhokaew, W., Kleebkaow, P., Chaisuriya, N., & Kietpeerakool, C. (2019). Programmed Death Ligand 1 (PD-L1) Expression in Epithelial Ovarian Cancer: A Comparison of Type I and Type II Tumors. *Asian Pacific Journal of Cancer Prevention : APJCP*, *20*(4), 1161–1169. https://doi.org/10.31557/APJCP.2019.20.4.1161

Niehrs, C. (2012). The complex world of WNT receptor signalling. *Nature Reviews Molecular Cell Biology*, *13*(12), Article 12. https://doi.org/10.1038/nrm3470

Nieto, M. A., Sargent, M. G., Wilkinson, D. G., & Cooke, J. (1994). Control of Cell Behavior During Vertebrate Development by Slug, a Zinc Finger Gene. *Science*, *264*(5160), 835–839. https://doi.org/10.1126/science.7513443

Nimnual, A. S., Taylor, L. J., & Bar-Sagi, D. (2003). Redox-dependent downregulation of Rho by Rac. *Nature Cell Biology*, *5*(3), Article 3. https://doi.org/10.1038/ncb938

Noce, V., Battistelli, C., Cozzolino, A. M., Consalvi, V., Cicchini, C., Strippoli, R., Tripodi, M., Marchetti, A., & Amicone, L. (2019). YAP integrates the regulatory Snail/HNF4α circuitry controlling epithelial/hepatocyte differentiation. *Cell Death & Disease*, *10*(10), Article 10. https://doi.org/10.1038/s41419-019-2000-8

Nugteren, S., & Samsom, J. N. (2021). Secretory Leukocyte Protease Inhibitor (SLPI) in mucosal tissues: Protects against inflammation, but promotes cancer. *Cytokine & Growth Factor Reviews*, *59*, 22–35. https://doi.org/10.1016/j.cytogfr.2021.01.005

Ocaña, O. H., Córcoles, R., Fabra, A., Moreno-Bueno, G., Acloque, H., Vega, S., Barrallo-Gimeno, A., Cano, A., & Nieto, M. A. (2012). Metastatic colonization requires the repression of the epithelial-mesenchymal transition inducer Prrx1. *Cancer Cell*, *22*(6), 709–724. https://doi.org/10.1016/j.ccr.2012.10.012

Oda, H., Tsukita, S., & Takeichi, M. (1998). Dynamic Behavior of the Cadherin-Based Cell–Cell Adhesion System duringDrosophilaGastrulation. *Developmental Biology*, *203*(2), 435–450. https://doi.org/10.1006/dbio.1998.9047

Oestreich, K. J., Yoon, H., Ahmed, R., & Boss, J. M. (2008). NFATc1 Regulates PD-1 Expression upon T Cell Activation1. *The Journal of Immunology*, *181*(7), 4832–4839. https://doi.org/10.4049/jimmunol.181.7.4832

Oft, M., Heider, K.-H., & Beug, H. (1998). TGFβ signaling is necessary for carcinoma cell invasiveness and metastasis. *Current Biology*, *8*(23), 1243–1252. https://doi.org/10.1016/S0960-9822(07)00533-7

Okita, R., Shimizu, K., & Nakata, M. (2018). Epithelial-mesenchymal transition-induced metastasis could be a bait for natural killer cells. *Journal of Thoracic Disease*, *10*(Suppl 26), S3143–S3146. https://doi.org/10.21037/jtd.2018.08.19

Ovarian Tumor Tissue Analysis (OTTA) Consortium. (2017). Dose-Response Association of CD8+ Tumor-Infiltrating Lymphocytes and Survival Time in High-Grade Serous Ovarian Cancer. *JAMA Oncology*, *3*(12), e173290. https://doi.org/10.1001/jamaoncol.2017.3290

Owusu-Akyaw, A., Krishnamoorthy, K., Goldsmith, L. T., & Morelli, S. S. (2019). The role of mesenchymal–epithelial transition in endometrial function. *Human Reproduction Update*, *25*(1), 114–133. https://doi.org/10.1093/humupd/dmy035

Ozga, A. J., Chow, M. T., & Luster, A. D. (2021). Chemokines and the immune response to cancer. *Immunity*, *54*(5), 859–874. https://doi.org/10.1016/j.immuni.2021.01.012

Pagan, R., Martín, I., Llobera, M., & Vilaró, S. (1997). Epithelial-mesenchymal transition of cultured rat neonatal hepatocytes is differentially regulated in response to epidermal growth factor and dimethyl sulfoxide. *Hepatology (Baltimore, Md.)*, *25*(3), 598–606. https://doi.org/10.1002/hep.510250318

Paley, M. A., Kroy, D. C., Odorizzi, P. M., Johnnidis, J. B., Dolfi, D. V., Barnett, B. E., Bikoff, E. K., Robertson, E. J., Lauer, G. M., Reiner, S. L., & Wherry, E. J. (2012). Progenitor and Terminal Subsets of CD8+ T Cells Cooperate to Contain Chronic Viral Infection. *Science*, *338*(6111), 1220–1225. https://doi.org/10.1126/science.1229620

Palmer, M. B., Majumder, P., Cooper, J. C., Yoon, H., Wade, P. A., & Boss, J. M. (2009). YY1 regulates the expression of snail through a distal enhancer. *Molecular Cancer Research : MCR*, *7*(2), 221. https://doi.org/10.1158/1541-7786.MCR-08-0229

Parameswaran, N., & Patial, S. (2010). Tumor Necrosis Factor-α Signaling in Macrophages. *Critical Reviews in Eukaryotic Gene Expression*, *20*(2), 87–103.

Park, J.-J., Park, M.-H., Oh, E. H., Soung, N.-K., Lee, S. J., Jung, J.-K., Lee, O.-J., Yun, S. J., Kim, W.-J., Shin, E.-Y., & Kim, E.-G. (2018). The p21-activated kinase 4-Slug transcription factor axis promotes epithelial−mesenchymal transition and worsens prognosis in prostate cancer. *Oncogene*, *37*(38), Article 38. https://doi.org/10.1038/s41388-018-0327-8

Peinado, H., Portillo, F., & Cano, A. (2004). Transcriptional regulation of cadherins during development and carcinogenesis. *The International Journal of Developmental Biology*, *48*(5–6), Article 5–6. https://doi.org/10.1387/ijdb.041794hp

Peinado, H., Quintanilla, M., & Cano, A. (2003). Transforming Growth Factor β-1 Induces Snail Transcription Factor in Epithelial Cell Lines: MECHANISMS FOR EPITHELIAL MESENCHYMAL TRANSITIONS*. *Journal of Biological Chemistry*, *278*(23), 21113–21123. https://doi.org/10.1074/jbc.M211304200

Peiró, S., Escrivà, M., Puig, I., Barberà, M. J., Dave, N., Herranz, N., Larriba, M. J., Takkunen, M., Francí, C., Muñoz, A., Virtanen, I., Baulida, J., & de Herreros, A. G. (2006). Snail1 transcriptional repressor binds to its own promoter and controls its expression. *Nucleic Acids Research*, *34*(7), 2077–2084. https://doi.org/10.1093/nar/gkl141

Pernodet, N., Hermetet, F., Adami, P., Vejux, A., Descotes, F., Borg, C., Adams, M., Pallandre, J.-R., Viennet, G., Esnard, F., Jouvenot, M., & Despouy, G. (2012). High expression of QSOX1 reduces tumorogenesis, and is associated with a better outcome for breast cancer patients. *Breast Cancer Research*, *14*(5), R136. https://doi.org/10.1186/bcr3341

Piver, M. S. (2006). Treatment of ovarian cancer at the crossroads: 50 years after single-agent melphalan chemotherapy. *Oncology (Williston Park, N.Y.)*, *20*(10), 1156, 1158.

Pradella, D., Naro, C., Sette, C., & Ghigna, C. (2017). EMT and stemness: Flexible processes tuned by alternative splicing in development and cancer progression. *Molecular Cancer*, *16*(1), 8. https://doi.org/10.1186/s12943-016-0579-2

Prakash, V., Carson, B. B., Feenstra, J. M., Dass, R. A., Sekyrova, P., Hoshino, A., Petersen, J., Guo, Y., Parks, M. M., Kurylo, C. M., Batchelder, J. E., Haller, K., Hashimoto, A., Rundqivst, H., Condeelis, J. S., Allis, C. D., Drygin, D., Nieto, M. A., Andäng, M., … Vincent, C. T. (2019). Ribosome biogenesis during cell cycle arrest fuels EMT in development and disease. *Nature Communications*, *10*(1), Article 1. https://doi.org/10.1038/s41467-019-10100-8

Prat, J. (2012). Ovarian carcinomas: Five distinct diseases with different origins, genetic alterations, and clinicopathological features. *Virchows Archiv: An International Journal of Pathology*, *460*(3), 237–249. https://doi.org/10.1007/s00428-012-1203-5

Priglinger, C. S., Obermann, J., Szober, C. M., Merl-Pham, J., Ohmayer, U., Behler, J., Gruhn, F., Kreutzer, T. C., Wertheimer, C., Geerlof, A., Priglinger, S. G., & Hauck, S. M. (2016). Epithelial-to-Mesenchymal Transition of RPE Cells In Vitro Confers Increased β1,6-N-Glycosylation and Increased Susceptibility to Galectin-3 Binding. *PLOS ONE*, *11*(1), e0146887. https://doi.org/10.1371/journal.pone.0146887

Qian, J., Olbrecht, S., Boeckx, B., Vos, H., Laoui, D., Etlioglu, E., Wauters, E., Pomella, V., Verbandt, S., Busschaert, P., Bassez, A., Franken, A., Bempt, M. V., Xiong, J., Weynand, B., van Herck, Y., Antoranz, A., Bosisio, F. M., Thienpont, B., … Lambrechts, D. (2020). A pan-cancer blueprint of the heterogeneous tumor

microenvironment revealed by single-cell profiling. *Cell Research*, *30*(9), Article 9. https://doi.org/10.1038/s41422-020-0355-0

Qin, Q., Xu, Y., He, T., Qin, C., & Xu, J. (2012). Normal and disease-related biological functions of Twist1 and underlying molecular mechanisms. *Cell Research*, *22*(1), 90–106. https://doi.org/10.1038/cr.2011.144

Rådestad, E., Klynning, C., Stikvoort, A., Mogensen, O., Nava, S., Magalhaes, I., & Uhlin, M. (2018). Immune profiling and identification of prognostic immune-related risk factors in human ovarian cancer. *Oncoimmunology*, *8*(2), e1535730. https://doi.org/10.1080/2162402X.2018.1535730

Rafehi, S., Valdes, Y. R., Bertrand, M., McGee, J., Préfontaine, M., Sugimoto, A., DiMattia, G. E., & Shepherd, T. G. (2016). TGFβ signaling regulates epithelial–mesenchymal plasticity in ovarian cancer ascites-derived spheroids. *Endocrine-Related Cancer*, *23*(3), 147–159. https://doi.org/10.1530/ERC-15-0383

Ran, G. he, Lin, Y. qing, Tian, L., Zhang, T., Yan, D. mei, Yu, J. hua, & Deng, Y. cai. (2022). Natural killer cell homing and trafficking in tissues and tumors: From biology to application. *Signal Transduction and Targeted Therapy*, *7*(1), Article 1. https://doi.org/10.1038/s41392-022-01058-z

Ribatti, D., Tamma, R., & Annese, T. (2020). Epithelial-Mesenchymal Transition in Cancer: A Historical Overview. *Translational Oncology*, *13*(6), 100773. https://doi.org/10.1016/j.tranon.2020.100773

Rivera-Cruz, C. M., Shearer, J. J., Figueiredo Neto, M., & Figueiredo, M. L. (2017). The Immunomodulatory Effects of Mesenchymal Stem Cell Polarization within the

Tumor Microenvironment Niche. *Stem Cells International*, *2017*, 4015039. https://doi.org/10.1155/2017/4015039

Roby, K. F., Taylor, C. C., Sweetwood, J. P., Cheng, Y., Pace, J. L., Tawfik, O., Persons, D. L., Smith, P. G., & Terranova, P. F. (2000). Development of a syngeneic mouse model for events related to ovarian cancer. *Carcinogenesis*, *21*(4), 585–591. https://doi.org/10.1093/carcin/21.4.585

Rodriguez, G. M., Galpin, K. J. C., Cook, D. P., Yakubovich, E., Maranda, V., Macdonald, E. A., Wilson-Sanchez, J., Thomas, A. L., Burdette, J. E., & Vanderhyden, B. C. (2022). The Tumor Immune Profile of Murine Ovarian Cancer Models: An Essential Tool for Ovarian Cancer Immunotherapy Research. *Cancer Research Communications*, *2*(6), 417–433. https://doi.org/10.1158/2767-9764.CRC-22-0017

Rodriguez, G. M., Yakubovich, E., & Vanderhyden, B. C. (2023). Unveiling the Immunogenicity of Ovarian Tumors as the Crucial Catalyst for Therapeutic Success. *Cancers*, *15*(23), Article 23. https://doi.org/10.3390/cancers15235694

Rudd, C. E., Chanthong, K., & Taylor, A. (2020). Small Molecule Inhibition of GSK-3 Specifically Inhibits the Transcription of Inhibitory Co-receptor LAG-3 for Enhanced Anti-tumor Immunity. *Cell Reports*, *30*(7), 2075-2082.e4. https://doi.org/10.1016/j.celrep.2020.01.076

Ruffo, E., Wu, R., Bruno, T. C., Workman, C. J., & Vignali, D. A. A. (2019). Lymphocyte-Activation Gene 3 (LAG3): The Next Immune Checkpoint Receptor. *Seminars in Immunology*, *42*, 101305. https://doi.org/10.1016/j.smim.2019.101305

Rutten, M. J., Dijk, F., Savci-Heijink, C. D., Buist, M. R., Kenter, G. G., van de Vijver, M. J., & Jordanova, E. S. (2014). HLA-G Expression Is an Independent Predictor for Improved Survival in High Grade Ovarian Carcinomas. *Journal of Immunology Research*, *2014*, 274584. https://doi.org/10.1155/2014/274584

Ryan, J. M., Barry, F. P., Murphy, J. M., & Mahon, B. P. (2005). Mesenchymal stem cells avoid allogeneic rejection. *Journal of Inflammation (London, England)*, *2*, 8. https://doi.org/10.1186/1476-9255-2-8

Sabbatino, F., Liguori, L., Polcaro, G., Salvato, I., Caramori, G., Salzano, F. A., Casolaro, V., Stellato, C., Dal Col, J., & Pepe, S. (2020). Role of Human Leukocyte Antigen System as A Predictive Biomarker for Checkpoint-Based Immunotherapy in Cancer Patients. *International Journal of Molecular Sciences*, *21*(19), 7295. https://doi.org/10.3390/ijms21197295

Sahoo, S., Nayak, S. P., Hari, K., Purkait, P., Mandal, S., Kishore, A., Levine, H., & Jolly, M. K. (2021). Immunosuppressive Traits of the Hybrid Epithelial/Mesenchymal Phenotype. *Frontiers in Immunology*, *12*, 797261. https://doi.org/10.3389/fimmu.2021.797261

Saitoh, M. (2018). Involvement of partial EMT in cancer progression. *Journal of Biochemistry*, *164*(4), 257–264. https://doi.org/10.1093/jb/mvy047

Sakata, J., Kajiyama, H., Suzuki, S., Utsumi, F., Niimi, K., Sekiya, R., Shibata, K., Senga, T., & Kikkawa, F. (2017). Impact of positive ZEB1 expression in patients with epithelial ovarian carcinoma as an oncologic outcome-predicting indicator. *Oncology Letters*, *14*(4), 4287–4293. https://doi.org/10.3892/ol.2017.6658

Santoiemma, P. P., Reyes, C., Wang, L.-P., McLane, M. W., Feldman, M. D., Tanyi, J. L., & Powell, D. J. (2016). Systematic evaluation of multiple immune markers reveals prognostic factors in ovarian cancer. *Gynecologic Oncology*, *143*(1), 120–127. https://doi.org/10.1016/j.ygyno.2016.07.105

Sarikonda, G., Wallace, B. K., Wiesner, C., Krishnan, S., Lewicki, J. A., & Kapoun, A. M. (2022). 111P Interim biomarker analysis of a phase Ib/II study of anti-TIGIT etigilimab (MPH313) and nivolumab in subjects with select locally advanced or metastatic solid tumors (ACTIVATE). *Annals of Oncology*, *33*, S589. https://doi.org/10.1016/j.annonc.2022.07.143

Sathe, A., Grimes, S. M., Lau, B. T., Chen, J., Suarez, C., Huang, R. J., Poultsides, G., & Ji, H. P. (2020). Single-Cell Genomic Characterization Reveals the Cellular Reprogramming of the Gastric Tumor Microenvironment. *Clinical Cancer Research*, *26*(11), 2640–2653. https://doi.org/10.1158/1078-0432.CCR-19-3231

Sato, E., Olson, S. H., Ahn, J., Bundy, B., Nishikawa, H., Qian, F., Jungbluth, A. A., Frosina, D., Gnjatic, S., Ambrosone, C., Kepner, J., Odunsi, T., Ritter, G., Lele, S., Chen, Y.-T., Ohtani, H., Old, L. J., & Odunsi, K. (2005). Intraepithelial CD8+ tumor-infiltrating lymphocytes and a high CD8+/regulatory T cell ratio are associated with favorable prognosis in ovarian cancer. *Proceedings of the National Academy of Sciences of the United States of America*, *102*(51), 18538–18543. https://doi.org/10.1073/pnas.0509182102

Savagner, P., Kusewitt, D. F., Carver, E. A., Magnino, F., Choi, C., Gridley, T., & Hudson, L. G. (2005). Developmental transcription factor slug is required for effective re-

epithelialization by adult keratinocytes. *Journal of Cellular Physiology*, *202*(3), 858–866. https://doi.org/10.1002/jcp.20188

Saxena, K., Jolly, M. K., & Balamurugan, K. (2020). Hypoxia, partial EMT and collective migration: Emerging culprits in metastasis. *Translational Oncology*, *13*(11), 100845. https://doi.org/10.1016/j.tranon.2020.100845

Schwartzkopff, S., Gründemann, C., Schweier, O., Rosshart, S., Karjalainen, K. E., Becker, K.-F., & Pircher, H. (2007). Tumor-Associated E-Cadherin Mutations Affect Binding to the Killer Cell Lectin-Like Receptor G1 in Humans1. *The Journal of Immunology*, *179*(2), 1022–1029. https://doi.org/10.4049/jimmunol.179.2.1022

Sestito, R., Tocci, P., Roman, C., Di Castro, V., & Bagnato, A. (2022). Functional interaction between endothelin-1 and ZEB1/YAP signaling regulates cellular plasticity and metastasis in high-grade serous ovarian cancer. *Journal of Experimental & Clinical Cancer Research : CR*, *41*, 157. https://doi.org/10.1186/s13046-022-02317-1

Shayesteh, L., Lu, Y., Kuo, W. L., Baldocchi, R., Godfrey, T., Collins, C., Pinkel, D., Powell, B., Mills, G. B., & Gray, J. W. (1999). PIK3CA is implicated as an oncogene in ovarian cancer. *Nature Genetics*, *21*(1), 99–102. https://doi.org/10.1038/5042

Shetty, S. S., Sharma, M., Fonseca, F. P., Jayaram, P., Tanwar, A. S., Kabekkodu, S. P., Satyamoorthy, K., & Radhakrishnan, R. (2020). Signaling pathways promoting epithelial mesenchymal transition in oral submucous fibrosis and oral squamous cell carcinoma. *Japanese Dental Science Review*, *56*(1), 97–108. https://doi.org/10.1016/j.jdsr.2020.07.002

Shibata, K., Kajiyama, H., Ino, K., Terauchi, M., Yamamoto, E., Nawa, A., Nomura, S., & Kikkawa, F. (2008). Twist expression in patients with cervical cancer is associated with poor disease outcome. *Annals of Oncology*, *19*(1), 81–85. https://doi.org/10.1093/annonc/mdm344

Shiina, T., Hosomichi, K., Inoko, H., & Kulski, J. K. (2009). The HLA genomic loci map: Expression, interaction, diversity and disease. *Journal of Human Genetics*, *54*(1), 15–39. https://doi.org/10.1038/jhg.2008.5

Shim, S., Lee, S., Hisham, Y., Kim, S., Nguyen, T. T., Taitt, A. S., Hwang, J., Jhun, H., Park, H.-Y., Lee, Y., Yeom, S. C., Kim, S.-Y., Kim, Y.-G., & Kim, S. (2022). A Paradoxical Effect of Interleukin-32 Isoforms on Cancer. *Frontiers in Immunology*, *13*. https://www.frontiersin.org/articles/10.3389/fimmu.2022.837590

Siemens, H., Jackstadt, R., Hünten, S., Kaller, M., Menssen, A., Götz, U., & Hermeking, H. (2011). miR-34 and SNAIL form a double-negative feedback loop to regulate epithelial-mesenchymal transitions. *Cell Cycle*, *10*(24), 4256–4271. https://doi.org/10.4161/cc.10.24.18552

Simeonov, K. P., Byrns, C. N., Clark, M. L., Norgard, R. J., Martin, B., Stanger, B. Z., Shendure, J., McKenna, A., & Lengner, C. J. (2021). Single-cell lineage tracing of metastatic cancer reveals selection of hybrid EMT states. *Cancer Cell*, *39*(8), 1150-1162.e9. https://doi.org/10.1016/j.ccell.2021.05.005

SINGH, A. B., SHARMA, A., SMITH, J. J., KRISHNAN, M., CHEN, X., ESCHRICH, S., WASHINGTON, M. K., YEATMAN, T. J., BEAUCHAMP, R. D., & DHAWAN, P. (2011). Claudin-1 Up-regulates the Repressor ZEB-1 to Inhibit E-Cadherin

Expression in Colon Cancer Cells. *Gastroenterology*, *141*(6), 2140–2153. https://doi.org/10.1053/j.gastro.2011.08.038

Slack, R. J., Mills, R., & Mackinnon, A. C. (2021). The therapeutic potential of galectin-3 inhibition in fibrotic disease. *The International Journal of Biochemistry & Cell Biology*, *130*, 105881. https://doi.org/10.1016/j.biocel.2020.105881

Smith, D. E., Amo, F. F. D., & Gridley, T. (1992). Isolation of Sna, a mouse gene homologous to the Drosophila genes snail and escargot: Its expression pattern suggests multiple roles during postimplantation development. *Development*, *116*(4), 1033–1039. https://doi.org/10.1242/dev.116.4.1033

Sordo-Bahamonde, C., Lorenzo-Herrero, S., González-Rodríguez, A. P., Payer, Á. R., González-García, E., López-Soto, A., & Gonzalez, S. (2021). LAG-3 Blockade with Relatlimab (BMS-986016) Restores Anti-Leukemic Responses in Chronic Lymphocytic Leukemia. *Cancers*, *13*(9), Article 9. https://doi.org/10.3390/cancers13092112

Soria, G., & Ben-Baruch, A. (2008). The inflammatory chemokines CCL2 and CCL5 in breast cancer. *Cancer Letters*, *267*(2), 271–285. https://doi.org/10.1016/j.canlet.2008.03.018

Spits, H., Bernink, J. H., & Lanier, L. (2016). NK cells and type 1 innate lymphoid cells: Partners in host defense. *Nature Immunology*, *17*(7), Article 7. https://doi.org/10.1038/ni.3482

Steele, N. G., Carpenter, E. S., Kemp, S. B., Sirihorachai, V. R., The, S., Delrosario, L., Lazarus, J., Amir, E. D., Gunchick, V., Espinoza, C., Bell, S., Harris, L., Lima, F., Irizarry-Negron, V., Paglia, D., Macchia, J., Chu, A. K. Y., Schofield, H.,

Wamsteker, E.-J., … Pasca di Magliano, M. (2020). Multimodal mapping of the tumor and peripheral blood immune landscape in human pancreatic cancer. *Nature Cancer*, *1*(11), Article 11. https://doi.org/10.1038/s43018-020-00121-4

Stemmler, M. P., Eccles, R. L., Brabletz, S., & Brabletz, T. (2019). Non-redundant functions of EMT transcription factors. *Nature Cell Biology*, *21*(1), Article 1. https://doi.org/10.1038/s41556-018-0196-y

Stoeckius, M., Hafemeister, C., Stephenson, W., Houck-Loomis, B., Chattopadhyay, P. K., Swerdlow, H., Satija, R., & Smibert, P. (2017). Simultaneous epitope and transcriptome measurement in single cells. *Nature Methods*, *14*(9), Article 9. https://doi.org/10.1038/nmeth.4380

Stoker, M., Gherardi, E., Perryman, M., & Gray, J. (1987). Scatter factor is a fibroblast-derived modulator of epithelial cell mobility. *Nature*, *327*(6119), Article 6119. https://doi.org/10.1038/327239a0

Stoker, M., & Perryman, M. (1985). An epithelial scatter factor released by embryo fibroblasts. *Journal of Cell Science*, *77*(1), 209–223. https://doi.org/10.1242/jcs.77.1.209

Stuart, T., Butler, A., Hoffman, P., Hafemeister, C., Papalexi, E., Mauck, W. M., Hao, Y., Stoeckius, M., Smibert, P., & Satija, R. (2019). Comprehensive Integration of Single-Cell Data. *Cell*, *177*(7), 1888-1902.e21. https://doi.org/10.1016/j.cell.2019.05.031

Stuelten, C. H., Barbul, A., Busch, J. I., Sutton, E., Katz, R., Sato, M., Wakefield, L. M., Roberts, A. B., & Niederhuber, J. E. (2008). Acute Wounds Accelerate

Tumorigenesis by a T-Cell Dependent Mechanism. *Cancer Research*, *68*(18), 7278–7282. https://doi.org/10.1158/0008-5472.CAN-08-1842

Subhadarshini, S., Markus, J., Sahoo, S., & Jolly, M. K. (2023). Dynamics of Epithelial–Mesenchymal Plasticity: What Have Single-Cell Investigations Elucidated So Far? *ACS Omega*, *8*(13), 11665–11673. https://doi.org/10.1021/acsomega.2c07989

Sun, Y., Song, G.-D., Sun, N., Chen, J.-Q., & Yang, S.-S. (2014). Slug overexpression induces stemness and promotes hepatocellular carcinoma cell invasion and metastasis. *Oncology Letters*, *7*(6), 1936–1940. https://doi.org/10.3892/ol.2014.2037

Sung, H.-J., Ahn, J.-M., Yoon, Y.-H., Na, S.-S., Choi, Y.-J., Kim, Y.-I., Lee, S.-Y., Lee, E.-B., Cho, S., & Cho, J.-Y. (2018). Quiescin Sulfhydryl Oxidase 1 (QSOX1) Secreted by Lung Cancer Cells Promotes Cancer Metastasis. *International Journal of Molecular Sciences*, *19*(10), 3213. https://doi.org/10.3390/ijms19103213

Taki, M., Abiko, K., Baba, T., Hamanishi, J., Yamaguchi, K., Murakami, R., Yamanoi, K., Horikawa, N., Hosoe, Y., Nakamura, E., Sugiyama, A., Mandai, M., Konishi, I., & Matsumura, N. (2018). Snail promotes ovarian cancer progression by recruiting myeloid-derived suppressor cells via CXCR2 ligand upregulation. *Nature Communications*, *9*(1), 1685. https://doi.org/10.1038/s41467-018-03966-7

Taki, M., Abiko, K., Ukita, M., Murakami, R., Yamanoi, K., Yamaguchi, K., Hamanishi, J., Baba, T., Matsumura, N., & Mandai, M. (2021). Tumor Immune Microenvironment

during Epithelial–Mesenchymal Transition. *Clinical Cancer Research*, *27*(17), 4669–4679. https://doi.org/10.1158/1078-0432.CCR-20-4459

Tam, S. Y., Wu, V. W. C., & Law, H. K. W. (2020). Hypoxia-Induced Epithelial-Mesenchymal Transition in Cancers: HIF-1α and Beyond. *Frontiers in Oncology*, *10*, 486. https://doi.org/10.3389/fonc.2020.00486

Tang, Y., & Weiss, S. J. (2017). Snail/Slug-YAP/TAZ complexes cooperatively regulate mesenchymal stem cell function and bone formation. *Cell Cycle*, *16*(5), 399–405. https://doi.org/10.1080/15384101.2017.1280643

Tashiro, E., Henmi, S., Odake, H., Ino, S., & Imoto, M. (2016). Involvement of the MEK/ERK pathway in EGF-induced E-cadherin down-regulation. *Biochemical and Biophysical Research Communications*, *477*(4), 801–806. https://doi.org/10.1016/j.bbrc.2016.06.138

Tato-Costa, J., Casimiro, S., Pacheco, T., Pires, R., Fernandes, A., Alho, I., Pereira, P., Costa, P., Castelo, H. B., Ferreira, J., & Costa, L. (2016). Therapy-Induced Cellular Senescence Induces Epithelial-to-Mesenchymal Transition and Increases Invasiveness in Rectal Cancer. *Clinical Colorectal Cancer*, *15*(2), 170-178.e3. https://doi.org/10.1016/j.clcc.2015.09.003

Taylor, A., & Rudd, C. E. (2017). Glycogen Synthase Kinase 3 Inactivation Compensates for the Lack of CD28 in the Priming of CD8+ Cytotoxic T-Cells: Implications for anti-PD-1 Immunotherapy. *Frontiers in Immunology*, *8*, 1653. https://doi.org/10.3389/fimmu.2017.01653

Taylor, B. C., & Balko, J. M. (2022). Mechanisms of MHC-I Downregulation and Role in Immunotherapy Response. *Frontiers in Immunology*, *13*. https://www.frontiersin.org/articles/10.3389/fimmu.2022.844866

Terme, M., Ullrich, E., Aymeric, L., Meinhardt, K., Desbois, M., Delahaye, N., Viaud, S., Ryffel, B., Yagita, H., Kaplanski, G., Prévost-Blondel, A., Kato, M., Schultze, J. L., Tartour, E., Kroemer, G., Chaput, N., & Zitvogel, L. (2011a). IL-18 induces PD-1-dependent immunosuppression in cancer. *Cancer Research*, *71*(16), 5393–5399. https://doi.org/10.1158/0008-5472.CAN-11-0993

Terme, M., Ullrich, E., Aymeric, L., Meinhardt, K., Desbois, M., Delahaye, N., Viaud, S., Ryffel, B., Yagita, H., Kaplanski, G., Prévost-Blondel, A., Kato, M., Schultze, J. L., Tartour, E., Kroemer, G., Chaput, N., & Zitvogel, L. (2011b). IL-18 Induces PD-1–Dependent Immunosuppression in Cancer. *Cancer Research*, *71*(16), 5393–5399. https://doi.org/10.1158/0008-5472.CAN-11-0993

Terry, S., Savagner, P., Ortiz-Cuaran, S., Mahjoubi, L., Saintigny, P., Thiery, J., & Chouaib, S. (2017). New insights into the role of EMT in tumor immune escape. *Molecular Oncology*, *11*(7), 824–846. https://doi.org/10.1002/1878-0261.12093

Thuault, S., Tan, E.-J., Peinado, H., Cano, A., Heldin, C.-H., & Moustakas, A. (2008). HMGA2 and Smads Co-regulate SNAIL1 Expression during Induction of Epithelial-to-Mesenchymal Transition*. *Journal of Biological Chemistry*, *283*(48), 33437–33446. https://doi.org/10.1074/jbc.M802016200

Tian, Y.-C., Chen, Y.-C., Chang, C.-T., Hung, C.-C., Wu, M.-S., Phillips, A., & Yang, C.-W. (2007). Epidermal growth factor and transforming growth factor-β1 enhance HK-2 cell migration through a synergistic increase of matrix metalloproteinase

and sustained activation of ERK signaling pathway. *Experimental Cell Research*, *313*(11), 2367–2377. https://doi.org/10.1016/j.yexcr.2007.03.022

Tinoco, R., Alcalde, V., Yang, Y., Sauer, K., & Zuniga, E. I. (2009). Cell-Intrinsic Transforming Growth Factor-β Signaling Mediates Virus-Specific CD8+ T Cell Deletion and Viral Persistence In Vivo. *Immunity*, *31*(1), 145–157. https://doi.org/10.1016/j.immuni.2009.06.015

Torre, L. A., Trabert, B., DeSantis, C. E., Miller, K. D., Samimi, G., Runowicz, C. D., Gaudet, M. M., Jemal, A., & Siegel, R. L. (2018). Ovarian cancer statistics, 2018. *CA: A Cancer Journal for Clinicians*, *68*(4), 284–296. https://doi.org/10.3322/caac.21456

Tripathi, S. C., Peters, H. L., Taguchi, A., Katayama, H., Wang, H., Momin, A., Jolly, M. K., Celiktas, M., Rodriguez-Canales, J., Liu, H., Behrens, C., Wistuba, I. I., Ben-Jacob, E., Levine, H., Molldrem, J. J., Hanash, S. M., & Ostrin, E. J. (2016). Immunoproteasome deficiency is a feature of non-small cell lung cancer with a mesenchymal phenotype and is associated with a poor outcome. *Proceedings of the National Academy of Sciences*, *113*(11), E1555–E1564. https://doi.org/10.1073/pnas.1521812113

Trivanović, D., Krstić, J., Djordjević, I. O., Mojsilović, S., Santibanez, J. F., Bugarski, D., & Jauković, A. (2016). The Roles of Mesenchymal Stromal/Stem Cells in Tumor Microenvironment Associated with Inflammation. *Mediators of Inflammation*, *2016*, 7314016. https://doi.org/10.1155/2016/7314016

Tuna, M., Ju, Z., Yoshihara, K., Amos, C. I., Tanyi, J. L., & Mills, G. B. (2020). Clinical relevance of TP53 hotspot mutations in high-grade serous ovarian cancers.

British Journal of Cancer, *122*(3), Article 3. https://doi.org/10.1038/s41416-019-0654-8

Tyler, M., & Tirosh, I. (2021). Decoupling epithelial-mesenchymal transitions from stromal profiles by integrative expression analysis. *Nature Communications*, *12*, 2592. https://doi.org/10.1038/s41467-021-22800-1

Uhlen, M., Zhang, C., Lee, S., Sjöstedt, E., Fagerberg, L., Bidkhori, G., Benfeitas, R., Arif, M., Liu, Z., Edfors, F., Sanli, K., von Feilitzen, K., Oksvold, P., Lundberg, E., Hober, S., Nilsson, P., Mattsson, J., Schwenk, J. M., Brunnström, H., … Ponten, F. (2017). A pathology atlas of the human cancer transcriptome. *Science*, *357*(6352), eaan2507. https://doi.org/10.1126/science.aan2507

Uhlitz, F., Bischoff, P., Peidli, S., Sieber, A., Trinks, A., Lüthen, M., Obermayer, B., Blanc, E., Ruchiy, Y., Sell, T., Mamlouk, S., Arsie, R., Wei, T., Klotz-Noack, K., Schwarz, R. F., Sawitzki, B., Kamphues, C., Beule, D., Landthaler, M., … Morkel, M. (2021). Mitogen-activated protein kinase activity drives cell trajectories in colorectal cancer. *EMBO Molecular Medicine*, *13*(10), e14123. https://doi.org/10.15252/emmm.202114123

Uttamsingh, S., Bao, X., Nguyen, K. T., Bhanot, M., Gong, J., Chan, J. L.-K., Liu, F., Chu, T. T., & Wang, L.-H. (2008). Synergistic effect between EGF and TGF-β1 in inducing oncogenic properties of intestinal epithelial cells. *Oncogene*, *27*(18), Article 18. https://doi.org/10.1038/sj.onc.1210915

Vallés, A. M., Boyer, B., Badet, J., Tucker, G. C., Barritault, D., & Thiery, J. P. (1990). Acidic fibroblast growth factor is a modulator of epithelial plasticity in a rat

bladder carcinoma cell line. *Proceedings of the National Academy of Sciences of the United States of America*, *87*(3), 1124–1128.

Vincent, T., Neve, E. P. A., Johnson, J. R., Kukalev, A., Rojo, F., Albanell, J., Pietras, K., Virtanen, I., Philipson, L., Leopold, P. L., Crystal, R. G., de Herreros, A. G., Moustakas, A., Pettersson, R. F., & Fuxe, J. (2009). A SNAIL1–SMAD3/4 transcriptional repressor complex promotes TGF-β mediated epithelial–mesenchymal transition. *Nature Cell Biology*, *11*(8), Article 8. https://doi.org/10.1038/ncb1905

Vitale, M., Pelusi, G., Taroni, B., Gobbi, G., Micheloni, C., Rezzani, R., Donato, F., Wang, X., & Ferrone, S. (2005). HLA Class I Antigen Down-Regulation in Primary Ovary Carcinoma Lesions: Association with Disease Stage. *Clinical Cancer Research*, *11*(1), 67–72. https://doi.org/10.1158/1078-0432.67.11.1

Walton, J. B., Farquharson, M., Mason, S., Port, J., Kruspig, B., Dowson, S., Stevenson, D., Murphy, D., Matzuk, M., Kim, J., Coffelt, S., Blyth, K., & McNeish, I. A. (2017). CRISPR/Cas9-derived models of ovarian high grade serous carcinoma targeting Brca1, Pten and Nf1, and correlation with platinum sensitivity. *Scientific Reports*, *7*, 16827. https://doi.org/10.1038/s41598-017-17119-1

Walton, J., Blagih, J., Ennis, D., Leung, E., Dowson, S., Farquharson, M., Tookman, L. A., Orange, C., Athineos, D., Mason, S., Stevenson, D., Blyth, K., Strathdee, D., Balkwill, F. R., Vousden, K., Lockley, M., & McNeish, I. A. (2016). CRISPR/Cas9-Mediated Trp53 and Brca2 Knockout to Generate Improved Murine Models of Ovarian High-Grade Serous Carcinoma. *Cancer Research*, *76*(20), 6118–6129. https://doi.org/10.1158/0008-5472.CAN-16-1272

Wang, G., Xu, D., Zhang, Z., Li, X., Shi, J., Sun, J., Liu, H.-Z., Li, X., Zhou, M., & Zheng, T. (2021). The pan-cancer landscape of crosstalk between epithelial-mesenchymal transition and immune evasion relevant to prognosis and immunotherapy response. *NPJ Precision Oncology*, *5*, 56. https://doi.org/10.1038/s41698-021-00200-4

Wang, H., Wang, H.-S., Zhou, B.-H., Li, C.-L., Zhang, F., Wang, X.-F., Zhang, G., Bu, X.-Z., Cai, S.-H., & Du, J. (2013). Epithelial–Mesenchymal Transition (EMT) Induced by TNF-α Requires AKT/GSK-3β-Mediated Stabilization of Snail in Colorectal Cancer. *PLoS ONE*, *8*(2), e56664. https://doi.org/10.1371/journal.pone.0056664

Wang, J., Sanmamed, M. F., Datar, I., Su, T. T., Ji, L., Sun, J., Chen, L., Chen, Y., Zhu, G., Yin, W., Zheng, L., Zhou, T., Badri, T., Yao, S., Zhu, S., Boto, A., Sznol, M., Melero, I., Vignali, D. A. A., … Chen, L. (2019). Fibrinogen-like Protein 1 Is a Major Immune Inhibitory Ligand of LAG-3. *Cell*, *176*(1), 334-347.e12. https://doi.org/10.1016/j.cell.2018.11.010

Wang, K., Hou, H., Zhang, Y., Ao, M., Luo, H., & Li, B. (2023). Ovarian cancer-associated immune exhaustion involves SPP1+ T cell and NKT cell, symbolizing more malignant progression. *Frontiers in Endocrinology*, *14*. https://www.frontiersin.org/articles/10.3389/fendo.2023.1168245

Wang, R., Löhr, C. V., Fischer, K., Dashwood, W. M., Greenwood, J. A., Ho, E., Williams, D. E., Ashktorab, H., Dashwood, M. R., & Dashwood, R. H. (2013). Epigenetic inactivation of endothelin-2 and endothelin-3 in colon cancer. *International Journal of Cancer*, *132*(5), 1004–1012. https://doi.org/10.1002/ijc.27762

Wang, S., Jiang, J., Liang, X., & Tang, Y. (2015). Links between cancer stem cells and epithelial–mesenchymal transition. *OncoTargets and Therapy*, *8*, 2973–2980. https://doi.org/10.2147/OTT.S91863

Wang, X., Li, C., Chen, T., Li, W., Zhang, H., Zhang, D., Liu, Y., Han, D., Li, Y., Li, Z., Luo, D., Zhang, N., & Yang, Q. (2021). Identification and Validation of a Five-Gene Signature Associated With Overall Survival in Breast Cancer Patients. *Frontiers in Oncology*, *11*. https://www.frontiersin.org/articles/10.3389/fonc.2021.660242

Wang, Y., Shi, J., Chai, K., Ying, X., & Zhou, B. P. (2013). The Role of Snail in EMT and Tumorigenesis. *Current Cancer Drug Targets*, *13*(9), 963–972.

Wang, Z. Y., Gaggero, A., Rubartelli, A., Rosso, O., Miotti, S., Mezzanzanica, D., Canevari, S., & Ferrini, S. (2002). Expression of interleukin-18 in human ovarian carcinoma and normal ovarian epithelium: Evidence for defective processing in tumor cells. *International Journal of Cancer*, *98*(6), 873–878. https://doi.org/10.1002/ijc.10268

Wawrocki, S., Druszczynska, M., Kowalewicz-Kulbat, M., & Rudnicka, W. (2016). Interleukin 18 (IL-18) as a target for immune intervention. *Acta Biochimica Polonica*, *63*(1), Article 1. https://doi.org/10.18388/abp.2015_1153

Weiss, A. R. R., & Dahlke, M. H. (2019). Immunomodulation by Mesenchymal Stem Cells (MSCs): Mechanisms of Action of Living, Apoptotic, and Dead MSCs. *Frontiers in Immunology*, *10*, 1191. https://doi.org/10.3389/fimmu.2019.01191

Wen, S., Hou, Y., Fu, L., Xi, L., Yang, D., Zhao, M., Qin, Y., Sun, K., Teng, Y., & Liu, M. (2019). Cancer-associated fibroblast (CAF)-derived IL32 promotes breast cancer

cell invasion and metastasis via integrin β3–p38 MAPK signalling. *Cancer Letters*, *442*, 320–332. https://doi.org/10.1016/j.canlet.2018.10.015

Westergaard, M. C. W., Milne, K., Pedersen, M., Hasselager, T., Olsen, L. R., Anglesio, M. S., Borch, T. H., Kennedy, M., Briggs, G., Ledoux, S., Kreuzinger, C., Decken, I. von der, Donia, M., Castillo-Tong, D. C., Nelson, B. H., & Svane, I. M. (2020). Changes in the Tumor Immune Microenvironment during Disease Progression in Patients with Ovarian Cancer. *Cancers*, *12*(12), Article 12. https://doi.org/10.3390/cancers12123828

Whitehair, R., Peres, L. C., & Mills, A. M. (2020). Expression of the Immune Checkpoints LAG-3 and PD-L1 in High-grade Serous Ovarian Carcinoma: Relationship to Tumor-associated Lymphocytes and Germline BRCA Status. *International Journal of Gynecological Pathology*, *39*(6), 558–566. https://doi.org/10.1097/PGP.0000000000000657

Wildenberg, G. A., Dohn, M. R., Carnahan, R. H., Davis, M. A., Lobdell, N. A., Settleman, J., & Reynolds, A. B. (2006). P120-Catenin and p190RhoGAP Regulate Cell-Cell Adhesion by Coordinating Antagonism between Rac and Rho. *Cell*, *127*(5), 1027–1039. https://doi.org/10.1016/j.cell.2006.09.046

Williams, E. J., Williams, G., Howell, F. V., Skaper, S. D., Walsh, F. S., & Doherty, P. (2001). Identification of an N-cadherin motif that can interact with the fibroblast growth factor receptor and is required for axonal growth. *The Journal of Biological Chemistry*, *276*(47), 43879–43886. https://doi.org/10.1074/jbc.M105876200

Willis, B. C., & Borok, Z. (2007). TGF-β-induced EMT: Mechanisms and implications for fibrotic lung disease. *American Journal of Physiology-Lung Cellular and Molecular Physiology*, *293*(3), L525–L534. https://doi.org/10.1152/ajplung.00163.2007

Wolf, K., & Friedl, P. (2009). Mapping proteolytic cancer cell-extracellular matrix interfaces. *Clinical & Experimental Metastasis*, *26*(4), 289–298. https://doi.org/10.1007/s10585-008-9190-2

Woo, S.-R., Turnis, M. E., Goldberg, M. V., Bankoti, J., Selby, M., Nirschl, C. J., Bettini, M. L., Gravano, D. M., Vogel, P., Liu, C. L., Tangsombatvisit, S., Grosso, J. F., Netto, G., Smeltzer, M. P., Chaux, A., Utz, P. J., Workman, C. J., Pardoll, D. M., Korman, A. J., … Vignali, D. A. A. (2012). Immune Inhibitory Molecules LAG-3 and PD-1 Synergistically Regulate T-cell Function to Promote Tumoral Immune Escape. *Cancer Research*, *72*(4), 917–927. https://doi.org/10.1158/0008-5472.CAN-11-1620

Woude, L. L. van der, Gorris, M. A. J., Halilovic, A., Figdor, C. G., & Vries, I. J. M. de. (2017). Migrating into the Tumor: A Roadmap for T Cells. *Trends in Cancer*, *3*(11), 797–808. https://doi.org/10.1016/j.trecan.2017.09.006

Wu, S. Z., Roden, D. L., Wang, C., Holliday, H., Harvey, K., Cazet, A. S., Murphy, K. J., Pereira, B., Al-Eryani, G., Bartonicek, N., Hou, R., Torpy, J. R., Junankar, S., Chan, C., Lam, C. E., Hui, M. N., Gluch, L., Beith, J., Parker, A., … Swarbrick, A. (2020). Stromal cell diversity associated with immune evasion in human triple-negative breast cancer. *The EMBO Journal*, *39*(19), e104063. https://doi.org/10.15252/embj.2019104063

Wu, S.-Y., Fu, T., Jiang, Y.-Z., & Shao, Z.-M. (2020). Natural killer cells in cancer biology and therapy. *Molecular Cancer*, *19*(1), 120. https://doi.org/10.1186/s12943-020-01238-x

Wu, T., Liu, T., Xing, L., & Ji, G. (2018). Baicalin and puerarin reverse epithelial-mesenchymal transition via the TGF-β1/Smad3 pathway in vitro. *Experimental and Therapeutic Medicine*, *16*(3), 1968–1974. https://doi.org/10.3892/etm.2018.6400

Wu, Y., Yi, M., Niu, M., Mei, Q., & Wu, K. (2022). Myeloid-derived suppressor cells: An emerging target for anticancer immunotherapy. *Molecular Cancer*, *21*(1), 184. https://doi.org/10.1186/s12943-022-01657-y

Xu, H., Wang, H., Li, G., Jin, X., & Chen, B. (2021). The Immune-Related Gene ELF3 is a Novel Biomarker for the Prognosis of Ovarian Cancer. *International Journal of General Medicine*, *14*, 5537. https://doi.org/10.2147/IJGM.S332320

Xu, W., Yang, Z., & Lu, N. (2015). A new role for the PI3K/Akt signaling pathway in the epithelial-mesenchymal transition. *Cell Adhesion & Migration*, *9*(4), 317–324. https://doi.org/10.1080/19336918.2015.1016686

Xu, Y., Lee, D.-K., Feng, Z., Xu, Y., Bu, W., Li, Y., Liao, L., & Xu, J. (2017). Breast tumor cell-specific knockout of Twist1 inhibits cancer cell plasticity, dissemination, and lung metastasis in mice. *Proceedings of the National Academy of Sciences of the United States of America*, *114*(43), 11494–11499. https://doi.org/10.1073/pnas.1618091114

Xu, Y., Qin, L., Sun, T., Wu, H., He, T., Yang, Z., Mo, Q., Liao, L., & Xu, J. (2017). Twist1 Promotes Breast Cancer Invasion and Metastasis by Silencing Foxa1 Expression. *Oncogene*, *36*(8), 1157–1166. https://doi.org/10.1038/onc.2016.286

Yang, J., Antin, P., Berx, G., Blanpain, C., Brabletz, T., Bronner, M., Campbell, K., Cano, A., Casanova, J., Christofori, G., Dedhar, S., Derynck, R., Ford, H. L., Fuxe, J., García de Herreros, A., Goodall, G. J., Hadjantonakis, A.-K., Huang, R. Y. J., Kalcheim, C., … Sheng, G. (2020). Guidelines and definitions for research on epithelial–mesenchymal transition. *Nature Reviews Molecular Cell Biology*, *21*(6), Article 6. https://doi.org/10.1038/s41580-020-0237-9

Yang, J., Mani, S. A., Donaher, J. L., Ramaswamy, S., Itzykson, R. A., Come, C., Savagner, P., Gitelman, I., Richardson, A., & Weinberg, R. A. (2004). Twist, a Master Regulator of Morphogenesis, Plays an Essential Role in Tumor Metastasis. *Cell*, *117*(7), 927–939. https://doi.org/10.1016/j.cell.2004.06.006

Yang, J., & Weinberg, R. A. (2008). Epithelial-Mesenchymal Transition: At the Crossroads of Development and Tumor Metastasis. *Developmental Cell*, *14*(6), 818–829. https://doi.org/10.1016/j.devcel.2008.05.009

Yang, L. (2010). TGFβ and cancer metastasis: An inflammation link. *Cancer Metastasis Reviews*, *29*(2), 263–271. https://doi.org/10.1007/s10555-010-9226-3

Ye, X., Tam, W. L., Shibue, T., Kaygusuz, Y., Reinhardt, F., Ng Eaton, E., & Weinberg, R. A. (2015). Distinct EMT programs control normal mammary stem cells and tumour-initiating cells. *Nature*, *525*(7568), Article 7568. https://doi.org/10.1038/nature14897

Ye, X., & Weinberg, R. A. (2017). The SUMO guards for SNAIL. *Oncotarget*, *8*(58), 97701–97702. https://doi.org/10.18632/oncotarget.22432

Yeh, H.-W., Hsu, E.-C., Lee, S.-S., Lang, Y.-D., Lin, Y.-C., Chang, C.-Y., Lee, S.-Y., Gu, D.-L., Shih, J.-H., Ho, C.-M., Chen, C.-F., Chen, C.-T., Tu, P.-H., Cheng, C.-F., Chen, R.-H., Yang, R.-B., & Jou, Y.-S. (2018). PSPC1 mediates TGF-β1 autocrine signalling and Smad2/3 target switching to promote EMT, stemness and metastasis. *Nature Cell Biology*, *20*(4), Article 4. https://doi.org/10.1038/s41556-018-0062-y

Yetkin, S., & Alotaibi, H. (2023). Selection and validation of novel stable reference genes for qPCR analysis in EMT and MET. *Experimental Cell Research*, *428*(1), 113619. https://doi.org/10.1016/j.yexcr.2023.113619

Yilmaz, M., & Christofori, G. (2009). EMT, the cytoskeleton, and cancer cell invasion. *Cancer and Metastasis Reviews*, *28*(1), 15–33. https://doi.org/10.1007/s10555-008-9169-0

Yook, J. I., Li, X.-Y., Ota, I., Hu, C., Kim, H. S., Kim, N. H., Cha, S. Y., Ryu, J. K., Choi, Y. J., Kim, J., Fearon, E. R., & Weiss, S. J. (2006). A Wnt–Axin2–GSK3β cascade regulates Snail1 activity in breast cancer cells. *Nature Cell Biology*, *8*(12), Article 12. https://doi.org/10.1038/ncb1508

Yu, L., Mu, Y., Sa, N., Wang, H., & Xu, W. (2014). Tumor necrosis factor α induces epithelial-mesenchymal transition and promotes metastasis via NF-κB signaling pathway-mediated TWIST expression in hypopharyngeal cancer. *Oncology Reports*, *31*(1), 321–327. https://doi.org/10.3892/or.2013.2841

Yu, M., Bardia, A., Wittner, B. S., Stott, S. L., Smas, M. E., Ting, D. T., Isakoff, S. J., Ciciliano, J. C., Wells, M. N., Shah, A. M., Concannon, K. F., Donaldson, M. C., Sequist, L. V., Brachtel, E., Sgroi, D., Baselga, J., Ramaswamy, S., Toner, M., Haber, D. A., & Maheswaran, S. (2013). Circulating Breast Tumor Cells Exhibit Dynamic Changes in Epithelial and Mesenchymal Composition. *Science*, *339*(6119), 580–584. https://doi.org/10.1126/science.1228522

Yuan, K., Zhao, S., Ye, B., Wang, Q., Liu, Y., Zhang, P., Xie, J., Chi, H., Chen, Y., Cheng, C., & Liu, J. (2023). A novel T-cell exhaustion-related feature can accurately predict the prognosis of OC patients. *Frontiers in Pharmacology*, *14*, 1192777. https://doi.org/10.3389/fphar.2023.1192777

Zeisberg, M., & Neilson, E. G. (2009). Biomarkers for epithelial-mesenchymal transitions. *The Journal of Clinical Investigation*, *119*(6), 1429–1437. https://doi.org/10.1172/JCI36183

Zhai, W., Zhou, X., Wang, H., Li, W., Chen, G., Sui, X., Li, G., Qi, Y., & Gao, Y. (2020). A novel cyclic peptide targeting LAG-3 for cancer immunotherapy by activating antigen-specific CD8+ T cell responses. *Acta Pharmaceutica Sinica B*, *10*(6), 1047–1060. https://doi.org/10.1016/j.apsb.2020.01.005

Zhang, H., Cui, B., Zhou, Y., Wang, X., Wu, W., Wang, Z., Dai, Z., Cheng, Q., & Yang, K. (2021). B2M overexpression correlates with malignancy and immune signatures in human gliomas. *Scientific Reports*, *11*(1), Article 1. https://doi.org/10.1038/s41598-021-84465-6

Zhang, J.-Y., Zhao, Y.-L., Lv, Y.-P., Cheng, P., Chen, W., Duan, M., Teng, Y.-S., Wang, T.-T., Peng, L.-S., Mao, F.-Y., Liu, Y.-G., Fu, X.-L., Yu, P.-W., Luo, P., Zhang, W.-J.,

Zou, Q.-M., & Zhuang, Y. (2018). Modulation of CD8+ memory stem T cell activity and glycogen synthase kinase 3β inhibition enhances anti-tumoral immunity in gastric cancer. *Oncoimmunology*, *7*(4), e1412900. https://doi.org/10.1080/2162402X.2017.1412900

Zhang, L., Conejo-Garcia, J. R., Katsaros, D., Gimotty, P. A., Massobrio, M., Regnani, G., Makrigiannakis, A., Gray, H., Schlienger, K., Liebman, M. N., Rubin, S. C., & Coukos, G. (2003). Intratumoral T Cells, Recurrence, and Survival in Epithelial Ovarian Cancer. *New England Journal of Medicine*, *348*(3), 203–213. https://doi.org/10.1056/NEJMoa020177

Zhang, X.-F., Wang, J., Jia, H.-L., Zhu, W.-W., Lu, L., Ye, Q.-H., Nelson, P. J., Qin, Y., Gao, D.-M., Zhou, H.-J., & Qin, L.-X. (2019). Core fucosylated glycan-dependent inhibitory effect of QSOX1-S on invasion and metastasis of hepatocellular carcinoma. *Cell Death Discovery*, *5*, 84. https://doi.org/10.1038/s41420-019-0164-8

Zhang, Y., & Weinberg, R. A. (2018). Epithelial-to-mesenchymal transition in cancer: Complexity and opportunities. *Frontiers of Medicine*, *12*(4), 361–373. https://doi.org/10.1007/s11684-018-0656-6

Zhao, L., Wang, H., Xu, K., Liu, X., & He, Y. (2022). Update on lymphocyte-activation gene 3 (LAG-3) in cancers: From biological properties to clinical applications. *Chinese Medical Journal*, *135*(10), 1203–1212. https://doi.org/10.1097/CM9.0000000000001981

Zheng, G. X. Y., Terry, J. M., Belgrader, P., Ryvkin, P., Bent, Z. W., Wilson, R., Ziraldo, S. B., Wheeler, T. D., McDermott, G. P., Zhu, J., Gregory, M. T., Shuga, J.,

Montesclaros, L., Underwood, J. G., Masquelier, D. A., Nishimura, S. Y., Schnall-Levin, M., Wyatt, P. W., Hindson, C. M., … Bielas, J. H. (2017). Massively parallel digital transcriptional profiling of single cells. *Nature Communications*, *8*(1), Article 1. https://doi.org/10.1038/ncomms14049

Zheng, M., Jiang, Y., Chen, W., Li, K., Liu, X., Gao, S., Feng, H., Wang, S., Jiang, J., Ma, X., Cen, X., Tang, Y., Chen, Y., Lin, Y., Tang, Y., & Liang, X. (2015). Snail and Slug collaborate on EMT and tumor metastasis through miR-101-mediated EZH2 axis in oral tongue squamous cell carcinoma. *Oncotarget*, *6*(9), 6794–6810. https://doi.org/10.18632/oncotarget.3180

Zvaifler, N. J. (2006). Relevance of the stroma and epithelial-mesenchymal transition (EMT) for the rheumatic diseases. *Arthritis Research & Therapy*, *8*(3), 210. https://doi.org/10.1186/ar1963